

Phosphorus forms in fertilized arable soil profiles and related ^{33}P uptake

Dissertation

zur

Erlangung des Grades
Doktor der Agrarwissenschaften
(Dr. agr.)

der

Landwirtschaftlichen Fakultät

der

Rheinischen Friedrich-Wilhelms-Universität Bonn

von

Maximilian Koch

aus Werneck

Bonn 2019

Tag der mündlichen Prüfung: 25. Juni 2019

Vorsitzender: Priv.-Doz. Dr. Gerd Welp

1. Gutachter: Prof. Dr. Wulf Amelung

2. Gutachter: Prof. Dr. Peter Leinweber

Fachnahes Mitglied: Prof. Dr. Claudia Knief

Angefertigt mit Genehmigung der Landwirtschaftlichen Fakultät der Universität Bonn

SUMMARY

Arable soils usually store several thousand kg phosphorus (P) per ha, thus far exceeding the recommended P fertilizer dose to sustain crop yields. However, the soil profile is frequently not considered in fertilizer recommendations, because P supply to the plants from the subsoil is lacking clarification. This thesis is determined by the overarching hypothesis that a large part of the P already present in the soil is neither physically accessible nor chemically available to plants and thus does not contribute to plant nutrition. Therefore, my goal was to evaluate the P bonding forms at different soil depth, and to determine the contribution of these P forms to plant nutrition.

My specific objectives were (i) to characterize and quantify the chemical speciation of P forms in soil profiles of agricultural long-term fertilizer experiments, (ii) to elucidate the supply potentials of moderately bioavailable P pools for plants, and finally (iii) to methodologically refine radiotracer-based digital autoradiography for quantifying spatial and temporal P uptake in plants. For this purpose I sampled (i) soil profiles (0 cm to 90 cm) from two long-term fertilizer experiments located in Rostock (Stagnic Cambisol, > 16 years duration) and Bad Lauchstädt (Haplic Chernozem, > 100 years duration); each experiment was comprised of an unfertilized control, an organic treatment (compost or manure), a mineral treatment (triple superphosphate or superphosphate), and a surplus treatment combining organic and mineral applications. Soil P analyses comprised the assessment of P stocks and speciation of P pools of varying chemical extractability, using sequential fractionation, nuclear magnetic resonance (NMR) as well as X-ray absorption near edge structure (XANES) spectroscopy. To trace P uptake from moderately bioavailable P pools, I (ii) conducted uptake studies including two soil orders; a Haplic Luvisol subsoil, that had never been P fertilized and an Orthic Ferralsol subsoil from Australia from a conventional agricultural background. Investigations were accompanied by digital autoradiography to trace plant uptake of P radiotracers. The experiment was conducted in rhizoboxes with ^{33}P loaded Fe and Al hydroxides in combination with diffusive gradients in thin films (DGT) techniques. The radiotracer method was then (iii) extended by advanced quantitative evaluation of the uptake of P radiotracers in wheat and maize. The ^{33}P quantification was carried out with co-exposed ^{14}C standard references during the imaging process.

The P fertilizer application (i) in excess of plant P demand significantly increased both top- and subsoil P stocks. Intriguingly, there was little if any difference in P stocks and the speciation of P forms for organically and inorganically fertilized plots, suggesting that the kind of fertilizer used had only limited effects on the soil P status in the long term. The P uptake study suggested that (ii) P supply from non-soluble, soil-inherent inorganic P bonding forms can compensate insufficient levels of available P in soil solution. Specifically, in the rhizobox experiments performed, even subsoil P bound to Fe and Al oxidic phases was able to contribute up to 30% of overall uptake of P by young wheat plants. Additionally, DGT applications indicated a better P availability from amorphous Fe hydroxide than from Al hydroxide. The overall P uptake, however, was regulated by soil moisture contents, indicating that water supply to plants controlled P uptake and the final amount of soluble P. These investigations were fundamentally supported by digital autoradiography, whose application resulted (iii) in a successful method for quantification of ^{33}P radiotracers in plant tissues.

In summary, P fertilizer applications control soil P stocks but effects on P speciation are minor. In the arable soil profiles studied here, P was predominantly bound to oxidic soil phases, suggesting that a significant portion of soil P dynamics is mediated by such inorganic P pools of varying availability, whereas organic P pools seem to be equilibrated with the general P status of the soil. The P supply rates from non-soluble, moderately labile P forms, rather than immediate mineralization processes, seem to control the long-term P supply for crops.

ZUSAMMENFASSUNG

Ackerböden speichern in der Regel mehrere tausend kg Phosphor (P) pro Hektar und übersteigen damit die empfohlenen P-Düngermengen zur Erhaltung der Ernteerträge. In den derzeitigen Düngeempfehlungen wird jedoch häufig nicht das gesamte Bodenprofil berücksichtigt, da die P-Versorgung der Pflanzen aus dem Untergrund nicht geklärt ist. Die vorliegende Arbeit wird daher durch die übergreifende Hypothese bestimmt, dass ein großer Teil des bereits im Boden vorhandenen P weder physikalisch zugänglich noch chemisch für Pflanzen verfügbar ist und somit nicht zur Pflanzenernährung beiträgt. In dieser Arbeit wurden die P-Bindungsformen in verschiedenen Bodentiefen bewertet und der Beitrag dieser P-Formen zur Pflanzenernährung untersucht.

Meine spezifischen Ziele waren (i) die Charakterisierung und Quantifizierung der chemischen Spezierung von P-Formen in Bodenprofilen landwirtschaftlicher Langzeitdüngerexperimente, (ii) die Aufklärung der Versorgungspotenziale mäßig bioverfügbarer P-Pools für Pflanzen und schließlich (iii) die methodische Verfeinerung der Radioisotopen-basierten digitalen Autoradiographie zur Quantifizierung der räumlichen und zeitlichen P-Aufnahme in Pflanzen. Zu diesem Zweck habe ich (i) Bodenprofile (0 cm bis 90 cm) aus zwei Langzeitdüngerexperimenten in Rostock (Stagnic Cambisol, > 16 Jahre Laufzeit) und Bad Lauchstädt (Haplic Chernozem, > 100 Jahre Laufzeit) entnommen; jedes Experiment bestand aus einer ungedüngten Kontrolle, einer organischen Behandlung (Kompost oder Gülle), einer mineralischen Behandlung (Dreifach-Superphosphat oder Superphosphat) und einer Überschussbehandlung, die organische und mineralische Anwendungen kombiniert. Die Boden-P-Analysen umfassten die Bewertung von P-Vorräten und die Spezierung von P-Pools unterschiedlicher chemischer Extrahierbarkeit mittels sequentieller Fraktionierung, Kernspinresonanz (NMR) sowie Röntgenabsorptionsnahkantenstruktur (XANES) Spektroskopie. Um die P-Aufnahme aus mäßig bioverfügbaren P-Pools zu verfolgen, führte ich (ii) Aufnahmestudien mit zwei Bodenordnungen durch: einem ungedüngten Haplic Luvisol-Unterboden und einem Orthic Ferralsol-Unterboden aus Australien mit konventionellem landwirtschaftlichen Hintergrund. Die Untersuchungen wurden durch digitale Autoradiographie ergänzt, um die Aufnahme von P-Radioisotopen in die Pflanzen zu verfolgen. Das Experiment wurde in Rhizoboxen mit ^{33}P beladenen Fe und Al Hydroxiden in Kombination mit einer neuartigen Technik mit Dünnschicht-diffusen-Gradienten (DGT) durchgeführt. Die autoradiographische Methode wurde anschließend (iii) durch eine quantitative Bewertung der Aufnahme von ^{33}P in Weizen und Mais erweitert. Diese ^{33}P -Quantifizierung wurde durch Zuhilfenahme von ^{14}C -Standardreferenzen ermöglicht.

Phosphordüngung (i) über den Pflanzenbedarf hinaus erhöhte die P-Vorräte im Ober- als auch im Unterboden deutlich. Interessanterweise gab es einen geringen oder gar keinen Unterschied der P-Vorräte und Spezierung in Abhängigkeit von organisch und anorganisch gedüngten Versuchsflächen, was darauf hindeutet, dass die Art des verwendeten Düngers langfristig nur begrenzte Auswirkungen auf den P Status eines Bodens hat. Die Untersuchung der P-Aufnahme zeigte, dass (ii) die P-Mobilisierung von unlöslichen, Boden-inhärenten anorganischen P-Bindungsformen ineffiziente Konzentrationen an verfügbarem P in der Bodenlösung kompensieren kann. Insbesondere in den durchgeführten Rhizobox-Experimenten konnte selbst der an Fe und Al gebundene P bis zu 30 % zur Gesamtaufnahme von P durch junge Weizenpflanzen beitragen. Darüber hinaus zeigte die DGT-Anwendung eine bessere P-Verfügbarkeit von P gebunden an amorphes Fe Hydroxid als von Al Hydroxid. Die Gesamtaufnahme von P wurde jedoch durch die Bodenfeuchte reguliert, was darauf hindeutet, dass die Wasserversorgung der Pflanzen die Aufnahme von P und die Menge an löslichem P kontrollierte. Diese Untersuchungen wurden grundlegend durch die digitale Autoradiographie unterstützt, deren Anwendung (iii) zu einer erfolgreichen Weiterentwicklung der quantitativen digitalen Autoradiographie von ^{33}P in Pflanzengewebe führte.

Zusammenfassend lässt sich sagen, dass P-Dünger Zugaben die Gehalte an P-Vorräte im Boden kontrollieren, aber die Einflüsse auf die chemische Form von Boden-P gering sind. In den hier untersuchten Ackerbodenprofilen war P überwiegend an oxidische Bodenphasen gebunden. Dies deutet daraufhin, dass ein bedeutender Teil der Boden-P-Dynamik durch solche anorganischen P-Pools unterschiedlicher Verfügbarkeit bewerkstelligt wird, während die organischen P-Pools passiv mit dem allgemeinen P-Status des Bodens äquilibriert sind. Die P-Mobilisierung aus unlöslichen, mäßig labilen P-Formen und nicht aus unmittelbaren Mineralisierungsprozessen scheint die langfristige P-Versorgung für Nutzpflanzen zu kontrollieren.

CONTENT

Summary	I
Zusammenfassung	II
Content	III
List of figures	VII
List of tables	XI
List of abbreviations.....	XIII
I GENERAL INTRODUCTION.....	1
1 RATIONALE.....	2
2 STATE OF THE ART	3
2.1 Phosphorus availability in arable soils	3
2.2 Phosphorus forms in fertilized arable soils.....	4
2.3 Subsoil phosphorus utilization	5
2.4 Why to study phosphorus dynamics in long-term agricultural experiments	6
2.5 Methodological approaches.....	7
2.5.1 Spectroscopic methods for phosphorus research.....	7
2.5.2 Radioisotope techniques to study phosphorus cycling in the soil-plant system.....	9
3 OBJECTIVES	10
II PHOSPHORUS STOCKS AND SPECIATION IN SOIL PROFILES OF A LONG-TERM FERTILIZER EXPERIMENT: EVIDENCE FROM SEQUENTIAL FRACTIONATION, P K-EDGE XANES, AND ³¹P-NMR SPECTROSCOPY.....	13
1 INTRODUCTION	14
2 MATERIAL AND METHODS	15
2.1 Soil sampling and basic soil characteristics	15
2.2 Sequential phosphorus fractionation	16
2.3 Phosphorus K-edge XANES spectroscopy.....	17
2.4 Solution ³¹ P-phosphorus-NMR spectroscopy	17
2.5 Statistical analyses.....	18
3 RESULTS	18
3.1 Soil characteristics.....	18
3.2 Sequentially extracted phosphorus fractions	19
3.3 P-XANES analyses.....	23
3.4 Solution ³¹ P-NMR spectroscopy	26
4 DISCUSSION	28
4.1 Influence of fertilizers on phosphorus stocks and proportions.....	28
4.2 Influence of fertilizer on phosphorus speciation	30
5 IMPLICATIONS.....	31

III	INSIGHTS INTO ³³P UTILIZATION FROM FE AND AL HYDROXIDES IN LUVISOL AND FERRALSOL SUBSOILS	33
1	INTRODUCTION	34
2	MATERIAL AND METHODS	35
2.1	Soil characteristics.....	35
2.2	Experimental	35
2.3	Plant growth	37
2.4	Radiotracer treatment and application.....	37
2.5	Plant analyses	39
2.6	Digital autoradiography.....	40
2.7	Statistics.....	40
3	RESULTS	40
3.1	Soil characteristics and plant biomass.....	40
3.2	Digital autoradiography – ³³ P distribution in plant and soil	42
3.3	Total shoot phosphorus concentrations and ³³ P allocation	43
4	DISCUSSION	44
4.1	Soil phosphorus buffering capacity and plant development.....	44
4.2	³³ P acquisition from phosphorus sources having different availabilities	45
5	CONCLUSION	46
IV	QUANTITATIVE IMAGING OF ³³P IN PLANT MATERIALS USING ¹⁴C POLYMER REFERENCES	47
1	INTRODUCTION	48
2	MATERIAL AND METHODS	49
2.1	Standardized preconditioning of the digital imaging plates	49
2.2	Co-exposure of ¹⁴ C polymer references and ³³ P phosphoric acid.....	49
2.3	Quantification of ³³ P activity in excised leaves	50
3	RESULTS	53
3.1	Linear relationship between ¹⁴ C and ³³ P activities	53
3.2	³³ P activities in leaves calculated from digital autoradiography images	55
4	DISCUSSION	57
4.1	Linear dynamic range and plate sensitivity	57
4.2	Quantification of ³³ P leaf tissue concentration.....	58
V	FINAL DISCUSSION	61
1	SUMMARY OF THE RESEARCH OBJECTIVES.....	62
2	SYNTHESIS AND OUTLOOK	64
2.1	Limitations of phosphorus supply in fertilized arable soils.....	64
2.2	Phosphorus stocks in fertilized arable soil profiles as modified by fertilizer usage.....	66

CONTENT

2.3	Phosphorus speciation in arable soil profiles as modified by fertilizer usage	68
2.4	Plant availability and accessibility of ³³ P from dominant phosphorus forms	71
2.5	Methodological advances of digital autoradiography for phosphorus research	73
3	CONCLUSIONS.....	75
VI	REFERENCES.....	77
VII	APPENDIX A	93
VIII	APPENDIX B.....	97
IX	APPENDIX C	101
X	APPENDIX D	105
XI	APPENDIX E	118
XII	APPENDIX F	122
	Lebenslauf	129
	Danksagung.....	131

LIST OF FIGURES

- Figure II-1 Phosphorus (P) stocks of labile (sum of Resin-P, $\text{NaHCO}_3\text{-P}_i$, and $\text{NaHCO}_3\text{-P}_o$), moderately labile (sum of NaOH-P_i , NaOH-P_o), and stable P fractions (sum of $\text{H}_2\text{SO}_4\text{-P}$ and Residual-P) of the three sampling depths (0 to 30 cm, 30 to 60 cm, and 60 to 90 cm) of the four treatments control, compost, TSP, and compost+TSP are displayed. Statistically differences are illustrated: Numbers with the same upper case letter are not significantly different to the depth of other treatments. Numbers with the same lower case letter within a treatment are not significantly different. $n=3$ 22
- Figure II-2 Phosphorus (P) speciation (% proportion of total P (P_{tot})) as obtained by linear combination fitting (LCF) on averaged ($n=3$) P K -edge XANES spectra of four different treatments (control, compost, TSP, and compost+TSP). All possible combinations with up to four standard components (total 12 standard components) were calculated. Best fit was chosen according to the lowest r -factor and fits were tested for significant differences using the Hamilton test ($p < 0.05$). Proportions of fits not significantly different from each other were averaged. 25
- Figure II-3 Phosphorus (P) stocks (kg ha^{-1}) and proportions (numbers in bars) of categorized chemical shift regions on the total ^{31}P -NMR signals of four treatments (control, compost, TSP, and compost+TSP) and three sampling depths (0 to 30, 30 to 60, and 60 to 90 cm). The recovery rate of NaOH-EDTA extraction is stated in relation to total P concentrations from aqua regia digestion before the lyophilization step, determined by ICP-OES. Proportions of the monoester region (identified peaks and an unidentified rest) were summarized as orthophosphate monoesters. Inorganic P and organic P ratios (P_i/P_o) calculated from identified compound classes are shown above the bars. 27
- Figure III-1 Digital autoradiography image (left) and photo (right) of a representative example of 14 days old wheat plants of a ^{33}P labeled KH_2PO_4 treatment in the left chamber (1) and a ^{33}P labeled Fe-P hydroxide treatment in the right chamber (2) grown in Ferralsol subsoil. The high contrasted regions in the left picture represented the ^{33}P radiotracer distributions in the soil band and the plant tissues. High contrasts are devoted to regions of higher ^{33}P activities. The imaging plates were exposed for 16 h to the rhizoboxes and then scanned in 100 μm sensitive mode (Bioimager CR35 Bio, ELYSIA-Raytest, Straubenhardt, Germany) and processed with the software AIDA Image Analyzer 2D densitometry program (ELYSIA-Raytest, Straubenhardt, Germany). 36
- Figure III-2 Soil water properties (matrix potential [kPa], pF value [as LOG (-hPa)] and soil moisture [Vol. %]) during 14 days of plant growth in Ferralsol and Luvisol under controlled conditions. Soil moisture was set to approximately 75% of maximal water holding capacity at the onset of the experiment (day 0), which equated water potentials in the range of field capacity (12 ± 1 kPa in both soils; the frame represents the limit of field capacity at -33 kPa). The measurements were valid from day 2 on (before day 2 shaded lines), after soil bands of the rhizoboxes were filled with the ^{33}P radioactive-labeled soil treatments and the rhizoboxes were sealed with plastic foil). The data was conducted by dielectric water potential sensors (MPS2) (Ferralsol, $n=2$; Luvisol, $n=1$) and moisture sensors (both soils, $n=2$) for the volumetric water content. It is noteworthy that only the data points from night measurements are presented here, as extreme and artificial diurnal matrix potential amplitudes indicated significant temperature influences on sensor reading (see also Fig. B2). Sensor accuracy error was estimated to be around 25%. 38
- Figure III-3 Shoot dry weights [mg] (A), shoot P derived from applied P source [%] (B), and proportions of P recovery [%] (C) determined from wheat plants grown in rhizoboxes with banded ^{33}P sources (at day 14). The radioactive-labeled ^{33}P treatments ($^{33}\text{P-Fe}$: ^{33}P associated to amorphous Fe hydroxide; $^{33}\text{P-Al}$: ^{33}P associated to amorphous Al hydroxide; $^{33}\text{P-OrthoP}$: ^{33}P applied in KH_2PO_4 solution; $^{33}\text{P-NoP}$: ^{33}P radiotracer applied alone without P addition) were banded in Ferralsol ($n=3$) and Luvisol ($n=5$) subsoil. Shoot dry weights were measured after drying at 40°C for 12h at the end of the experiment. Shoot ^{33}P activities were determined by liquid scintillation counting after acid digestion of plant material. Significant differences at 5% probability level between samples are designated by different letters (testing: two-way ANOVA combined with the Tukey post hoc test for comparison of means). *Treatment between soils*: numbers with the same capital case letter are not significantly different from the treatment of the other soil group. *Treatments within one soil*: numbers with the same lower case letter within a soil type are not significantly different. 41

- Figure IV-1 Digital images of selected regions of interest (ROI) of (A) the reference experiments (EXP 1 and EXP 2) with ^{33}P phosphoric acid activities (contrasted circles) and ^{14}C polymer reference activities (contrasted squares), and of (B) excised leaf experiments with maize and wheat leaves containing ^{33}P phosphoric acid and co-exposed ^{14}C polymer references. Imaging plates were exposed for 4 h to radioactivity, and then scanned in sensitive mode with a pixel size resolution of 100 μm . A: At the beginning (EXP 1) and at the end of the study (after 20 exposures, EXP 2) we applied ^{33}P phosphoric acid solution with different activities into circular 100 μm deep recesses on an aluminum plate. The surface area of every recess was 1 cm^2 . Commercial ^{14}C polymer references (with also 1 cm^2 surface area) were co-exposed to imaging plates. B: ^{33}P phosphoric acid solutions having different activities were supplied to excised leaves for 3 days in a climate chamber, after uptake, leaves were dried and exposed to the imaging plates. Images are received and presented under identical conditions (incubation time, gamma resolution of 2). 52
- Figure IV-2 Linear relationship between photostimulated luminescence intensities (PSL) and exposed radioactivity of ^{14}C and ^{33}P radioisotopes applied on an aluminum plate for the reference experiments. Linear relationship between both radioisotopes was only found within the range of 50 and 2000 Bq cm^{-2} . The exposure time was 4 h followed by digital autoradiography scanning. Results are averaged values over 7 plate exposure events (including EXP 1 and EXP 2). 53
- Figure IV-3 Schematic illustration of the methodological approach for digital autoradiographic quantification of ^{33}P by photostimulated luminescence intensity (PSL) in leaves, gained from the co-exposure of ^{14}C polymer references. First, in reference experiments (EXP1 and EXP2), the ratio γ between ^{14}C and ^{33}P intensities at different known activities was analyzed. By using γ to transform the known relationship α between ^{14}C radioactivity and responding PSL, the activity of ^{33}P can be calculated by dividing respective PSL intensities by β_{calc} 54
- Figure IV-4 Relationship between photostimulated luminescence (PSL) intensities and applied ^{14}C and ^{33}P activities over the whole range of applied radioactivity in two reference experiments (EXP1 and EXP2). At the end of the study, after more than 20 exposure events the linearity in the plate response reaction of PSL to increasing ^{33}P activities was lost (EXP2) and we therefore recommend to apply the method within the dynamic linear range between 50 and 2000 Bq cm^{-2} for ^{33}P radioisotopes. 55
- Figure IV-5 Relationship between leaf tissue density [g cm^{-3}] of maize and wheat leaves and the ratio of measured photostimulated luminescence (PSL) assessed via autoradiography and ^{33}P activities assessed by liquid scintillation counting (LSC). The ^{33}P labeled excised leaves of maize ($n=3$) and wheat ($n=5$) plants were first dried and then exposed for 4 h to imaging plates and afterwards scanned by the Bioimager CR35. For LSC analyses leaf materials were digested (HNO_3 pressure digestion) and 3 aliquots of every digest were analyzed. 56
- Figure IV-6 Relationship between measured ^{33}P activities [Bq cm^{-2}] assessed by liquid scintillation counting (LSC) and calculated ^{33}P activities [Bq cm^{-2}] from autoradiography. All activities of single ^{33}P excised leaves of maize ($n=3$; over 3 imaging events) as well as of wheat ($n=5$; over 5 imaging events) are displayed. The results revealed a highly significant linear correlation between measured ^{33}P activities in the excised leaves (obtained via LSC) and the calculated ^{33}P activities using the outlined quantification method. 57
- Figure A1 Stacked normalized P *K*-edge XANES spectra of used P reference compounds and the four treatments separated by sampling depths 0 to 30 cm, 30 to 60 cm, and 60 to 90 cm. 94
- Figure A2 Solution ^{31}P -NMR spectra of the NaOH-EDTA extracts of the topsoil and subsoil samples from 0 to 90 cm soil depths of the control and the fertilizer treatments compost, TSP and compost+TSP with highlighted orthophosphate and orthophosphate monoester region. Shift regions of P compounds are marked with capital letters. Showing orthophosphate (A), the orthophosphate monoester region (B), the orthophosphate diester region (C), and the pyrophosphate region (D). The identified orthophosphate monoester species, are illustrated with small letters from a to e, displaying (a) *neo*-inositol hexakisphosphate, (b) *chiro*-inositol hexakisphosphate, (c) orthophosphate, (d) *myo*-inositol hexakisphosphate, and (e) *scyllo*-inositol hexakisphosphate. Spiking experiments revealed the diester degradation products (f) *alpha*-glycerophosphate, and (g) *beta*-glycerophosphate. 95

- Figure A3 Spiking experiment of a topsoil sample of the TSP treatment, showing the orthophosphate and orthophosphate monoester region. The original solution ^{31}P -NMR spectrum is presented (black line) and the spiked spectra (dotted line) of (I) *myo*-inositol hexakisphosphate, (II) *alpha*-glycerophosphate, and (III) *beta*-glycerophosphate is superimposed to identify and separate these monoesters. 96
- Figure B1 Digital autoradiographic images of 14 days old wheat plants grown in rhizoboxes with different ^{33}P labeled treatments (^{33}P -Fe: ^{33}P associated to amorphous Fe hydroxide; ^{33}P -Al: ^{33}P associated to amorphous Al hydroxide; ^{33}P -OrthoP: ^{33}P applied in KH_2PO_4 solution; ^{33}P -NoP: ^{33}P radiotracer applied alone without P addition) in Ferralsol and Luvisol subsoil. Imaging plates were exposed for 4 h to the plant material followed by a 100 μm sensitive scan with the scanner unit Bioimager CR35 Bio. Images are processed with AIDA software and presented with a gamma resolution at 2. 98
- Figure B2 Average diurnal temperature [$^{\circ}\text{C}$] and soil matrix potentials [kPa] data points from Luvisol (Luvisol sensor 1 + 2) Ferralsol (Ferralsol sensor 1 + 2) subsoil during a 14 days growth period of wheat plants in rhizoboxes. Valid measurement started after filling the ^{33}P radioactive-labeled soil treatments in soil bands of rhizoboxes, which were sealed with plastic foil at day 2 of growth. The data was conducted by dielectric water potential sensors (MPS2) and moisture sensors for the volumetric water content. In this figure all data points from night and day measurements are presented. It is obvious, that matrix potentials were artificially affected by increasing temperature at the start of each day time similar observations are stated by other users. Others authors also assumed effects by plant transpiration when plants reached the sensor area, but these effects were not that pronounced than the effects of temperature variations. However, plant transpiration can be expected to gain influence on the matrix potential after day 7. Furthermore, matrix potential producer estimated the sensor accuracy at -9 to -100 kPa to be approximately 25% (Decagon Devices Inc. 2016). However, these variations cannot explain the steep increase of the matrix potentials measured by Luvisol Sensor 2, and we therefore assume that sensor-soil connectivity was not appropriate for this sensor. 99
- Figure C1 Technical illustration of the aluminum plate with specific tolerances. 102
- Figure C2 In this example, the ^{33}P activity in specific plant sections of whole plants was analyzed. Results showed that $101 \pm 4\%$ ($n=2$; 3 plate exposures) of the measured activity by liquid scintillation counting (LSC) (in both, M1 and M2) was quantified. Whole maize plants in the three leaf stage were cut at the rhizome and directly placed in 20 mL of dH_2O spiked with $3.6 \text{ Bq } \mu\text{L}^{-1} \text{ }^{33}\text{P}$. After 2 days of incubation in a climate chamber, the plants were carefully removed from the solution. Thereafter, the first 2 cm from the bottom of the stem that were in contact with the solution were cut and discarded. The plants were dried at 40°C for 24 h and thereafter leaf sections of 5 to 10 cm were marginally incised at the edge of a leaf. This was done to retrieve the specific leaf area for processing with AIDA Image Analyzer 2D software (ELYSIA-Raytest, Straubenhardt, Germany). For plate exposure, single plants were placed together with a ^{14}C polymer reference set in a cassette for radiography and exposed for 4 h to a freshly erased imaging plate, covered with a thin plastic foil. The ROI, representing the labeled leaf section were surrounded within the software, giving the PSL intensity and the size of the region in mm^2 . Overall, 3 different imaging plates were exposed to two maize plants (giving $n=6$), respectively. After exposure, the marked leaf sections were carefully cut at the incisions. Then, the tissue thickness was measured and the material was digested with subsequent ^{33}P activities liquid scintillation counting (LSC). The Figure demonstrates that even within a whole plant it is possible to identify and quantify ^{33}P uptake into individual plant sections. 104
- Figure D1 Averaged stocks of labile (sum of Resin-P, $\text{NaHCO}_3\text{-P}_i$, and $\text{NaHCO}_3\text{-P}_o$), moderately labile (sum of NaOH-P_i , NaOH-P_o), and stable P fractions (sum of $\text{H}_2\text{SO}_4\text{-P}$ and Residual-P) of the three sampling depths (0 to 30 cm, 30 to 60 cm, and 60 to 90 cm) of fertilizer treatments (compost, triple superphosphate (TSP), and the combination compost + TSP ($n=3$)) as delta to the P stocks of the unfertilized control treatment (kg ha^{-1}). Long-term fertilizer experiment Rostock 108
- Figure D2 Averaged stocks of labile (sum of Resin-P, $\text{NaHCO}_3\text{-P}_i$, and $\text{NaHCO}_3\text{-P}_o$), moderately labile (sum of NaOH-P_i , NaOH-P_o), and stable P fractions (sum of $\text{H}_2\text{SO}_4\text{-P}$ and Residual-P) of the three sampling depths (0 to 30 cm, 30 to 60 cm, and 60 to 90 cm) of fertilizer treatments (manure, superphosphate (SP), and the combination manure + SP ($n=1$)) as delta to the P stocks of the unfertilized control treatment (kg ha^{-1}). Long-term fertilizer experiment Bad Lauchstädt (data analysis by Theresa Funk – Master Thesis FZJ 2018) 109

Figure D3 Inorganic P (P_i) to organic P (P_o) ratio, estimated from sequential P fractionation procedure in three sampling depths (0 to 30 cm, 30 to 60 cm, and 60 to 90 cm) of fertilizer treatments of a fertilizer experiment in Rostock (control (no P), compost, triple superphosphate (TSP), and the combination compost + TSP (n=3) and of a fertilizer experiment in Bad Lauchstädt (control (no P), manure, superphosphate (SP), and the combination manure + SP (n=1)).....	111
Figure D4 ^{31}P -NMR P stocks of orthophosphate (ortho-P), ortho-P monoesters and ortho-P diesters after NaOH-EDTA extraction of fertilizer treatments (compost, triple superphosphate (TSP), and the combination compost + TSP (n=3)) as delta to the NaOH-EDTA P stocks of the unfertilized control treatment (kg ha^{-1}). Long-term fertilizer experiment Rostock.....	112
Figure D5 ^{31}P -NMR P stocks of orthophosphate (ortho-P), ortho-P monoesters and ortho-P diesters after NaOH-EDTA extraction of fertilizer treatments of fertilizer treatments (manure, superphosphate (SP), and the combination manure + TSP (n=1)) as delta to the NaOH-EDTA P stocks of the unfertilized control treatment (kg ha^{-1}). Long-term fertilizer experiment Bad Lauchstädt (data analysis by Theresa Funk – Master Thesis FZJ 2018).....	113
Figure D6 Dry weights (DW) and ^{32}P proportions of selected plant compartments and agar nutrition medium after 18 days of growth. ^{32}P recovery was between 95% and 100% at the end of the experiment. Significant at * $p < 0.05$	115
Figure E1 Exemplified ^{33}P autoradiographic image of soil blended with (A) ^{33}P -Fe, (B) ^{33}P -Al, (C) ^{33}P -K, and (D) ^{33}P -solution.....	119
Figure E2 Exemplified ^{33}P autoradiographic image of a diffusive gradient in thin films (DGT) sheet applied for 48 h to soil blended with (A) ^{33}P -Fe, (B) ^{33}P -Al, (C) ^{33}P -K, and (D) ^{33}P -solution. Following the order, ^{33}P -solution ($3841 \pm 721^c \text{ Bq cm}^{-2}$) > ^{33}P -K ($1389 \pm 543^b \text{ Bq cm}^{-2}$) > ^{33}P -Fe ($84 \pm 22^a \text{ Bq cm}^{-2}$) = ^{33}P -Al ($53 \pm 54^a \text{ Bq cm}^{-2}$).	120
Figure F1 Digital autoradiographic images of ^{33}P labeled soil bands of a Ferralsol and a Luvisol with associated and ^{33}P radioisotopes (^{33}P Fe hydroxide, ^{33}P Al hydroxide, ^{33}P -SurplusP, and ^{33}P -NoP) in duplicates (two replicated chambers). The standard deviation (SD) \pm standard error of the mean bulk soil signature is displayed below the digital image.	125
Figure F2 Statistical analysis of blending homogeneities evaluated by the digital image data of the soil bands (with the treatments ^{33}P Fe hydroxide, ^{33}P Al hydroxide, ^{33}P -SurplusP, and ^{33}P -NoP). The analysis is separated into the number of high activity regions, the average size of high activity regions, and the percentage area covered by high activity regions as parameters for soil radiotracer blending homogeneity. Significant differences at 5% probability level between samples are designated by different letters.	126

LIST OF TABLES

Table II-1 Basic soil characteristics and elemental stocks of the soil samples of the four studied treatments (control, compost, TSP, and compost+TSP), and three sampling depths (0 to 30, 30 to 60, and 60 to 90 cm) with \pm standard deviation (SD).	21
Table II-2 Phosphorus (P) stocks of the sequential P fraction and total P (P_{tot}) stocks of the four studied treatments (control, compost, TSP, and compost+TSP) and three sampling depths (0-30, 30-60, and 60-90 cm) with \pm standard deviation (SD). Values in brackets represent the proportions of the P stock fractions (as 100%) in relation to P_{tot} and significances are designated to both, the stocks and the proportions of the sequential P fractions.	24
Table III-1 Soil characteristics of Ferralsol and Luvisol subsoil. Both subsoils were sampled below a soil depth of 50 cm, air-dried and 2mm sieved. Significant differences at 5% probability level between samples are designated by different small case letters.	42
Table III-2 Basic results of total shoot P concentration per plant, specific shoot P concentration, shoot ^{33}P activity, and specific shoot ^{33}P activity (at day 14 of growth). The radioactive-labeled ^{33}P treatments (^{33}P -Fe: ^{33}P associated to amorphous Fe hydroxide; ^{33}P -Al: ^{33}P associated to amorphous Al hydroxide; ^{33}P -OrthoP: ^{33}P applied in KH_2PO_4 solution; ^{33}P -NoP: carrier-free ^{33}P radiotracer) were banded in Ferralsol (n=3) and Luvisol (n=5) subsoil. The P concentrations were determined colorimetrically using the molybdate blue method. The ^{33}P activities were determined by liquid scintillation counting after acid digestion of plant material.	44
Table C1 Average leaf tissue thickness, leaf area, weight, and density of the excised leaves of maize and wheat plants.	103
Table D1 Basic soil characteristics and elemental stocks of the samples of the four studied treatments (control (no P additions), manure, superphosphate (SP), and manure + SP), and three sampling depths (0 to 30, 30 to 60, and 60 to 90 cm). Long-term fertilizer experiment Bad Lauchstädt (data analysis by Theresa Funk – Master Thesis FZJ 2018)	106
Table D2 Stocks of extractable P of the individual fractions determined by sequential fractionation (n=2) in kg ha^{-1} , extractability with respect to total P stocks (P_t), proportions of inorganic P (P_i) and organic P (P_o) in %, and the ratio of P_i and P_o stocks. The P stocks of the four fertilizer treatments, control (no P additions), manure, superphosphate (SP), and the combination with manure and SP within three soil depths (0 to 30, 30 to 60 and 60 to 90 cm) and the standard deviation are listed. Significant differences between the control and the treatments with fertilizer inputs are marked by * ($p < 0.5$). Long-term fertilizer experiment Bad Lauchstädt (data analysis by Theresa Funk – Master Thesis FZJ 2018)	107
Table D3 Phosphorus (P) speciation (% proportion of total P (P_t)) as obtained by linear combination fitting (LCF) on averaged (n= 3) P K-edge XANES spectra of two treatments (Control (no P additions) and Manure + Superphosphate (SP) from the long-term fertilizer treatments Bad Lauchstädt. All possible combinations with up to four standard components (total 12 standard components) were calculated comprising P associated with calcium species (Ca-P and Apatite), aluminum species (Al-P), iron species (Fe-P) and organic P species (here phytic acid). Best fit was chosen according to the lowest r-factor and fits were tested for significant differences using the Hamilton test ($p < 0.05$). Long-term fertilizer experiment Bad Lauchstädt (data analysis by Theresa Funk – Master Thesis FZJ 2018)	110
Table D4 Phosphorus loading levels on amorphous Fe and Al hydroxide surfaces. The weight proportions are shown after acid digestion of the P loaded hydroxides and subsequent inductively coupled plasma emission spectroscopy (ICP-OES) measurement. For acid digestion 50 mg replicate sample were dissolved in 3 mL HCl / 3 mL HNO_3 each and make up to 50 mL volume. For the ICP-OES element determination, two aliquots of each of the sample solutions obtained were diluted to 1 to 100.	114

LIST OF TABLES

Table D5 Photo and bioimager image of plant-aga system after 18 days of growth. P sources were provided as (1) P sorbed to amorphous iron oxide and (2) on to amoprhous aluminum oxide, both labeled with ³² P orthophosphate mixed in agar gel and implmented in sorounding agar gel with basal nutrition solution containing (a) 5 mM and (b) 0.2 mM of KH ₂ PO ₄	115
--	-----

LIST OF ABBREVIATIONS

Al	Aluminum
Al-P	Phosphate associated to aluminum (hydr)oxides
C	Carbon
Ca	Calcium
Ca-P	Phosphate associated to calcium minerals
DGT	diffusive gradients in thin films technique
Fe	Iron
Fe-P	Phosphate associated to iron (hydr)oxides
ICP-OES	Inductively coupled plasma – optical emission spectroscopy
IHP6	Inositol hexakisphosphate
K	Potassium
LCF	Linear combination fitting
LSC	Liquid scintillation counting
Mg	Magnesium
N	Nitrogen
NMR	Nuclear magnetic resonance (spectroscopy)
O	Oxygen
P	Phosphorus
P _{CAL}	Calcium-acetate-lactate extractable phosphorus
P _i	Inorganic phosphorus
P _o	Organic phosphorus
P _{ox}	Ammonium oxalate extractable phosphorus
P _{tot}	Total phosphorus
PSC	Phosphorus sorption capacity
DPS	Degree of phosphorus saturation
ortho-P	Orthophosphate
TSP	Triple superphosphate
SP	Superphosphate
³³ P	Radioisotope (P-33) of phosphorus
¹⁴ C	Radioisotope (C-14) of carbon

I

GENERAL INTRODUCTION

1 RATIONALE

In Germany, the arable land area covers about 52% of the land surface (Statistisches Bundesamt 2017). Most of this arable land is intensively used for food and renewable energy production. A continuing trend of agricultural land use intensification is expected and promotes issues of soil degradation and erosion as well as the loss of non-renewable resources, such as mineral fertilizers and biodiversity. Therefore, preservation of soil fertility along with the development of sustainable agricultural systems is obligatory to continuously produce sufficient food for the expanding human world population. Johnston and Poulton (2018) defined sustainable agricultural food production as a system that has to maintain yields without excessive price increases along with the prohibition of environmental contaminations and negative effects on habitats due to pollution mediated through the transfer of soil nutrients – mostly applied to soils by fertilizers – into water bodies.

Phosphorus (P) is one of the most indispensable nutrients to ensure plant vigor and development. Although required in lower quantities than other essential macronutrients (e.g., nitrogen (N) and potassium (K)), an insufficient P supply results in growth limitations from the very beginning of plant growth (Schachtman *et al.* 1998; Grant *et al.* 2005; Mengel *et al.* 2006). The dry matter of terrestrial plants contains about 0.2% P (Epstein 1972). It is taken up by the roots mainly as free, inorganic orthophosphate ions (PO_4^{3-} , in the following referred to as ortho-P) (Hinsinger 2001). In the living cell of higher plants P serves as a structural key component of phospholipids and nucleosides (e.g., the universal energy carrier adenosine triphosphate) as well as an essential constituent of nucleic acids, the carrier of genetic information of all living cells (Veneklaas *et al.* 2012).

In order to keep pace with the increasing demand for food and thus with plant productivity since the beginning of the last century, mineral P fertilizers were industrially produced from rock phosphate (sedimentary marine phosphorites) as basic raw material. The use of mineral P fertilizers has maintained soil fertility and high crop yields through adequate P supply according to crop requirements. Although, government authorities are observing a declining trend in the use of mineral P fertilizers (below 16 kg P ha⁻¹ in 2017, (LWK Nordrhein-Westfalen 2015, 2017), agricultural intensification is heavily dependent on the annual supply of mineral P fertilizers due to the decoupling of livestock production and arable farming. Moreover, the absence of adequate alternatives still ties the growing human world population on the continued use of mineral fertilizers for food production (Smil 2000; Dawson and Hilton 2011; Rittmann *et al.* 2011).

The total global rock phosphate resources are estimated at more than 300,000 million tons, but mineral P fertilizers are expected to be a finite and non-renewable resource, with less than 23% of the deposits are technically minable to date (Jasinski 2018). Estimations for the longevity of the remaining P reserves vary between 50 and 300 years (Cordell and White 2011; Rosemarin *et al.* 2011). In addition, according to Heffer and Prud'homme (2017) global P fertilizer demand is predicted to grow on average by 1.5% per annum till 2022. Such an increase in fertilizer use carries the risk of scarcity of rock phosphate reserves (Vaccari 2009) and the exploration of new, more contaminated deposits leads to mineral P fertilizers laden with heavy metals such as cadmium and uranium (Kratz and Schnug 2006; Nziguheba and Smolders 2008; Roberts 2014). Furthermore, the unequal distribution of the known deposits among politically unstable countries harbors further uncertainties, e.g., with regard to long-term access to mineral P resources (Tiess 2010). The largest mineable rock phosphate deposits are geologically concentrated in North Africa (> 78% of known minable deposits) followed by the Middle East (6%), China (4%), and the United States (1.4%) (Jasinski 2018).

From an economic and ecological perspective, it is therefore imperative to develop new management approaches in order to make use of P fertilizers more efficient without jeopardizing yields (Kruse

et al. 2015). A sustainable P management must improve the efficiency of fertilizer uptake and to make better use of the advantages of soil-inherent P pools or suitable alternatives from renewable resources (e.g., Leinweber *et al.* 2019) which are not yet generally included into agricultural management strategies. In this context, the subsoil can account for up to 80% of the P supply to the crops (Kuhlmann and Baumgartel 1991; Kautz *et al.* 2012). Nevertheless, only few studies have addressed its exploration as a promising P reservoir for crop nutrition (e.g., Garz *et al.* 2000; McBeath *et al.* 2012; Barej *et al.* 2014; Bauke *et al.* 2017a). In a first step, it is therefore important to evaluate the potentially available P stocks as P nutrient reservoir. This also implies analyzing the chemical form of dominant soil P pools throughout the soil profile to understand their full potential for plant P supply, including their accessibility to plant roots.

2 STATE OF THE ART

2.1 Phosphorus availability in arable soils

Soils contain between 1,200 to 30,000 kg P ha⁻¹ (Stevenson and Cole 1999). The form of P present in soils is mainly determined by the soil parent material and changes systematically over time (Walker and Syers 1976). During pedogenesis, soil weathering and acidification mediate the dissolution of primary P minerals such as Ca-P minerals (predominantly apatite, Ca₅[(F,Cl,OH)(PO₄)₃]), which are the origin of endogenous soil P in native soils (Stevenson and Cole 1999). Due to strong sorption characteristics of soil P, soil constituents are decisive for P solubility and mediate abiotic soil P dynamics (sorption desorption and precipitation dissolution reactions) between P in soil solution and soil P pools with variable solubility. Hedley *et al.* (1982) and subsequently Negassa and Leinweber (2009) designated these P pools as moderately labile and stable or rather residual soil P forms. In fertilized arable soils, these pools mainly comprise inorganic P, which is complexed with Fe, Al, Ca, and silicate minerals predominantly in an oxidized state, also referred to as secondary soil minerals (Stevenson and Cole 1999). The solubility of soil oxides depends primarily on the pH value of the soil. In acid soils, the surface charge of these oxides is positive, which enables a strong binding of ortho-P (Hinsinger 2001). On the reactive and hydroxylated mineral surfaces, in the first instance, free P is bound via ligand exchange and mono- or bidentate complexes are formed (Goldberg and Sposito 1985; Torrent 1997; Fink *et al.* 2016). In the long term, slow diffusion reactions prevail, occluding P into the adsorbing materials, also referred to as “phosphorus aging” (Barrow 1987; Bünemann 2015; de Campos *et al.* 2016). Depending on the soil properties, these interactions (association and/or occultation reactions) favor strong P retentions in the soil (Walker and Syers, 1976; Gérard, 2016) and transform free P from a moderately labile binding to secondary minerals into stable, non-soluble compounds (Schwertmann and Taylor, 1989; Hinsinger, 2001). In neutral to alkaline soils, free P reacts predominantly with CaCO₃ to Ca-P precipitates (Ca-P species with increasing chemical stability over time) comprising mainly stable, primarily non-soluble P forms (Lindsay *et al.* 1989; Torrent 1997; Hinsinger 2001).

Both, ortho-P and organic P compounds serve as source of plant available P (Friesen and Blair 1988). The incorporation of dead organic material increases the organic P pool in the upper soil layers (Williams and Saunders 1956; Lal and Stewart 2016). In cultivated soils, they mainly comprise of ortho-P monoesters, which are the degradation products of complex organic compounds such as ortho-P diesters, phospholipids, phosphoproteins, and sugar phosphates (Condrón *et al.* 1990). In particular, phytic acid, known as inositol hexakisphosphate (IHP6), is a non-digestible (not bioavailable to ruminant animals) ortho-P monoester (Klopfenstein *et al.* 2002), which accounts for up to half of soil the organic P in fertilized arable soils (Turner *et al.* 2012). In principle, the recycling (mineralization and hydrolyzation) of degradable organic materials and thus of organic P is controlled by microbial

mediated processes (Bünemann, 2015), which release soluble P into soil solution (Oberson *et al.* 1993) and can be an important source of available P for plants (Hayes *et al.* 2000). For example, in a study conducted by Friesen and Blair (1988), P was found as soluble P_i after 11 days from plant residues applied to the soil. If it is not readily degradable, organic P can also be associated and complexed into stable compounds that form non-soluble, occluded, mainly residual P forms (Sattari *et al.* 2012). However, the potential relevance of organic soil P to build up soil P repositories (involvement in the formation of stable and residual P forms) and its role in maintaining acceptable level of P plant availability in soil (Oehl *et al.* 2002) is not well understood and needs further clarification.

The P uptake of plants in general is determined by ortho-P in soil solution (generally in the form of PO_4^{3-} , HPO_4^{2-} , or $H_2PO_4^-$ as pH dependent valences). The maximum plant availability of P is between pH 6 to 7.2 in the form of HPO_4^{2-} (Lindsay 1979). The concentration of P ions in soil solution ranges within the micro molar range between 0.1 and 10 μM (Frossard *et al.* 2000; Mengel *et al.* 2006), which is primarily determined by the soil pH value (Gustafsson *et al.* 2012). However, soil texture, soil moisture, ionic strength, and microbial activity also control the abundance of ortho-P in soil solution (Hinsinger 2001). Thus, in general, only a small proportion of P_i and P_o is dissolved at any time in soil solution (Bünemann *et al.* 2016). When it is depleted, i.e., due to plant uptake, P from moderately labile (but also stable and residual P fractions) replenish the P concentration in soil solution (Guo *et al.* 2000; Blake *et al.* 2003; Selles *et al.* 2011). Therefore, besides the above mentioned soil parameters, also the amount and the chemical form (i.e., molecular speciation/ degree of crystallinity) of soil secondary minerals are deterministic factors for the soil P buffering capacity to replenish P into solution (Yuan and Lavkulich 1994; Agbenin and Goladi 1997; Igwe *et al.* 2010) and hence for soil P availability in general.

Especially in fertilized arable soils, processes and factors (including plant-induced processes) determining the form in which P is present in the soil, are not fully understood (Hinsinger 2001; Gérard 2016; Weihrauch and Opp 2018). Results shown by Requejo and Eichler-Löbermann (2014) indicated that soil P availability is independent of the type of fertilizer applied in the long term, however, the chemical form of P residues in soil and how the different P pools are interlinked still remains unclear (Weihrauch and Opp 2018). For a more complete picture of the P status and to improve our understanding of the general P dynamics also the P speciation in fertilized soils need careful evaluation. Thus, **it is necessary to reveal the influence of P fertilizer application on the soil P status in the whole soil profile, including also the immobile (but potentially available) P species.**

2.2 Phosphorus forms in fertilized arable soils

Some soils have low P supply while others have excellent P status, particularly fertilized arable soils in Europe are well supplied (Tóth *et al.* 2014). Annual fertilizer recommendations, nowadays, correspond to the crop P requirements but in the past they exceeded crop needs (Sattari *et al.* 2012; Tóth *et al.* 2014), which often resulted in P surpluses (P input minus P output) over several decades (Selles *et al.* 1995; Requejo and Eichler-Löbermann 2014). The excessive applications of mineral P fertilizer in the past, of which approximately only half found its way into the harvested crop (Rittmann *et al.* 2011), led to strong accumulation of soil P (Sattari *et al.* 2012).

Selles *et al.* (1995); (2011) analyzed the effect of mineral fertilization on P availability and found that fertilizer P remaining in the soil (further referred to as residual fertilizer P) accumulated predominantly in plant available inorganic forms. For a more complete picture, Eriksson *et al.* (2016a); and Eriksson *et al.* (2016b) analyzed evolution and dynamics of P speciation in fertilized arable soils. They reported that the formation of poorly crystalline secondary Fe and Al hydroxides in the topsoil during pedogenesis as well as the presence of apatite in the subsoil are predominantly affecting P speciation within the soil profile. They found that fertilizer P is mainly retained by Al and Fe soil hydroxides

besides the formation of Ca-P and organic P complexes. The same P speciation patterns were found by Beauchemin *et al.* (2003), Kizewski *et al.* (2011), and Liu *et al.* (2014b). **However, all these study results were not related to the use of P fertilizer, leaving the question behind if the observed P forms were affected by the kind and the duration of fertilizer applied to the analyzed soils.**

Blake *et al.* (2000) analyzed P dynamics with regard to the use of P fertilizer of three long-term experiments in Europe. They found that the form in which fertilizer P is retained in the soil is affected by complex interrelations, which depend primarily on the soil type and the soil texture. With regard to the type of fertilizer applied, they stated that both mineral and organic fertilizer applications had an effect on the behavior of residual fertilizer P in the soil. They highlighted that P availability from manure applications exceeded that of applied mineral fertilizers. Hao *et al.* (2008) supported this finding, as their results indicated that organic fertilizers increased P levels in all soil P pools in the long-term; however, these results are not justified by better availabilities of the applied organic P forms in the soil. They found that the organic P forms accounted for less than 5% of total P in the soil profile after 30 (annual) manure applications, and thus most of the organic amendments applied were already mineralized after application and enriched, in particular, the inorganic soluble P pools. In four arable soils from Sweden, Ahlgren *et al.* (2013) found no apparent build-up of organic P, independent of the soil type. Hence, it seems reasonable that P originating from organic fertilizers rapidly transforms into inorganic soil P pools. Yet all these studies did not analyze the exact chemical form (speciation) the fertilizer P was applied in and transformed to arriving in the soil. However, this needs to be done in order to fully understand the effects of organic P fertilizers on soil P speciation and thus on soil P long-term availability in fertilized arable soils (Sattari *et al.* 2012).

To comprehensively understand the effects of fertilizer applications on soil P pools in the whole soil profiles of arable soils, it is important to **not only quantitatively investigate P availability but rather to qualitatively understand the interrelations of P fertilization, the effect on all soil P forms, and their contributions to plant P utilization also on the molecular scale.**

2.3 Subsoil phosphorus utilization

In the past, excessive applications of highly soluble mineral P fertilizer increased P levels of arable fields in Europe. The resulting soil P surplus subsequently depleted the sorption capacity of soil constituents (Pizzeghello *et al.* 2011), especially in the topsoils, and provoked P movements into deeper soil layers (Godlinski *et al.* 2004; Andersson *et al.* 2015; Rupp *et al.* 2018). This resulted in massive topsoil and subsoil P stocks up to several tons P per hectare (Rubæk *et al.* 2013). Current estimates indicated that subsoils in Europe hold 50 to 80% of the total P stock of a soil profile (Kautz *et al.* 2012; Barej *et al.* 2014). As one of the first researches Kuhlmann and Baumgartel (1991) reported the importance of subsoil P utilization (it can vary between 10 and 50%, in extreme cases even up to 80% of total plant P supply), if P supply from the topsoil was inadequate. Similarly, Oehl *et al.* (2002) studied P balances in arable soil profiles fertilized for more than 20 years and found an upward P movement, respectively P utilization from subsoil P repositories after decreasing available P concentration in the topsoil. Bauke *et al.* (2018) analyzed the oxygen isotope composition of soil P in soil profiles under varying long-term fertilizer applications and highlighted the requirement of sufficient topsoil nutrient availability. Moreover, they showed that topsoil N fertilization promoted subsoil root exploration and thus subsoil nutrient acquisition. These findings seem reasonable, as the topsoil serves young crop plants as the initial compartment of nutrient supply. However, the opposite was found by other scientists claiming that under nutrient depleted topsoil root growth is adapted by increasingly assessing the soil volume of the subsoil below the plough horizon (> 30 cm) (Lambers *et al.* 2006; Richardson *et al.* 2009). Other scientists analyzed highly weathered and claimed instead, that subsoil root growth is only promoted by subsoil fertilization (McLaren *et al.* 2013). Along these

findings scientists highlighted that beneficial physicochemical soil conditions and sufficient soil moisture are favorable for subsoil P accessibility. This seems reasonable as adequate growth conditions have to be established first to access a larger soil volume (Gliński and Lipiec 1990). A study conducted by McBeath *et al.* (2012) showed that the subsoil P access by plants was stimulated by topsoil P fertilization in combination with adequate soil water conditions. However, these general findings are not new, Blake *et al.* (2000) have already highlighted the importance of soil physicochemical properties, climate, and the chemical form of the applied P fertilizer on P availability of three well-known long-term fertilizer experiments, even if they did not related their findings to subsoil nutrition levels. **These sometimes contradictory findings reveal that knowledge on the accessibility and utilization of P from deeper, less-rooted soil regions is complex and raise the question, whether subsoil P pools can serve as an alternative for adequate crop P supply.**

Concluding, the vast majority of organic and inorganic P in top- as well as subsoils is obviously not used by microorganisms and plants, either because it is not readily released from stable chemical bonds (not bioavailable) or because it is not seen (not bioaccessible) (Kautz *et al.* 2012). The effect of soil order and related soil conditions (but also the soil P concentration in general) significantly affects the soil P speciation (Eriksson *et al.* 2015) and thus P availability under long-term fertilization. This implies that no general answer on subsoil P utilization can be given and shows that soil P dynamics in fertilized arable soil profiles under varying fertilization managements are still not well understood and thus require greater research efforts. **Further studies, have to include active plant growth in the soil to compare plant availability of specific P forms and related P plant uptake potentials over time** (Audette *et al.* 2016). Especially long-term fertilizer experiments offer a unique opportunity to fill this knowledge gap.

2.4 Why to study phosphorus dynamics in long-term agricultural experiments

Long-term agricultural experiments are suitable large-scale field experiments to study crop production, nutrient cycles and related impacts in a controlled environment (Rasmussen *et al.* 1998). Due to controlled long-term management, often in replicated field plots within a mostly but not always randomized design, long-term experiments are seen as the only practical way to assess management induced fertilizer effects on yields and their impact on soil P within the soil profile (Johnston and Poulton 2018). Therefore, they provide an indispensable source of knowledge for understanding and proving changes in soil fertility as a result of common agricultural practices (Debreczeni and Körschens 2003).

Rasmussen *et al.* (1998) have defined long-term agricultural experiments as experiments conducted for longer than 20 years, however, also shorter field experiments over several years can provide merits and need to receive sufficient attention because their maintenance, also in the early stages, is costly and work intensive (Körschens 2006). The best example for the beneficial capability to expand knowledge from long-term agricultural experiments is the oldest long-term experiment at the Rothamsted experimental site located in Harpenden, United Kingdom. Around 174 years ago, in 1844, well-known scientists such as Justus von Liebig have already discussed benefits of nutrient recycling which resulted in the foundation of Rothamsted (Debreczeni and Körschens 2003). Due to the long-term storage of input and output samples from this experiment it was shown that under appropriate agricultural management yields were maintained without fertilizer applications; however, they also found that yields were doubled due to intensive fertilizer usage (Rothamsted Research 2017). Similar observations were reported by (Edmeades 2003) reviewing results from 14 long-term experiments in which nutrient inputs had increased soil productivity, e.g., yields by 150 to 1000%.

General statements on fertilizer induced yield increases can be made by every farmer, but the knowledge on the fate and the effective P balance can only be assessed by monitoring experiments

year by year, which highlights the importance of long-term fertilizer experiments for future agricultural development.

2.5 Methodological approaches

2.5.1 Spectroscopic methods for phosphorus research

For plants to take up nutrients, it is essential that they are present in a specific chemical form, as it determines their bioavailability. In the scientific literature, there are many methods described that illuminate the bioavailability of P in soils (Kruse *et al.* 2015). In the early stages of P research the first approaches comprised of single wet-chemical extractions, conventionally applied to analyze the concentration of labile soil P (e.g., Riehm 1948; Olsen 1954). However, these methods aimed only on analyzing the proportion of soil P that is already dissolved or present in a labile and thus easily-extractable form and neglected the amount of P in more stable P forms (not readily extractable) that can possibly become available if the former is depleted. For a more comprehensive understanding of the dynamics of soil P pools, sequential extraction procedures are applied, including the evaluation of these dominant more stable P pools.

A widely applied sequential P fractionation scheme developed by Hedley *et al.* (1982) is conventionally used to characterize P pools in soils, soil amendments, and their effects on the P plant availability. The pools are determined by their mode of extraction, removing labile P fractions with milder reagents and more stable P fractions with reagents of increasing extraction strength (e.g., Blake *et al.* 2003; Kruse and Leinweber 2008; Siebers *et al.* 2013; Barej *et al.* 2014). With his approach Hedley *et al.* (1982) postulated the classification of P into soil fractions of soluble (labile) and non-soluble (stable and residual) inorganic and organic P pools. Nonetheless, in the past many reviews identified inconsistencies of sequentially extracted P fractions in terms of P fraction distinction and their relative bioavailability (e.g., Levy and Schlesinger 1999; Golterman 2002; Turner *et al.* 2005; Condrón and Newman 2011). Furthermore, attention has to be addressed to the “inaccuracy” of the underlying determination of organic P as the difference between total P and colorimetrically determined inorganic P (the latter is suffering insufficient measurement of total inorganic P, as only the ortho-P is measured which reacts with the color reagent) (Cade-Menun and Liu 2013). Therefore, wet chemical methods are well standardized and applicable to obtain an overview about P pools and their abundance in soils; however, they cannot measure the chemical speciation on the molecular level and thus are lacking of significant detailed insights.

As affected by the high complexity of even a single soil order, just a single method often will be insufficient to comprehensively characterize the broad range of inorganic and organic P forms in soils. The appealed shortcomings of wet-chemical extractions can be overcome with multi-methodological approaches to integrate and enhance the individual advantages of specific methods (Kruse *et al.* 2015). Highlighted by Negassa and Leinweber (2009) and Kizewski *et al.* (2011) spectroscopically techniques have to be applied simultaneously for a sophisticated characterization of the molecular chemical form of soil P, as every single method only provides unique information in dependence on matrix complexity.

X-ray absorption near edge structure (XANES) spectroscopy enables an element-specific and non-invasive direct P speciation in the solid phase. In brief, XANES spectroscopy is based on the absorption of high energetic X-ray photons by the photoelectric effect of matter and the measurement of its release afterwards. By reaching a specific binding energy of core electrons of a target atom a sharp increase in the absorption occurs, whereas further energy increases reduces the electron absorption again, which leads to an edge like structure in the absorption coefficient also called absorption edge. Thereby, the excited core electrons reach higher core levels, transferring the target atom in an unstable, excited state. By refilling the atomic core hole with electrons from higher energy levels characteristic fluorescence or Auger electrons (as the difference between the energy levels) are

emitted (Kruse *et al.* 2015). Finally, the oxidation state and the chemical environment of the target atom distinctively characterize the spectrum. Variations of the absorption coefficient of a solid sample as a function of the applied X-ray energy are therefore characteristic for specific P binding forms and can be identified by comparing with spectra of known P species.

Speciation of P in soil amendments like manure, mineral and organic P fertilizer (Sato *et al.* 2005; Toor *et al.* 2005), and the receiving arable soils (e.g., Beauchemin *et al.* 2003; Lombi *et al.* 2006; Ajiboye *et al.* 2008; Khatiwada *et al.* 2012; Liu *et al.* 2013b; Siebers *et al.* 2013; Eriksson *et al.* 2015) using P *K*-edge XANES is already well established. A combination of P *K*-edge XANES spectroscopy with sequential fractionation methods to analyze predominance of certain P species and their bioavailability in arable soils found strong correlations between Ca-P compounds and the HCl-extractable P as well as Fe and Al bound P species and the NaOH fraction of inorganic P determined by the sequential fractionation method (e.g., Beauchemin *et al.* 2003; YanHong *et al.* 2014).

These results clearly show the applicability of XANES spectroscopy and the benefits from a multiple-method approach for P research. However, like for every single method, there are also drawbacks, e.g., the need of relatively high sample P concentrations to obtain an acceptable signal to noise ratio, the limited number of samples that can be analyzed due to limited beam time at synchrotron facilities, and the inappropriate differentiation of organic P compounds (Kruse *et al.* 2015).

In contrast to P *K*-edge XANES spectroscopy solution ^{31}P liquid nuclear magnetic resonance spectroscopy (^{31}P -NMR) is better suited to differentiate especially organic P forms and has a wide scope of applications in P research (Leinweber *et al.* 1997; Amelung *et al.* 2001; Cade-Menun and Liu 2013). It enables structural elucidation and quantification of various classes of P species such as ortho-P, polyphosphate, pyrophosphates, phosphonates, as well as ortho-P mono- and diesters, and correlates them to bioavailability (Turner *et al.* 2003a; Richardson *et al.* 2007; Ahlgren *et al.* 2013). The physical basis of NMR spectroscopy is based on nuclear magnetism. The interaction of the magnetic core moments of a substance with an applied magnetic field leads to nuclear energy pattern, as each nucleus can only exist in its own energy states (Günther 1992). Magnetic moments are often observed in isotopes having an atomic spin quantum of one-half (odd-numbered protons or neutrons). By repeatedly applying a high frequent magnetic field, the magnetic moment excites the atomic nuclei from its basic state and after the magnetic field is removed it relaxes back to its initial state. The specific resonance energy emitted during this process results in different chemical shifts which are affected by the chemical environment of the nuclei. To be able to obtain reproducible signal patterns, the resonance frequency is expressed relative to a standard, generating the so called chemical shift (in ppm) in the same spectra, which allows interpretation of the chemical constitution of nuclei present in the sample as a function of electron density surrounding the respective nuclei (Gorenstein 2012; Wilson 2013). Thus, detailed information of the electronic structure on the monomolecular level and the attached functional groups can be elucidated.

Phosphorus contains one stable isotope, namely ^{31}P and this is half integer. This 100% isotopic abundance makes ^{31}P -NMR highly P sensitive and enables easy interpretation of the spectra. However, there are also shortcomings of this technique for soil P research. For example, the soil sample needs to be in liquid form and thus require a preparation step of systematic extraction of P from the solid phase, which may degrade instable organic P forms. Furthermore, insufficient P concentrations (especially in deeper soil layers) and the co-extraction of paramagnetic ions, such as Fe and Mn, accelerate spectral line broadening, which impairs the spectral resolution (Cade-Menun 2005). The advantages and disadvantages of different soil extraction procedures for ^{31}P -NMR research are summarized in a review by Cade-Menun and Liu (2013). Despite these disadvantageous impairments arising from sample preparation, no alternative for organic P speciation exists and many scientists successively applied ^{31}P -NMR analyzing organic soil P species and pools. As one of the first Newman and Tate (1980) applied NMR spectroscopy to analyze organic P forms in arable topsoils of New Zealand and

found that inorganic ortho-P and ortho-P monoesters were predominant in their soil extracts. Due to great scientific effort these days, the chemical shifts of mainly all predominant organic soil P compounds are characterized (e.g., Turner *et al.* 2003b; Turner and Richardson 2004; Turner *et al.* 2012; Cade-Menun 2014). Even if ^{31}P -NMR was applied to analyze the composition of organic P in organic fertilizers such as manure (Turner and Leytem 2004; Kruse *et al.* 2010), only a few ^{31}P -NMR studies aimed to characterize the composition of the organic P pool (Soinne *et al.* 2011) or specific organic P forms in terms of their potential plant availability (Gatiboni *et al.* 2005) in arable fertilized soils, which resulted in the limited understanding of fertilizer introduced interrelations.

Thus, to improve our understanding of processes and factors for sufficient plant P supply from predominant soil P forms, the application of the techniques presented here is urgently needed to first comprehensively elucidate soil P chemical composition and their dynamics induced by fertilizer use. However, the current knowledge-gap on plant soil P acquisition potentials from the whole soil profile can only be overcome if we apply complementary techniques that are able to track down the plant P uptake (plant availability and accessibility) from the previously identified dominant P forms in the plant-soil system of arable soils.

2.5.2 Radioisotope techniques to study phosphorus cycling in the soil-plant system

In general, isotopes are defined by a varied atomic mass (corresponding to the total number of protons and neutrons) in the nucleus of elements which change atomic weights but leave the nuclear charge, the atomic number, and hence the chemical identity unchanged. With varying abundances, elements commonly contain several isotopes of which certain undergo spontaneous disintegrations along the emission of atomic particles (this process is called radiation) (Comar 1955; L'annunziata 1979; Wahid 2001). Such unstable isotopes are called radioisotopes. Phosphorus contains, besides its stable and naturally occurring ^{31}P isotope, two radioisotopes, which are considered as radiotracers for P in a great variety of scientific applications.

Especially for studies on plant-soil interactions the exact and quantitative monitoring of, e.g., the uptake of radioisotopes by the plant enables the determination of its contribution to plant nutrition. Therefore, for studies on the utilization of specific soil P forms by plants, the use of the P radioisotopes ^{33}P or ^{32}P has increased in recent years. Limitations for their use only arise from the short half-life of both radioisotopes, being 25.3 (^{33}P) and 14.3 (^{32}P) days. Nevertheless, Fardeau *et al.* (1995) suggested that experiments with ^{33}P might last at maximum for three to eight months, which is sufficient, e.g., for quantifying P availability and dynamics in soils across a vegetation season of most crops, measuring root activity, testing the efficiency of P fertilizers, and following the decomposition of plant materials (e.g., Wahid 2001; Hedley and McLaughlin 2005).

Radioactive-labeling of fertilizers, soil constituents or residual plant materials, which were added to soils, bears great advantages to determine the uptake from different P sources by microorganisms (McLaughlin *et al.* 1988b) and by plants (e.g., Friesen and Blair 1988; McLaughlin *et al.* 1988a; McLaren *et al.* 2016), or to quantify how the availability of different P fractions declined over the course of incubations followed by sequential extraction procedures (e.g., Daroub *et al.* 2000; Bühler *et al.* 2002; Bühler *et al.* 2003). Most of the radioisotopic techniques applied in the above mentioned studies are well summarized by Di *et al.* (1997). However, they did not include a technical approach that enables the spatial visualization of radiation emitted from a radioactive source or tissues containing radioisotopes.

Digital autoradiography systems were developed for the visualization of conventional radioactive β -emitters (e.g., Amemiya and Miyahara 1988; Johnston *et al.* 1990; Nakajima 1993), and have their infancies in medical studies in the early 1980ies in so called “whole body autoradiography studies” for

drug metabolism analysis and direct analyses of radio thin-layer chromatography. The general principles, as well as the advantages and disadvantages, of digital autoradiography are summarized by Johnston *et al.* (1990); and Upham and Englert (2003). In P research only a few studies utilized digital autoradiography to spatially-visualize or to semi-quantitative measure P amounts and P dynamics in plant leaves (Hüve *et al.* 2007; Anil Kumar *et al.* 2009), plant roots (Rubio *et al.* 2004), arbuscular mycorrhizas (Nielsen *et al.* 2002) and soils (Lewis and Quirk 1967; Bhat and Nye 1973).

However, none of these studies were able to successfully quantify P radioisotope concentrations in the mentioned compartments, as it is common practice in medical digital autoradiography applications (e.g., Eakin *et al.* 1994; Coe 2000; Cremer *et al.* 2009). A quantitative and spatially resolved analysis of, e.g., ^{33}P uptake in plants but also the mobility of sorbed P in soils is urgently required for P research, as the commonly applied quantitative estimation procedure of liquid scintillation counting after acid digestion or extraction is time consuming and cost intensive. In particular the possibility of a spatially resolved and non-destructive quantification of P radiotracers, e.g., in different compartments and repeatedly of the same sample can be seen as the biggest achievement of such a method, as it allows also time-resolved evaluation of soil P utilization. Hence, **quantitative estimations of P uptake in plants using digital autoradiography may be the next step to better understand the accessibility of soil P for plant nutrition and will enable also to visualize soil P distribution in less-rooted soil zones.** As science calls for a technique precisely quantifying the plant available P fraction in soils that is inexpensive and easily to apply to a great number of samples, an approach using digital autoradiography may be able to accomplish this.

3 OBJECTIVES

To shed light on the specific P status of fertilized arable soil profiles, the following study addresses the availability (quantity and speciation) of P forms in fertilized soil profiles of a long-term fertilizer experiments located in Rostock and Bad Lauchstädt under inorganic and organic fertilizer management. After identifying the predominant subsoil P forms, the plant accessibility of ^{33}P associated to amorphous Fe and Al oxidic subsoil phases to wheat plants will be evaluated. The use of liquid scintillation counting of radioisotope activities enabled the quantification of utilized ^{33}P in the plant shoots. Special emphasis was given to a method development that refines quantification of ^{33}P uptake and thus advances P research through a spatially and temporally resolved quantitative digital autoradiography imaging method.

Based on these research highlights, I addressed the following research questions:

i) **How are P stocks and P speciation in arable soil profiles affected by long-term application of organic and inorganic P fertilizers?**

Along the agricultural intensification at the beginning of the last century, especially in Europe, most of the arable fertilized soils were supplied with mineral P fertilizers. The fertilizer dose often exceeded the crop P needs which subsequently affected P stocks in the whole soil profile. Therefore, I investigated soil P dynamics, including P stocks and the P speciation under long-term inorganic and organic P fertilization in whole soil profiles by applying an advantageous range of specific methods of soil P research.

ii) **Can P from oxidic (sub)soil P forms sufficiently contribute to plants soil P demand?**

Fertilized arable soils often exhibit great proportions of mainly inorganic, moderately labile P species, consisting of mainly Fe- and Al-P species. I questioned if and to which degree these P

forms can supply the crops P demand? Therefore, I supplied two different subsoils of two different soil orders with ^{33}P labelled Fe and Al hydroxides and let young wheat plants grow in these soils. Afterwards I accounted the proportions of ^{33}P translocated into the plant tissues.

iii) Is digital autoradiography an efficient, non-destructive, and spatially resolved method for ^{33}P radioisotope quantification in plant leaves?

Quantitative approaches of digital autoradiography were successively applied to estimate in situ hybridization of rare mRNAs and for other mainly medical purposes. However, what has worked in the laboratory at the small scale may also be applicable for estimating ^{33}P activities in plant leaves or whole plants after radioisotope uptake or translocation. Therefore, I developed a ^{33}P quantification method using digital autoradiography. Thereby, the co-application of ^{14}C polymer references to ^{33}P -labeled plant leaves bears the possibility for a spatially resolved quantification of the ^{33}P radioactivity.

II

PHOSPHORUS STOCKS AND SPECIATION IN SOIL PROFILES OF A LONG-TERM FERTILIZER EXPERIMENT: EVIDENCE FROM SEQUENTIAL FRACTIONATION, P *K*-EDGE XANES, AND ^{31}P -NMR SPECTROSCOPY

Modified on the basis of the manuscript

Koch, M.; Kruse, J.; Eichler-Löbermann, B.; Zimmer, D.; Willbold, S.; Leinweber, P.; Siebers, N., Phosphorus stocks and speciation in soil profiles of a long-term fertilizer experiment: Evidence from sequential fractionation, P *K*-edge XANES, and ^{31}P -NMR spectroscopy. *Geoderma* 2018, 316, 115-126.

1 INTRODUCTION

Phosphorus (P) plays a key role in agricultural productivity (Cordell *et al.* 2009), and seems to be a future constraint in agricultural systems (Gilbert 2009). The arising uncertainties and ongoing discussions about unevenly distributed, and above all finite P rock reserves are summarized by Baveye (2015). For future agriculture, a more sufficient (not more than required) and efficient (higher yields per P applied) use of P is necessary whereas also alternative ways of P supply must be developed (Kruse *et al.* 2015). In this respect, the unexploited subsoil P reserves deserve special attention. Actual P stocks in soil profiles vary between 1200 to 30000 kg P ha⁻¹ (Stevenson and Cole 1999), and in particular European agricultural important soils seem to have an high P supply due to high and excessive P fertilizer applications in the past (Smil 2002; Tunney *et al.* 2003; Sattari *et al.* 2012; Tóth *et al.* 2014).

So far the fate of surplus fertilizer P in soil is not known for all important agricultural soils in central and northern Europe. It is well established that some of the surplus P ends up in aquatic systems (Smith and Schindler 2009) but processes of intermediate binding and remobilization in soil profiles, depending on different fertilization strategies are far from being understood. Fertilizer P is mainly associated to silicate clay minerals, Fe and Al (hydro)oxides, Ca carbonates, humic substances, or in the soil biomass shortly after application (e.g., Sattari *et al.* 2012; Tóth *et al.* 2014; Kruse *et al.* 2015; Eriksson *et al.* 2016b).

Various studies investigated and compared the effects of organic and inorganic P fertilization on the P status and P availability in soils (Fuentes *et al.* 2008). A few studies indicated that the kind of fertilizer application had no effect on P speciation (e.g., Friesen and Blair 1988; Wang *et al.* 2007; Requejo and Eichler-Löbermann 2014) whereas others found that the application of organic P (P_o) fertilizers (such as compost or manure), compared to mineral P fertilizers, improved the P utilization in soils (e.g., Hue *et al.* 1994; Bah *et al.* 2006; Pizzeghello *et al.* 2011; Yan *et al.* 2013). Although many studies delivered valuable insights to P fertilizer effects in the topsoils, they totally omitted the subsoil, the soil below the plough horizon (> 30 cm). Beside the P rich agricultural topsoils, also the subsoils hold immense P reserves, which account for 25% up to 70% of total P (P_{tot}) in the soil profile (Godlinski *et al.* 2004; Kautz *et al.* 2012; Barej *et al.* 2014). Current estimates indicated that the plants acquire 10 to 50% (Kautz *et al.* 2012), in extreme cases even up to 80% of their P_{tot} supply from the subsoil when the topsoil P supply is decreased (Kuhlmann and Baumgartel 1991). However, Kautz *et al.* (2012) summarized that only rare and divisive information about plant accessible and plant available subsoil P exist because its distribution and speciation were not yet assessed widely. Disclosing the role of subsoil as P reservoir for crop requires detailed elucidation of chemical speciation of abundant soil P components by state-of-the art methods (Liu *et al.* 2013b; Kruse *et al.* 2015).

The commonly applied sequential P fractionation approach developed by Hedley *et al.* (1982) is used to differentiate labile, moderately labile, and stable organic and inorganic P fractions in soils (e.g., Bühler *et al.* 2002; Kruse *et al.* 2010; Alamgir and Marschner 2013; Siebers *et al.* 2013). Limitations arise from inconsistencies about carryover or neutralization reactions between the successive P fractionation steps as well as the nature and quality of the Residual-P, which massively depends on the previous extraction steps as critically discussed by Condon and Newman (2011). Therefore, complementary spectroscopic techniques are applied to obtain an overview about the P speciation in environmental samples. Phosphorus K-edge X-ray absorption near edge structure (XANES) spectroscopy is an element-specific and non-invasive direct P speciation method for identifying P species in complex soil matrices (e.g., Ajiboye *et al.* 2008; Eriksson *et al.* 2015; Kruse *et al.* 2015). Solution ³¹P liquid nuclear magnetic resonance (³¹P-NMR) spectroscopy, first applied to soil research by Newman and Tate (1980), enables the identification and speciation of P_o classes such as ortho-P

monoesters and diesters (Turner *et al.* 2005; Doolette and Smernik 2011; Ahlgren *et al.* 2013). However, this method is unsuitable for identification of inorganic P (P_i) species associated with soil particles and requires an extraction step before analysis, which can alter the sample probe (Cade-Menun and Liu 2013).

Complementary studies with the above mentioned techniques facilitate a substantiated characterization of P speciation and precise quantification of predominant P species in agriculturally used soils on the molecular scale (e.g., Kizewski *et al.* 2011; Liu *et al.* 2014a; Kruse *et al.* 2015). Such an approach has been firstly applied in a study by Liu *et al.* (2013b), but have not yet been applied for the investigation of fertilizer effects on the P status in whole soil profiles of long-term fertilizer experiments.

Therefore we would like to answer the following research questions in the present study: What is the difference between the P stocks and the P speciation of the topsoil (0 to 30 cm) and the underlying subsoil (30 to 60 cm, and 60 to 90 cm)? Which impact has long-term application of different P fertilizers on the P stocks and P speciation in the topsoil compared to the subsoil? Is there a P reservoir in the subsoil, which can be utilized by the plants? Therefore, our objectives were to (i) estimate if different long-term P fertilizer applications altered the soil P stocks within the soil profile, (ii) to evaluate the P dynamics and differences in P speciation under different P fertilizer treatments, and (iii) to evaluate whether subsoil P stocks accumulated from long-term fertilizer applications can contribute to an efficient and sufficient P plant supply. Consequently, the availability of predominant inorganic and organic P species in top- and subsoils up to 90 cm depths from a long-term fertilizer experiment were studied and related to the potential use efficiency of plants. We hypothesize that fertilizer P inputs sustained or increased P distributions in the whole soil profile and with that also the speciation of soil P affecting P bioavailability.

2 MATERIAL AND METHODS

2.1 Soil sampling and basic soil characteristics

Soil samples were collected from an agricultural long-term experimental site (54° 3' 41.47'' N; 12° 5' 5.59'' E) at the University of Rostock, Germany, which was established in 1998. The soil is classified as a non-calcareous soil, predominantly a Stagnic Cambisol according to the World Reference Base for Soil Resources (IUSS Working Group WRB 2015). A full description of the experimental design and soil characteristics were published by Requejo and Eichler-Löbermann (2014). For the present study soil samples were taken at the end of April 2015 from four different fertilization treatments: control with no P fertilization, compost (in total 378 kg ha⁻¹ P within 16 years; mainly green waste from a composting plant near Rostock), triple superphosphate (TSP) (in total 393 kg ha⁻¹ P within 16 years), and a combination of compost and TSP (compost+TSP) (in total 771 kg ha⁻¹ P within 16 years). Fertilization with compost was triennial at a level of 69 kg P ha⁻¹, while TSP was applied annually. The N:P ratio in the compost was between 3 and 5.6 from the start of the experiment in 1998 till the last triennial fertilizer application in 2016. To avoid soil nutrient imbalances, soil N was monitored by mineral N measurements and if needed an additional mineral fertilizer application was performed. Application concentrations were according to the plant need under consideration of the mineral N concentration in soil in spring (before the vegetation period). However, the differences between mineral N concentrations in soil between the treatment were low (Table II-1). Maize was grown at the various plots before and after soil sampling. For each treatment three replicate plots were sampled. At each replicate plot, soil samples were taken at three randomly selected spots and three depths, namely 0 to 30 cm (topsoil), 30 to 60 cm (subsoil1), and 60 to 90 cm (subsoil2) using an auger with 4 cm

diameter. Afterwards, samples from the same depth interval of each plot were compiled into a homogenous composite sample. The bulk densities of the samples were calculated for each depth by multiplying soil dry weights (g) after drying at 105 °C and the auger volumes (cm³) at certain sampling depths with a factor of 0.01.

The soil samples were air-dried and ground to pass through a 2 mm sieve. Soil texture was determined after chemical disaggregation (H₂O₂, Na₄P₂O₇) by wet sieving (2 to 0.063 mm) and automated sedimentation analyses (Sedimat 4-12, UGT GmbH, Müncheberg, Germany) according to Köhn (DIN ISO 11277) (< 63µm to 2µm silt, < 2µm clay). Soil pH (0.01 M CaCl₂) was measured according to Godlinski *et al.* (2004). Soil C and N analyses were done using dry combustion followed by heat conductivity detection of the released trace gases (vario MICRO cube, Elementar, Hanau, Germany). Total elemental concentrations of P from bulk soil (P_{tot}), iron (Fe_{tot}), aluminum (Al_{tot}), manganese (Mn_{tot}), magnesium (Mg_{tot}), potassium (K_{tot}), calcium (Ca_{tot}), and sodium (Na_{tot}) were determined after microwave-assisted digestion of 150 mg with 0.7 mL HNO₃ and 2 mL HCl using an inductively coupled plasma-optical emission spectroscopy (ICP-OES; Thermo Fisher iCAP™ 7600). Total elemental stocks were calculated for every sampling depth with the certain bulk density. Ammonium oxalate extractable phosphorus (P_{ox}), aluminum (Al_{ox}), iron (Fe_{ox}), and manganese (Mn_{ox}) were determined by extraction with 0.2 M ammonium oxalate and 0.2 M oxalic acid (pH 3.1) for 2 h in the dark (Schwertmann 1964) and elemental analysis by ICP-OES. The P sorption capacity (PSC) and the degree of P saturation (DPS) were calculated according to Eckhardt and Leinweber (1997). The total concentration of organic P (P_{o,tot}) was estimated by subtraction of the total concentration of inorganic P (P_{i,tot}) from P_{tot}.

2.2 Sequential phosphorus fractionation

A slightly modified sequential fractionation method according to Hedley *et al.* (1982), Tiessen *et al.* (1984) and Tiessen and Moir (2008) was used to extract different P fractions from soil. In short, 0.5 g soil was weighed into 50 mL centrifuge tubes and 30 mL of double distilled water was added. Samples were shaken at 22 rpm for 18 h followed by centrifugation at 10000 g for 30 min, and decanted. Subsequent extractions were performed with: (1) resin (2), 0.5 M NaHCO₃, (3) 0.1 M NaOH, and (4) 1 M H₂SO₄. The residues after each extraction step were washed with deionized water to completely remove the extractant before the next fractionation step. The P fractions were interpreted as suggested by Hedley *et al.* (1982); resin P (Resin-P) representing the easily exchangeable and soil solution P, inorganic (NaHCO₃-P_i) and organic (NaHCO₃-P_o) bicarbonate P representing labile (adsorbed) inorganic and organic P as well as microbial P, inorganic (NaOH-P_i) and organic P (NaOH-P_o) hydroxide representing moderately labile inorganic and organic P sorbed and/or fixed by aluminum- and iron (hydr)oxide (accessory minerals) and P in humic and fulvic acids potentially bioavailable. The H₂SO₄-P fractions represent insoluble (stable) P associated with Ca and Mg minerals being in occluded or non-occluded forms (Walker and Syers 1976; Hedley *et al.* 1982; Tiessen and Moir 1993; Torrent 1997; Guo *et al.* 2000; YanHong *et al.* 2014). The P_i concentration in the extracts was determined colorimetrically using the molybdate blue method as described by (Ohlinger 1996) using a UV-Spectrometer (Vario EL, Elementar Analysensysteme, Hanau, Germany). Total P in the extracts was measured using an inductively coupled plasma-optical emission spectroscopy (ICP-OES; Thermo Fisher iCAP™ 7600) and the concentration of P_o was estimated by subtracting P_i from P_{tot}. The concentration of not extractable P (Residual-P) was calculated as the difference between the sum of the P fractions and the P_{tot} concentration of the samples.

2.3 Phosphorus K-edge XANES spectroscopy

To achieve a sufficient signal to noise ratio in spectra of the low P subsoil samples, we relatively enriched P by isolating the < 20 μm size fraction because most P is concentrated in clay to medium silt (Leinweber *et al.* 1997). In this way we achieved a P_{tot} -enrichment by a factor of 4 to 5 than in the bulk soil samples. Spectra were collected at the Soft X-ray Microcharacterization Beamline (SXRMB) at Canadian Light Source (CLS), Saskatoon, Canada. The air-dried and homogenized samples were spread as thin film onto a double-sided carbon (C) tape and mounted onto a copper sample holder before being placed in the vacuum chamber. The spectra were recorded in fluorescence yield mode (samples) and total electron yield mode (reference standards), respectively, at photon energies between 2130 and 2200 eV (Fig. A1). For each sample at least two scans were recorded. Subsequent data treatment and evaluation such as spectra averaging, background correction and normalization as well as linear combination fitting (LCF) were done using the ATHENA software package (Demeter 0.9.20) (Ravel and Newville 2005).

Linear combination fitting was performed on averaged, normalized spectra in the energy range between -10 and +31 eV, relative to the E_0 . Fitting was done for all possible binary to quaternary combinations of the 12 most probable P reference standards in the sample: CaHPO_4 , $\text{CaHPO}_4 \cdot 2\text{H}_2\text{O}$, $\text{Ca}(\text{H}_2\text{PO}_4)_2 \cdot \text{H}_2\text{O}$, $\text{Ca}_{10}(\text{PO}_4)_6(\text{OH})_2$, AlPO_4 , $\text{FePO}_4 \cdot 4\text{H}_2\text{O}$, P adsorbed on gibbsite, P adsorbed on iron goethite, $\text{Mg}_3(\text{PO}_4)_2 \cdot 8\text{H}_2\text{O}$, $\text{Mg}_2\text{O}_7\text{P}_2$, $\text{MgHPO}_4 \cdot 3\text{H}_2\text{O}$, and $(\text{C}_6\text{H}_{18}\text{O}_{24}\text{P}_6 \cdot \text{Na} \cdot y\text{H}_2\text{O})$ = phytic acid sodium salt hydrate). The R-factor values were used as goodness-of-fit criteria and their significance between fits was evaluated using the Hamilton test ($p < 0.05$) (Calvin 2013) with the number of independent data points calculated by Athena, estimated as data range divided by core-hole lifetime broadening. If by adding a further reference compound to a fit the r-factor was not significantly better according to the Hamilton test, the fit with a lower number of reference compounds was chosen. If fits with the same number of reference compounds were not significantly different from each other, fit proportions were averaged.

2.4 Solution ^{31}P -NMR spectroscopy

The NMR samples were prepared as follows: 5 g of air-dried and sieved (2 mm) soil from composite samples from the three replicates per treatment were shaken for 16 h at 20 °C with a 1:20 solution of 0.25 M NaOH and 0.05 M EDTA (Cade-Menun and Liu 2013). The extracts were deep-frozen at -18 °C and lyophilized to dryness with a Christ BETA 1-8 LD plus freeze dryer. For ^{31}P -NMR analyses 500 mg of the lyophilized samples were re-dissolved in 1.5 mL 1 M NaOH and 0.1 M EDTA solution and 250 μL deuterated water (D_2O) were added for frequency-field lock. The standard compound methylendioxypropylamphetamine (MDPA) was added as external standard, for controlling the measurement conditions. After vortexing for 1 min, an additional centrifugation step (14000 g for 10 min) followed to separate fine particles caused by NaOH-EDTA re-dissolving (recommended by Cade-Menun and Liu (2013)). For estimating the extraction efficiency, several pellets of fine particles were analyzed by microwave assisted digestion as described above (results are not shown).

The NMR spectra were recorded on a Bruker 600 Advance NMR-Spectrometer operating at 242.95 MHz. The spectra were recorded in 5 mm NMR tubes at 20 °C using a 30° pulse with 32 K data points over an acquisition time of 0.7 s, and a pulse delay of 0.5 s. Chemical shifts were analyzed using MestreNova 7. The organic P resonances were identified by their chemical shift deviation related to the dominant ortho-P peak at 5.5 to 5.6 ppm, as recommended by Cade-Menun (2014). To assign the measured resonances in the orthophosphate monoester region, spiking experiments were performed (Fig. A2), and among others the resonances of the ubiquitous *myo*-inositol hexakisphosphate (*myo*-IHP6) were confirmed. The signal ratio resulted in a pattern of 1:2:2:1, which was previously reported by Turner *et al.* (2012).

Spiking experiments were also conducted to test for diester hydrolysis. In our NMR spectra diesters were not present, which is typical for an agricultural soil (Cade-Menun, 2005). However, we were aware that small quantities of ortho-P diesters could be hydrolyzed to monoesters during extraction times for NMR analysis. In order to assure that results are not significantly biased by hydrolysis, literature recommends spiking experiments to identify the common known diester hydrolysis products such as α - and β -glycerophosphate (Cade-Menun and Liu, 2013; Cade-Menun, 2014). For this reason we ran spiking experiments (α - and β -glycerophosphate, Sigma Aldrich) with the topsoil sample of the TSP treatment (Fig. A2), as from this treatment sufficient amounts of lyophilization product were left which enabled to run multiple NMR measurements. The resonances of α -glycerophosphate were present in the spectra between 4.4 and 4.3 ppm (Fig. A2), yet the signal was very weak and we had to assume that the standard was degraded. Nevertheless, the β -glycerophosphate signal was distinct (Fig. A2) and we obtained proportions for α - and β -glycerophosphate between 0 and 2.8%. However, it still remains unclear, if these small quantities of diester hydrolysis products formed during processing or were present in the soil before. Therefore, effects of hydrolyses on proportions of diesters and monoesters were neglected. By comparing the chemical shifts reported in literature, it was possible to identify additional resonances of the stereoisomers *neo*-, *scyllo*-, and *D-chiro*-IHP6 (Turner *et al.* 2005; Turner *et al.* 2012), in the following summarized as ortho-P monoesters. The P_i/P_o ratios were calculated by the sum of area integrals of the signals in the ortho-P and pyrophosphate region divided by the sum of area integrals of signals in the ortho-P monoester regions.

2.5 Statistical analyses

Statistical analyses were carried out with Sigmaplot 13.0. For testing significant effects, a two-factor, two-way analysis of variance (ANOVA) was used combined with a Tukey multiple comparison test over all treatments and depths. Mean values are listed with (\pm) the standard deviation (SD).

3 RESULTS

3.1 Soil characteristics

The bulk density was higher in subsoil2 than in subsoil1 and the topsoil (Table II-1), but differences were not significant. The soil pH_{CaCl_2} of all treatments and sampling depths was between 5.5 and 6.0. Only the subsoil2 of the compost+TSP treatment had significantly higher pH values than the same sampling depth of the control and the TSP treatment (Table II-1). The C/N ratios averaged between 9.0 ± 0.2 , 9.9 ± 0.2 , and 8.6 ± 0.8 in the topsoil, subsoil1, and subsoil2 across all treatments, respectively. Yet only subsoil2 of the control showed a significantly lower C/N ratio than in subsoil1. In general, the C and N stocks in the topsoils of all treatments significantly exceeded those at the other two depths but subsoil1 and subsoil2 were mostly not significantly different. Only in the compost treatment the C and N stocks significantly decreased with depths (Table II-1).

Among treatments the C and N stocks in the topsoil of the compost+TSP treatment were significantly larger (C: by a factor of 1.5, N: by a factor of 1.4) than in the control (Table II-1). In this treatment, the Fe_{tot} , Al_{tot} , and Mn_{tot} stocks in the topsoil were significantly lower than in the subsoil2. No further significant differences between the sampling depths of treatments were obvious. The P_{tot} stocks varied greatly between the sampling depths with generally lower P_{tot} stocks in the subsoils (Table II-1). Among the treatments only the P_{tot} stock of the compost+TSP treatment in subsoil2 was significantly higher compared to the same depths of the control (Table II-1). The highest topsoil P_{tot} stocks were found in the compost treatment, which exceeded that of the control by a factor of 1.4. Yet the P_{tot} stock of the compost treatment decreased the most in subsoil2. The combined P_{tot} stocks of both subsoils

(sum of subsoil1 and 2) of the compost+TSP treatment exceeded the control by a factor of 1.5 and by 1.3 times in the single compost and TSP treatments, respectively. The proportions of the subsoil P_{tot} stocks (sum of subsoil1 and 2) related to P_{tot} stock of the complete soil profile (sum of all sampling depths) were $51\pm9\%$ (control), $48\pm9\%$ (compost), $53\pm5\%$ (TSP), and $54\pm5\%$ (compost+TSP).

Across all treatments the P_{ox} stocks were significantly larger in the topsoils than in subsoil2, whereas the treatments with TSP had significantly larger topsoil P_{ox} stocks than in both subsoil depths (Table II-1). In contrast, the Fe_{ox} and Al_{ox} stocks showed no significant differences among the sampling depths and treatments. Based on the Fe_{ox} , Al_{ox} , and Mn_{ox} we estimated average PSC stocks of $90\pm3.5 \text{ mol ha}^{-1}$ (control), $99\pm4.2 \text{ mol ha}^{-1}$ (compost), $120\pm18.8 \text{ mol ha}^{-1}$ (TSP), and $112\pm2.0 \text{ mol ha}^{-1}$ (compost+TSP) over all depths, yet no significant differences between the sampling depths and the treatments were found (Table II-1). The DPS in the topsoil of all treatments were significantly larger than those of the subsoils.

3.2 Sequentially extracted phosphorus fractions

The average P extractability in comparison to P_{tot} was $61\pm3\%$ in the topsoil, $72\pm3\%$ in subsoil1, and $70\pm7\%$ in subsoil2 (Table II-2). The stocks of all P fractions across the treatments and depths increased in the topsoil in the order Resin-P < $\text{NaHCO}_3\text{-P}_o$ < $\text{NaHCO}_3\text{-P}_i$ < NaOH-P_o < $\text{H}_2\text{SO}_4\text{-P}$ < NaOH-P_i , in the subsoil1 in the order Resin-P < $\text{NaHCO}_3\text{-P}_o$ < $\text{NaHCO}_3\text{-P}_i$ < NaOH-P_o < NaOH-P_i < $\text{H}_2\text{SO}_4\text{-P}$, and in the subsoil2 in the order Resin-P < $\text{NaHCO}_3\text{-P}_o$ < NaOH-P_o < $\text{NaHCO}_3\text{-P}_i$ < NaOH-P_i < $\text{H}_2\text{SO}_4\text{-P}$ (Table II-2).

Generally, P stocks of most of the fractions significantly decreased with increasing sampling depths. Among the treatments, mainly the P_i stocks in the subsoil of the fertilizer treatments were higher than in the subsoil of the control; nevertheless, significantly smaller $\text{NaHCO}_3\text{-P}_i$ stocks in both subsoils of the compost treatment than in the subsoils of the control were found. The topsoil P_o stocks were higher in the fertilizer treatments than in the control. The differences in the NaOH-P_o stocks between the subsoil2 of the fertilizer treatments were insignificantly lower than between the fertilizer treatments and the same depths of the control. By summing up the P fractions into labile (sum of Resin-P, $\text{NaHCO}_3\text{-P}_i$, and $\text{NaHCO}_3\text{-P}_o$), moderately labile (sum of NaOH-P_i , NaOH-P_o), and stable (sum of $\text{H}_2\text{SO}_4\text{-P}$ and Residual-P) P pools, we determined significantly higher labile P stocks in the topsoil than in the subsoil2 within all treatments (Fig. II-1). Across the treatments labile P stocks were only significantly higher in the topsoil of the compost+TSP treatment than in the control (Fig. II-1). Similarly, within all treatments moderately labile P stocks were significantly larger in the topsoil than in subsoil2. No significant differences of the moderately labile P stocks were found among the treatments. The stocks of stable P were higher in the topsoils than in the subsoils, except for the compost+TSP treatment with no differences of the stable P pool with depth. Among the treatments significantly higher stable P stocks in the topsoil of the compost treatment as well as in the subsoil2 of the compost+TSP treatment compared to the respective sampling depths of the control were found (Fig. II-1). Between the three sampling depths of the treatments no significantly different proportions of Resin-P were observed (values in brackets; Table II-2). Among treatments, subsoil2 of the compost+TSP treatment had significantly lower proportions of Resin-P than the same subsoil of the TSP treatment. Also the proportions of $\text{NaHCO}_3\text{-P}_i$ were not significantly different between sampling depths. Yet proportions were significantly smaller in subsoil2 of the compost treatment than in the control and the compost+TSP treatment (Table II-2). The greatest differences between fertilizer treatments and the control were found for the proportions of $\text{NaHCO}_3\text{-P}_o$ with significantly larger proportions in the topsoil of the TSP treatment but significantly lower in subsoil1 of the compost treatment. Furthermore, subsoil2 of the control and the compost treatment had significantly larger proportions of $\text{NaHCO}_3\text{-P}_o$ than subsoil2 of the compost+TSP treatment. The proportions of NaOH-P_i

were the highest, yet within the soil profiles (topsoil, subsoil1, and subsoil2) they were inconsistently distributed among sampling depths. Among the treatments the highest proportion of NaOH-P_i was measured in subsoil2 of the TSP treatment, which was significantly above the control. Moreover, the proportion of NaOH-P_i was significantly smaller in the topsoil of the compost treatment than in the control. The proportions of NaOH-P_o significantly decreased with depths across all treatments; proportions of the compost and the compost+TSP treatments approached almost zero in subsoil2 (Table II-2). Besides significantly reduced proportions in subsoil1 of the TSP treatment also the proportions of NaOH-P_o in subsoil2 of all three fertilizer treatments were significantly smaller than in the control. The proportions of $\text{H}_2\text{SO}_4\text{-P}$ were significantly larger in subsoil2 than in the topsoils (Table II-2). The same was true for subsoil1 of the compost+TSP treatment. The proportions of Residual-P in the topsoil of the control and the compost treatment significantly exceeded those of the subsoils. Nevertheless, no significantly different proportions of Residual-P among the treatments were observed.

Table II-1: Basic soil characteristics and elemental stocks of the soil samples of the four studied treatments (control, compost, TSP, and compost+TSP), and three sampling depths (0 to 30, 30 to 60, and 60 to 90 cm) with \pm standard deviation (SD).

Sample	Unit	Control			Compost			TSP			Compost+TSP		
		0-30 cm	30-60 cm	60-90 cm	0-30 cm	30-60 cm	60-90 cm	0-30 cm	30-60 cm	60-90 cm	0-30 cm	30-60 cm	60-90 cm
Sand		66	78	89	65	64	59	62	60	58	65	66	59
Silt	%	23	16	7.7	25	25	26	26	26	27	26	22	25
Clay		11	5.5	3.4	10	11	15	12	14	16	9.3	12	16
bulk density	g cm ⁻³	1.0 \pm 0.2 ^{Aa}	1.2 \pm 0.2 ^{Aa}	1.3 \pm 0.1 ^{Aa}	1.1 \pm 0.2 ^{Aa}	1.3 \pm 0.2 ^{Aa}	1.3 \pm 0.2 ^{Aa}	1.2 \pm 0.2 ^{Aa}	1.3 \pm 0.1 ^{Aa}	1.4 \pm 0.2 ^{Aa}	1.2 \pm 0.1 ^{Aa}	1.3 \pm 0.0 ^{Aa}	1.4 \pm 0.1 ^{Aa}
pH _{CaCl2}	-	5.8 \pm 0.0 ^{ABa}	5.5 \pm 0.3 ^{ABa}	5.7 \pm 0.3 ^{Aa}	5.8 \pm 0.1 ^{ABa}	5.7 \pm 0.1 ^{ABa}	5.9 \pm 0.1 ^{ABa}	5.6 \pm 0.2 ^{ABa}	5.6 \pm 0.2 ^{ABa}	5.7 \pm 0.2 ^{Aa}	5.9 \pm 0.1 ^{ABa}	5.8 \pm 0.2 ^{ABa}	6.0 \pm 0.7 ^{Ba}
C/N	-	8.8 \pm 0.4 ^{Aab}	9.7 \pm 0.6 ^{Aa}	7.5 \pm 0.8 ^{Ab}	9.2 \pm 0.2 ^{Aa}	10.2 \pm 0.8 ^{Aa}	8.9 \pm 0.7 ^{Aa}	8.9 \pm 0.2 ^{Aa}	9.8 \pm 0.8 ^{Aa}	9.0 \pm 1.6 ^{Aa}	9.1 \pm 0.5 ^{Aa}	9.9 \pm 1.2 ^{Aa}	11.4 \pm 4.6 ^{Aa}
C _{tot}		2462 \pm 309 ^{Aa}	1305 \pm 381 ^{ABb}	685 \pm 322 ^{ABb}	3354 \pm 514 ^{ABa}	1964 \pm 362 ^{ABb}	929 \pm 261 ^{ABc}	2793 \pm 448 ^{ABa}	1409 \pm 184 ^{ABb}	948 \pm 180 ^{ABb}	3612 \pm 171 ^{Ba}	1887 \pm 967 ^{ABb}	1583 \pm 979 ^{ABb}
N _{tot}		279 \pm 34 ^{Aa}	136 \pm 48 ^{ABb}	92 \pm 45 ^{ABb}	363 \pm 49 ^{ABa}	191 \pm 20 ^{ABb}	104 \pm 23 ^{ABc}	315 \pm 54 ^{ABa}	146 \pm 32 ^{ABb}	106 \pm 5 ^{ABb}	397 \pm 38 ^{Ba}	185 \pm 73 ^{ABb}	131 \pm 30 ^{ABb}
Fe _{tot}		24859 \pm 3713 ^{Aa}	37275 \pm 11862 ^{Aa}	49300 \pm 30125 ^{Aa}	27864 \pm 1807 ^{Aa}	42560 \pm 8401 ^{Aa}	55527 \pm 12585 ^{Aa}	29040 \pm 5061 ^{Aa}	47896 \pm 19350 ^{Aa}	58190 \pm 11814 ^{Aa}	33053 \pm 3381 ^{Aa}	48490 \pm 18725 ^{Aab}	67930 \pm 35089 ^{Ab}
Al _{tot}		22327 \pm 3978 ^{Aa}	42170 \pm 15599 ^{Aa}	54000 \pm 37647 ^{Aa}	26555 \pm 2590 ^{Aa}	47340 \pm 9561 ^{Aa}	60680 \pm 15819 ^{Aa}	26778 \pm 4595 ^{Aa}	54340 \pm 22485 ^{Aa}	60620 \pm 13167 ^{Aa}	28804 \pm 4810 ^{Aa}	53820 \pm 19312 ^{Aab}	73789 \pm 40299 ^{Ab}
Mn _{tot}		815 \pm 56 ^{Aa}	950 \pm 394 ^{Aa}	812 \pm 403 ^{Aa}	859 \pm 70 ^{Aa}	956 \pm 100 ^{Aa}	1094 \pm 206 ^{Aa}	897 \pm 220 ^{Aa}	1043 \pm 272 ^{Aa}	1091 \pm 131 ^{Aa}	1014 \pm 114 ^{Aa}	1164 \pm 209 ^{Aab}	1530 \pm 318 ^{Ab}
Ca _{tot}	kg ha ⁻¹	4246 \pm 632 ^{Aa}	5388 \pm 1599 ^{Aa}	6180 \pm 3488 ^{Aa}	6487 \pm 1716 ^{Aa}	6962 \pm 1182 ^{Aa}	7587 \pm 1331 ^{Aa}	4818 \pm 1280 ^{Aa}	6940 \pm 2362 ^{Aa}	7491 \pm 1518 ^{Aa}	6709 \pm 793 ^{Aa}	7553 \pm 1080 ^{Aa}	8267 \pm 3583 ^{Aa}
Mg _{tot}		4135 \pm 673 ^{Aa}	6559 \pm 2711 ^{Aa}	9138 \pm 6327 ^{Aa}	4962 \pm 641 ^{Aa}	7632 \pm 1881 ^{Aa}	10108 \pm 2742 ^{Aa}	4852 \pm 1230 ^{Aa}	8386 \pm 3659 ^{Aa}	10046 \pm 2588 ^{Aa}	5390 \pm 1598 ^{Aab}	9152 \pm 4754 ^{Aa}	13232 \pm 8161 ^{Ab}
P _{tot}		1890 \pm 474 ^{ABa}	1144 \pm 134 ^{ABb}	794 \pm 190 ^{Ab}	2704 \pm 1004 ^{ABa}	1474 \pm 255 ^{ABb}	1005 \pm 200 ^{ABb}	2239 \pm 449 ^{ABa}	1282 \pm 117 ^{ABb}	1198 \pm 338 ^{ABb}	2556 \pm 132 ^{ABa}	1645 \pm 429 ^{ABb}	1332 \pm 179 ^{Bb}
P _{ox}		1161 \pm 345 ^{Aa}	711 \pm 142 ^{Aab}	394 \pm 39 ^{Ab}	1354 \pm 334 ^{Aa}	1045 \pm 276 ^{Aab}	526 \pm 136 ^{Ab}	1380 \pm 264 ^{Aa}	802 \pm 52 ^{Ab}	693 \pm 271 ^{Ab}	1608 \pm 237 ^{Aa}	982 \pm 451 ^{Ab}	683 \pm 252 ^{Ab}
Fe _{ox}		5420 \pm 1366 ^{Aa}	5217 \pm 449 ^{Aa}	5079 \pm 4536 ^{Aa}	5811 \pm 1108 ^{Aa}	6394 \pm 562 ^{Aa}	6075 \pm 1532 ^{Aa}	6401 \pm 944 ^{Aa}	7017 \pm 1656 ^{Aa}	8616 \pm 477 ^{Aa}	6858 \pm 440 ^{Aa}	6724 \pm 734 ^{Aa}	7234 \pm 2768 ^{Aa}
Al _{ox}		1905 \pm 574 ^{Aa}	1960 \pm 297 ^{Aa}	1981 \pm 737 ^{Aa}	2056 \pm 361 ^{Aa}	2219 \pm 185 ^{Aa}	1991 \pm 401 ^{Aa}	2130 \pm 238 ^{Aa}	2699 \pm 1054 ^{Aa}	3016 \pm 1102 ^{Aa}	2404 \pm 171 ^{Aa}	2356 \pm 271 ^{Aa}	2282 \pm 464 ^{Aa}
Mn _{ox}		542 \pm 79 ^{ABa}	492 \pm 196 ^{ABa}	394 \pm 159 ^{Aa}	578 \pm 99 ^{ABa}	568 \pm 43 ^{ABa}	684 \pm 195 ^{ABa}	600 \pm 139 ^{ABa}	570 \pm 161 ^{ABa}	740 \pm 211 ^{Ba}	774 \pm 111 ^{ABa}	705 \pm 66 ^{ABa}	792 \pm 175 ^{Ba}
PSC	mol ha ⁻¹	89 \pm 23 ^{Aa}	88 \pm 6 ^{Aa}	94 \pm 41 ^{Aa}	95 \pm 18 ^{Aa}	104 \pm 9 ^{Aa}	97 \pm 23 ^{Aa}	102 \pm 13 ^{Aa}	118 \pm 27 ^{Aa}	140 \pm 22 ^{Aa}	113 \pm 8 ^{Aa}	110 \pm 12 ^{Aa}	114 \pm 32 ^{Aa}
DPS	%	42 \pm 2 ^{Aa}	26 \pm 5 ^{Ab}	16 \pm 7 ^{Ab}	46 \pm 4 ^{Aa}	32 \pm 7 ^{Aa}	17 \pm 2 ^{Ab}	44 \pm 4 ^{Aa}	23 \pm 7 ^{Ab}	16 \pm 5 ^{Ab}	46 \pm 5 ^{Aa}	29 \pm 13 ^{Ab}	21 \pm 11 ^{Ab}

TSP = Triple superphosphate

tot = total elemental stocks

P_{ox}, Fe_{ox}, Al_{ox}, Mn_{ox} = ammonium-oxalate extractable stocks of P, Fe, Al, and Mn

PSC = Phosphorus sorption capacity

DPS = Degree of phosphorus sorption

Significant differences at 5% probability level between samples are designated by different letters.

Depths between treatments: numbers with the same capital letter are not significantly different to the depth of other treatments. Depths within

a treatment: numbers with the same lower case letter within a treatment are not significantly different.

n = 3

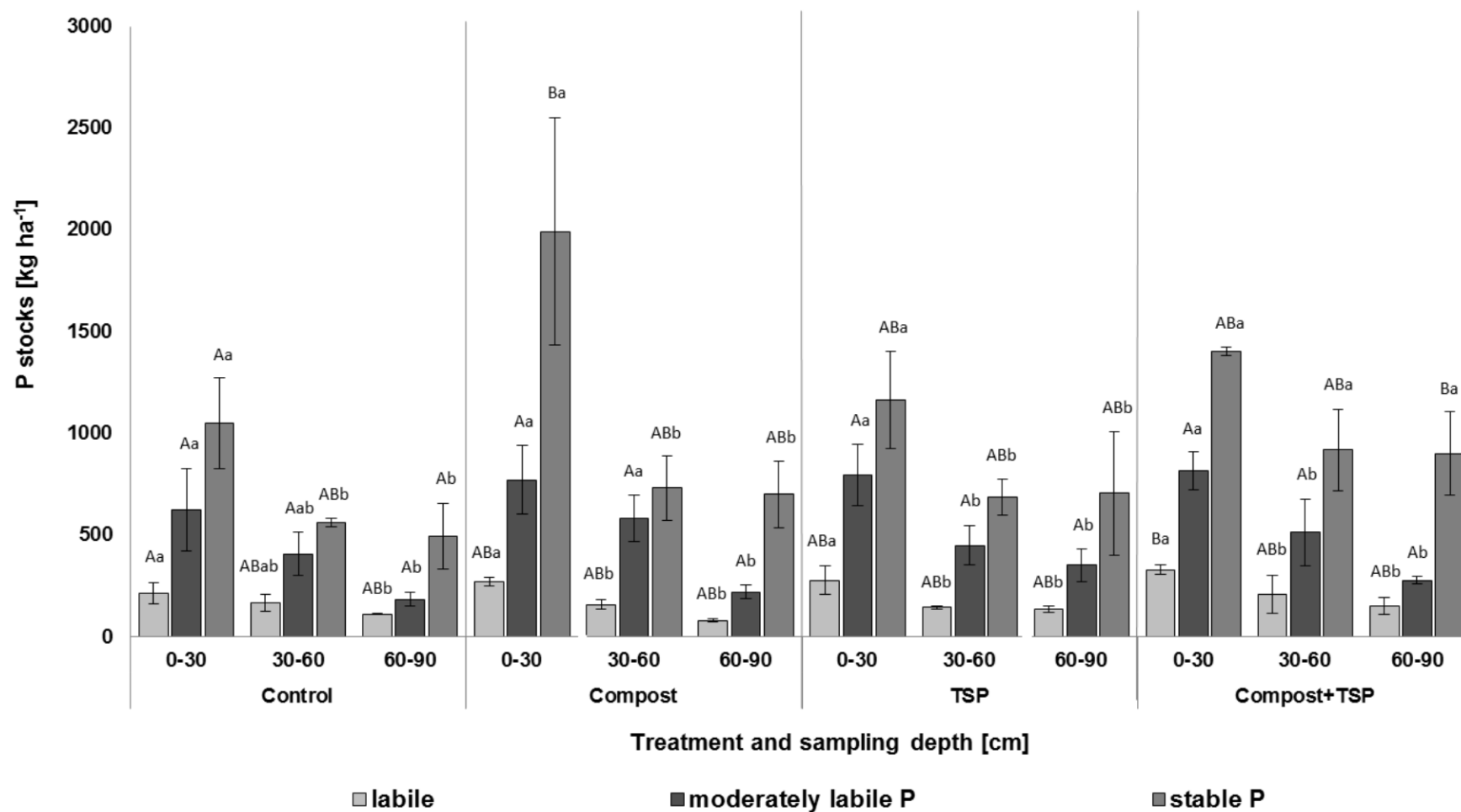


Figure II-1: Phosphorus (P) stocks of labile (sum of Resin-P, $\text{NaHCO}_3\text{-P}_i$, and $\text{NaHCO}_3\text{-P}_o$), moderately labile (sum of NaOH-P_i , NaOH-P_o), and stable P fractions (sum of $\text{H}_2\text{SO}_4\text{-P}$ and Residual-P) of the three sampling depths (0 to 30 cm, 30 to 60 cm, and 60 to 90 cm) of the four treatments control, compost, TSP, and compost+TSP are displayed. Statistical differences are illustrated: Numbers with the same upper case letter are not significantly different to the depth of other treatments. Numbers with the same lower case letter within a treatment are not significantly different. $n=3$

The summed proportions of total inorganic P ($P_{i,t}$) (sum of Resin-P, $\text{NaHCO}_3\text{-P}_i$, NaOH-P_i , and $\text{-H}_2\text{SO}_4\text{-P}$) increased with depths in all four treatments, these proportions were significantly higher in the subsoils than in the topsoil (Table II-2). In contrast, the proportion of total organic P ($P_{o,t}$) (sum of proportions of $\text{NaHCO}_3\text{-P}_o$ and NaOH-P_o) was highest in the topsoil of the TSP and compost+TSP treatments and in subsoil1 of the control and the compost treatment. In general, $P_{o,t}$ proportions in the topsoils were significantly larger than in subsoil2. In the TSP treatment the proportion of $P_{o,t}$ decreased significantly with every depth step. Between the treatments the proportion of $P_{o,t}$ in subsoil1 of the control significantly exceeded those of the TSP and the compost+TSP treatments. Likewise, proportions of $P_{o,t}$ in subsoil2 were reduced; here also subsoil2 of the compost treatment was significantly lower than the same depth of the control. The stepwise increases in the $P_{i,t}/P_{o,t}$ ratios followed the order control < TSP < compost < compost+TSP (Table II-2).

3.3 P-XANES analyses

Visually the obtained spectra had similar shapes in showing the major “white line” peak at around 2152 eV and only slight differences in the post-edge region (Fig. A1), indicating the dominance of ortho-P in these samples. In general, spectral shape between treatments did not vary considerably but differences, mostly peak intensities, were obvious between the topsoil and the subsoils. All samples were characterized by a weak pre-edge feature around 2149 eV, which is characteristic for Fe associated P. Spectral features known for Ca associated P (shoulder at the higher energy side of the white line peak at 2161 eV) were not visually pronounced. The LCF of spectra using 13 soil-relevant spectra of reference compounds indicated that overall the P composition among all treatments and depths could be described with two to three compounds. P associated to Fe was always the most dominant (46 to 92%), followed varying proportions of P associated to Al (0 to 40%), P associated to Ca (0 to 21%), and organic P compounds (0 to 12%) (Fig. II-2).

Table II-2: Phosphorus (P) stocks of the sequential P fraction and total P (P_{tot}) stocks of the four studied treatments (control, compost, TSP, and compost+TSP) and three sampling depths (0-30, 30-60, and 60-90 cm) with \pm standard deviation (SD). Values in brackets represent the proportions of the P stock fractions (as 100%) in relation to P_{tot} and significances are designated to both, the stocks and the proportions of the sequential P fractions.

Treatment	Depth	P_{tot}	extractable P	Resin-P	$\text{NaHCO}_3\text{-P}_i$	$\text{NaHCO}_3\text{-P}_o$	NaOH-P_i	NaOH-P_o	$\text{H}_2\text{SO}_4\text{-P}$	Residual-P	$P_{i,t}$	$P_{o,t}$	P_i/P_o
	cm	kg ha ⁻¹ (%)										%	-
Control	0-30	1890±474 ^{ABa}	1139±308 (60)	27±9 ^{Aa} (1 ^{ABa})	166±60 ^{ABCDa} (9 ^{ABa})	23±16 ^{Ab} (1 ^{ACDEFa})	339±123 ^{ABa} (18 ^{ABa})	285±84 ^{Aa} (15 ^{ABCDa})	299±55 ^{ABa} (16 ^{Aa})	751±168 ^{ABa} (40 ^{Aa})	44±3 ^{Aa}	16±2 ^{ABCDa}	2.7
	30-60	1144±134 ^{ABb}	833±171 (72)	19±8 ^{Aa} (2 ^{ABa})	107±31 ^{ABCDab} (9 ^{ABa})	43±7 ^{ABa} (4 ^{ABCEfb})	241±66 ^{ABab} (21 ^{ABa})	168±41 ^{Ab} (15 ^{ACDa})	254±50 ^{ABa} (22 ^{Aa})	311±44 ^{ABb} (28 ^{Ab})	54±6 ^{Ab}	18±2 ^{ACDa}	2.9
	60-90	794±190 ^{Ab}	565±94 (72)	12±1 ^{Aa} (2 ^{ABa})	82±6 ^{ACDb} (11 ^{Aa})	18±5 ^{ABb} (2 ^{ABCEa})	132±27 ^{Ab} (17 ^{Aa})	55±8 ^{Ac} (7 ^{ABCb})	267±64 ^{Aa} (34 ^{Ab})	229±97 ^{Ab} (28 ^{Ab})	63±5 ^{Ac}	9±2 ^{ABCb}	6.8
Compost	0-30	2704±1004 ^{ABa}	1449±234 (57)	42±9 ^{Aa} (2 ^{ABa})	169±5 ^{ABCDa} (7 ^{ABa})	61±17 ^{Ba} (2 ^{ABCEFa})	466±102 ^{ABa} (18 ^{ABa})	307±66 ^{Aa} (12 ^{ABCDa})	404±67 ^{ABa} (16 ^{Aa})	1255±835 ^{ABa} (43 ^{Aa})	43±11 ^{Aa}	14±3 ^{ABCDa}	2.9
	30-60	1474±255 ^{ABb}	1104±197 (75)	26±12 ^{Ab} (2 ^{ABa})	85±1 ^{ABCb} (6 ^{ABa})	48±14 ^{ABa} (3 ^{ABCEFa})	387±50 ^{ABa} (26 ^{ABb})	197±67 ^{Aa} (13 ^{ABCDa})	361±73 ^{ABa} (24 ^{Aab})	371±98 ^{ABb} (25 ^{Ab})	58±2 ^{Ab}	17±3 ^{ABCDa}	3.5
	60-90	1005±200 ^{ABb}	627±59 (63)	11±3 ^{Ab} (1 ^{ABa})	43±11 ^{BcDc} (4 ^{Ba})	28±2 ^{ABa} (3 ^{ABCEa})	220±28 ^{ABa} (22 ^{ABab})	6±8 ^{Ab} (0 ^{ABDb})	323±27 ^{ABa} (33 ^{Ab})	379±14 ^{ABb} (37 ^{Ac})	60±6 ^{Ab}	3±0 ^{ABDb}	20.3
TSP	0-30	2239±449 ^{ABa}	1434±284 (64)	42±13 ^{Aa} (2 ^{ABa})	156±50 ^{ABCDa} (7 ^{ABa})	80±12 ^{Ba} (4 ^{BCDEFa})	474±89 ^{ABa} (21 ^{ABa})	322±62 ^{Aa} (14 ^{ABCDa})	359±70 ^{ABa} (16 ^{Aa})	805±169 ^{ABa} (36 ^{Aa})	46±1 ^{Aa}	18±0 ^{ABCDa}	2.6
	30-60	1282±117 ^{ABb}	913±125 (71)	26±3 ^{Ab} (2 ^{ABa})	88±8 ^{ABCDb} (7 ^{ABa})	32±1 ^{ABb} (2 ^{ABCEfb})	334±77 ^{ABa} (26 ^{ABa})	117±22 ^{Ab} (9 ^{BCDb})	316±41 ^{ABa} (25 ^{Aa})	370±72 ^{ABb} (29 ^{Aa})	60±5 ^{Ab}	12±1 ^{BCDb}	5.2
	60-90	1198±338 ^{ABb}	909±195 (78)	20±3 ^{Ab} (2 ^{Aa})	94±8 ^{ACDb} (8 ^{ABa})	23±7 ^{ABb} (2 ^{ABCEfb})	330±93 ^{Ba} (29 ^{Ba})	48±47 ^{Ab} (1 ^{ABDc})	418±102 ^{ABa} (36 ^{Ab})	444±281 ^{ABab} (22 ^{Aa})	75±24 ^{Ab}	3±1 ^{ABDc}	18.5
Compost+	0-30	2556±132 ^{ABa}	1595±122 (62)	42±2 ^{Aa} (2 ^{ABa})	234±21 ^{ABCDa} (9 ^{ABa})	56±21 ^{Ba} (2 ^{ABCEFa})	463±52 ^{ABa} (18 ^{ABa})	355±73 ^{Aa} (14 ^{ABCDa})	445±57 ^{ABa} (17 ^{Aa})	961±55 ^{ABa} (38 ^{Ab})	46±1 ^{Aa}	16±3 ^{ABCDa}	2.9
TSP	30-60	1645±429 ^{ABb}	1116±277 (68)	22±8 ^{Ab} (1 ^{ABa})	153±64 ^{ABDab} (9 ^{ABa})	34±24 ^{ABab} (2 ^{ABDEFa})	343±97 ^{ABab} (21 ^{ABa})	172±70 ^{Ab} (10 ^{ABCDa})	391±41 ^{ABa} (24 ^{Ab})	529±163 ^{ABab} (32 ^{Aa})	56±3 ^{Ab}	12±3 ^{BCDa}	4.4
	60-90	1335±215 ^{Bb}	865±109 (65)	12±6 ^{Ab} (1 ^{Ba})	130±29 ^{ACb} (10 ^{Aa})	11±11 ^{ABb} (1 ^{ABCEFa})	273±34 ^{ABb} (21 ^{ABa})	36±26 ^{Ac} (0 ^{ABDb})	433±110 ^{Ba} (32 ^{Ab})	470±124 ^{Bab} (35 ^{Aa})	64±6 ^{Ab}	1±2 ^{ABDb}	18.4

TSP = Triple superphosphate

$P_{i,t}$ = total extractable inorganic phosphorus

$P_{o,t}$ = total extractable organic phosphorus

Significant differences at 5% probability level between samples are designated by different letters.

Depths between treatments: numbers with the same capital letter are not significantly different to the depth of other treatments.

Depths within a treatment: numbers with the same lower case letter within a treatment are not significantly different.

n = 3

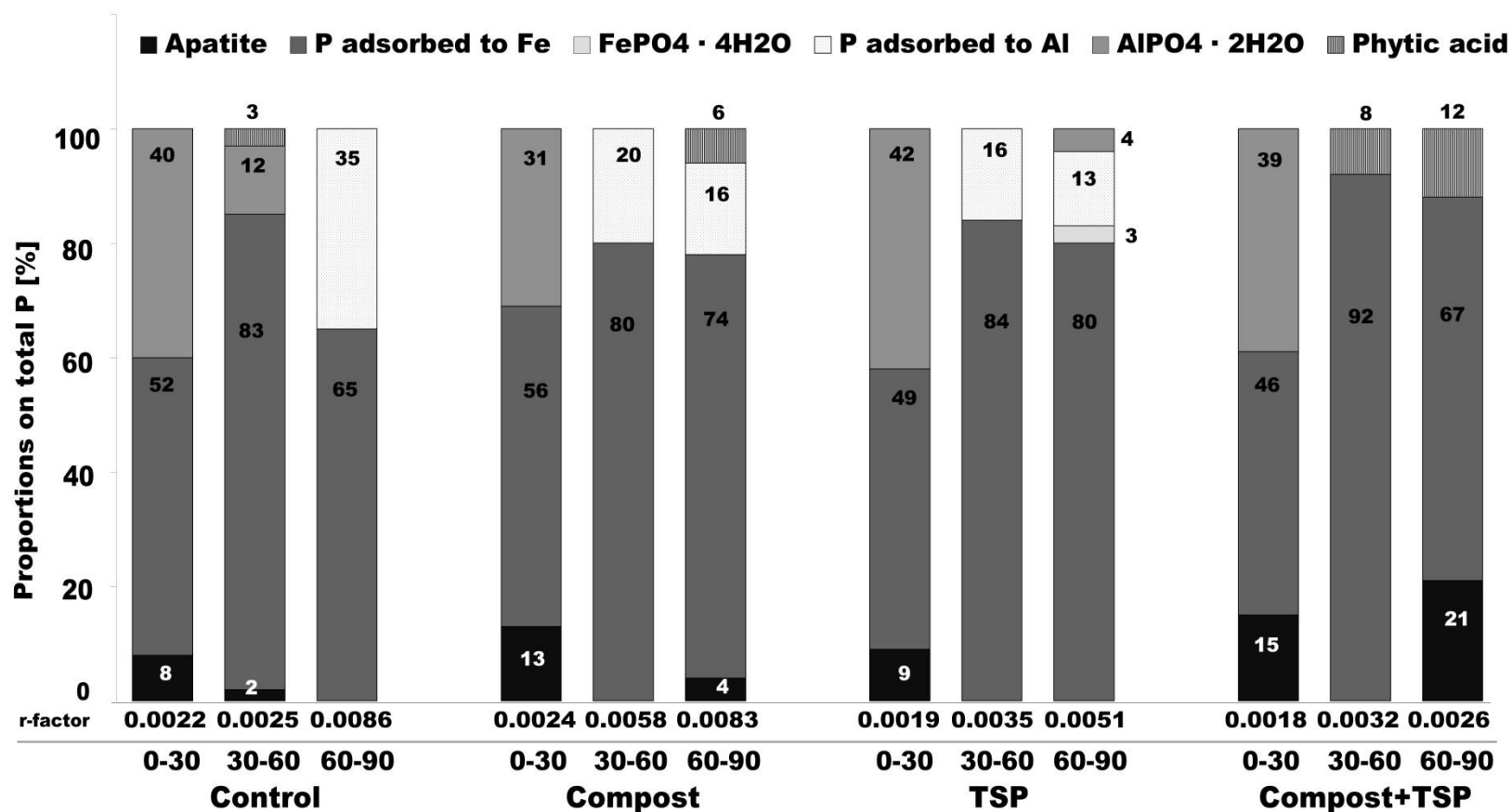


Figure II-2: Phosphorus (P) speciation (% proportion of total P (P_{tot})) as obtained by linear combination fitting (LCF) on averaged ($n=3$) P K-edge XANES spectra of four different treatments (control, compost, TSP, and compost+TSP). All possible combinations with up to four standard components (total 12 standard components) were calculated. Best fit was chosen according to the lowest r-factor and fits were tested for significant differences using the Hamilton test ($p < 0.05$). Proportions of fits not significantly different from each other were averaged.

The visible spectral differences between topsoil and subsoil were also reflected in the LCF results. In all topsoils of the fertilizer treatments Fe associated P was still the dominant P compound (46% to 56%), followed by Al associated P in the form of $\text{AlPO}_4 \cdot 2\text{H}_2\text{O}$ (31% to 42%) and varying proportions of apatite (8% to 15%). A treatment effect in the topsoils was not indicated by LCF, if taking an error of approximately 10% into account. In general, the proportions of P associated to Fe were higher in all treatments in the subsoils (92 to 65%) than in the topsoil, with indications of a trend towards lower proportion in subsoil2 (Fig. II-2). Proportions of P_o compounds were assigned only in both subsoils of the compost+TSP treatment and the subsoils of the compost treatment. In the latter the proportion of P_o compounds is uncertain as another not significantly better fit did not indicate P_o . Proportions of P associated with Al were always lower in the subsoils than in the topsoil. In the subsoil, P adsorbed predominately to Al. This might indicate that a higher proportion of P is stronger bound to Al. Only subsoil2 of the control treatment showed contributions of $\text{AlPO}_4 \cdot 2\text{H}_2\text{O}$, whereas both subsoils of the compost+TSP treatment showed no Al-associated P. Subsoil1 of the compost+TSP treatment showed clear contributions of apatite (21%), whereas the obtained small proportions of apatite from insignificantly different fits in subsoil1 of the control (2%) and subsoil2 of the compost treatment (4%) are insecure.

3.4 Solution ^{31}P -NMR spectroscopy

Results from ^{31}P -NMR showed that the resonance intensities and chemical shifts of the designated P species were not visibly different from each other (Fig. A2). The P recovery of the NaOH-EDTA extraction step before lyophilization on P_{tot} stocks ranged between 51% and 77%. All spectra were dominated by the orthophosphate peak at 5.5 to 5.6 ppm (Fig. A2). Several resonances in the orthophosphate monoester region between 6.1 and 3.3 ppm and distinctive resonances in the region of pyrophosphates (-4.6 to -4.7 ppm) were detected but no resonances in the diesters region (2.0 to 0.0 ppm) appeared (Fig. A2). Corresponding to the observed negative depth gradient of P_{tot} in the soil profile, also the summed total peak areas of the NMR spectra and so the calculated stocks of the identified P_o compounds of all treatments successively decreased from the topsoil to the second subsoil sampling depth (Fig. II-3). The proportions of orthophosphate on NaOH-EDTA extractable P increased with depths across all treatments; here the topsoils of TSP and compost+TSP had the highest proportions of orthophosphate. Vice versa, proportions of the sum of orthophosphate monoesters decreased with sampling depth in all treatments, following the order compost > control > TSP > compost+TSP. Among the treatments, proportions of orthophosphate monoesters in the topsoils were relatively equal; here the compost treatment showed the highest proportions followed by the control (Fig. II-3). The biggest differences appeared in subsoil2; the orthophosphate monoester stocks of the compost+TSP treatment were higher than in the other treatments. This finding was supported by the small P_i/P_o ratio of 7 in subsoil2 of this treatment and wider P_i/P_o ratios in the TSP (ratio: 13), compost (ratio: 11), and the control (ratio: 13) treatments (Fig. II-3).

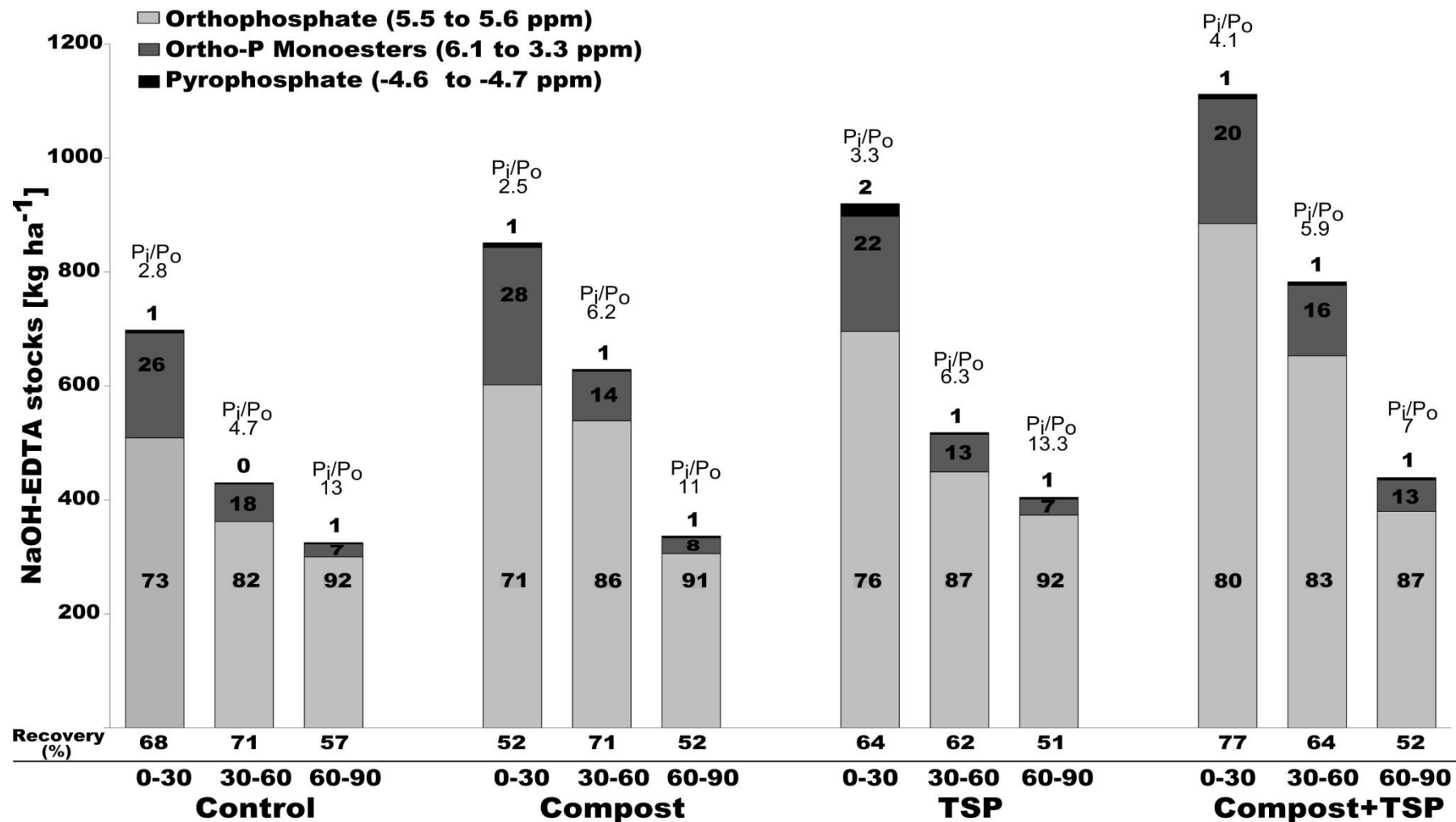


Figure II-3: Phosphorus (P) stocks (kg ha⁻¹) and proportions (numbers in bars) of categorized chemical shift regions on the total ³¹P-NMR signals of four treatments (control, compost, TSP, and compost+TSP) and three sampling depths (0 to 30, 30 to 60, and 60 to 90 cm). The recovery rate of NaOH-EDTA extraction is stated in relation to total P concentrations from aqua regia digestion before the lyophilization step, determined by ICP-OES. Proportions of the monoester region (identified peaks and an unidentified rest) were summarized as orthophosphate monoesters. Inorganic P and organic P ratios (P_i/P_o) calculated from identified compound classes are shown above the bars.

Within the orthophosphate monoester region *neo*-IHP6, *chiro*-IHP6, *scyllo*-IHP6 and *myo*-IHP6 were identified (Fig. A2). The latter was always most dominant with higher proportions on NaOH-EDTA extractable P in the topsoils than in the subsoils of all treatments (data not shown). The proportions of *myo*-IHP6 on the total orthophosphate monoester signal (summed as 100%) increased substantially with depths across all treatments (data not shown).

4 DISCUSSION

4.1 Influence of fertilizers on phosphorus stocks and proportions

The significantly increased P_{tot} stocks in subsoil2 of the compost+TSP treatment compared to the unfertilized control (Table II-1) indicate P accumulation of P from fertilizer above plant P uptake after 16 years. Requejo and Eichler-Löbermann (2014) showed for the same experiment that after 14 years the differences between P_{tot} removal (P removed in the harvested biomass) and P input was marginal among all treatments (including the control). Thus, the observed difference in the P balance between the treatments (ranging between -345 to +258 kg ha⁻¹, see Requejo and Eichler-Löbermann (2014)) was mainly due to differences in the amount of P application, especially for the compost+TSP treatment. The higher P_{tot} stocks in the subsoil of the compost+TSP treatment (about 54% above the control) suggest a downward movement of the surplus fertilizer P within the soil profile. This was also observed when P applications by far exceed plant uptake, and if the P sorption/storage capacity of the topsoils was exhausted (e.g., Godlinski *et al.* 2004; Kautz *et al.* 2012). This so called P leaching into deeper soil layers can be facilitated by preferential flow pathways, along biopores or in water flow areas that are depleted by P sorption sites, such as Fe and Al (hydro)oxides (Sinaj *et al.* 2002).

The comparison of the P_{tot} stocks of soil profiles (control 3828 kg ha⁻¹; compost 5184 kg ha⁻¹; TSP 4720 kg ha⁻¹; and compost+TSP 5532 kg ha⁻¹; Table II-1) with the annually P inputs indicates that the latter account for only < 2% of soil P_{tot} stocks. Thus, the impact of fertilizer P on the soil P stocks seemed to be low after 16 years, and only the excessive compost+TSP treatment seemed to effectively affect the soil P pool. By contrast, a negative P balance (-345 kg ha⁻¹) was reported for the control treatment (Requejo and Eichler-Löbermann 2014). This implies that the P fertilization in the single TSP and the compost treatments may have maintained the original profile P stocks at start of the experiment and the compost+TSP treatment increased the P_{tot} stock due to higher application levels, whereas plant P removal in the control reduced the P stocks, which was also reported by Oehl *et al.* (2002). The plant uptake in the control treatment might be facilitated through P mobilizing from moderately labile and stable P pools, as also assumed by Gransee and Merbach (2000), who measured negative yield responses in their unfertilized control treatment first after 25 years. Also Liu *et al.* (2014a), stated the release of P from soil Al-P and Ca-P sources. This might explain the low NaHCO₃-P_o stocks – especially in the topsoil – found in the control treatment. This suggests a more progressive P_o mineralization of incremental more stable P_o pools to compensate P_i removals by plants, which is more or less compensated via fertilization in the other treatments. Hence, in cultivated soils the mineralization of P_o depends on the amount of P_i in the soil. Therefore, P_o mineralization does not seem to be a main pathway for the supply of easily plant available P_i in soils with high available P_i concentrations, whereas when the available P_i concentrations are low (e.g., in an unfertilized soil) NaHCO₃-P_o mineralization contributes to efficient plant P availability by refilling soil solution (Guo *et al.* 2000).

The generally higher labile P stocks in the topsoils of the fertilizer treatments (Fig. II-1) can be explained by the addition of easily available P forms to the soil via the fertilizers. This P_i is rapidly

turned over or can be fixed by interacting with soil sorption sites. However, Dorahy *et al.* (2007) reported that this P still remains adequately accessibly by the plants. Other authors showed that fertilizer P_i was insufficiently available in the year of application especially in soils known for high sorption capacities (McLaughlin *et al.* 2011; McLaren *et al.* 2016). Therefore, the residual value of applied fertilizer P still improves P availability and P supply rates for plants within the following seasons (Morel *et al.* 1989). Another aspect which explains the higher labile P, especially in the compost+ TSP treatment, is the application of mineral P fertilizers in combination with organic amendments. The combined application of these fertilizers can lead to a competition for sorption sites between fertilizer P_i , organic anions and low-molecular acids released during decomposition processes of the organic amendments (Hue 1991; Iyamuremye *et al.* 1996; Reddy *et al.* 2005). Blocking of sorption sites by these organic anions and acids can result in an increase of free P in soil solution (Reddy *et al.* 2005), which in the following also affects the PSC (Table II-1). However, as stated in a review by Guppy *et al.* (2005), it is most likely that this is rather a result of higher P releases by decomposition of organic matter rather than from competition for sorption sites by the organic matter. Guppy *et al.* (2005) further suggested a potential increase of DPS through metal-chelate linkages mediated by humic- and fulvic acids, which by implication reduced soil sorption sites in the soil. Indeed, the DPS of subsoil were higher after the introduction of organic amendments (compost treatments) (Table II-1), indicating a lower capacity of P retention in the soil due to organic fertilization. This positively influenced soil P availability by increasing the soil P solution concentration, and thus improving potentially plant P availability (Nziguheba *et al.* 1998; Xavier *et al.* 2009).

It can be concluded that the significant increase of labile P stocks in the compost+TSP treatment over all soil depths compared to the control (Fig. II-1) is likely, apart from the higher P quantities, an effect of high solubility of TSP (Siebers *et al.* 2013) and a generally enhanced P solubility due to organic matter (Negassa *et al.* 2008). Therefore, the high labile P stocks have facilitated P leaching in the compost+TSP treatment (as stated above). In order to avoid the risk of P leaching a further accumulation of subsoil P due to excessive P fertilizer application must be avoided. However, future management and fertilization strategies should be adjusted to enable a more efficient utilization of the already existing but often unused subsoil P reserves.

Different to mineral P fertilizers, compost directly introduces moderately labile and stable P species (Audette *et al.* 2016). This was also visible in our results as significantly higher stable P stocks in the topsoil of the compost treatment were observed compared to the other treatments (Table II-2 and Fig. II-1). However, Reddy *et al.* (2005) stated that in treatments fertilized with organic amendments or in combination with mineral fertilizers both the labile (Resin- and $\text{NaHCO}_3\text{-}P_i + P_o$) and moderately labile P pool (NaOH-P_o and NaOH-P_i) build up, whereas after application of mineral P fertilizer short-term transformations of the applied P_i towards moderately labile and stable P compounds (only NaOH-P_i) occurred. This was partially also confirmed by our results, where topsoil $\text{NaHCO}_3\text{-}P_o$ was significantly increased (Table II-2) and the moderately labile and stable P pools were most pronounced in the subsoils in all fertilizer treatments (Fig. II-1). In a long-term view, this can contribute to the refilling of labile P reaction by a continuous release of P_i (Hedley *et al.* 1982; Tiessen *et al.* 1984).

The general distribution of the proportions of the five P fractions (Table II-2) agreed with the proportions found in other studies (e.g., Negassa and Leinweber 2009; Siebers *et al.* 2013). The low influence of fertilizer application on the P proportions likely resulted from the small amount of applied P in relation to the large P_{tot} stocks already in soil profiles. This is supported by the fact that the proportions of the labile, moderately labile and stable P pools did not significantly vary with depths and/or due to fertilizer application compared to the control. A P fertilizer effect was mainly visible in decreasing P_o proportions with depths as a result of a decreasing migration ability of complex P_o .

species with soil depths (Hedley *et al.* 1982). Inconsistency between P_o stocks and proportions is explained by the presence of high proportions of P_o in the residual-P pool, that resists extraction and its P composition still remains vague (Sattari *et al.* 2012; Velásquez *et al.* 2016).

4.2 Influence of fertilizer on phosphorus speciation

Most differences in XANES spectra appeared between sampling depths instead of treatments which indicate a stronger influence of P speciation during pedogenesis and soil profile formation on the soil P composition rather than from fertilizer applications (Fig. II-2). Phosphorus associated with Fe and Al (hydr)oxides was identified as the dominant P form followed by Ca-P compounds. This agrees with results from sequential fractionation also showing highest P proportions in the NaOH- P_i and H₂SO₄-P fractions (representing P associated to amorphous Fe and Al (hydr)oxides and Ca minerals). The dominance of P associated to Fe (hydr)oxides in all samples and especially in both subsoil samples is explained by the high content of secondary Fe and/or Al minerals in the weathered glacial till. This also corresponded well to the high proportion of P_{ox} in all treatments, accounting for 50% to 71% of P_{tot} (Table II-1).

The fact that Fe-associated P species increased with depth and were always the highest in subsoil1 can be explained by secondary enrichment and formation of Fe (hydr)oxides at this depth, which is the diagnostic property for the weathered brown B horizon of a Cambisol between 30 and 60 cm soil depths or even deeper. A similar trend of Fe-P accumulation in fertilized and unfertilized treatments were reported by Liu *et al.* (2013b) and Liu *et al.* (2014a). However, they also reported declining amounts of P associated to Al (hydr)oxides in the control, which we could not observe in our study. Among treatments, P species associated to Al (hydr)oxides showed large proportions especially in the topsoils (Fig. II-2), which might be related to the low pH of soils being around 5.5 to 6, which also favors the association of P to soil (hydr)oxides and accelerates the dissolution of Ca-associated P (Hinsinger 2001).

The fact that only rather small amounts of Ca-P were detected in contrast to relative large proportions of H₂SO₄-P (16% to 36%) (Table II-2 and Fig. II-2) can be explained by the use of particles < 20 µm for XANES analyses. It is generally known that the weathered primary Ca minerals (mainly of the apatite type) which are usually enriched in the silt to fine sand fraction (Saunders 1959) are lost when isolating the small particle size fractions (Tiessen *et al.* 1983; Schoenau *et al.* 1989; Eriksson *et al.* 2015). This also agreed with Eriksson *et al.* (2015) who found a depletion in apatite-P in the clay fraction in favor to P associated with poorly crystalline Fe and Al (hydr)oxides along a soil profile. Proportions of P_o – represented by phytic acid – were detected only in the subsoils of both treatments that received compost. This disagreed to low proportions of NaOH- P_o and the highest P_i/P_o ratio in the sequential fractionation (Table II-2), but can be plausibly explained by known low sensitivity of XANES to identify and quantify P_o species (Kruse *et al.* 2015). For this reason, it is likely that P_o proportions were underestimated by XANES and portions of other P forms with similar spectral features might be overestimated. Especially the high proportions of assigned $AlPO_4 \cdot 2H_2O$ may partly also represent P_o compounds, as spectral features of $AlPO_4 \cdot 2H_2O$ are not distinctively different from the used P_o reference compound phytic acid. XANES spectroscopy cannot clearly differentiate whether P_i or P_o is sorbed on Al and Fe (Kruse *et al.* 2015) and the evidence of high specific sorption affinities of P_o species on soil Al (hydr)oxides (Liu *et al.* 2013a) may support the underestimating of P_o by XANES. The same may be true for the assigned proportion of P sorbed on Fe (hydr)oxides (here the reference standard P_i sorbed on goethite was used). Therefore, it is likely that particularly the topsoil proportions of P sorbed to Fe also include P_o sorbed to Fe, especially in the particle fractions < 20 µm, which are known to be enriched in organic matter and thus P_o . This would correspond to the observed P_i/P_o ratios that were always the smallest in the topsoils.

The complementary liquid ^{31}P -NMR spectroscopy showed that orthophosphate was the most abundant P species in the NaOH-EDTA extracts, which increased with depth in all treatments (Fig. II-3). Such findings were also reported by McKercher and Anderson (1968) for Chernozems. The fact that application of organic fertilizer did not lead to an enrichment of NMR P_o stocks agrees to Ahlgren *et al.* (2013), who did not find any accumulation of P_o under long-term fertilizer application with both mineral and/or organic fertilizers in a wide range of soil types. This affirmed that the applied P_o in both compost treatments undergoes a rapid and nearly complete turnover (Annaheim *et al.* 2015) and, thus, contributes to plant nutrition by the steady release of more plant available P_i (as already stated above). In the present study the majority of P_o was identified as IHP6 monoesters including all of its known stereoisomers, with *myo*-IHP6 being always the most dominant form (Turner *et al.* 2012; Liu *et al.* 2013b). It is well known, that *myo*-IHP6 has a great affinity to react with the surface of soil particles (Celi and Barberis 2005; Jørgensen *et al.* 2015), such as amorphous Fe (Celi *et al.* 2003) or amorphous Al soil compounds (Yan *et al.* 2014). Especially, the affinity of *myo*-IHP6 towards goethite is higher than that of inorganic orthophosphate (Yan *et al.* 2015), which underlines the strong ambition of this orthophosphate monoester to form less plant available P_o complexes (Celi *et al.* 1999). The fact that NMR detected significant proportions of non-complex, NaOH-EDTA extractable orthophosphate monoesters (up to 28% in the compost treatment), especially in the topsoils, supports the suggestion that XANES may have overestimated proportions of P_i sorbed to Fe at the expense of P_o .

The absence of orthophosphate diesters (such as phospholipids) in the NMR spectra, which was previously reported in small quantities for agricultural soils (Cade-Menun 2005), can be explained by their fast hydrolytic degradation towards orthophosphate monoesters during the extraction and measurement preparation (Turner *et al.* 2003a). Therefore, the long extraction step of 16 h applied in this study may have facilitated this degradation (Cade-Menun and Liu 2013). However, the presence of small quantities of diesters, e.g., phosphatidyl choline, before extraction is rather likely, as distinctive main degradation products such as α - and β -glycerophosphates (Doolette and Smernik 2011; Cade-Menun 2014) were detected in the spectra mainly in the topsoil and subsoil1 (Fig. A2), where they accounted for up to 3% of NaOH-EDTA extractable P (data not shown). The fact that proportions of orthophosphate diester breakdown products only occurred in the upper soil layers seems reasonable because of predominating aerobic conditions, facilitating fast microbial turnover, and thus support the above discussed degradation of the organic P fertilizer sources. This can be explained by the higher amount of microbial biomass (soil bacteria and fungi) at these soil depths than in subsoil2, whose degradation products are the important sources of orthophosphate monoesters and diesters in soils (Bünemann *et al.* 2008). However, proportions of diesters in agricultural soils are often relatively small < 9%; (Condon *et al.* 1990)), also when shorter extraction times were used.

5 IMPLICATIONS

This study combined wet-chemical and spectroscopic analyses and evaluated the effects of different P fertilizers on soil P status and P speciation of whole soil profiles of a European agriculturally used Stagnic Cambisol. Our results suggested that the largest differences on P stocks and P speciation were found between the three soil sampling depths rather between fertilization treatments. Sequential fractionation showed that irrespective of the fertilizer P source the moderately labile NaOH-P fraction was predominant in the soil profiles. This was in line with results obtained by XANES spectroscopy, which identified P associated to Fe and Al (hydr)oxides followed by Ca-P compounds as the main dominant binding forms. The ^{31}P -NMR analyses revealed no differences between the P_o pools among the treatments, with always IHP6 monoesters as the predominant P_o form.

Therefore, we assume that 16 years of continuous fertilizer application and cropping were too short to lead to pronounced management-induced differences in P stocks, P speciation, and P dynamics in the soil profiles. However, in the fertilized topsoils there were significant, but minor fertilization effects on labile P pools, when compared to the unfertilized control. These marginal effects on P pools and speciation, as well as the constant and comparable removals of P via crops within all treatments irrespective of P application, suggest that redistribution and turnover even within the soil-inherent P pools is sufficiently dynamic to supply enough P to the bioavailable P pool to meet plants' P requirements even in the unfertilized control treatment. However, the combined application of mineral and organic fertilizers exceeded the levels of plants' P uptake and thus over the longer term will lead to a further accumulation of P in the profile. This, together with exhausting P sorption capacities in the topsoils may lead to progressive leaching of P into the subsoil, which will further increase the subsoil P stock but will also increase risk for groundwater contamination. Therefore, excessive P application exceeding plant needs must be prevented in order to stop future P leaching in to the subsoil ground water. However, already existing P stock in the subsoil built up from past excessive P fertilizer application might act as a valuable P nutrient reservoir, implying that such subsoil P stocks are also accessible by plant roots. Since the subsoil P reservoirs are currently ignored in soil P tests for fertilizer recommendations, ongoing studies should focus on management strategies to increase the plant accessibility of these unused P stocks in subsoils.

III

INSIGHTS INTO ^{33}P UTILIZATION FROM FE AND AL HYDROXIDES IN LUVISOL AND FERRALSOL SUBSOILS

Modified on the basis of the manuscript

Koch, M., Guppy, C., Amelung, W., Gypser, S., Bol, R., Seidel, S., Siebers, N., Insights into ^{33}P phosphorus utilisation from Fe and Al hydroxides in Luvisol and Ferralsol subsoils. Soil Research 2019 57, 447 – 458.

1 INTRODUCTION

To optimize crop growth, P fertilizers are frequently applied to topsoils, disregarding the supply potential of subsoils, the soil below the plough horizon (> 30 cm), for sustaining P for crop nutrition (Gransee and Merbach 2000; Kautz *et al.* 2012; Barej *et al.* 2014). Little is known about subsoil P utilization, but it is generally determined by interdependences of soil and plant factors. For instance, the spatial accessibility of subsoil P depends on beneficial soil conditions, such as soil moisture, soil structure, and topsoil nutrient concentrations (Kuhlmann and Baumgartel 1991; McBeath *et al.* 2012; Bauke *et al.* 2018). Promoted root growth at the early stage of plant growth accesses a greater soil volume and is beneficial for multiple resource acquisition (Römer and Schilling 1986; Ho *et al.* 2005; Bauke *et al.* 2017a) also from the subsoil. Hence, subsoil P stocks can only be efficiently utilized by plants if the physical conditions of both the topsoil and the subsoil are adequate, allowing the plant to exploit soil fertility throughout the soil profile.

Beside beneficial physical soil conditions, the soil chemistry controls bioavailability of soil P forms (Hedley *et al.* 1982; Beauchemin *et al.* 2003; Eriksson *et al.* 2016b). Subsoil P forms can be seen as a potential P repository but are often present in moderately labile and stable P forms and thus cannot be directly taken up by the plants (Kautz *et al.* 2012; Weihrauch and Opp 2018). In highly weathered, clay rich soils, e.g., Ferralsols and Ultisols, the majority of P is associated with or precipitated by secondary soil minerals, e.g., Fe and Al (hydr)oxides, accompanied by low available soil solution P concentrations (Dubus and Becquer 2001; Bertrand *et al.* 2003; Igwe *et al.* 2010). Similarly, secondary minerals (oxides and hydroxides) play also in many European agricultural soils an important role as predominant soil P sorption sites (Eriksson *et al.* 2016a; Gérard 2016). However, mediated by biotic and abiotic dissolution processes, also these non-soluble subsoil P forms are suspected to effectively contribute to the plant available soil P pool (Kuhlmann and Baumgartel 1991; Gransee and Merbach 2000; Kautz *et al.* 2012). Although the importance of P-oxide reactions in controlling soil P mobility and plant availability in the soil solution is well known (Hinsinger 2001), specific knowledge on subsoils (hydr)oxide-P contributions to plant nutrition are still lacking.

General information on speciation as well as sorption desorption dynamics between dominant soil P pools may be obtained from wet chemical extractions and spectroscopic approaches (Kruse *et al.* 2015). However, only when applying direct isotope tracing ($^{32}\text{P}/^{33}\text{P}$) a reliable quantification of P uptake by crops from specific soil P pools is feasible (Fardeau *et al.* 1995; Di *et al.* 1997; Frossard *et al.* 2011), since plants do not discriminate between ^{31}P and its radioisotopes (Bühler *et al.* 2003; Randriamanantsoa *et al.* 2013). Thus, an approach using ^{33}P associated to Fe and Al hydroxides, homogeneously located in soil, may allow quantifying the role of P forms of variable solubility for plant nutrition.

The complex issue between soil physical conditions and soil P availability has not received much attention in the past. An approach using ^{33}P associated to Fe and Al hydroxides in different soil orders may allow for the first time to gain insights into the linkage between the role of moderately labile soil P forms and soil physical conditions for plant nutrition. Therefore, the objectives of this study were (i) to analyze the effect of soil order on P use efficiency in the early stage of plant growth and (ii) to determine the plants P utilization potential of subsoil P sources having different availabilities. For this purpose, we performed a rhizobox experiment with subsoils of a Ferralsol and a Luvisol from which we expected different plant P uptake evolving from different physicochemical soil conditions. Soil bands were blended with ^{33}P spiked P forms of different availability (i.e., ^{33}P associated to synthetic Fe and Al hydroxides and easily available ^{33}P spiked KH_2PO_4 solution) to assess the short-term uptake of ^{33}P by wheat. Initial water contents were adjusted to 75% water holding capacity to provide optimum water supply at the beginning of the experiment; subsequent irrigation was not performed. The study

was supported by digital autoradiography imaging in order to visualize the distribution of ^{33}P radiotracer in the soil band and plant shoots.

2 MATERIAL AND METHODS

2.1 Soil characteristics

Subsoils (taken from 50 to 60 cm soil depths) of an Australian Orthic Ferralsol (> 60 % clay; classification according to World Reference Base for Soil Resources, IUSS Working Group WRB (2015)) and a German Haplic Luvisol (classification according to World Reference Base for Soil Resources, IUSS Working Group WRB (2015)) were chosen for this study, since both exhibited low soil solution P concentrations, along with high degrees of P sorption capacity, but different soil textures and thus physicochemical conditions (Table III-1). The Luvisol was obtained from an unfertilized control plot (no P applied since 1931) at the former experimental research station Dikopshof of the University of Bonn (50°48'17" N, 6°57'17" E), described in Mertens *et al.* (2008). The Ferralsol subsoil was sampled from a conventional used arable land close to Kingaory (26°35' S 151°49' E), Queensland, Australia.

The soils were air-dried, sieved to 2 mm, and analyzed for particle-size distribution (DIN ISO 11277), pH (0.01 mol L⁻¹ CaCl₂) at a soil:solution ratio of 1:2.5, total elemental concentrations of calcium (Ca_t), magnesium (Mg_t), potassium (K_t), iron (Fe_t), aluminum (Al_t), manganese (Mn_t), and P (P_t) after aqua regia digestion (Crosland *et al.* 1995), and subsequent analyzes using inductively-coupled plasma optical emission spectroscopy (ICP-OES; Thermo Fisher iCAP™ 7600). The loam soil reference ERMCC141 (Merck, Taufkirchen, Germany) was provided for analyzes and result validation. The concentrations of soil P available to plants were determined by double lactate extraction (DL-P) according to Riehm (1948). Olsen-P using 0.5 M NaHCO₃ extraction solution (Olsen 1954) was performed to assess the amount of soil P that is potentially plant available. Although Olsen-P is not recommended for acidic soils, Speirs *et al.* (2013) showed that Olsen-P produced appropriate results in Ferralsols. Similar observations were reported by Horta and Torrent (2007) claiming that Olsen-P was appropriate for estimating P release from acidic soils. Ammonium oxalate extractable Fe (Fe_{ox}), Al (Al_{ox}), Mn (Mn_{ox}), and P (P_{ox}) were determined after extraction with 0.2 mol L⁻¹ ammonium oxalate and 0.2 mol L⁻¹ oxalic acid (pH 3.1) for 2 h in the dark (Schwertmann 1964; McKeague and Day 1966) and subsequent analyzes with ICP-OES. Citrate-bicarbonate-dithionite extractable Fe (Fe_D), Al (Al_D), and Mn (Mn_D) were determined according to methods by Holmgren (1967) and Blakemore *et al.* (1977). The P sorption index of both soils was calculated using the P buffer index (PBI) according to Burkitt *et al.* (2002).

2.2 Experimental

In total 16 growth boxes were prepared from square petri dishes (24.3 x 24.3 x 2 cm; Laboglob, Gottmadingen, Germany), which were painted black on the outside. Every box was split into two chambers and every chamber was horizontally divided into bulk soil (0 to 15 cm and 20 to 24 cm; 77% of total soil volume) and a banded soil layer (15 to 20 cm; 23% of total soil volume) containing the ^{33}P radioactive-labeled treatments (Fig. III-1). The bulk soil space of the box was packed first (at day 0 of plant growth) whilst keeping the space for the soil band with a space holder. Afterwards (at day 2 of plant growth), this remaining space was filled with the same subsoil with different ^{33}P treatments blended before in a drum hop mixer for 24 h.

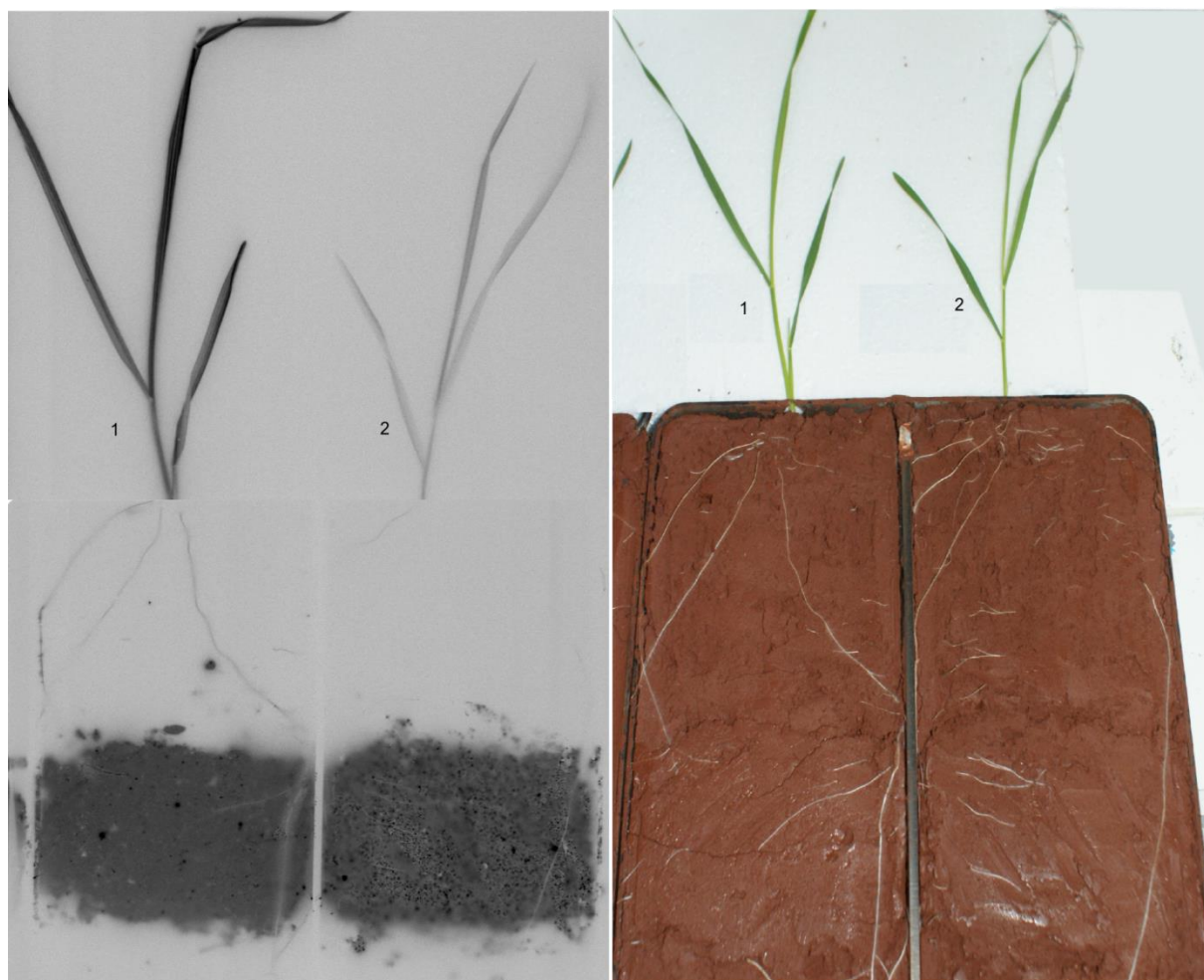


Figure III-1: Digital autoradiography image (left) and photo (right) of a representative example of 14 days old wheat plants of a ^{33}P labeled KH_2PO_4 treatment in the left chamber (1) and a ^{33}P labeled Fe-P hydroxide treatment in the right chamber (2) grown in Ferralsol subsoil. The high contrasted regions in the left picture represented the ^{33}P radiotracer distributions in the soil band and the plant tissues. High contrasts are devoted to regions of higher ^{33}P activities. The imaging plates were exposed for 16 h to the rhizoboxes, and then scanned in 100 μm sensitive mode (Bioimager CR35 Bio, ELYSIA-Raytest, Straubenhardt, Germany) and processed with the software AIDA Image Analyzer 2D densitometry program (ELYSIA-Raytest, Straubenhardt, Germany).

In both soils, the soil water content was individually set to 75% of the maximum water-holding capacity (WHC) (determined according to Forster 1995) to establish soil moisture at field capacity, yielding optimal water conditions for both soils at the beginning of plant growth. Thereafter, the soil was pre-incubated for 24 h in darkness. Afterwards the growth boxes were filled with the pre-wetted subsoils packed to a bulk density of 1.4 g cm^{-3} . This packing now resulted in only small differences in matrix potentials using dielectric water potential sensors (MPS2; Meter Environment, München, Germany), yielding $-12 \pm 1 \text{ kPa}$ (below pF 2.2) for both soils (Fig. III-2). Thus, starting water availability in both soils was within the borders of field capacities (border of field capacity was estimated to be around -33 kPa (pF 2.5) (Blume *et al.* 2011; Kirkham 2014). To monitor soil physical conditions during plant growth, we continuously determined the volumetric soil water content with moisture sensors and the soil matrix potential with the dielectric porous matrix potential sensors in both soils (Fig. III-2). Both sensors were carefully pressed into the soil of the control treatments (^{33}P -NoP, see below) during the filling process of the rhizoboxes (day 0) in order to ensure the maximal sensor-soil contact for reliable measurements. The sensors were placed before the beginning of the

radioactive soil band (from 20 to 25 cm depth) in a depth of 15 to 20 cm to avoid contamination of the equipment.

The accuracy of measured and calculated water moisture levels was checked at the first onset of the experiment and proofed functioning of soil moisture sensors (data not shown). For the Luvisol the data of only one matrix potential sensor was used as the soil-connectivity of the second sensor was not appropriate leading to erroneous results (Fig. B2). Overall, it is noteworthy that the sensor producer Decagon Devices Inc. (2016) claimed accuracy of MPS2 sensors being $\pm 25\%$ over the range of -9 to 100 kPa. Therefore, the matrix potential starting values of both soils were assumed to be identical. In addition, other scientists reported high temperature sensitivities of the sensor type MPS2 with artificial matrix potentials at increasing temperature (Richter *et al.* 2012; Hartner 2013). This effect was also visible in our data (diurnal shifts, Fig. B2); therefore, only data points of night measurements exhibiting more constant temperatures were utilized in Fig. III-2. Due to the adjustment of the soil moisture content to soil water holding capacity and thus water availability, i.e., to a certain potentiometric marker, soil water corresponded to slightly different gravimetric soil water contents (25 wt.% Ferralsol, 18 wt.% Luvisol), due to the different fine porosity of these soils at given packing density.

2.3 Plant growth

Wheat seeds (*Triticum aestivum* L. cv. Cornetto, KWS Saat SE, Einbeck, Germany) were germinated on filter paper and selected seedlings having the same development stage were carefully placed in the rhizoboxes, with one seedling per chamber (two per rhizobox; Fig. III-1), right after filling the boxes with the bulk soil (at day 0 of plant growth). The wheat plants were grown in a climate chamber with 16 h day-length at a light intensity of $320 \mu\text{mol m}^{-2} \text{s}^{-1}$. Day-time conditions were $20 \pm 5^\circ\text{C}$ and 60% relative air humidity, while night temperature decreased to approximately $14 \pm 2^\circ\text{C}$ and relative air humidity to 50%.

2.4 Radiotracer treatment and application

We applied four different treatments in the soil bands, which were all radioactive-labelled with 1.9 MBq ^{33}P -phosphoric acid (approximately $1.8 \times 10^{-8} \text{ mmol P}$). The amount of ^{33}P introduced into the system was negligibly small compared to the soil P concentration. In the soil bands, we applied ^{33}P spiked KH_2PO_4 either associated to Fe hydroxide (^{33}P -Fe) or to Al hydroxide (^{33}P -Al), as well as with a carrier free KH_2PO_4 solution (^{33}P -OrthoP) or in ^{33}P trace amounts without any additional P (^{33}P -NoP). The maximal P surface coverage of the hydroxides theoretically amounted for the Fe hydroxide: $0.75 \text{ mmol g oxide}^{-1}$ and the Al hydroxide: $0.9 \text{ mmol g oxide}^{-1}$ (Gypser *et al.* 2018). From this information, the P amount (as KH_2PO_4) for the P loading on the amorphous hydroxides were adjusted to cover about 80% of adsorptive mineral surface of the hydroxides in order to minimize significant physicochemical desorption of weakly adsorbed P at the beginning of the experiment. According to that, the Fe hydroxide were supplied with $0.64 \text{ mmol P g hydroxide}^{-1}$ and the Al hydroxide treatments with $0.77 \text{ mmol P g hydroxide}^{-1}$ (oxide preparation described in Gypser *et al.* (2018). The P associated to the amorphous hydroxides was assigned to build surface and structural OH non-hydrogen P bindings (Gypser *et al.* 2018); however, the character of P adsorption depends, beside the P concentration, on the hydroxide characteristics (Gypser *et al.* 2018), which were not further analyzed here.

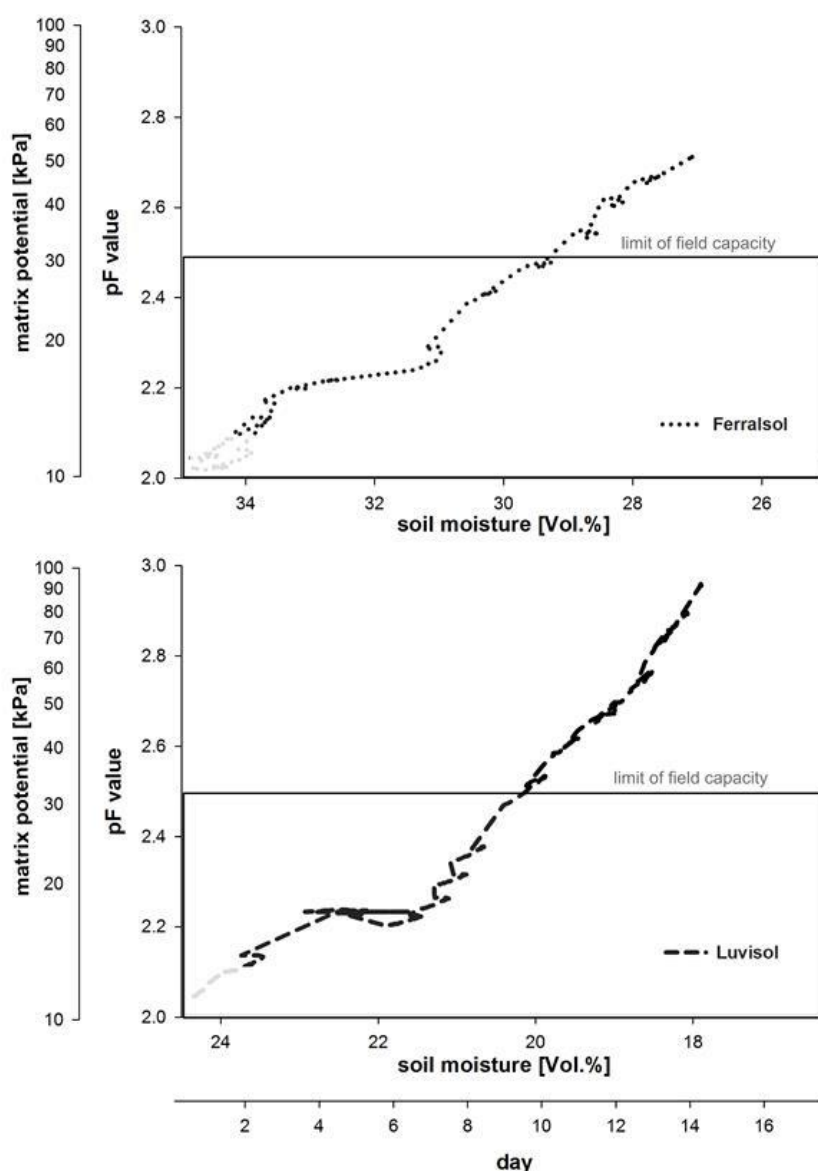


Figure III-2: Soil water properties (matrix potential [kPa], pF value [as LOG (-hPa)] and soil moisture [Vol. %]) during 14 days of plant growth in Ferralsol and Luvisol under controlled conditions. Soil moisture was set to approximately 75% of maximal water holding capacity at the onset of the experiment (day 0), which equated water potentials in the range of field capacity (12 ± 1 kPa in both soils; the frame represents the limit of field capacity at -33 kPa). The measurements were valid from day 2 on (before day 2 shaded lines), after soil bands of the rhizoboxes were filled with the ³³P radioactive-labeled soil treatments and the rhizoboxes were sealed with plastic foil). The data was conducted by dielectric water potential sensors (MPS2) (Ferralsol, n=2; Luvisol, n=1) and moisture sensors (both soils, n=2) for the volumetric water content. It is noteworthy that only the data points from night measurements are presented here, as extreme and artificial diurnal matrix potential amplitudes indicated significant temperature influences on sensor reading (see also Fig. B2). Sensor accuracy error was estimated to be around 25%.

In order to create a gradient of different P availabilities between the treatments, we increased the P concentration of the hydroxide treatments and the ³³P-OrthoP treatment (applied in the soil band) by about 100% of the endogenous soil P_t, being equal to P additions of 300 kg ha⁻¹ in the Ferralsol treatments and 390 kg ha⁻¹ in the Luvisol treatments. However, due to the mineral washing steps during the adsorption process, the amount of total P in the hydroxide treatments was reduced to 290 kg ha⁻¹ (³³P-Fe; Ferralsol), 224 kg ha⁻¹ (³³P-Al; Ferralsol), 382 kg ha⁻¹ (³³P-Fe; Luvisol), and 367 kg ha⁻¹ (³³P-Al; Luvisol), which equates to a final hydroxide P loading of 0.62 mmol P g hydroxide⁻¹ (Ferralsol) and 0.63 mmol P g hydroxide⁻¹ (Luvisol) for the ³³P-Fe treatments and of 0.58 mmol P g hydroxide⁻¹ (Ferralsol) and 0.72 mmol P g hydroxide⁻¹ (Luvisol) for ³³P-Al treatments, respectively.

The plants were grown for 14 days in the rhizoboxes and not longer to avoid emerging microbial mineralization, and thus, artificial P dissolution of the ³³P treatments. Overall, the combination of two soils with application of four different ³³P treatments resulted in eight treatments being tested in triplicate (n=3) for the Ferralsol and in quintuplicate (n=5) for the Luvisol. It was not possible to test the Ferralsol also in quintuplicate due to the limited amount of this Australian soil available for

experimental purposes. The hydroxide treatments (³³P-Fe and ³³P-Al) were applied as powder to the soil, whereas the other treatments (³³P-OrthoP and ³³P-NoP) were blended with the soil as a liquid. For all treatments a homogenous soil-radiotracer blending could be confirmed by using digital autoradiography (data not shown).

2.5 Plant analyses

The shoot dry weights (DW) were measured after drying at 40 °C for 24 h. Dry plants were further processed with pressure digestion of 0.5 g in 4 mL nitric acid according to Bauke *et al.* (2017a). Afterwards the plant shoot P_i concentration was determined colorimetrically using the molybdate blue method as described by Murphy and Riley (1962) using a UV-Spectrometer (Specord 250 plus; Analytik Jena AG, Germany), a calibration curve measured before and after samples guaranteed accuracy of measurements.

From subsamples of the above described digests the ³³P activity was measured in duplicate via liquid scintillation counting (LSC), as outlined by Bauke *et al.* (2017a). All ³³P data were adjusted to the time of application in order to account for the radioactive decay. The specific ³³P activity (SA) for ³³P applied in the soil band at the beginning of the experiment and afterwards, translocated in the plant and was calculated using equation III-1. At the onset of the experiment, the ³³P-Fe and ³³P-Al treatments blended in the soil had a SA of 0.023 MBq mg P⁻¹ (Luvisol) and 0.029 MBq mg P⁻¹ (Ferralsol). The SA of the liquid applied P in the soil (³³P-OrthoP and ³³P-NoP) were for the Luvisol: 0.021 MBq mg P⁻¹ (³³P-OrthoP) and 0.022 MBq mg P⁻¹ (³³P-NoP), and for the Ferralsol: 0.025 MBq mg P⁻¹ (³³P-OrthoP) and 0.030 MBq mg P⁻¹ (³³P-NoP). The ³³P SA of the plant shoot ranged between 0.002 and 0.022 MBq mg P⁻¹ (Table III-2). In order to estimate which proportion of the P taken up by the plants originates from the applied ³³P source in the soil band, we estimated the proportion of P in the shoot derived from the applied ³³P treatments (PPDS) by dividing the ³³P SA in the plant and ³³P SA of applied P sources at the beginning of the experiment (equation III-2). The plant's recovery of ³³P applied in the soil band was calculated as shown in equation III-3. The calculation of plant's recovery of ³³P has been outlined by McBeath *et al.* (2012) and McLaren *et al.* (2016). This parameter is helpful to study the fate of fertilizers in the soil and is a more accurate value for the amount of total P taken up from a particular source in the soil, as it takes the whole plant's development into account.

(III-1) Specific activity (SA) (MBq mg P⁻¹) =

$$\frac{^{33}\text{P in the shoot (MBq kg shoot DW}^{-1})}{\text{total P in the shoot (mg P kg shoot DW}^{-1})} \times 100$$

(III-2) ³³P in shoot derived from applied P source (PPDS; %) =

$$\frac{\text{SA of shoot (MBq mg P}^{-1})}{\text{SA of applied P source (MBq mg P}^{-1})} \times 100$$

(III-3) Recovery of ³³P (%) =

$$\frac{\text{total P in sample (mg P shoot)} \times \frac{\text{PPDS (\%)}}{100}}{\text{total P applied (mg P applied with source)}}$$

Nearly all of the applied ³³P activity (Ferralsol: 100%; Luvisol: 98.6%) could be accounted for at the end of the experiment. In total, around 0.026% (Ferralsol) and 0.020% (Luvisol) of the applied ³³P activity was located in the plant, around 97.9% (Ferralsol) and 98.3% (Luvisol) of the ³³P activity

remained in the soil bands. The rest of the ³³P activities, between 0.33% (Luvisol) and 2.9% (Ferralsol), have to be accounted as losses during the experimental setup.

2.6 Digital autoradiography

Digital autoradiography enabled us to locate ³³P radiotracer distribution within the plant and the soil. Due to the low penetration depth of ³³P radioisotopes, having an energy emission of 0.249 MeV, only the ³³P radioisotopes located at the direct surface of the soil band were tracked (see Fig. III-1). Immediately before harvest, the growth boxes were placed horizontally on a table and the surface of the soil and the plant was covered with phosphor imaging plates (20 x 40 cm, normal resolution image plate; DÜRR NDT GmbH, Bietigheim-Bissingen, Germany), wrapped in a thin plastic foil to avoid contamination. The exposure time of the plates to the rhizotrons was 16 h to ensure the capture of low radioactivity doses. Thereafter, the imaging plates were scanned with the scanner unit (Bioimager CR 35 Bio, Raytest, Straubenhardt, Germany) in sensitive mode at a resolution of 100 µm. The scanner produced a digital image (DI), which was processed with software (AIDA Image Analyzer 2D densitometry program; ELYSIA-Raytest, Straubenhardt, Germany). Contrasted regions as a spatial map on the DI showed the signal intensities of radioactive decay and enabled to document the ³³P radiotracer distribution and densities in the soil and the translocation in the plants (Fig. III-1; representative examples for all treatments see Fig. B1).

2.7 Statistics

All statistical analyzes were carried out using Sigmaplot 13.0.0.83 (Systat Software Inc., USA). Basic soil characteristics were tested for significant differences by using t-test ($p < 0.05$). Normal distribution and homogeneity of variance of the data was tested using the Shapiro-Wilk test and the Brown-Forsythe test, respectively. If normality assumption of data was violated, a log transformation of the data was performed. For determination of significant differences of the treatment means within one soil and for the same treatment between both soils at the 5% level ($p < 0.05$) of significance, we used a two-way analysis of variance (ANOVA) combined with the Tukey post hoc test for comparison of means.

3 RESULTS

3.1 Soil characteristics and plant biomass

Gravimetric soil moisture contents decreased in both soils (Luvisol, -5.1 wt.%; Ferralsol, -5.2 wt.%) at similar degree (see Vol.% at 1.4 g cm³ soil packing, Fig. III-2). At the start of the experiment the water availability in both soils was in the similar range of field capacity (pF values below 2.2 (day 2)); however, the soil water availability in the Luvisol declined steeper and reached the boarder of field capacity (at -33 kPa and pF 2.5 (Kirkham 2014)) at day 9; thus, one day earlier than the Ferralsol (Fig. III-2). At similar starting water conditions (12 ± 1 kPa) the matrix potential in the Ferralsol was more stable, i.e., it declined less (by about -40 kPa (n=2)) than in the Luvisol (by about -78 kPa (n=1)) towards the end of the experiment (Fig. III-2). Final water availability in the Ferralsol was thus more favorable for plant growth than in the Luvisol.

The Ferralsol subsoil was more acidic, contained higher clay proportions, greater amounts of sesquioxides with high crystallinities; moreover it exhibited a lower total soil concentration in base cations, as well as in C, N, and P than did the Luvisol (Table III-1). This also resulted in a lower soil solution P buffering of the Ferralsol than in the Luvisol, as also confirmed by the analyses of DL-P, Olsen-P, and PBI (Table III-1).

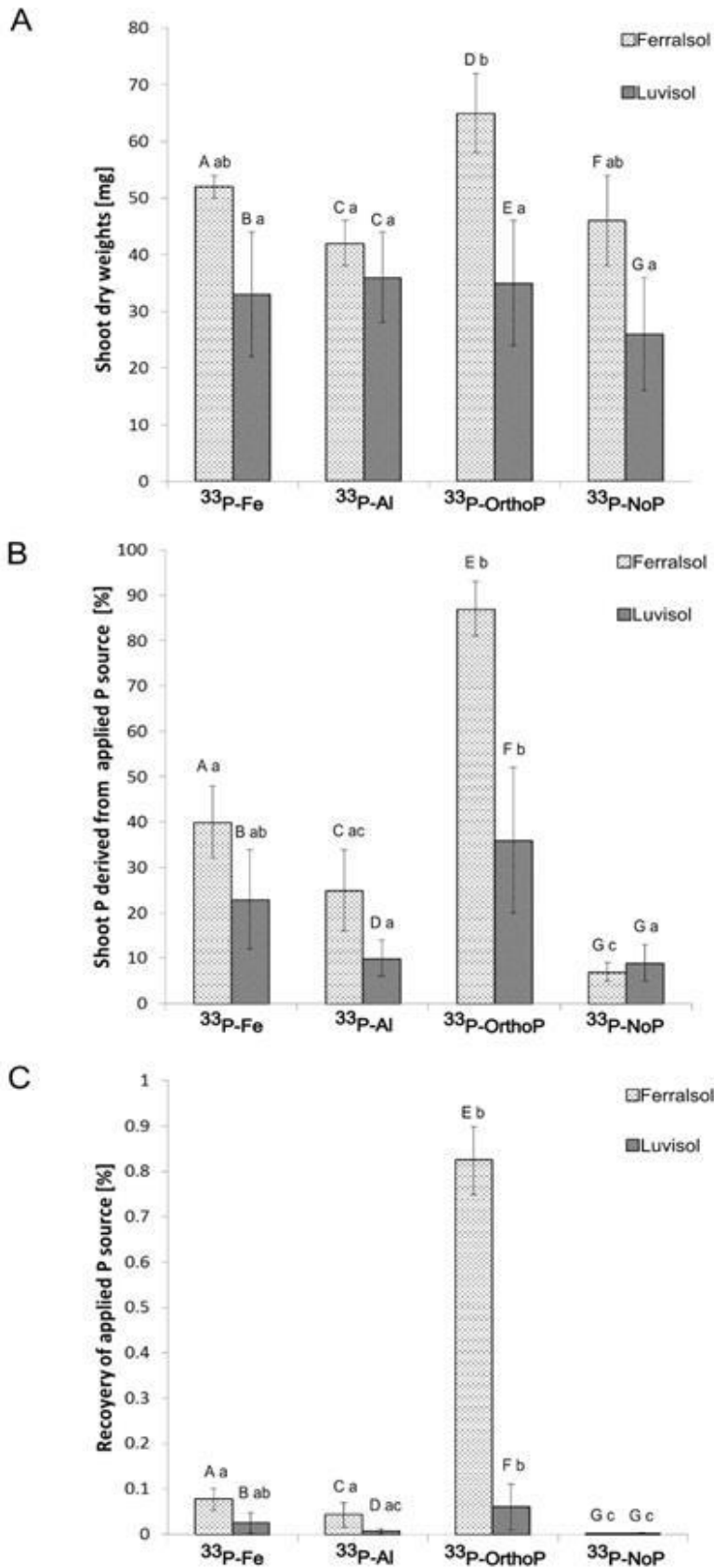


Figure III-3: Shoot dry weights [mg] (A), shoot P derived from applied P source [%] (B), and proportions of P recovery [%] (C) determined from wheat plants grown in rhizoboxes with banded ^{33}P sources (at day 14). The radioactive-labeled ^{33}P treatments ($^{33}\text{P-Fe}$: ^{33}P associated to amorphous Fe hydroxide; $^{33}\text{P-Al}$: ^{33}P associated to amorphous Al hydroxide; $^{33}\text{P-OrthoP}$: ^{33}P applied in KH_2PO_4 solution; $^{33}\text{P-NoP}$: ^{33}P radiotracer applied alone without P addition) were banded in Ferralsol (n=3) and Luvisol (n=5) subsoil. Shoot dry weights were measured after drying at 40°C for 12h at the end of the experiment. Shoot ^{33}P activities were determined by liquid scintillation counting after acid digestion of plant material. Significant differences at 5% probability level between samples are designated by different letters (testing: two-way ANOVA combined with the Tukey post hoc test for comparison of means). *Treatment between soils*: numbers with the same capital case letter are not significantly different from the treatment of the other soil group. *Treatments within one soil*: numbers with the same lower case letter within a soil type are not significantly different.

The effect of different levels of soil on the level of treatment is as follows:

Interaction between soil and treatment ($p = 0.05$)

Shoot dry weights	0.111
P proportion derived from applied P source	< 0.001
Recovery of applied P source	0.002

Table III-1: Soil characteristics of Ferralsol and Luvisol subsoil. Both subsoils were sampled below a soil depth of 50 cm, air-dried and 2mm sieved. Significant differences at 5% probability level between samples are designated by different small case letters.

		Ferralsol	Luvisol
Sand		13	9
Silt	%	25	62
Clay		61	29
pH _{bulk}		5.33	6.38
C _t		9.6±0.5 ^a	5.6±1.3 ^b
N _t		0.8±0.1 ^a	0.9±0.2 ^a
Ca _t		1.9±0 ^a	3.5±0.3 ^b
Mg _t		1.2±0 ^a	5±0.2 ^b
K _t		0.6±0 ^a	6.5±0.4 ^b
Fe _t		122±0.9 ^a	28±1 ^b
Fe _{Dit}	g kg ⁻¹	103.9±2.9 ^a	12.5±0.3 ^b
Fe _{Ox}		1.8±0.1 ^a	2.2±0.1 ^b
Al _t		113±5.7 ^a	32±1 ^b
Al _{Dit}		5.7±0.2 ^a	1.8±0.1 ^b
Al _{Ox}		2.2±1.1 ^a	1.1±0.0 ^b
Mn _t		1.4±0.1 ^a	0.6±0 ^b
Mn _{Dit}		1.0±0.0 ^a	0.5±0.0 ^b
Mn _{Ox}		0.9±0.0 ^a	0.5±0.1 ^b
P _t	mg kg ⁻¹	381±3.2 ^a	499±17 ^b
P _{Ox}		51±2 ^a	177±4 ^b
Olsen-P		11.9±0.5 ^a	17.4±0.5 ^b
DL-P		<0.1	<0.1
PBI		325	98

Significant differences at 5% probability level between samples are designated by different letters (t-test, with passed normality test (Shapiro-Wilk) and equal variance test (Brown-Forsythe)).

bulk = bulk soil

t = total concentration

Dit = Citrate-bicarbonate-dithionite extractable

Ox = Oxalate-extractable

DL-P = double lactate extractable P

PBI = phosphorus buffer index

n=3

The plant shoot DW in the Ferralsol were 1.6 to 1.8 times greater for the ³³P-Fe ($p = 0.009$), ³³P-OrthoP ($p < 0.001$), and ³³P-NoP trials ($p = 0.006$) than in the respective Luvisol treatments (Fig. III-3A). Only for the ³³P-Al treatments, the DW was not significantly different among the soils (Fig. III-3A). Within the Ferralsol treatments, the ³³P-OrthoP treatment showed a significant higher shoot DW (factor 1.4; $p = 0.024$) compared to the ³³P-Al treatment of this soil. There were no significant differences in treatment effects towards the DW in the Luvisol.

3.2 Digital autoradiography – ³³P distribution in plant and soil

The ³³P radiotracer-blended soil band was clearly visible in all digital images as a broad band with high levels of ³³P activity (Fig. III-1). There was no infiltration and diffusion of radioactivity into the

surrounding soil and surrounding pores and soil solution. The digital images also indicated that ^{33}P translocated into the plant shoots in all treatments except in the ^{33}P -NoP treatments. Generally, it was shown that within the period of 14 days of growth, the quantities of ^{33}P activity taken up by the young wheat plants varied between the different treatments and between soils. Digital autoradiography allowed direct non-quantitative estimations of ^{33}P activity uptakes between the treatments, being in the order of ^{33}P -OrthoP > ^{33}P -Fe \geq ^{33}P -Al \geq ^{33}P -NoP (Fig. B1).

3.3 Total shoot phosphorus concentrations and ^{33}P allocation

The shoot P concentrations in the Ferralsol were consistently but not significantly greater than in treatments of plants grown in the Luvisol. Except of the ^{33}P -ortho-P treatments at which the specific shoot P concentrations per kg dry matter in the Ferralsols exceeded those of the Luvisol by a factor of 2 ($p < 0.001$; Table III-2), no significant differences between the soils were measured. The interaction between the soil and the ^{33}P treatments were significant ($p < 0.001$). Among the treatments of a given soil, both soils showed significantly greater total shoot P concentrations in the ^{33}P -OrthoP treatment than in the other treatments, while no differences for the specific P concentration among the treatments grown in the Luvisol were measured. Enhanced ^{33}P uptake from the oxide treatments relative to ^{33}P -NoP treatments were detected for the Ferralsol only (Table III-2).

Dividing the ^{33}P specific activity (SA) of the shoot by the ^{33}P SA of the applied P source located in the soil band allowed the calculation of the proportion of shoot P that derived from the applied P source (PPDS). For the treatments of the Ferralsol, PPDS was 1.8 to 13 times greater than for those of the Luvisol ($p < 0.05$); except for the PPDS of the ^{33}P -NoP treatments that were in a similar range (Fig. III-3B). Among the treatments of one soil (with significant interactions ($p < 0.001$)), the PPDS was largest for the ^{33}P -OrthoP treatment and statistically different from the other ones ($p < 0.01$; except of ^{33}P -Fe in the Luvisol $p < 0.18$; Fig. III-3B). The ^{33}P uptake trends were confirmed by digital autoradiography, which showed the sharpest contrast for ^{33}P activities between ^{33}P -OrthoP treatment and ^{33}P -Fe treatments (Fig. B1).

The overall ^{33}P recovery (Fig. III-3C), defined as the ratio of P in the shoot to the P amount applied to the soil ranged from 0.01 to 0.89%. Between soils, ^{33}P recoveries were significantly greater for all treatments of the Ferralsol than of the Luvisol ($p < 0.05$, Fig. III-3C), with expectation of the recoveries of the ^{33}P -NoP treatments. Generally, the recovery from the applied P source in the plant was up to 13 times greater in the Ferralsol than in the Luvisol (Fig. III-3C). Among treatments in the Ferralsol, ^{33}P recovery rates declined in the order ^{33}P -OrthoP > ^{33}P -Fe = ^{33}P -Al > ^{33}P -NoP. No clear trend was visible in the Luvisol treatments, except for significantly greater ^{33}P recoveries of the ^{33}P -OrthoP treatment compared to the ^{33}P -Al and ^{33}P -NoP treatment of this soil ($p < 0.001$; Fig. III-3C). Overall, the Ferralsol thus allowed better ^{33}P utilization than the Luvisol, despite more acidic soil conditions.

Table III-2: Basic results of total shoot P concentration per plant, specific shoot P concentration, shoot ³³P activity, and specific shoot ³³P activity (at day 14 of growth). The radioactive-labeled ³³P treatments (³³P-Fe: ³³P associated to amorphous Fe hydroxide; ³³P-Al: ³³P associated to amorphous Al hydroxide; ³³P-OrthoP: ³³P applied in KH₂PO₄ solution; ³³P-NoP: carrier-free ³³P radiotracer) were banded in Ferralsol (n=3) and Luvisol (n=5) subsoil. The P concentrations were determined colorimetrically using the molybdate blue method. The ³³P activities were determined by liquid scintillation counting after acid digestion of plant material.

Treatment		Total shoot P concentration μg P plant ⁻¹	Specific P concentration g P kg DW ⁻¹	Shoot ³³ P-activity MBq kg DW ⁻¹	Shoot specific ³³ P-activity MBq mg shoot P ⁻¹
Ferralsol	³³ P-Fe	127±16 ^a	2.4±0.5 ^a	29±8 ^a	0.012±0.002 ^{a**}
	³³ P-Al	88±20 ^a	2.1±0.4 ^a	15±8 ^{a*}	0.007±0.003 ^{a*}
	³³ P-OrthoP	634±33 ^{b**}	9.9±0.4 ^{b**}	219±41 ^{b**}	0.022±0.002 ^{b**}
	³³ P-NoP	74±13 ^a	1.6±0.4 ^a	3±1 ^c	0.002±0.001 ^c
Luvisol	³³ P-Fe	98±29 ^{ab}	3.1±0.8 ^a	18±12 ^{ab}	0.005±0.003 ^{ab**}
	³³ P-Al	80±24 ^a	2.2±1.1 ^a	5±2 ^{b*}	0.002±0.001 ^{b*}
	³³ P-OrthoP	138±59 ^{b**}	4.0±0.9 ^{a**}	34±29 ^{a**}	0.007±0.003 ^{a**}
	³³ P-NoP	73±13 ^a	3.2±0.9 ^a	6±2 ^b	0.002±0.001 ^b
Interaction between soil and treatment (<i>p</i> = 0.05)		<0.001	<0.001	0.001	<0.001

Significant differences at 5% probability level between different treatments of the same soil are designated by different small case letters. Significant differences between the two soils and the same ³³P treatment at *p* < 5% probability are marked by *; and at < 1% probability level by **.

DW = dry weight

4 DISCUSSION

4.1 Soil phosphorus buffering capacity and plant development

Lower Olsen extractable P concentration along a smaller P buffering potential in the Ferralsol confirmed that overall soil P availability was lower than in the Luvisol, despite this methodology is usually biased towards better P extractability at more acidic soil conditions (Blume *et al.* 2011). Generally, P availability is reduced under more acidic soil conditions (Lal and Stewart 2016), evidenced here for the advanced weathered Ferralsol, leading to elevated concentrations of kaolinite, soil Fe (hydr)oxides, and Al (hydr)oxides (Table III-1), and greater P sorption strength (Schwertmann and Taylor 1989; Burkitt *et al.* 2002; Gérard 2016), i.e., greater PBI values.

Nevertheless, we found greater shoot DW in the Ferralsol than in the Luvisol for all treatments (Fig. III-3A) which suggested improved plant growth despite reduced P availability. We attribute this finding to the better maintenance of matrix potential. It maintained hydraulic conductivity and provided more available water for plant growth in the Ferralsol than in the Luvisol (Fig. III-2). In Ferralsols, pseudo-silt and pseudo-sand structures usually maintain soil physical stability with larger pores at similar degree of soil compaction (Balbino *et al.* 2002; Balbino *et al.* 2004). This probably resulted in stable, large aggregates that did not collapse to form micropores upon wetting in the rhizobox environment. As a result, the energy required by the plant roots to extract water was less than in soils with siltier textures, such as the Luvisol. Therefore, the soil moisture in the Ferralsol but not in the Luvisol remained in a range of optimal availability throughout the experiment as reviewed by Gliński and Lipiec (1990). It should be noted that this difference in water supply may not only have directly promoted plant growth, it may well also comprise indirect effects on improved performance,

e.g., stimulation of rhizosphere microbial communities (Brockett *et al.* 2012), enhanced mineralization of inorganic nitrate (Kladivko and Keeney 1987), or facilitated P diffusion (Bhadoria *et al.* 1991).

Overall, our data showed that differences between the soil orders affected the plant development already after 14 days, and thus, influenced the P utilization capacity on commencing wheat development between both subsoils. We therewith support findings by He *et al.* (2014) who modelled higher water sensitivities by wheat in silty than in clayey soils. Our results also support findings by McBeath *et al.* (2012) who showed that adequate soil moisture improved subsoil P utilization in a field trail with high rainfall. On the plant basis, a sufficient and stable soil moisture improves root architecture (Ho *et al.* 2005) and results in larger shares of subsoil roots (Bauke *et al.* 2017a), allowing the plant to exploit larger soil volumes and, thus, to acquire more soil P.

4.2 ^{33}P acquisition from phosphorus sources having different availabilities

Initial seedling P requirements are sufficiently covered by seed reserves for less than 10 days; thereafter, plants' vigor soon depends on P uptake from soil (Veneklaas *et al.* 2012). Similarly, Nadeem *et al.* (2011) reported that maize already took up significant amounts of ^{32}P only five days after sowing, indicating that the present short-term P uptake study was appropriate to analyze early growth related uptake of ^{33}P . The P amounts added in the soil bands were above the P fertilizer requirement of wheat being about 40 kg P ha^{-1} for a season of growth (LWK Nordrhein-Westfalen 2015). However, this was intended since spatial P soil accessibility of young wheat plants is restricted. Römer and Schilling (1986) reported that root density of wheat plants was as low as 0.27 cm cm^{-3} soil before Feekes stage 3 (before tillering; Large (1954)), which was the development stage the plants reached at the end of this study. Thus, even though the rich ^{33}P resources in this experiment were homogenously blended in the soil bands, only small P proportions in the soil bands were encountered by root surfaces, which consequently reduced spatial P accessibility. The relative low recoveries of the ^{33}P tracer in the plants were much smaller than those reported in literature (3% to 30%; (Sharpley 1986; McLaughlin *et al.* 1988a; McBeath *et al.* 2012), which may also be attributed to the early development stage of wheat plants in the present study. The recoveries of the ^{33}P radiotracers generally followed the order of increasing bioaccessibility of P among the treatments (Fig. III-3B+C).

Abiotic desorption experiments with the same hydroxides showed that less than 1% of P associated to Fe-hydroxide and only 37% of P onto Al hydroxides desorbed after more than 14 d (Gypser *et al.* 2018). In this regard, P availability in the present study decreased in the order: $^{33}\text{P-OrthoP} > ^{33}\text{P-Al} > ^{33}\text{P-Fe} > ^{33}\text{P-NoP}$. Nevertheless, elevated shoot P concentrations in the plants (Table III-2) and PPDS (Fig. III-3B) of ^{33}P from the Fe hydroxide treatments compared to the Al hydroxide treatments suggested improved plant P accessibility of this P form. This was unexpected since the P sorption strength of the Fe-hydroxide was actually stronger (potentially desorbing $\text{P} < 1\%$) than that of the Al-hydroxides (potentially desorbing $\text{P} < 37\%$) (Gypser *et al.* 2018). Yet the pH value in the soil band of the Al hydroxide treatment was lower by one unit: it dropped from 5.3 to 5.1 in the Ferralsol and from 6.4 to 5.6 in the Luvisol (Fig. III-1). While this is still outside common pH values for Al^{3+} toxicity ($< \text{pH } 5$) (Panda *et al.* 2009), it likely reduced the availability of sorbed P by forming amorphous analogues of variscite (Veith and Sposito 1977) or other insoluble solid phase Al-P compounds (Lindsay *et al.* 1959; Subbarao 1977). However, these findings were also indicated by the mass ratios of non-radioactive P-loaded Al hydroxide samples after digestion and ICP-OES measurement. The mass ratio of Al with $27.5 \pm 0.9\%$ was close to that of AlPO_4 (around 22%) Table D4). These assumptions are in line with Lookman *et al.* (1994), who proposed that P associated to Al hydroxides dried at low temperatures (in this thesis at 45°C) precipitated more rapidly to AlPO_4 than at high temperature drying. However, detailed analyses of hydroxide speciation were beyond the scope

of this thesis and thus characterization of P loaded (hydr)oxide samples is highly recommended in future studies.

Intriguingly, and despite the generally low plant availability of P adsorbed to Fe and Al hydroxides, these P sources still contributed up to 30% to overall plant P uptake (Fig. III-3B) (when PPDS of ³³P-NoP treatment representing soil P acquisition is subtracted). Our data thus support the classification of Negassa and Leinweber (2009), who designated the applied P associated with the hydroxides as moderately labile soil P forms, i.e., as a P form that may still be acquired by the plant. Overall, the results demonstrated that wheat plants are unlikely to meet their early P requirement for growth from sorbed oxide-P compounds only, especially because requirements are larger at early growth stage (Römer and Schilling 1986).

The ³³P-OrthoP treatment showed 8 and 13 times greater shoot P and ³³P recoveries than the oxide treatments in the Ferralsol, respectively (Table III-2 and Fig. III-3C). By overwhelming soil P sorption sites with excess additional P the ³³P-OrthoP treatment likely produced a P surplus. Consequently, soil P sorption capacity of variably-charged surface sites was heavily reduced, leading to elevated soil solution P concentrations in both soils. This demonstrates benefits of banding high and easily available P additions in soils leaving surplus P in soil solution and hence accessible by plant roots. However, the soil P surplus was sufficiently accessed only by the plants grown in the Ferralsol. Due to restrained physical conditions for growth, the plants in the Luvisol were unable to exploit the potentially available P sufficiently, leading to lower shoot P uptake from the Luvisol than from the Ferralsol, affecting the whole plant development.

5 CONCLUSION

Providing P to subsoil mineral phases showed that there were differences in P supply to young wheat plants, which were largest after adding carrier-free potassium phosphate in solution and smallest for Al associated P; P associated to Fe hydroxides showed an intermediate P plant supply. We showed that under favorable soil physical conditions these subsoil P forms efficiently contributed to up to 30% to the plant P requirements, already in the very early stages of plant growth. An analysis of the fate of ³³P from the subsoil P forms into different soil P pools should also help to explain differences in plant P uptake and should be focus of future investigations. Noteworthy, performing this experiment for two different soil orders revealed an improved P uptake from the Ferralsol than from the Luvisol, irrespective of the initially lower P concentration in the highly weathered Ferralsol. We attribute this finding to the soil physical parameters. At similar gravimetric soil water losses during plant growth, the Ferralsol maintained matrix potential and thus water availability at more favorable conditions for plant growth than did the Luvisol, thus improving the P utilization potential from subsoil. In other words, subsoil P forms appear to contribute sufficiently to plants P requirements only when optimum soil physical conditions are established.

From a methodological point of view, our study renews old discussions on controlling soil physical conditions when studying P uptake from subsoil. For a model-supported quantitative differentiation of the interaction of physical and chemical effects on subsoil P uptake, future studies should likely control all, water availability (as done here), gravimetric and potentiometric water contents, and temporal variation of water uptake dynamics; the latter thus resulting in significant multiplication of the trials, respectively.

IV

QUANTITATIVE IMAGING OF ^{33}P IN PLANT MATERIALS USING ^{14}C POLYMER REFERENCES

Modified on the basis of the manuscript

Koch, M.; Schiedung, H.; Siebers, N.; McGovern, S.; Hofmann, D.; Vereecken, H.; Amelung, W., Quantitative imaging of ^{33}P in plant materials using ^{14}C polymer references. Analytical and Bioanalytical Chemistry 2019, 1-8.

1 INTRODUCTION

The use of ^{33}P radioisotopes for tracing soil phosphorus (P) utilization in plants and soils has increased in recent years. By adding ^{33}P labeled P sources such as organic residues or mineral fertilizers to soil, the P uptake of microorganism (McLaughlin *et al.* 1988b) and plants (McLaughlin *et al.* 1988a; McLaren *et al.* 2016) can be studied in space and time in more detail. Determination of the ^{33}P activity is typically done by destructive sampling followed by liquid-scintillation counting (LSC). In general, autoradiography systems avoid destructive sampling by visualization of β -emitters in a great variety of organic tissues (e.g., Amemiya and Miyahara 1988; Johnston *et al.* 1990; Nakajima 1993). Compared to the X-ray film autoradiography, this technique utilizes more sensitive imaging plates for two-dimensionally resolved mapping of radiation (Nakajima 1993) and captures due to the linearity in response within a high dynamic range. The imaging plate consists of uniformly coated photostimulable luminescence materials, also called phosphors, which are mostly solid inorganic materials such as barium fluorobromide crystals containing traces of bivalent europium as the center of luminescence (written as BaFX:Eu^{2+} ($\text{X} = \text{Cl, Br, I}$)) (Takahashi *et al.* 1985). In principle, the technology is based on the detection of photostimulated luminescence (PSL), which involves two successive processes, i) the absorption of energy (excitation process) from radioactive decay and ii) the subsequent emission of photons (emission process) (Shinde *et al.* 2012). The general principles, as well as the advantages and disadvantages, of digital autoradiography are summarized by Upham and Englert (2003).

In P research, digital autoradiography was applied to trace the transport of ^{33}P radioisotopes in leaf veins (Hüve *et al.* 2007) and to visualize ^{33}P plant uptake after translocation from soil (Bauke *et al.* 2017a). Until now, information obtained from digital images were only semi-quantitative (e.g., positive, negative or intermediate results) and no direct approach has been reported in literature to quantify ^{33}P activities in soil and plants using digital autoradiography. Only in the field of medical sciences, where Cremer *et al.* (2009) studied the hybridization of mRNAs, the authors stated that they successfully quantified the ^{33}P activity in homogenized brain paste slices of rats. We therefore hypothesized that a total quantification of ^{33}P activity should in principle also be possible using digital autoradiography for plant materials.

Any quantitative imaging approach, to estimate radioactivity in a sample always requires the exposure of references of known activity at the same time. It was the manufacturing of ^{33}P activity references from brain paste that enabled a standardization of tissue thickness of paste slices and the valuation of its influence on signal intensity response during autoradiography (Cremer *et al.* 2009). Similarly, we have to manufacture standardized ^{33}P plant materials as referenced standards. However, both practices are not suited for routine research, due to the short half-life of ^{33}P radioisotopes (25.34 days) and the time consuming process of preparing reference standards. Therefore, a long-lasting and an easy-to-manufacture reference standard is required for temporally resolved ^{33}P quantification of a soil-plant system using digital autoradiography. A promising alternative reference substance is commercially available ^{14}C polymers (Eakin *et al.* 1994; Cremer *et al.* 2009), with reference series of different activities. Combining the latter with ^{33}P radioisotopes is suitable for autoradiography because of the long half-life time of the ^{14}C radionuclides and the fact that both radioisotopes exhibit approximately similar emission energies (Baskin and Stahl 1993). The PSL intensities of the ^{14}C references therewith comprise lower emission intensities (0.156 MeV) than for ^{33}P radioisotopes (0.249 MeV), since exposed imaging plates indirectly capture information from the radioactive decay as a function of radioactive energy (in the context of radiation flux; the amount of radiation received by an object from a given source) and exposure time (Upham and Englert 2003). By using low-energy electron emitters, unlike high-energy electron emitters such as ^{32}P , a finer resolution of captured radiation can be facilitated. On the other hand, the imaging sensitivity of low-electron emitters (here the radiation flux) is strongly affected by the samples composition. In the case of volume samples, absorption of radiation is

primarily influenced by the density of the radioactivity containing material but hardly if at all by its thickness (Robu and Giovani 2009) (provided that distance between the origin of radiation and the imaging plate is small). For this reason, absorption of radiation in environmental sampled, due to, e.g., varying material densities have to be taken into account to validate the quantitative success of digital autoradiography applications.

We hypothesized that digital autoradiography may easily be converted into a quantitative ^{33}P imaging method for plants by simultaneous analyzes of ^{14}C polymer reference materials. To be able to achieve this, it is necessary to establish a factor of equivalence between the PSL response of both radioisotopes, which is adapted to the co-exposure of the standards and allows the calculation of the true ^{33}P activities in plant materials. Hence, we applied this technique to excised leaves of maize and wheat, therewith using both C3 and C4 plant materials for the establishment of ^{14}C radioisotopes as a reference for quantitative ^{33}P imaging in digital autoradiography. In order to understand selective P uptake and transformation processes, we should finally also be able to quantify ^{33}P radioactivity in a spatially resolved manner into the respective above-ground biomass tissues.

2 MATERIAL AND METHODS

2.1 Standardized preconditioning of the digital imaging plates

It is well-known that phosphor imaging plates are highly sensitive towards photon emitting sources such as day light or electric light as they contain photosensitive crystals. In order to obtain reproducible high quality digital autoradiographic imaging we needed to standardize the sensitivity of the imaging plates. We therefore conducted a two-step erasing process for resetting the imaging plates' sensitivity to its maximal storage capacity. First, we erased the imaging plates for 30 min under a high energy white light imaging plate eraser (Fujifilm, Tokyo, Japan) followed by erasing with the Bioimager CR35 Bio (Raytest, Straubenhardt, Germany) before and after every exposure event. Flooding the imaging plate with bright visible or high energy laser beam returns most of the phosphor crystals to ground state and achieved the lowest background; important for quantitative purposes (Upham and Englert 2003). The successful re-adjusting of imaging plate sensitivity and storage capacity for ^{14}C radioisotopes was proven by repeated scanning and erasing events of the ^{14}C polymer references (Raytest, Straubenhardt, Germany) for different imaging plates (20 x 40 cm; Raytest, Straubenhardt, Germany) at the outset of the experiment (data not shown).

After plate erasing, it is highly recommended to avoid any light influence before plate exposure. For quantitative purposes the plate exposure should take place in special cassettes for radiography (e.g., from Fujifilm, Tokyo, Japan) and in a lead shielded cupboard to avoid any influence of background radiation. After exposure, imaging plates were immediately scanned with the scanner unit Bioimager CR35 Bio in sensitive mode at a resolution of 100 μm in darkness. During the scanning process the photostimulated luminescence (PSL) intensities were measured and a digital autoradiographic image was processed. The standard imager software, AIDA Image Analyzer 2D densitometry program (ELYSIA-Raytest, Straubenhardt, Germany) was used for quantitative measurement of PSL intensities of regions of interest (ROI). In the following, the established erasing and imaging procedures were applied for every exposure event.

2.2 Co-exposure of ^{14}C polymer references and ^{33}P phosphoric acid

In order to estimate the relationship between ^{14}C and ^{33}P radioisotopes having different emission energies, we analyzed their response of PSL by repeated co-application of different ^{33}P activities. For

this purpose, an aluminum plate with 36 recesses, each 100 μm deep with a surface area of 1 cm^2 , was constructed (see technical illustration; Fig. C1). Within two experiments (here called EXP1 and EXP2), we randomly applied ^{33}P phosphoric acid activities (^{33}P activities) diluted in a volume of 150 μL deionized water (dH_2O) to the spots, and exhibiting radioactive decays of 55, 270, 555, 1709, 3368, and 4597 Bq cm^{-2} (EXP1) as well as of 55, 261, 708, 1583, 3094, 5053, 7969, and 10531 Bq cm^{-2} (EXP2) (3 application aliquots measured by liquid scintillation counting (LSC) with daily calibration of an external standard (Tri-Carb 3110 Liquid Scintillation Counter, Perkin Elmer, Waltham, US)). The application solution covered the area of 1 cm^2 , enabling an approximately homogeneous ^{33}P distribution of the activity in every spot. Afterwards, the solution was evaporated at room temperature overnight. Before plate exposure, ^{14}C polymer references with six activities, each also covering a surface area of 1 cm^2 were applied on the plate, namely 66, 223, 692, 1867, 7067, and 18450 Bq cm^{-2} (Fig. IV-1). All ^{33}P data were adjusted to the time of the imaging event in order to account for the radioactive decay. Overall, in EXP1 we supplied 24 spots with six ^{33}P activities in quadruplicate and six ^{14}C polymer references in duplicate and exposed them to three imaging plates (20 x 40 cm; ELYSIA-Raytest, Straubenhardt, Germany). In EXP2 we applied eight ^{33}P activities in triplicate and six ^{14}C polymer references in duplicate and exposed them to four imaging plates, respectively.

For imaging plate exposure, the prepared aluminum plate was placed in a radiographic cassette and a freshly erased imaging plate, covered with a thin plastic foil (< 10 μm cellophane; to avoid any contamination), was placed on top and exposed for 4 h. Afterwards the plates were scanned and processed with the imaging software AIDA Image Analyzer 2D. The ROIs, here the ^{33}P spots and the ^{14}C reference squares, were selected manually. By also selecting background spots of a 1 cm^2 area, the software calculated the PSL intensities per area of ROI under automatic background subtraction (PSL cm^{-2} - BKG cm^{-2}), which in the following are referred to as PSL intensities.

2.3 Quantification of ^{33}P activity in excised leaves

Maize and wheat seeds were germinated in a standard cultivation soil and grown with daily watering in a climate chamber with 16 h day-length at a light intensity of 320 $\mu\text{mol m}^{-2} \text{s}^{-1}$. Day-time conditions were 20 $^{\circ}\text{C}$ and 60 % relative air humidity, while at night-time temperature decreased to 16 $^{\circ}\text{C}$ and 50% relative air humidity. From plants in the three-leaf stage (approximately 14 days of growth), single leaves of about 6 cm length from the top were cut and immediately placed in 200 μL dH_2O with additions of different ^{33}P activities, namely 23, 49, 100, 150, and 184 $\text{Bq } \mu\text{L}^{-1}$ (maize) and 12, 24, 49, 77 and 92 $\text{Bq } \mu\text{L}^{-1}$ (wheat). After 2 days in a climate chamber, when most of the solution was taken up, the leaves were dried at 40 $^{\circ}\text{C}$ for 12 h. Afterwards, the first 1 cm (maize) and 2.5 cm (wheat) of each leaf, which had contact with the radioactive solution, were cut and discarded. The average leaf tissue thickness was calculated after measuring the leaf thickness of the top and the bottom of every leaf (Foil Thickness Gauge, Model 497; Erichsen, Hemer, Germany). Leaf density (g cm^{-3}) was calculated by the leaf area, leaf thickness, and the leaf dry weight (Table C1).

For imaging plate exposure, leaves were placed in a radiographic cassette keeping the horizontal space on the imaging plate of one leaf to another free (similar to the ^{14}C reference material). This was necessary since the applied bioimager unit horizontally scans the whole imaging plate surface at once and photon emissions from high active areas create flare signals when the released photons reach the sensitive photomultiplier tube of the scanner unit. Thus, if the horizontal space of one leaf overlaps with others, the PSL intensities of leaves are artificially affected. A ^{14}C polymer reference was enclosed and the imaging plate was exposed for 4 h in a lead-shielded box. After exposure and scanning of the imaging plate, the digital image was processed and the total PSL intensities were obtained with AIDA Image Analyzer 2D, by selecting the leaf areas as ROI. The ^{33}P containing leaves were exposed to 3 (maize) and 5 (wheat) imaging plates in order to demonstrate reproducibility of

results. To compare total ^{33}P activity, the leaves were digested (HNO_3 acid pressure digestion, 6 h at 180 °C) with subsequent LSC counting, according to Bauke *et al.* (2017a). The ^{33}P data were adjusted to the time of imaging, considering the short half-life time for ^{33}P . Overall, for maize leaves we exposed five ^{33}P activities in triplicate together with one ^{14}C polymer reference set with 6 different specific activities to three imaging plates. For wheat leaves we exposed five ^{33}P activities in quadruplicate together with two ^{14}C polymer references sets to five imaging plates (Fig. IV-1). This resulted in 45 and 100 single PSL intensities, corresponding to the ^{33}P activities in the excised leaves, respectively.

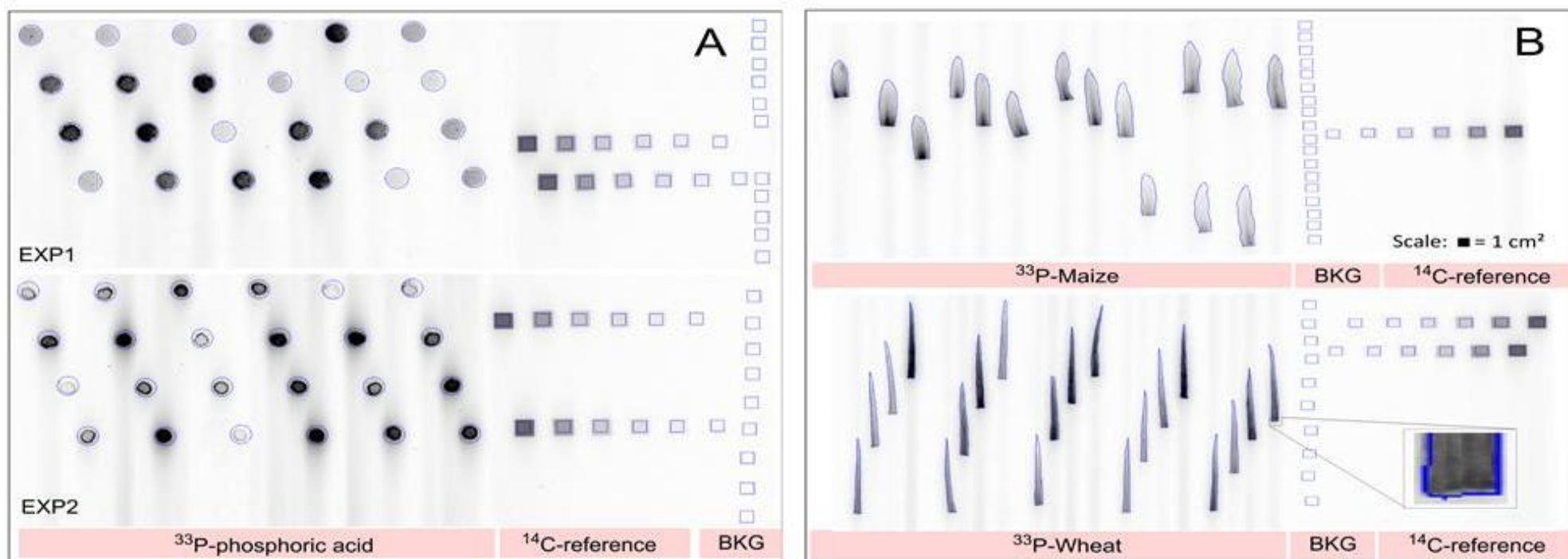


Figure IV-1: Digital images of selected regions of interest (ROI) of (A) the reference experiments (EXP 1 and EXP 2) with ^{33}P phosphoric acid activities (contrasted circles) and ^{14}C polymer reference activities (contrasted squares), and of (B) excised leaf experiments with maize and wheat leaves containing ^{33}P phosphoric acid and co-exposed ^{14}C polymer references. Imaging plates were exposed for 4 h to radioactivity, and then scanned in sensitive mode with a pixel size resolution of 100 μm . A: At the beginning (EXP 1) and at the end of the study (after 20 exposures, EXP 2) we applied ^{33}P phosphoric acid solution with different activities into circular 100 μm deep recesses on an aluminum plate. The surface area of every recess was 1 cm^2 . Commercial ^{14}C polymer references (with also 1 cm^2 surface area) were co-exposed to imaging plates. B: ^{33}P phosphoric acid solutions having different activities were supplied to excised leaves for 3 days in a climate chamber, after uptake, leaves were dried and exposed to the imaging plates. Images are received and presented under identical conditions (incubation time, gamma resolution of 2).

3 RESULTS

3.1 Linear relationship between ^{14}C and ^{33}P activities

In a first step, the relationship between PSL intensity and exposed ^{14}C and ^{33}P activities of several exposure events was analyzed. This aimed to replace a time consuming and inefficient preparation of ^{33}P references by commercially available ^{14}C polymer references. From seven plate exposure events (sum of EXP1 and EXP2), average PSL intensities for the known ^{33}P activities were obtained (Fig. IV-1). From 4 h exposures, a linear relationship (^{14}C : $R^2 = 1$, $p < 0.0001$; ^{33}P : $R^2 = 0.99$, $p = 0.001$) for both radioisotopes was estimated (Fig. IV-2).

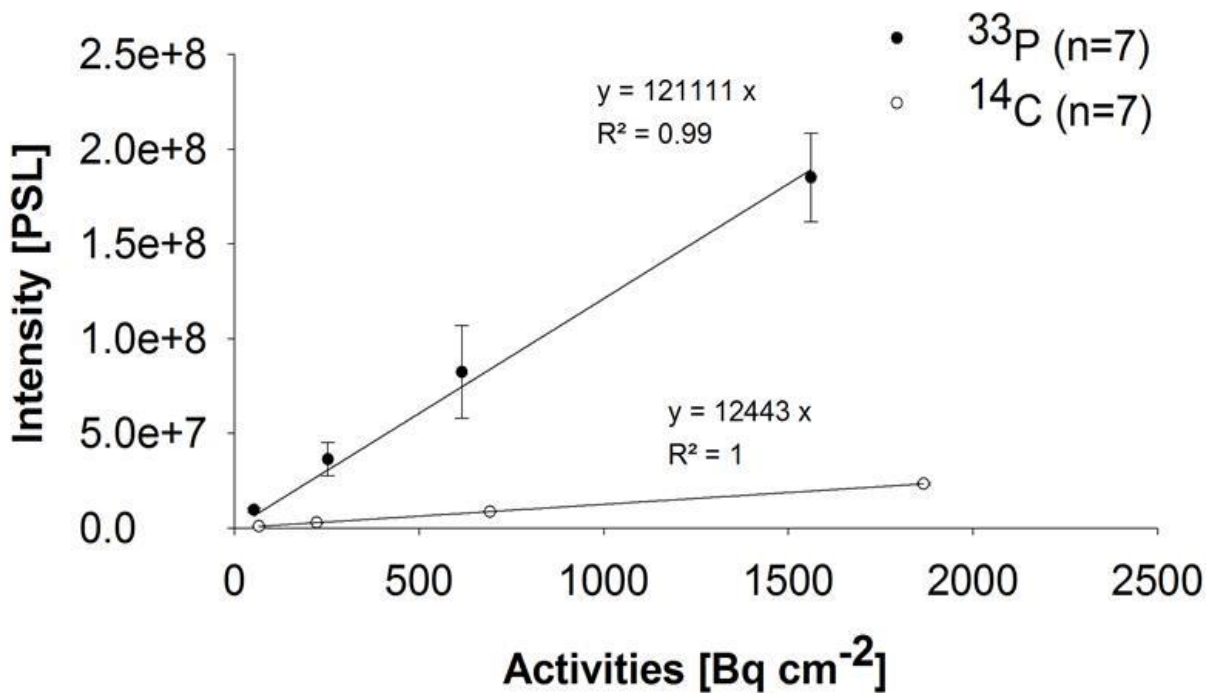


Figure IV-2: Linear relationship between photostimulated luminescence intensities (PSL) and exposed radioactivity of ^{14}C and ^{33}P radioisotopes applied on an aluminum plate for the reference experiments. Linear relationship between both radioisotopes was only found within the range of 50 and 2000 Bq cm^{-2} . The exposure time was 4 h followed by digital autoradiography scanning. Results are averaged values over 7 plate exposure events (including EXP 1 and EXP 2).

We found linear photostimulated-luminescence equivalence in the range between 50 to 2000 Bq cm^{-2} by dividing the ^{14}C PSL intensities and ^{33}P PSL intensities. The linear relationship can be expressed by the factor 9.73 ($R^2 = 1$, $p < 0.0001$) (called γ in Fig. IV-3). In the following, this slope will be referred to as PSL equivalence factor γ (Fig. IV-3). This allowed that ^{33}P activities can be calculated from obtained ^{14}C slope co-exposed for single plate exposures.

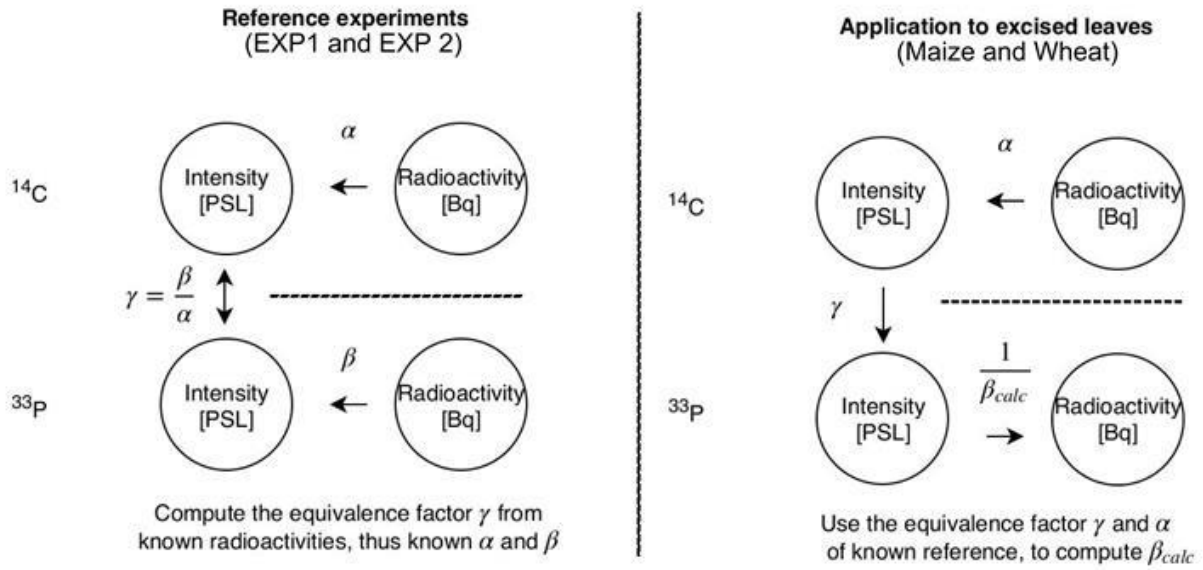


Figure IV-3: Schematic illustration of the methodological approach for digital autoradiographic quantification of ^{33}P by photostimulated luminescence intensity (PSL) in leaves, gained from the co-exposure of ^{14}C polymer references. First, in reference experiments (EXP1 and EXP2), the ratio γ between ^{14}C and ^{33}P intensities at different known activities was analyzed. By using γ to transform the known relationship between ^{14}C radioactivity and responding PSL, the activity of ^{33}P can be calculated by dividing respective PSL intensities by β_{calc} .

Our data showed in this context, that higher ^{33}P activities led to respective PSL intensities outside the linear range (Fig. IV-4). In EXP2 this led to a sigmoid exponential function ($R^2 = 0.99$, $p < 0.0001$) (Fig. IV-4). The cut-off for linearity was different for both experiments being $> 4000 \text{ Bq cm}^{-2}$ for EXP1 and $> 2000 \text{ Bq cm}^{-2}$ for EXP2. The linearity between PSL intensities for exposed ^{14}C activities, however, was similar in both experiments ($R^2 = 1$, $p < 0.0001$) (Fig. IV-4). Based on these results, sensitivity losses of imager plates occurring between the reference experiments at the beginning (EXP1) and at the end (EXP2) of the experiment cannot be excluded, since imaging plates were not used too often during the experiment: approximately 20 exposure events with approximately 80 h exposure time in combination with the described erasing procedure. Usually, however data indicates that this accounts for radioisotopes having higher emission energies than ^{14}C .

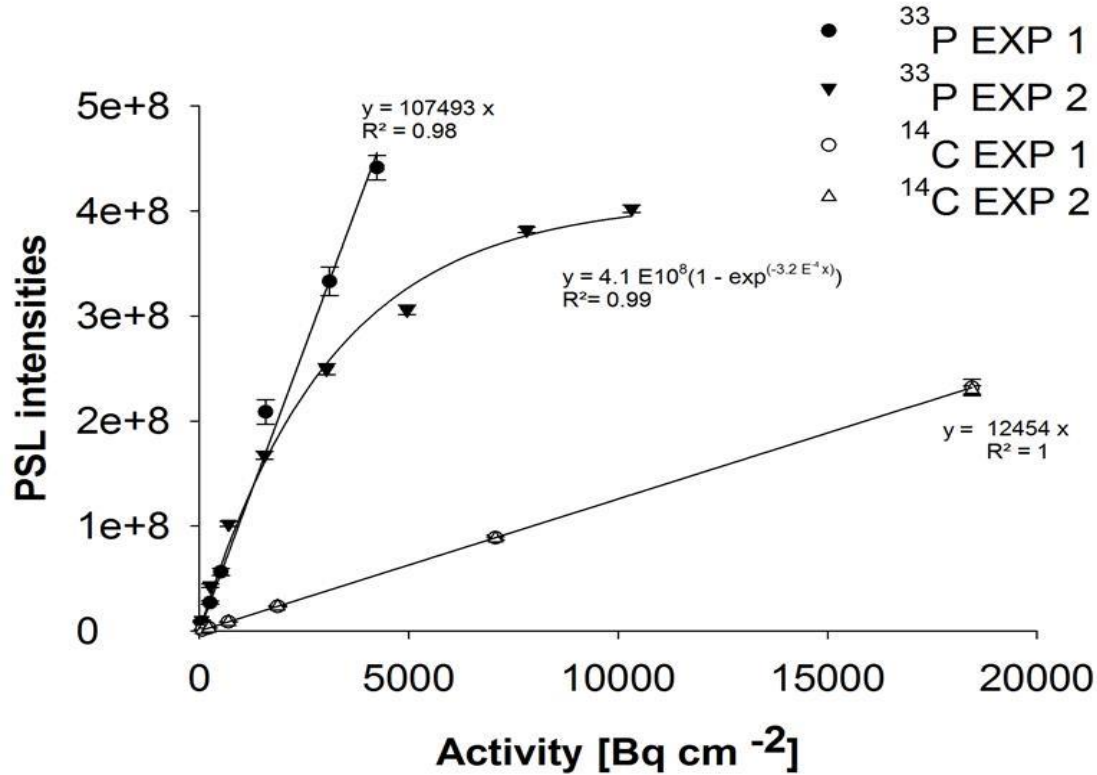


Figure IV-4: Relationship between photostimulated luminescence (PSL) intensities and applied ^{14}C and ^{33}P activities over the whole range of applied radioactivity in two reference experiments (EXP1 and EXP2). At the end of the study, after more than 20 exposure events the linearity in the plate response reaction of PSL to increasing ^{33}P activities was lost (EXP2) and we therefore recommend to apply the method within the dynamic linear range between 50 and 2000 Bq cm^{-2} for ^{33}P radioisotopes.

3.2 ^{33}P activities in leaves calculated from digital autoradiography images

In an excised leaf experiment, ^{14}C polymer references were co-exposed with ^{33}P labeled plant leaves, both designated here as ROI (Fig. IV-1). After exposure, the ^{14}C slope (different for every single exposure event) was calculated and multiplied by the equivalence factor (Fig. IV-2 and Fig. IV-3), which resulted in the equivalent ^{33}P slope, calculated from activities < 2000 Bq cm^{-2} (Fig. IV-2). Afterwards, ^{33}P PSL intensities were divided by the calculated ^{33}P slope (Fig. IV-3), which resulted in calculated ^{33}P activities for single ROIs.

To estimate the effect of tissue density as a factor of ^{33}P activity absorption, the average leaf tissue thickness was measured and multiplied by the leaf area and the dry weight. The density ranged between 0.29 and 0.48 g cm^{-3} for maize and 0.44 and 0.49 g cm^{-3} for wheat leaves. The relationship between leaf density and the ratio of PSL intensities and applied ^{33}P activities showed no significant correlation (maize: $R^2 = 0.08$, $p = 0.31$; wheat: $R^2 = 0.007$, $p = 0.72$) (Fig. IV-5). With greater leaf densities no declining PSL to Bq ratios were found (Fig. IV-5).

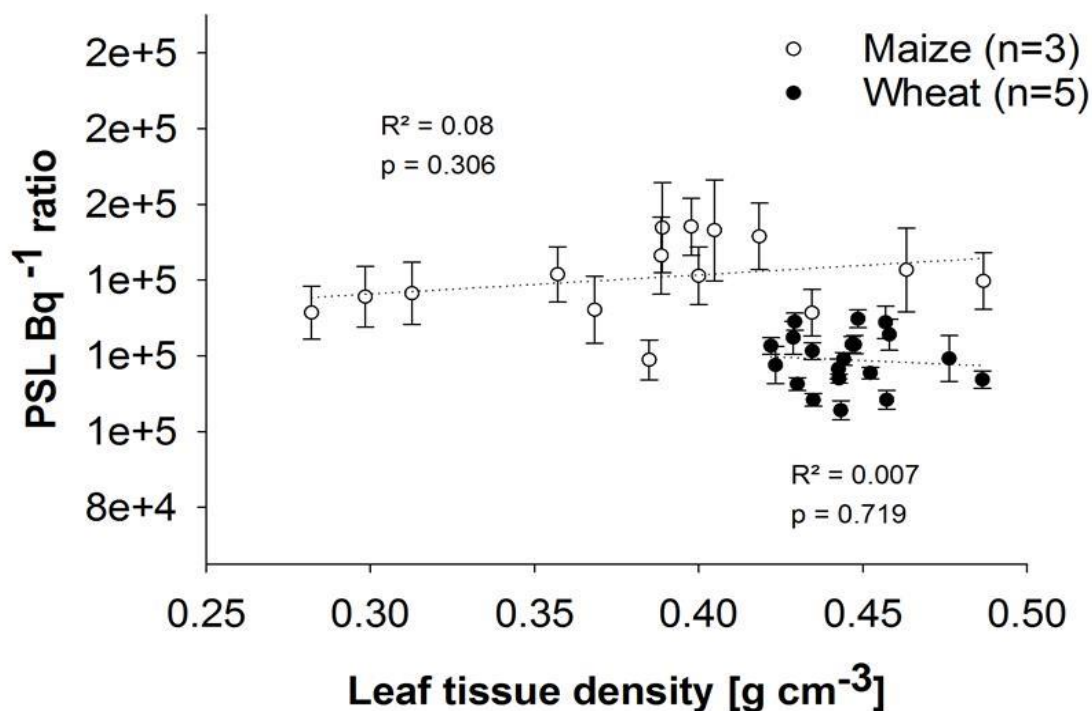


Figure IV-5: Relationship between leaf tissue density [g cm^{-3}] of maize and wheat leaves and the ratio of measured photostimulated luminescence (PSL) assessed via autoradiography and ^{33}P activities assessed by liquid scintillation counting (LSC). The ^{33}P labeled excised leaves of maize ($n=3$) and wheat ($n=5$) plants were first dried and then exposed for 4 h to imaging plates and afterwards scanned by the Bioimager CR35. For LSC analyses leaf materials were digested (HNO_3 pressure digestion) and 3 aliquots of every digest were analyzed.

We plotted the calculated ^{33}P activities of plant leaves against their ^{33}P activities, which were estimated by LSC analyzes (Fig. IV-6). A significant linear correlation was found for both the excised maize ($R^2 = 0.99$, $p < 0.0001$) and wheat leaves ($R^2 = 0.99$, $p < 0.0001$) (Fig. IV-6). Generally, the calculated activities were in good agreement with the ^{33}P activities measured by LSC, with overall recoveries averaging $100\% \pm 12\%$ (for single plant species: maize = $114\% \pm 8\%$; wheat = $94\% \pm 6\%$).

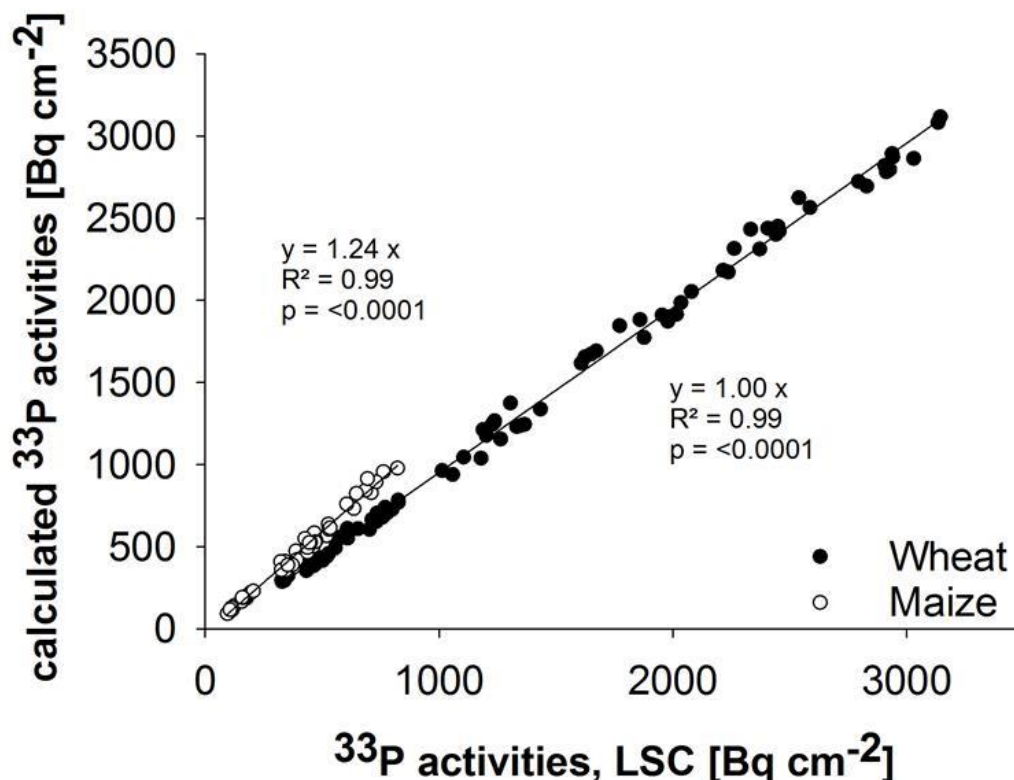


Figure IV-6: Relationship between measured ^{33}P activities [Bq cm^{-2}] assessed by liquid scintillation counting (LSC) and calculated ^{33}P activities [Bq cm^{-2}] from autoradiography. All activities of single ^{33}P excised leaves of maize ($n=3$; over 3 imaging events) as well as of wheat ($n=5$; over 5 imaging events) are displayed. The results revealed a highly significant linear correlation between measured ^{33}P activities in the excised leaves (obtained via LSC) and the calculated ^{33}P activities using the outlined quantification method.

4 DISCUSSION

4.1 Linear dynamic range and plate sensitivity

The present study aimed to develop a fast quantitative application of digital autoradiography. It provides here for the very first time a standardized processing and calculation procedure to quantify ^{33}P activities in plant leaves after uptake of labeled P. The high linear agreement of PSL response for ^{33}P and ^{14}C activities (Fig. IV-2) confirms earlier suggestions of Eakin *et al.* (1994) and Cremer *et al.* (2009) who also found a constant relationship between ^{14}C and ^{33}P activities for a specific range of activity. The procedure described here can be used routinely up to ^{33}P activities of 2000 Bq cm^{-2} and a routine limit of detection of approximately 50 Bq cm^{-2} , and it should be possible to adapt it easily also to other radioactive isotopes such as ^{32}P , ^{35}S or ^{59}Fe . Notably, results with ^{33}P labeled wheat leaves, however, indicated that the range of application can be expanded up to 3000 Bq cm^{-2} , or even higher activities (Fig. IV-6).

In this study, an exposure time of 4 h was found to be optimal. It captured the intensity responses of the applied ^{14}C and ^{33}P activities, and avoided imaging plate overexposure in EXP1 and the excised leaf experiment. A loss of linear PSL response at higher activities of ^{33}P radioisotopes occurred in EXP2, the reference experiment at the end of the study. Results indicated that the imaging plate sensitivity can be exceeded or exhausted by repeated exposure (Upham and Englert 2003), even after repeated erasing processes. This was visible in the decrease of sensitivity in EXP2 towards the end of

the study (Fig. IV-4); the increment of PSL intensities with increasing radioactivity was not linear anymore. After 20 process iterations (approximately 80 h exposure with the outlined erasing procedure), the total plate sensitivity losses were evident (Fig. IV-4). Reichert *et al.* (1992) stating the same observation, therefore recommended to ‘flood’ imaging plates with white light for 24 to 48 h for erasing remaining local artifacts on the imaging plate, which was not done here.

Interestingly, the loss of linearity occurred only for ^{33}P and not for the co-exposed ^{14}C in EXP2. Generally, during imaging plate exposure, the energy emitted by radioactive decay is absorbed by an activator ion of the phosphoric materials in the plate, and then transported through the luminescence material to the host lattice. In the case of BaFX:Eu^{2+} , the quantum of energy emitted by the radioactive decay ionizes the activator ion Eu^{2+} and converts it to Eu^{3+} ($4f-5d$ transition). This liberates excited electrons, which are trapped in a bromine vacancy in the host lattice ($\text{BaFBr}^{\cdot-}$) to form F centers (type of crystallographic defect in which an anionic vacancy in a crystal is filled by one or more unpaired electrons). The electrons are thereby stored in a meta-stable energy state (Takahashi *et al.* 1984; Takahashi *et al.* 1985; Takahashi 2006). Due to higher emission energies of ^{33}P radioisotopes, compared to ^{14}C radioisotopes, the excitation from ^{33}P radioactive decay is larger during imaging plate exposure. Hence, more electrons are captured from ^{33}P in the meta-stable energy state during a given time interval. Therefore, the maximum imaging plate storage capacity was reached faster for ^{33}P than for ^{14}C exposure. Care has to be addressed to the exposure time and the amount of the most active radioisotope (Upham and Englert 2003). We recommend careful pre-testing and imaging plate replacing after experiments with radioisotopes of high emission energies when quantification is intended.

4.2 Quantification of ^{33}P leaf tissue concentration

The PSL responses of imaging plates to exposed radioactive decay can be described by a function of distance of the radioactive source, its activity, and the material density (affecting self-absorption) (Johnston *et al.* 1990; Robu and Giovani 2009). By multiplying ^{14}C PSL intensities with the equivalence factor of 9.73 (Fig. IV-2 and Fig. IV-3), and dividing it by the measured ^{33}P PSL intensities (from the excised leaves) (Fig. IV-3), we were able to provide a highly significant, linear correlation between calculated and measured ^{33}P activities for both crops (Fig. IV-6).

The thickness of the leaf tissue correlated slightly negatively with both the PSL response ($R^2 < 0.24$; $p < 0.005$) on the imaging plate as well as with LSC response ($R^2 < 0.19$; $p < 0.05$). Yet any absorption and subsequent self-attenuation of radioactivity must result from interactions with tissue material, i.e., as outlined in the introduction section it is a function of tissue density rather than of tissue thickness (Robu and Giovani 2009; L'Annunziata 2012). The leaf tissue densities, however, did not affect the quantitation of ^{33}P activities (Fig. IV-5). As the measured leaf densities are representative for a range of monocotyledon plants (Robu and Giovani 2009), we conclude that natural ranges of plant leaf tissues are not significantly attenuating radiation.

A lacking impact of biological tissue thickness on the PSL response of ^{33}P activity appears to contradict results found earlier by other researchers working with brain paste slices (Eakin *et al.* 1994; Cremer *et al.* 2009). They analyzed ^{33}P activities in slices of different thickness and found a linear increase of radioactivity with tissue thickness on the one hand and PSL intensity variations, especially with increasing tissue thickness on the other. Eakin *et al.* (1994) recommended that uniformity of tissue thickness is therefore important to obtain consistent quantitative results. This is reasonable for materials with tissue densities close to 1 g cm^{-3} as likely investigated for the brain slices used in that study, because this at such density absorption of radioactivity is increasingly captured when thickness increases. In dried plants and thus in our study, however, averaged leaf densities were $0.38 \pm 0.06 \text{ g cm}^{-3}$ (maize) and $0.46 \pm 0.02 \text{ g cm}^{-3}$ (wheat), taking into account the mesophyll

intercellular air spaces and total leaf dryness. At thus lower density, absorption of radioactive decay by plant leaves obviously plays a minor role, which was also supported by the close agreement of calculated and measured radioactivity concentrations in the plants (Fig. IV-6). A subsequent study using the described method for ^{33}P quantification in plant sections of whole plants (Fig. C2) demonstrated that it is also applicable for random leaf parts, and not only leaf tips.

In summary, we developed an enhanced, fast and quantitative autoradiography method for imaging ^{33}P activities, which is now applicable for plants and probably other biological systems up to a spatial resolution of 100 μm . Our results suggest that after drying, ^{33}P activity in specific plant compartments can be appropriately quantified by digital autoradiography under the following conditions: (a) appropriate erasing and sensitivity maintenance of the imaging plates, (b) co-application of ^{14}C polymer references, (c) applications of the radiotracers within the linear response range of radioisotopes (here, between 50 and 2000 Bq cm^{-2}), (d) adequate exposure times to maintain PSL linearity, and (e) the calibration of an equivalence factor for PSL intensities of ^{14}C and ^{33}P radioisotopes, being 9.73 in our experiments.

V

FINAL DISCUSSION

1 SUMMARY OF THE RESEARCH OBJECTIVES

Uncertainties regarding scarcity of phosphorus (P) reserves for the production of mineral P fertilizers in the long term, but also environmental effects resulting from excessively high concentrations of P in surface waters and its value as essential crop nutrient to meet the demands of the expanding world population's food supply have encouraged scientific efforts to find ways to improve the efficiency of P use in fertilized arable soils (Syers *et al.*, 2008). There is a broad scientific consensus to improve the understanding of the fate and residual value of P fertilizers supplied to the soil. Information gained can be used to increase its use efficiency and utilization rate in order to reduce fertilizer usage to the required level, while at the same time it ensures the mandatory high yields in agricultural production. Therefore, an objective of modern P research is to orientate the already existing knowledge on soil P dynamics beyond the frequently only methodologically defined P fractions towards a primarily **environmentally relevant understanding of the existing chemical P speciations** in agricultural important soils. The investigation of existing and sometimes massive soil P deposits, their quantities and detailed chemical differentiation is indispensable and urgently required. This information can then be linked to a sustainable fertilizer management. However, this also includes the evaluation of the soil-inherent potential to contribute to adequate supply with plant available P (the so-called P buffer capacity of a soil). An adequate soil P supply potential is particularly important when it is needed by the crop, i.e., in the most active period of growth (Syers *et al.*, 2008). Therefore, also the development, combination and improvement of efficient methods for the evaluation of readily available P in soils must be promoted in order **to enable rapid and functionally-defined P analysis** (Condon and Newman 2011; Kruse *et al.* 2015).

This work comprises three interlinked areas of current P research outlined above. In a first study, the dominant chemical forms of soil P stocks under the influence of different long-term fertilizer applications were elucidated. Therefore, the effect of P fertilizer inputs on the composition of P in the entire soil profile was considered and the hypothesis was pursued that the P fertilizer source and the amount applied have direct influence on the dynamics of soil P as well as on the accumulation of P from fertilization, especially in the subsoil. The knowledge gained formed the basis to investigate efficient utilization of P stocks located in the whole soil profile. In the second study, the contribution of predominant soil P forms to the overall soil P supply of plants was analyzed. This P accessibility study comprised two soil orders since it was known from the literature that not only the chemical form of P in the soil but also soil physical properties determine the efficiency of P uptake by plants. The investigations carried out were mostly hampered by the destructive analysis of the plant materials for ^{33}P concentration analysis at the end of the study, which, however, also permitted a time resolved monitoring of the uptakes of ^{33}P into the shoots. To avoid destructive sampling, therefore, a new quantification method was established to determine the activity of ^{33}P radioisotopes in dry plant leaves, and thus the plant's P uptake. On the basis of a cost-efficient, fast, and high-throughput application, this method contributes to the elucidation of spatial P dynamics and uptake of soil P, and thus to an overall progress in P research.

The results gained allowed to answer the main research questions outlined in chapter I:

I. How are phosphorus stocks and phosphorus speciation in arable soil profiles affected by long-term application of inorganic and organic phosphorus fertilizers?

As agricultural productivity depends on the use of P – of which not only the topsoil but also the subsoil can provide P to the plants – this study hypothesized that past P fertilizer inputs sustained or increased the P stocks in the whole soil profile and with that influenced the P speciation and thus bioavailability of soil P. To assess the availability of soil P forms for plant nutrition, the P status of Stagnic Cambisol profiles (0 cm to 90 cm soil depth; long-term fertilizer experiment at the University of Rostock) in experimental plots that received different P fertilizer applications for 16 years were compared. Sequential fractionation was combined with P *K*-edge XANES spectroscopy and liquid ³¹P-NMR spectroscopy to characterize the chemical form of dominant, inorganic and organic P species. Fertilized topsoils showed P stocks being larger by a factor of 1.2 to 1.4, and subsoil stocks being larger by a factor of 1.3 to 1.5 than the unfertilized control treatments. The P-XANES analyses revealed the predominance of mainly inorganic P species, such as moderately labile Fe- (46 to 92%), Al- (0 to 40%) and Ca-P (0 to 21%) compounds besides organic P (0 to 12%). These findings were supported by ³¹P-NMR analyses who indicated decreasing proportions of orthophosphate monoesters from topsoil (20 to 28%) towards the second subsoil layer (7 to 13%). In summary, the investigation showed that fertilizer application maintained or increased P stocks along the whole soil profile but only slightly altered the P speciation throughout the profiles after 16 years of fertilization. Hence, the kind of fertilizers had no significant effect on the final soil P status, only the amount of applied P in total affected mainly the inorganic P pools.

Results from another long-term fertilizer experiment located in Bad Lauchstädt (Haplic Chernozem, 4 different fertilized soil profiles 0 to 90 cm, longer duration (> 100 years); analyzed in accordance to chapter II) are implemented in the following synthesis as they showed supporting trends of P stocks and speciation in a different soil order. Differences between the fertilizer treatments and the unfertilized control treatment were more pronounced, which may result from the longer duration of this fertilizer experiment.

II. Can P from oxidic (sub)soil forms sufficiently contribute to plants soil P demand?

There is currently relatively little available information on subsoil P use for crop production as a function of soil order. In this study, a rhizobox experiment was performed using subsoils of two reference soil groups, an Orthic Ferralsol and a Haplic Luvisol. To evaluate the immediate P uptake by wheat (*Triticum aestivum* L.) from different subsoil P pools during 14 days of growth, subsoil bands were spiked with KH₂PO₄ solution associated to Fe-hydroxide (³³P-Fe), to Al-hydroxide (³³P-Al), in free form (³³P-OrthoP), or in trace amounts without any additional ³¹P (³³P-NoP). At the beginning of the experiment, the soil water content was set at 75% of water-holding capacity, corresponding to an initial soil matric potential of -12 ± 1 kPa. During plant growth, soil moisture decreased in both soils, but soil matric potentials in both soils did not drop below field capacity (-33 kPa; pF 2.5). The shoot dry weights of the Ferralsol were 1.2 to 1.8 times those of the Luvisol. The amount of ³³P taken up by the shoots from the oxide phases was 15 to 40% greater in the Ferralsol treatments than in those in the Luvisol treatments. It was concluded that the more favorable physical soil conditions facilitated ³³P uptake from both oxidic phases from the Ferralsol subsoil relative to the Luvisol subsoil, despite better P phytoavailability in the latter.

III. Is digital autoradiography an efficient, non-destructive and spatially resolved method for ^{33}P radioisotope quantification in plant leaves?

Phosphorus uptake studies in the past were hampered by the processing and analyzing conditions of P, i.e., the destructive pressure-digestion of the plant material and subsequent wet-chemical analysis of P concentrations. This is also notably as P research still lacks techniques for rapid imaging of P uptake by plants and P allocation in different soil, sediment, and biological systems in a quantitative manner. In this study, we describe a time saving and cost-efficient digital autoradiographic method for in-situ quantitative imaging of ^{33}P radioisotopes in plant materials. The described method combines digital autoradiography of the radiotracer applications with additions of commercially available ^{14}C polymer references to obtain ^{33}P activities in a quantitative manner up to 2000 Bq cm². I showed that linear standard regressions for both radioisotopes are obtained, allowing to establish a photostimulated luminescence equivalence between both radioisotopes with a factor of 9.73. Validating experiments revealed good agreement between the calculated and applied ^{33}P activity ($R^2 = 0.96$). This finding was also valid for the co-exposure of ^{14}C polymer references and ^{33}P radioisotope specific activities in excised plant leaves for both maize ($R^2 = 0.99$) and wheat plants ($R^2 = 0.99$). The outlined digital autoradiographic quantification procedure retrieved 100±12% of the ^{33}P activity in the plant leaves, irrespective of plant tissue density. The simplicity of this methodology opens new perspectives for fast quantitative imaging of ^{33}P in biological systems and likely, thus, also for other environmental compartments.

2 SYNTHESIS AND OUTLOOK

The results of this thesis showed that long-term excess P fertilizer applications had increased the stocks of P pools with different availabilities in the soil profile. However, it was also indicated that the soil-inherent P availability without any P fertilization was still sufficient to supply P to the plants over decades, even if the P uptake by the crop tended to exhaust the readily available soil-inherent P reserves. It can be assumed that the subsequent replenishment of plant available P via, i.e., desorption from moderately labile P forms (provided that they are spatially accessible) can compensate for the absence of soluble P from fertilizer applications. The results, therefore, indicated that the current fertilizer recommendations underestimate the intrinsic P supply potential of long-term fertilized arable soils. It is conjecturable that especially European arable soils even without excessive P fertilization can sufficiently cover the annual demand for P by the crop, presumed the subsoil P pool is physically accessible (Gransee and Merbach 2000). In addition, other factors such as climate, vegetation control, and a balanced nutrient ratio contributed to the general P use efficiency, which depended also on the respective soil order and related physicochemical soil properties, such as the potential of soil water replenishment. Moreover, with the third chapter of this thesis I may now offer an efficient modern instrument on the basis of digital autoradiography, that enables a spatially resolved and quantitative determination of P radiotracer concentrations in plants. The fields of application include further biological systems as well as other environmental compartments.

2.1 Limitations of phosphorus supply in fertilized arable soils

Long-term fertilizer experiments have shown that soil P stocks were maintained or increased due to the P inputs via fertilizers over many decades. However, also the unfertilized control treatments were not lacking available P (Resin-P and $\text{NaHCO}_3\text{-P}$ stocks) over long durations of cultivation (Table II-2 and Table D2) so that sometimes only after decades yield losses arose (Selles *et al.* 1995; Gransee and Merbach 2000). The use of P fertilizers on arable soils in Europe can thus be seen as a kind of “luxury treatment” considering that there is a sufficient supply of P to the crop P needs. A decisive reason for

this is a low level of weathering in European soils, which implies that the soil-inherent P reserves, e.g., from the parent rock are sufficiently available. With pedogenesis, these reserves can be mobilized over time and thus continuously contribute (however to a lesser extend) to the P supply of the crop (Bauke *et al.* 2018). In heavily weathered soils, such as Australian Ferralsols, the available, soil-inherent P reserves have been largely exhausted or lost through advanced pedogenesis (Walker and Syers 1976). The advanced chemical weathering of these soils led to lower soil pH and high concentrations of amorphous and crystalline Fe and Al (hydr)oxides (Table III-1), which limit P mobility and thus sufficient soil P plant availability (Yang and Post 2011). Such differences between general soil groups indicate right from the beginning, that the P dynamics and the general P supply of the crop in a given soil are strongly related to the present chemical and physical soil conditions.

Since crop growth depends on adequate supply of dissolved P, an optimal P plant availability in the soil can only be sustained by steadily maintaining a certain P concentration in the soil solution. During the vegetative phase, especially in the first 6 to 10 weeks, when the P uptake by the crop is highest (Römer and Schilling 1986; Veneklaas *et al.* 2012), more P is required daily (approximately 0.3 to 0.5 kg ha⁻¹ (Syers *et al.* 2008)) than is actually present in the soil solution (less than 0.2 kg ha⁻¹ (bulk soil) and 0.075 kg ha⁻¹ (rhizosphere) (Syers *et al.* 2008)). Therefore, the available P concentration in soil solution is restricted during the period of the highest P requirement in the growing season. Due to higher demands, the P concentration in the soil solution tends to be replenished multiple times a day, e.g., by diffusion of desorbing soil-inherent P or by dissolving external P from fertilizers.

Fertilizer applications by introducing high soluble P into the soil should guarantee such a sufficient P concentration in the soil solution according to crop requirements. After application, the main component (monocalcium phosphate) of mineral fertilizers, i.e., superphosphate and triple superphosphate, is initially converted by hydrolysis processes into a meta-stable acidic composition of monocalcium phosphate, dicalcium phosphate dihydrate, and phosphoric acid. Within a short period, the more stable dicalcium phosphate dihydrate continues to dissolve, while highly insoluble components such as hydroxyl apatite precipitate (Sanyal and De Datta 1991). Due to this fast solubilization of the superphosphate the soil solution is, on the one hand, saturated with freely available ortho-P after fertilizer applications (Sample *et al.* 1980). However, on the other, in excess applied P interacts with the soil matrix and is thus rapidly adsorbed by soil particles (this can account for up to 76% of the fertilizer P applied) (Wechsung and Pagel 1993; Blake *et al.* 2000; Tunney *et al.* 2003). Overtime this “remaining fertilizer P” can be mobilized again and contribute to the supply of P to crops (Pheav *et al.* 2003; McLaren *et al.* 2016).

The main limitations for an accurate determination of soil P supply to plants, which have to be carefully considered, arise from the limited potential of the plant roots to explore the entire soil volume. Estimations suggested that only 25% of the topsoil volume in a vegetation period stands in close contact with the root zone (Jungk 1984). However, it can be assumed that the presence of roots in the topsoil (especially the root length density) is always high, whereas the subsoil is less penetrated by roots with increasing depth (Bauke *et al.* 2017a). **Therefore, the spatial distributions and quantities of P stocks in the soil profile are decisive for the evaluation of a sufficient supply of P to the crop, irrespective of the soil depth where the external P fertilizers are applied.**

Beside spatial limitations, adequate P supplies strongly rely on the chemical nature of the P forms close to the plants' roots, as it determines their availability for the plants. The P concentration gradient in the root-ambient soil phase (also known as **rhizosphere**), mainly caused by the P uptake of the crop, can reach sufficient P desorption and diffusion rates providing plant available P. This so-called intrinsic soil **P buffer potential** is generally influenced by soil physical parameters such as soil acidity, moisture and temperature. Hence, the “speed” and potential of P replenishment depends

overall on the "soil P composition", i.e., the amount and chemical form of the P stocks in the soil. **The elucidation of the chemical nature of dominant soil P species must, therefore, receive attention first in order to comprehensively assess the potential for P supply for plants in a specific soil.**

2.2 Phosphorus stocks in fertilized arable soil profiles as modified by fertilizer usage

Phosphorus applications on agricultural important soils in Europe, i.e., Anthrosols, Luvisol, Cambisols, and Chernozems, often exceeded the P requirements of the crop or are applied in an unbalanced nutrient ratio. Surplus P from fertilizer applications thus subsequently accumulated in the topsoil but also leached out into deeper soil layers (Khan *et al.* 2018). Results from 10 long-term fertilizer experiments, summarized by (Hooda *et al.* 2001) showed a net accumulation of 16 to 232 kg P ha⁻¹ year⁻¹. Gransee and Merbach (2000) published results of a long-term fertilizer experiment in Halle (Luvic Phaeozem) which has received different amounts of P fertilizer (0, 15, and 45 kg P ha⁻¹ year⁻¹) for 50 years. The P balance (P inputs minus P output) over the duration of the experiment was only positive (+800 kg P ha⁻¹) for the treatment which has received 45 kg P ha⁻¹ year⁻¹. Literature reported for the treatments with surplus P analyzed in this thesis (combination of organic and mineral fertilizer applications) a surplus over 14 years of +258 kg ha⁻¹ (Rostock, Stagnic Cambisol, additions of approximately 47 kg P ha⁻¹ year⁻¹ (Requejo and Eichler-Löbermann 2014)) and a surplus over 84 years of +2652 kg ha⁻¹ (Bad Lauchstädt, Haplic Chernozem, additions of approximately 50 kg P ha⁻¹ year⁻¹ (Wechsung and Pagel 1993; Körschens 1994)). These fertilizer P surpluses were in line with the here found significantly higher P stocks in the soil profile of these fertilizer treatments (total P stocks: Table II-2 (Rostock) and Table D1 (Bad Lauchstädt)).

However, at annual P fertilizer applications of up to 15 kg P ha⁻¹ year⁻¹ in Halle, the P balance was already negative (-349 kg ha⁻¹). Hence, this P fertilizer dose did not meet the crops requirements, leaving an average annual loss of approximately 7 kg P ha⁻¹ over the last 50 years behind. Interestingly, despite the P surpluses in the treatment with highest P inputs the average yields of the three fertilizer treatments (0, 15, and 45 kg P ha⁻¹ year⁻¹) were not significantly different (Gransee and Merbach 2000), especially when compared to the control treatment which has received any P additions. Hence, **lower total P stocks in the soil profile of the treatments with negative P balances suggested a re-supply and/or acquisition by the crops from soil-inherent P forms from deeper soil depths** (Gransee and Merbach 2000).

Assuming an average annual P removal of 20 to 28 kg P ha⁻¹ (estimated from P removals from the investigated long-term fertilizer experiments Rostock and Bad Lauchstädt (annual removals stated by Wechsung and Pagel (1993); Gransee and Merbach (2000); Requejo and Eichler-Löbermann (2014)) the single fertilizer treatments with either organic or mineral amendments (average annual P application of 25 to 34 kg ha⁻¹ year⁻¹) were able to cover the crops P requirements in the season. Similar to the negative P balance in the fertilizer treatment with 15 kg ha⁻¹ year⁻¹ in Halle, Requejo and Eichler-Löbermann (2014) stated that the P balance of the compost treatment in Rostock was still negative (soil P removals of -4.4 kg ha⁻¹ year⁻¹). The opposite was found in Bad Lauchstädt, Wechsung and Pagel (1993) calculated positive P balances for organic and mineral single P fertilizer applications, leaving an annual P surplus of +7.4 to +16.4 kg ha⁻¹ year⁻¹ over 84 years behind. In conclusion, Wechsung and Pagel (1993) reported that P inputs of 12.9 kg P ha⁻¹ would have already compensated for the P removals at the experimental site in Bad Lauchstädt. Hence, in the first instance an excess P supply via the annual fertilization in Bad Lauchstädt could be assumed. However, if one considers the average annual P requirement, e.g., of wheat of 35 to 40 kg P ha⁻¹ (LWK Nordrhein-Westfalen, 2017) it has to be assumed here that these P fertilizer quantities have covered only a part of the P requirements. This, however, legitimates the official fertilizer recommendations (of up to 40 kg P ha⁻¹) but also indicates that in the single fertilizer treatments (P inputs of up to 34 kg P ha⁻¹) **soil-inherent P**

stocks must have undergone annual reductions over the duration of the long-term experiments, if the crop's P requirement in a season is not met by the applied P fertilizer quantities. Concluding, a general fertilizer influence on the soil P stocks between the treatments was measurable (lowest total P stocks were always found in the unfertilized control treatment and the highest in the surplus treatments (Table II-2 and Table D2)) but the sum of P stocks of the soil profile in Rostock (total P stocks: 3827 to 5532 kg ha⁻¹) and in Bad Lauchstädt (total P stocks: 5019 to 9652 kg ha⁻¹) were relatively high. This agrees to the fact that annual soil P losses of 4 to 7 kg P ha⁻¹ as outlined above, affected these P stocks in the soil profile, even over many years only slightly.

With regard to the P stock in the soil profiles; all treatments showed comparable depth related differences. The distribution of the P stocks in the soil profile of both long-term fertilizer experiments decreased with increasing soil depth. This seemed reasonable, since the surface application of P fertilizers, but also the exploration and acquisition of P from the subsoil or the parent rock by the crop, generally leads to an accumulation of larger P reserves in the topsoil. However, the results also showed that the P stocks in the soil profile were equally distributed half within the topsoil (0 to 30 cm) and half within the subsoil (30 to 90 cm) irrespective of the fertilization regime. The migration of surplus P (here with emphasis to the surplus treatments) into deeper soil layers due to increased mobility of P can be explained by the saturation of the soil sorption sites (the degree of P adsorption (DPS) was > 30% in the fertilizer treatments, Table II-1, Table D1), especially in the topsoil, and a subsequent migration of unbound P, i.e., via preferential paths (Bauke *et al.* 2017b) into deeper soil layers. Medinski *et al.* (2018) just recently reported increased P stocks up to soil depths of 60 cm in Bad Lauchstädt due to P fertilizer inputs. On the other side, rhizotron experiments conducted by Bauke *et al.* (2017a) clearly showed that **the transport of topsoil P into deeper soil layers mediated by plant roots has a decisive role for reallocations of soil P within the soil profile and thus has also to be taken into consideration when analyzing soil P dynamics.**

Limitations arose, since the exact contributions from massive soil-inherent top- and subsoil P stocks at negative P balances cannot be estimated since no data are available reporting original P stocks up to 90 cm at the beginning of the long-term experiments. It is therefore not certain whether the treatments with organic or mineral fertilization also led to an accumulation of P stocks or P additions just have sustained the endogenous level of soil P stocks. Valid answers on the P status without fertilizer usage can only be obtained by the control treatment without P inputs. As highlighted above, yields in the control treatment were not reduced due to the absence of P inputs for many decades, which indicated that **the annual crop-related soil P removals in the control treatments also must have originated from either readily available external P or from available P stocks from the soil profiles.**

By mobilizing P from moderately labile and stable P fractions, the demand for P by crops can be met for many years (Spratt *et al.* 1980). The sequential P fractionation revealed that, especially in the control treatment in Bad Lauchstädt the P stocks of different P fractions in the topsoil but also in the first subsoil layer were reduced compared to the treatments with P inputs (Table D2). In the relatively young long-term experiment in Rostock these findings were not pregnant. Gransee and Merbach (2000) also stressed the importance of the P re-supply from moderately labile P fractions with respect to soil P dynamics of a long-term test site in Halle. The authors emphasized potential importance of moderately labile subsoil P stocks providing readily available P, when labile P stocks in the topsoil are depleted. **It can be assumed that the differences found between both control treatments of the long-term experiments indicate that not only the fertilizer application but also the period of cultivation and thus the amount of easy available soil P removed from the soil profile is decisive and significantly affects the P status (towards less available, stable P species in the long-term) in the soil profile.**

2.3 Phosphorus speciation in arable soil profiles as modified by fertilizer usage

Current P research is still lacking information on the extent to which the P forms present in the soil profile are physically available (spatial accessibility with depth) to the crop, and if, how they are utilized in terms of their chemical availability (Kuhlmann and Baumgartel 1991; Syers *et al.* 2008; Kautz *et al.* 2012). The use of soil depth-resolved sequential P fractionation in combination with spectroscopic methods in this thesis made it possible to elucidate P forms at the molecular level as influenced by the use of P fertilizer.

Independent of the type of fertilizer applied (i.e., inorganic or organic), the soil P forms vary only slightly, since both inorganic and organic P fertilization generally result in the introduction of soluble inorganic P being present in the soil solution (Sharpley 1986; Hao *et al.* 2008; McLaren *et al.* 2016). Selles *et al.* (1995) analyzed the effect of fertilization on soil P availability and found that fertilizer P not taken up by the plants (above already designated as “remaining fertilizer P”) accumulated predominantly in plant available P forms. Thus, in the first instance, fertilizer P increases the inorganic labile (NaHCO_3 -extractable) and moderately labile (NaOH -extractable) soil P fractions (Pheav *et al.* 2003) in the topsoil. Similar hints were found in chapter II of this thesis. When considering the P fractions of the fertilized treatments as delta to the control, in Bad Lauchstädt the delta of the labile (Resin-P and NaHCO_3 -P) and moderately labile P fractions (NaOH -P) dominated in the treatments with P inputs (Fig. D2). As assumed above, this indicated that especially in the control treatment in Bad Lauchstädt the labile and moderately labile P stocks were more depleted (effects of seasonal depletion due to P removal by the crop has to be expected) most likely because of the long-term absence of P inputs with continuous soil P utilization by crops and the subsequent removal of harvest products. A similar trend, was already shown by Blake *et al.* (2003) and suggests a soil P re-supply potential by continuous replenishing of P in soil solution from the soil, if no yield losses occurred (Körschens 1994). This may have reduced the moderately labile soil P species over time – as already assumed above – leaving less available, stable P species in the control treatment augmented. However, the delta of the stable P fractions (here mainly Residual-P) dominated the soil profiles in Rostock (Table II-2 and Fig. D1). In such a relatively young long-term fertilizer experiment, labile P depletions in the absence of P inputs seemed not far advanced (low delta of the labile P fractions in the fertilized treatments, Fig. D1) and thus the effect of P re-supply from moderately labile P pools was not that pronounced. However, it is known that also seasonal variations affect the soil P pool (Saunders and Metson 1971; Magid and Nielsen 1992), which limits the significance of a comparison between the fertilizer induced effects on soil P pools in both long-term experimental sites; the samples in Rostock were taken before and in Bad Lauchstädt after the cultivation season in 2015. These differences were especially visible in the concentrations of readily available P in soil solution (P_{CAL} values, Table D1). In Bad Lauchstädt differences between the fertilized treatments and the control treatment were significant (between 6 to 26 times higher P_{CAL} concentrations); whereas in Rostock no significant differences appeared (0.9 to 1.4 times higher P_{CAL} concentrations; hence here a re-equilibration after the cropping period, during winter can be assumed). This indicated that effects on P availability affected by plant growth and harvest have to be considered too, also for further conclusions. **Nevertheless, from these findings also fundamental indications arose that the moderately labile P species indirectly contributed to the P supply of the crop by assumingly buffering the available soil solution P concentrations in the long term.**

When P is being applied in excess to the soil, i.e., above the short-term requirements of the crop, it is distributed between different soil P pools with time. In dependence on the soil group, it can be predominantly fixed by surface-reactive amorphous Fe and Al (hydr)oxides (Sanyal and De Datta 1991). This was also found here with fertilizer-induced shifts towards higher NaOH-P_i proportions (representing moderately labile inorganic P sorbed or fixed by Fe and Al (hydr)oxides) especially in

the mineral fertilizer treatments in Rostock and Bad Lauchstädt as revealed by sequential P fractionation (Table II-2 and Table D2). This was confirmed by higher proportions of P associated with Fe and Al soil compounds in the soil profiles of all treatments in the Cambisol (between 46 and 92%, Rostock), but also in the Chernozem soil (between 0 and 50%, Bad Lauchstädt) as determined by XANES spectroscopy (Fig. II-2 and Table D3). **The proportion of P associated to Fe-species increased with depth in all treatments, whereas the opposite was found for Al-P species. Therefore, slight influence on the inorganic P speciation due to the introduction of fertilizer P can be confirmed** in this thesis. These trends were also found by other scientist showing that especially mineral fertilizer P was first associated with Al compounds in the topsoil (Eriksson *et al.* 2015).

Audette *et al.* (2016) suggested that the remaining fertilizer P not taken up by crops, either applied as inorganic and organic form, transforms into labile and moderately labile P forms in the first place along the migration into more stable P pools with time. Hence, a trend towards phase saturations can allow migration into deeper soil layers, which then can also contribute to the formation of less-soluble Ca-P species in the subsoil (Schmieder *et al.* 2018). Khatiwada *et al.* (2012) showed that 6 month after fertilizer application (if not taken up by the plant) most of the remaining fertilizer P was transformed into stable Ca-P and Fe-P soil species, irrespective of the form the fertilizer was applied to the topsoil. Similarly, Ahlgren *et al.* (2013) showed in a ^{31}P -NMR study, that the amount of extractable inorganic P did not increase as much as the total inorganic P proportions under fertilizer applications. They assumed that a part of the inorganic P-build-up from fertilizers went into more stable, not extractable P pools. However, the altering of P speciation due to fertilization and thus also the formation of Ca-P species is influenced by the soil group (including its properties such as weathering stage and parent rock material) (Beauchemin *et al.* 2003; Ulen and Snall 2007; Eriksson *et al.* 2016b).

A general dominance of the stable P pool (especially the H_2SO_4 -extractable P) in Chernozem soils as present in Bad Lauchstädt, which build up on calcareous loose rocks being mainly loess from the last ice age 12000 years ago (Altermann *et al.* 2005), was expected. The XANES spectroscopy revealed that in Bad Lauchstädt up to 50% of P were Ca-P compounds (Table D3). These results were in line with the relatively high H_2SO_4 -P stocks comprising of mainly insoluble P associated with Ca and Mg minerals (Chang and Jackson 1957; Golterman and Booman 1988; Pierzynski *et al.* 2005), which increased with soil depth (Table D2). At soil pH in the neutral to alkaline range, as found in Bad Lauchstädt, the precipitation of P as Ca-P (including amorphous Ca-P species in addition to subclasses of apatite and hydroxyapatite) is probable (Lindsay *et al.* 1989). However, also in the slightly acidic Cambisol in Rostock increasing proportions of H_2SO_4 -P stocks with increasing depths were found (Table II-2), whereas XANES spectroscopy did not show dominant proportions of Ca-P compounds in these soil profile (Fig. II-2). Since XANES spectroscopy is based on the use of standard substances, which will hardly be present in the sample in such purity, but rather in mixed or transitional forms, XANES results can only be an approximation of reality of the P speciation in the soil. Therefore, XANES spectroscopy is used to detect the dominant P compounds (usually only up to 4 compounds), but there is always a higher number of P forms in the sample than can be identified by linear combination fitting (Kruse *et al.* 2015). More insights into soil Ca-P speciation may be obtained by the complementary application of Ca-K-edge XANES spectroscopy. In the slightly acidic Cambisol, some Ca-P may remain overall acidic soil conditions, i.e., in incorporated and complexed forms. **A sufficient comparison with the operationally defined fractions from sequential fractionation and XANES spectroscopy will always vary imprecisely because of possible carryovers from one fraction to another** and re-adsorption of P during on extraction step which will enrich the proportions of the acid extraction step (Williams *et al.* 1971; He *et al.* 2006; Condon and Newman 2011).

The overall dominance of P associated to soil oxidic mineral phases but also Ca-P compounds in fertilized arable soils was proven and thus **P fertilizer applications may reduce the diversity of the soil-inherent P species** (Hawkes *et al.* 1984; Leinweber *et al.* 1997; Cade-Menun 2005). Mediated by the annual P inputs, the concentrations but also relative proportions of the “most affected” P species increases, whereas without P additions the P species that are less affected/ less accessible by the crop increase. Therefore, this may explain the low delta to the control of the stable P fraction in Bad Lauchstädt, especially the H₂SO₄-P fractions, being pronounced in the control treatments even after 84 years of continuous P removals (Table D2).

On the contrary to the inorganic P speciation, the organic P fractions in the soil profiles of both long-term fertilizer treatments were of minor importance and not sustainably affected by fertilization. With minor exceptions the P_i/P_o ratios of the treatment with P inputs corresponded to the ratios found in the control treatments (Fig. D3). Similarly to this, a trend towards a higher significance of inorganic P with increasing soil depth could be routinely confirmed in all treatments (Table II-2 and Table D2). In the soil profile of the unfertilized control of the Chernozem in Bad Lauchstädt considerable proportions of organic P were determined by XANES spectroscopy (Table D3); this seems reasonable for the topsoil with its high soil organic matter content (SOM) but not for the subsoils, where the loess layer is found already at shallow depth (approximately below 40 cm; Altermann *et al.* (2005)).

Despite of the total organic P concentration, the ³¹P-NMR analysis of the NaOH-EDTA-extracts showed that the composition of the organic P pool was relatively similar for the treatments of both long-term experiments. A general accumulation of organic P in the topsoil independent of fertilizer usage was not found. Also the annual input of organic residues from the organic fertilizer treatments did not or only slightly increased the organic P content in the soils (Fig. II-3, Fig. D4, and Fig. D5). Same results were reported by Ahlgren *et al.* (2013) who found that the relative composition of organic P species identified by NMR did not change, regardless of the amounts or the kind of P fertilizer (either mineral or cattle manure, alone or in combination).

Low-molecular weight ortho-P monoester compounds dominated the organic P fraction in the topsoil independently of the fertilizer treatment. In Bad Lauchstädt also small proportions of diesters were found, which is generally quite atypical for mineral arable soils (Cade-Menun 2005) but may represent the higher SOM in the topsoil of the Chernozem soil. The great proportions of ortho-P monoesters can partly be considered as degradation products of ortho-P diesters, such as RNA and phosphatidyl choline (Turner *et al.* 2003a). Bol *et al.* (2006) analyzed the short-term dynamics of soil organic P derived from higher organic P compounds in cattle manure and explained that degradation of organic P towards ortho-P monoester as the dominant soil organic P forms was positively correlated with the manure applications. However, it can be assumed that ortho-P monoesters were already enriched in the organic fertilizers as they normally show a high degree of decomposition and therefore already consist to a large extent of inorganic P compounds and low-molecular organic, mainly monoesteric compounds (Sharpley and Moyer, 2000; Turner and Leytem, 2004; Pagliari and Laboski, 2012). In particular, the ortho-P monoester compounds, which comprise of stereoisomers of inositol hexakisphosphate, are considered to be poorly mineralizable and thus its ortho-P is also not directly plant available (Turner and Leytem, 2004). Their high stability and affinity to react with abiotic soil constituents (Celi and Barberis 2005) as well as the introduction by dead organic matter into the soil explains their dominance in the topsoil and suggests an accumulation with increased supply. However, the organically fertilized treatments had no or only slightly increased ortho-P monoester contents than the mineral fertilizer treatments or the control treatments of both long-term experiments. Surprisingly, the relative proportions of ortho-P monoesters in the control treatment were comparable or only slightly lower than in the fertilized treatments (Fig. D4 and Fig. D5). A theoretical accumulation of ortho-P monoester compounds and generally organic P in the topsoil by fertilizer application is

therefore doubtful (Ahlgren *et al.* 2013). Hence, **it still remains unclear if organic compounds introduced by the application of organic fertilizer, especially including the ortho-P monoesters, experienced a turnover in soil (e.g., in the case of low soil P availabilities) and thus providing readily available P, as it was assumed by Turner *et al.* (2003b).**

Alternatively, incorporation or complexation of organic P into stable and non-extractable Residual-P compounds was likely (Velásquez *et al.*, 2016). Residual-P, can consist of occluded inorganic P and organic P forms, i.e., stable humic acids and larger humus-complexes (Cross and Schlesinger 1995), but predominantly ortho-P monoesters (Velásquez *et al.* 2016) being covered or physically encapsulated. The increased stable P fractions (with emphasis to Residual-P) in the topsoil and first subsoil layer of the organic fertilizer treatments as well as in the surplus treatments of both long-term experiments supports this assumption. Interestingly, differences between the two organic fertilizer forms were found. The fertilizer treatment with cattle manure in Bad Lauchstädt showed lower proportions of the non-extractable Residual-P fraction than the treatment with green compost applications in Rostock. In the latter the non-extractable Residual-P fraction dominated the P proportions in the topsoil. Different degradation stages of the organic fertilizer forms, here cattle manure with an advanced degradation stage, but also effects on soil pH (Sato *et al.* 2005) explain these differences between the fertilizer types. Unfortunately, a direct comparison between the effects on soil chemistry due to green compost and manure application are not available in literature. **Furthermore, a more detailed consideration of the chemical structure of the Residual-P forms is not given in this thesis, but would be advisable for future studies, since the non-extractable Residual-P pool build up considerable proportions in soils (proportions of 30 to 80% in dependence on the weathering stage)** (Turner *et al.* 2005; Condrón and Newman 2011). Hence, due to its composition, it is expected that Residual-P is to a certain degree recalcitrant (Condrón and Newman 2011). However, its potential bioaccessibility is largely unexplored (Velásquez *et al.* 2016), mainly due to its chemical complexity.

It can be concluded that the type of fertilizer is of minor importance for long-term P availability in fertilized arable soils. However, the duration, the amount, and the frequency of P fertilizer application to a specific soil group influence its P speciation (Blake *et al.* 2000). Soil P stocks associated to mineral phases, such as amorphous Fe and Al hydroxides, increased or remained constant due to fertilizer P applications, also described in literature (Delgado and Torrent 2000; Wang *et al.* 2010). Also the opposite trend towards a replenishment of labile and moderately labile P species was indicated in this thesis. The reduction of these soil P fractions in absence of P additions over decades highlighted cropping induced effects on soil P pools in general (Blake *et al.* 2003), and especially on the moderately labile P species. The soil physicochemical properties of these prominent highly-adsorbing soil constituents were studied by several researchers (Barrow 1987; Fardeau 1995; Frossard *et al.* 2011); however, information about the dynamics and plants P utilization from these soil fractions under cultivation have not been resolved yet, despite their importance to control soil P mobility and availability by refilling soil solution P (Hinsinger 2001).

2.4 Plant availability and accessibility of ^{33}P from dominant phosphorus forms

Plant P uptake is limited to P in soil solution; therefore, the restricting factors to meet a sufficient P availability for optimal plant P supply are at first the concentration of ortho-P in soil solution and secondary the amount of P that can potentially leave the solid soil phase (Bühler *et al.* 2003; Syers *et al.* 2008). Soil P dynamics in fertilized arable soil profiles mainly rely on inorganic P stocks and results (cf. chapter II) showed that independently of the fertilizer regime, secondary soil minerals, such as Fe and Al (hydr)oxides, are found to be the predominant soil mineral constituents soil P is associated to or precipitated by (Walker and Syers 1976; Yuan and Lavkulich 1994; Gérard 2016). It is

well known that their degree of crystallinity (representative for the reactive surfaces) highly determines P adsorption levels, which in turn determines the P concentration in soil solution and thus the overall P availability in soils (e.g., Schwertmann and Taylor 1989; Torrent 1997; Hinsinger 2001). The relatively strong affinity of P for these mineral surfaces also affects the use efficiency of highly soluble P fertilizers (Khasawneh *et al.* 1980; McLaughlin *et al.* 1988a; Syers *et al.* 2008), as also the dissolving P from fertilizers is rapidly sorbed to or precipitated by the solid soil phase. Besides soil specific thermodynamic and physical parameters such as texture, soil acidity, and ionic strength, the equilibrium between P concentration in the liquid phase and P surface coverage, e.g., of Fe and Al (hydr)oxides is one of the most important drivers that determines adsorption and desorption strength of these P-loaded soil constituents.

In general it is important to emphasize that **it remains questionable whether the individual sorption and desorption assessment of single P species is fortunate to expand knowledge about the supply from soil-inherent P forms for plants** and thus on general P use efficiency in the complex soil matrix. Studies that focused on the elucidation of the P supply from specific P species being introduced into a soil matrix are limited, but being advised by literature (McBeath *et al.* 2012). Especially, P accessibility of introduced P-loaded synthetic oxidic phases in soils have not been reported yet; however, when combined with radiotracer techniques they can provide valuable information to the understanding of plant uptake related soil P dynamics as they dominate soil P pools (cf. chapter II). Therefore, the rhizobox experiment in chapter III served to investigate the accessibility of these predominant amorphous Fe and Al hydroxide P forms to plants, blended in two subsoils of different orders.

Different ^{33}P plant uptake rates and probably P availabilities between the soil orders can be related to soil physical properties of the Ferralsol and Luvisol subsoil (Fig. III-2 and Table III-1). Most probably the differences in plant development (shoot dry weights) arose from the fact that no irrigation was planned in this experiment (irrigation can induce pH equilibrium changes, which can have influence on sorption and desorption equilibria of cations and anions bound to mineral phases, which may have affected P desorption behavior from the Fe and Al hydroxide surfaces (personal communication; F. Gérard, May 2018)). Thus, soil water availability was highly dependent on the soil order-inherent ability to replenish water, e.g., in the rhizosphere. Here, due to the more stabilized soil structure (Table III-1) (Goldberg *et al.* 1990) the water supply for the plants was better in the more oxidic and clayey Ferralsol than for the Luvisol (Fig. III-2). Better growth conditions with improved root developments and better spatial P accessibility in the Ferralsol manifested these results. However, improved P diffusion properties from the bulk soil to the rhizosphere in the Ferralsol could also be assumed, which guaranteed a constant P availability in soil solution for plant roots (Lewis and Quirk 1967; Bhadoria *et al.* 1991).

Different ^{33}P plant uptake rates between the ^{33}P -treatments (with greater ^{33}P uptake rates in the ^{33}P -Fe treatments, Table III-2) can be related to insoluble solid phase Al-P compounds (cf. chapter III) and a certain Al-phytotoxicity in the ^{33}P -Al treatments. To verify phytotoxic side effects, I applied a plant-agar system using either a ^{32}P loaded Fe and Al hydroxide treatment (see Table D5 and Fig. D6) with the same hydroxide-P-loadings (cf. chapter III). Plant-agar systems were already applied in another experiment (Schmidt *et al.* 2015) and provided good growth conditions for plants. After 18 days of growth, a trend towards reduced plant dry weights in the Al hydroxide treatments (Table D5), likewise in the rhizobox experiments (Fig. III-3), along a slight yellowing of the plant leaves (Fig. D6) indicated growth inhibiting toxic stress for the plants (Panda *et al.* 2009). These results, however, have to be seen critically since no Al concentrations in the plant tissues were analyzed. Uncertainties regarding phytotoxic Al availabilities for the young wheat plants could have been easily eliminated by

ICP-MS analysis of the digested plant material, however, unfortunately this was not possible due to contamination related problems for analysis, reducing interpretation of my results.

Overall, the ^{33}P uptake rates in the rhizobox experiment indicated a trend towards better P utilization from P-loaded Fe hydroxides (Fig. III-3), which was in contradiction to desorption experiments conducted in another study with the same hydroxides (Gypser *et al.* 2018). We therefore estimated the plant available P fraction without plant growth by using the diffuse gradient in thin films technology (DGT). A DGT sampler consists of a hydrogel layer containing an ion resin (ferrihydrite) covered by a diffusion layer and protected by a membrane. It mimics the actions of P uptake by plants from the soil solution by creating a sink for dissolved P but also for P which can be mobilized from the solid phase due to the creation of a concentration gradient being comparable to a plant root (Degryse *et al.* 2009; Santner *et al.* 2012). The application of DGT sampler to ^{33}P -loaded hydroxides being blended within the Luvisol soil (Fig. E1; $n=3$) revealed that within 48 h of DGT deployment it appears that the ^{33}P availability from the Fe hydroxides was greater ($84\pm 22 \text{ Bq cm}^{-2}$) than from the Al hydroxides ($53\pm 54 \text{ Bq cm}^{-2}$), even though the results were not significantly different (Fig. E2).

Hence, the outlined experiments with ^{33}P -loaded Fe and Al hydroxides mixed within different soil orders, gave detailed insights into general P supply potentials for plants from oxidic bound soil P. The results from the DGT experiment with lower ^{33}P diffusion rates into the gel sink from the ^{33}P -Al source than from the ^{33}P -Fe source showed comparable results than the specific plant ^{33}P uptake rates in the rhizobox experiment. Thus, the overall trends indicated lower P supply rates and thus lower P availabilities for plants from subsoil Al-P species in arable soils. Concluding, the detailed information gained in chapter III fundamentally supported the findings in chapter II. Especially in the first subsoil layer (from 30 to 60 cm soil depth) the dominance of Fe-P forms (in all treatments between 80 to 92% P adsorbed to Fe, Fig. II-2) was confirmed, which thus very likely represented great proportions of the labile (11 to 15%) and moderately labile (31 to 40%) P stocks found in this soil depth (Table II-2). Hence, the careful and comprehensive elucidation of P stocks, the chemical speciation of dominant P species (chapter II) in combination with investigations towards P accessibility for plant P nutrition (chapter III), provided in this thesis may allow the conclusion that **Fe-mineral soil P forms are of greater importance for soil P dynamics in arable soils and thus overall control the P availability and accessibility for plants** by governing slow, long-term dissolution reactions and thus may maintain continuous plant P supply.

2.5 Methodological advances of digital autoradiography for phosphorus research

Autoradiographic systems were developed for the visualization of conventional radioactive β -emitters (e.g., Amemiya and Miyahara 1988; Johnston *et al.* 1990; Nakajima 1993). They have their infancies in the early 50th in whole-body autoradiography for drug metabolism studies (mostly medical purposes) followed by direct analysis of radio-thin-layer chromatography (implemented in plant metabolism studies) (Barthe *et al.* 2012). Compared to the X-ray film autoradiography (which was widely used in various fields from the 1950s on), digital autoradiographic systems (also referred to as autoradioluminography being patented by Luckey (1975)) utilize sensitive sensor imaging plates (Nakajima 1993). The imaging plates consist of uniformly coated photostimulable luminescence material containing phosphors, which are mostly solid inorganic materials such as barium fluorobromide crystals containing traces of bivalent europium, as the center of luminescence (written as BaFX:Eu^{2+} (X = Cl, Br, I)) (Takahashi *et al.* 1985).

Due to an exact spatial storage of signals from the origin of the radioactive decay on the imaging plate material, this technique offers two-dimensional resolved mapping of radiotracers. In this thesis I determined the spatial distribution of ^{33}P or ^{32}P radioisotopes in plants, soils, or gels (Fig. III-1, Fig. D6, Fig. E1, and Fig. F1). However, due to capturing exact intensities from the radioactive decay on

the imaging plate and subsequent conversion into a digital signal, this method also allows quantitative analyses. According to Barthe *et al.* (2012) autoradiography was first used in a quantitative manner by Schweitzer *et al.* (1987) using a radioactive ^{14}C labeled blood scale standard for comparative whole-body autoradiography. In the following decades, many authors used ^{14}C standards for quantitative purposes, not only for ^{14}C radioisotope autoradiography but also for other radioisotopes (e.g., Bhat and Nye 1973; Miller 1991; Eakin *et al.* 1994).

In this thesis, digital autoradiography was applied (i) to analyze the distribution and success of blending ^{33}P associated to mineral phases into soil (cf. Appendix F) and (ii) to compare the uptake from ^{33}P associated mineral sources with different P availabilities by plants (cf. chapter III). These investigations raised the idea (iii) to advance and simplify analysis of P uptake studies by a non-destructive quantitative method development, using ^{14}C standards as references for intensity calculations of ^{33}P activities in leaf tissues (chapter IV). In the following, the benefits of digital autoradiography experiments but also further possibilities for its application are discussed.

The location of P fertilizer placement in a soil, i.e., when it is applied in a soil band, as point-source (as hotspot) or as homogenous incorporated particles into the entire soil volume can have enormous impact on its accessibility for growing roots (Borges and Mallarino 2001; Mallarino and Borges 2006). Fox and Kang (1978) proposed the advantages of a homogenous incorporation of P fertilizer into the entire cultivated soil volume, being most sufficient for crop uptake. Thus, also for the rhizobox experiments in this thesis (chapter III), a homogenous blending of particulate and liquid ^{33}P forms needed verification first, since such a method was not available in literature. By using digital autoradiography in combination with software-based pixel density evaluation after blending ^{33}P sources into subsamples of the soils, I was able to proof homogenous ^{33}P incorporation in the soil bands of the rhizoboxes of different ^{33}P treatments (Fig. F1 and Fig. F2). Hence, spatial disadvantages between root ^{33}P uptakes grown in different treatments could be excluded by proofing nearly the same spatial distribution and thus spatial conditions of the introduced ^{33}P sources in the soils (Appendix F).

Beside the evaluation of experimental conditions for the rhizobox experiment, digital autoradiography was applied to verify and compare ^{33}P uptake and activities in wheat plants (Fig. B1 and Bauke *et al.* 2017a). Varying contrasted leaf tissues first allowed only the visualization of differences in ^{33}P uptake of wheat plants and was then further deepened by the development of an approach enabling a quantitative analysis of the ^{33}P activities within leaves (chapter IV). However, the described quantification method for ^{33}P activities in plant tissues is currently limited to the application to dried leaves, since parameters for the shielding effects from tissue water content were not included into the calculations (no data on ^{33}P shielding by water are available in literature). This currently limits the application down to the level of dried plant leafs without the possibility of its application to living plants. Hence, a time-resolved quantification of radiotracer uptake by the living plant is currently still hampered. Real-time radioisotope imaging systems using photon counting camera units to analyze nutrient uptake in plants were already developed (Kanno *et al.* 2012; Hirose *et al.* 2013). However, they are still lacking true quantification in plants only analyzing radioisotopic activities relatively or in solution spots, most probably due to shielding effects from tissue water contents. An approach including multiple disciplines has to find ways to overcome this fundamental problem related to radioactive shielding but also to imaging plate sensitivity and capacity related restrictions. However, a conceivable area of applications for time resolved ^{33}P quantification may still be possible with the here outlined method. By analyzing the ^{33}P activity per leave area of dried leaves cut from growing plants, negative effects for the growing plant are limited and due to comparable conditions results can be estimated for different treatments. However, this has to be adopted carefully since it can change the physiological behavior of plants, and thus needs verification first.

Another field of application is to quantify P dynamics via radiotracers in soils; however, here similar constraints as for plants, i.e., shielding effects from soil constituents, shielding by soil water, and bulk density related inhomogeneities have to be expected. In a first approach outlined in this thesis DGT technology was applied to ^{33}P labeled soil (cf. Appendix E). It included the analyses of the direct soil surface with homogeneously introduced ^{33}P sources (cf. Fig. E1), which were compared to the bulk soil. As outlined in section V-2.4, different ^{33}P soil treatments, e.g., blended with ^{33}P labeled hydroxides or $^{33}\text{P}\text{-KH}_2\text{PO}_4$ were added as round soil spots to the bulk soil in quadratic petri dishes. Afterwards, I applied digital autoradiography and quantified the ^{33}P radiotracers following the order $^{33}\text{P}\text{-Al}$ ($496\pm30\text{b Bq cm}^{-2}$) > $^{33}\text{P}\text{-Fe}$ ($358\pm37\text{a Bq cm}^{-2}$), and $^{33}\text{P}\text{-K}$ ($340\pm79\text{a Bq cm}^{-2}$) on the direct soil surface (Fig.E1). The quantified activity of the $^{33}\text{P}\text{-Al}$ treatment was slightly higher but still in the same order of magnitude than to the other solid carrier P sources. On closer examination of the labeled area of the $^{33}\text{P}\text{-Al}$ treatment inhomogeneous regions of high contrast hinting at a higher surfaces ^{33}P activity were striking (Fig. E1, section B). Probably being the reason for the slightly higher ^{33}P activity of that treatment. Significantly higher ^{33}P activities ($3094\pm582\text{c Bq cm}^{-2}$) were found in the area where the same activity of ^{33}P was applied as liquid carrier-free ^{33}P -solution to the soil surface (Fig. E1, section D). Due to the application of DGT technique, the amount of bioavailable ^{33}P on the soil surface was additionally quantified (Fig. E2). After two days the DGT gel was removed and the ^{33}P activities were quantified; following the order: $^{33}\text{P}\text{-solution}$ ($3841\pm721\text{c Bq cm}^{-2}$) > $^{33}\text{P}\text{-K}$ ($1389\pm543\text{b Bq cm}^{-2}$) > $^{33}\text{P}\text{-Fe}$ ($84\pm22\text{a Bq cm}^{-2}$) = $^{33}\text{P}\text{-Al}$ ($53\pm54\text{a Bq cm}^{-2}$) (Appendix E). Hence, this first step indicated quantitative application of DGT to soils which suggests that the methods can successfully be applied together in the future.

Furthermore, if the methods can be applied to soil and plants together, soil science may have a strong tool to analyze soil dynamics of other radioisotopes. However, the here described restrictions of the imaging plate material (cf. chapter III) limited its application only to radioisotopes with similar β -emission energies than the ^{14}C radioisotope. The described method can be seen as first step, further studies have to target these suggestions.

3 CONCLUSIONS

My thesis supports the general consensus that fertilizer applications beyond the plants' requirements increase P stocks in the soil profile. Fertilizer levels maintaining P status in soils are recommended as they sustain the soil P status, but, I have also critically discussed that in unfertilized arable soils the soil-inherent P supply from primarily non-available P forms seemed to be adequate to replenish annual P removals from crops for several years or decades. The statements are subjected to limitations, as the general lack of reference soil samples at the beginning of the fertilizer experiment prevented comprehensive comparison with any initial soil P status in both long-term experiments.

However, the general assumptions made from the presented results are further limited to overcome soil order dependent variations, as results only comprise two soil orders under long-term fertilization in Germany; most studies presented in the literature are based on several soil orders. Therefore, I suggest that further investigations should include other agricultural important soil orders to confirm the results. Only if sufficient data are available agronomic considerations to optimize P fertilization management can also take the supply of soil P from preliminary non-soluble forms (soil-inherent P but also unused, remaining fertilizer P), and thus also P forms from subsoils into account. If these P sources are omitted in soil P tests for fertilizer recommendations, as is the case in the current extract-based methods, the P fertilizer requirements can be still vastly overestimated. The DGT technique can become a tool for soil testing to overcome these limitations.

In a multi-method approach of well standardized single and sequential wet chemical extraction methods combined with spectroscopic analyses, Fe and Al soil oxidic phases were identified as predominant forms to which P is bound in agricultural used Cambisols and Chernozems. By refining the understanding of P buffering and accessibility of exchangeable soil P associated with, e.g., soil oxidic surfaces, I have tried to contribute to the general questions of P use efficiency in soil profiles from 0 to 90 cm soil depth.

In a rhizobox experiment I have shown that such oxidic bound P forms can contribute to an adequate P supply for growing wheat plants in Luvisol and Ferralsol subsoil. However, I did not succeed to elucidate how the ^{33}P became available (included abiotic or biotic processes) for the wheat plants. The rhizobox results also suggested that despite the chemical form of P in the soil, soil physical conditions are important drivers for P mobilization from subsoils and can overrule chemical availability of moderately labile P forms for plant nutrition. This study can be considered a pioneering achievement, as for the first time the accessibility of moderately labile P forms by living plants grown in a soil-plant system under controlled conditions was investigated. In order to review these conclusions beyond the limited scope of this thesis, further investigations should focus on more controllable soil physical conditions and extend the range of P forms used in such an approach. Special emphasis is on clay mineral surfaces, being often neglected in soil related P dynamic studies.

As a promising technique for improving P research, digital autoradiography enabled me to conduct a comprehensive study of ^{33}P radiotracer uptake from less-soluble soil constituents by plants. Due to method refinement, a new methodology was conducted which should be further improved to utilize its advantageous application for broader analyses, e.g., soil nutrient dynamics as well as management strategies that promote efficient soil P acquisition strategies of plants to overcome the insufficient use of the limited P resource.

VI

REFERENCES

- Agbenin, J. O., Goladi, J. T. (1997) Carbon, nitrogen and phosphorus dynamics under continuous cultivation as influenced by farmyard manure and inorganic fertilizers in the savanna of northern Nigeria. *Sustainable Agriculture and Environment* **63** (1), 255-261.
- Ahlgren, J., Djodjic, F., Borjesson, G., Mattsson, L. (2013) Identification and quantification of organic phosphorus forms in soils from fertility experiments. *Soil Use and Management* **29** 24-35.
- Ajiboye, B., Akinremi, O. O., Hu, Y., Jurgensen, A. (2008) XANES speciation of phosphorus in organically amended and fertilized vertisol and mollisol. *Soil Science Society of America Journal* **72** (5), 1256-1262.
- Alamgir, M., Marschner, P. (2013) Short-term effects of application of different rates of inorganic P and residue P on soil P pools and wheat growth. *Journal of Plant Nutrition and Soil Science* **176** (5), 696-702.
- Altermann, M., Rinklebe, J., Merbach, I., Körschens, M., Langer, U., Hofmann, B. (2005) Chernozem-Soil of the Year 2005. *Journal of Plant Nutrition and Soil Science* **168** (6), 725-740.
- Amelung, W., Rodionov, A., Urusevskaja, I., Haumaier, L., Zech, W. (2001) Forms of organic phosphorus in zonal steppe soils of Russia assessed by ³¹P NMR. *Geoderma* **103** (3-4), 335-350.
- Amemiya, Y., Miyahara, J. (1988) Imaging plate illuminates many fields. *Nature* **336** (6194), 89-90.
- Andersson, H., Bergstrom, L., Ulen, B., Djodjic, F., Kirchmann, H. (2015) The role of subsoil as a source or sink for phosphorus leaching. *Journal of Environmental Quality* **44** (2), 535-544.
- Anil Kumar, R., Vasu, K., Velayudhan, K. T., Ramachandran, V., Suseela Bhai, R., Unnikrishnan, G. (2009) Translocation and distribution of ³²P labelled potassium phosphonate in black pepper (*Piper nigrum* L). *Crop Protection* **28** (10), 878-881.
- Annaheim, K. E., Doolette, A. L., Smernik, R. J., Mayer, J., Oberson, A., Frossard, E., Bünemann, E. K. (2015) Long-term addition of organic fertilizers has little effect on soil organic phosphorus as characterized by ³¹P NMR spectroscopy and enzyme additions. *Geoderma* **257–258** 67-77.
- Audette, Y., O'Halloran, I. P., Paul Voroney, R. (2016) Kinetics of phosphorus forms applied as inorganic and organic amendments to a calcareous soil. *Geoderma* **262** 119-124.
- Bah, A., Zaharah, A., Hussin, A. (2006) Phosphorus uptake from green manures and phosphate fertilizers applied in an acid tropical soil. *Communications in Soil Science and Plant Analysis* **37** (13-14), 2077-2093.
- Balbino, L. C., Bruand, A., Brossard, M., Grimaldi, M., Hajnos, M., Guimarães, M. F. (2002) Changes in porosity and microaggregation in clayey Ferralsols of the Brazilian Cerrado on clearing for pasture. *European Journal of Soil Science* **53** (2), 219-230.
- Balbino, L. C., Bruand, A., Cousin, I., Brossard, M., Quétin, P., Grimaldi, M. (2004) Change in the hydraulic properties of a Brazilian clay Ferralsol on clearing for pasture. *Geoderma* **120** (3), 297-307.
- Barej, J. A. M., Pätzold, S., Amelung, W. (2014) Phosphorus fractions in bulk subsoil and its biopores. *European Journal of Soil Science* **65** (4), 553-561.
- Barrow, N. J. (1987) The reaction of anions and cations with soil. In 'Reactions with Variable-Charge Soils'. pp. 54-80. (Springer Netherlands: Dordrecht)
- Barthe, N., Maîtrejean, S., Cardona, A. (2012) Chapter 19 - High-Resolution Beta Imaging. In 'Handbook of Radioactivity Analysis (Third Edition)'. (Ed. MF L'Annunziata.) pp. 1209-1242. (Academic Press: Amsterdam)
- Baskin, D. G., Stahl, W. L. (1993) Fundamentals of quantitative autoradiography by computer densitometry for in situ hybridization, with emphasis on ³³P. *Journal of Histochemistry & Cytochemistry* **41** (12), 1767-1776.
- Bauke, S., C. von Sperber, F. Tamburini, M. Gocke, B. Honermeier, K. Schweitzer, M. Baumecker, A. Don, A. Sandhage-Hofmann, Amelung, W. (2018) Subsoil phosphorus is affected by fertilization regime in long-term agricultural experimental trials. *European Journal of Soil Science* **69** (1), 103-112.
- Bauke, S. L., Landl, M., Koch, M., Hofmann, D., Nagel, K. A., Siebers, N., Schnepf, A., Amelung, W. (2017a) Macropore effects on phosphorus acquisition by wheat roots – a rhizotron study. *Plant and Soil* **416** (1-2), 67-82.
- Bauke, S. L., von Sperber, C., Siebers, N., Tamburini, F., Amelung, W. (2017b) Biopore effects on phosphorus biogeochemistry in subsoils. *Soil Biology and Biochemistry* **111** 157-165.

- Baveye, P. C. (2015) Looming scarcity of phosphate rock and intensification of soil phosphorus research *Revista Brasileira de Ciência do Solo* **39** (3), 637-642.
- Beauchemin, S., Hesterberg, D., Chou, J., Beauchemin, M., Simard, R. R., Sayers, D. E. (2003) Speciation of phosphorus in phosphorus-enriched agricultural soils using X-ray absorption near-edge structure spectroscopy and chemical fractionation. *Journal of Environmental Quality* **32** (5), 1809-1819.
- Bertrand, I., Holloway, R. E., Armstrong, R. D., McLaughlin, M. J. (2003) Chemical characteristics of phosphorus in alkaline soils from southern Australia. *Soil Research* **41** (1), 61-76.
- Bhadoria, P. B. S., Kaselowsky, J., Claassen, N., Jungk, A. (1991) Phosphate Diffusion Coefficients in Soil as Affected by Bulk Density and Water Content. *Zeitschrift für Pflanzenernährung und Bodenkunde* **154** (1), 53-57.
- Bhat, K. K. S., Nye, P. H. (1973) Diffusion of phosphate to plant roots in soil. *Plant and Soil* **38** (1), 161-175.
- Blake, L., Johnston, A. E., Poulton, P. R., Goulding, K. W. T. (2003) Changes in soil phosphorus fractions following positive and negative phosphorus balances for long periods. *Plant and Soil* **254** (2), 245-261.
- Blake, L., Mercik, S., Koerschens, M., Moskal, S., Poulton, P. R., Goulding, K. W. T., Weigel, A., Powlson, D. S. (2000) Phosphorus content in soil, uptake by plants and balance in three European long-term field experiments. *Nutrient Cycling in Agroecosystems* **56** (3), 263-275.
- Blakemore, L. C., Searle, P. L., Daly, B. (1977) 'Methods for chemical analysis of soils.' (Department of Scientific and Industrial Research: Lower Hutt, New Zealand)
- Blume, H.-P., Stahr, K., Leinweber, P. (2011) 'Bodenkundliches Praktikum: Eine Einführung in pedologisches Arbeiten für Ökologen, Land-und Forstwirte, Geo-und Umweltwissenschaftler.' (Springer-Verlag: Heidelberg)
- Bol, R., Amelung, W., Haumaier, L. (2006) Phosphorus-31–nuclear magnetic–resonance spectroscopy to trace organic dung phosphorus in a temperate grassland soil. *Journal of Plant Nutrition and Soil Science* **169** (1), 69-75.
- Borges, R., Mallarino, A. P. (2001) Deep Banding Phosphorus and Potassium Fertilizers for Corn Managed with Ridge Tillage Iowa Agric. Home Econ. Exp. Stn. Journal Paper no. J-18523. Project 3233. Research supported in part by the Leopold Center for Sustainable Agriculture. *Soil Science Society of America Journal* **65** (2), 376-384.
- Brockett, B. F. T., Prescott, C. E., Grayston, S. J. (2012) Soil moisture is the major factor influencing microbial community structure and enzyme activities across seven biogeoclimatic zones in western Canada. *Soil Biology and Biochemistry* **44** (1), 9-20.
- Bühler, S., Oberson, A., Rao, I. M., Friesen, D. K., Frossard, E. (2002) Sequential Phosphorus Extraction of ³³P-Labeled Oxisol under Contrasting Agricultural Systems. *Soil Science Society of America Journal* **66** 868-877.
- Bühler, S., Oberson, A., Sinaj, S., Friesen, D. K., Frossard, E. (2003) Isotope methods for assessing plant available phosphorus in acid tropical soils. *European Journal of Soil Science* **54** (3), 605-616.
- Bünemann, E. K. (2015) Assessment of gross and net mineralization rates of soil organic phosphorus – A review. *Soil Biology and Biochemistry* **89** 82-98.
- Bünemann, E. K., Augstburger, S., Frossard, E. (2016) Dominance of either physicochemical or biological phosphorus cycling processes in temperate forest soils of contrasting phosphate availability. *Soil Biology and Biochemistry* **101** 85-95.
- Bünemann, E. K., Smernik, R. J., Doolette, A. L., Marschner, P., Stonor, R., Wakelin, S. A., McNeill, A. M. (2008) Forms of phosphorus in bacteria and fungi isolated from two Australian soils. *Soil Biology and Biochemistry* **40** (7), 1908-1915.
- Burkitt, L. L., Moody, P. W., Gourley, C. J. P., Hannah, M. C. (2002) A simple phosphorus buffering index for Australian soils. *Soil Research* **40** (3), 497-513.
- Cade-Menun, B. J. (2005) Characterizing phosphorus in environmental and agricultural samples by ³¹P nuclear magnetic resonance spectroscopy. *Talanta* **66** (2), 359-371.
- Cade-Menun, B. J. (2014) Improved peak identification in ³¹P-NMR spectra of environmental samples with a standardized method and peak library. *Geoderma* **257-258** 102-114.

- Cade-Menun, B. J., Liu, C. W. (2013) Solution phosphorus-31 nuclear magnetic resonance spectroscopy of soils from 2005 to 2013: A review of sample preparation and experimental parameters. *Soil Science Society of America Journal* **78** 19-37.
- Calvin, S. (2013) 'XAFS for Everyone.' (CRC Press: Boca Raton)
- Celi, L., Barberis, E. (2005) Abiotic stabilization of organic phosphorus in the environment. In 'Organic Phosphorus in the Environment'. (Ed. BLF Turner, E. Baldwin, D.) pp. 113 - 132. CABI Publishing)
- Celi, L., De Luca, G., Barberis, E. (2003) Effects of interaction of organic and inorganic P with ferrihydrite and kaolinite-iron oxide systems on iron release. *Soil Science* **168** (7), 479-488.
- Celi, L., Lamacchia, S., Marsan, F. A., Barberis, E. (1999) Interaction of Inositol Hexaphosphate on clays: Adsorption and Charging Phenomena. *Soil Science* **164** (8), 574-585.
- Chang, S. C., Jackson, M. L. (1957) Fractionation of soil phosphorus. *Soil Science* **84** ((2)), 133-144.
- Coe, R. A. J. (2000) Quantitative Whole-Body Autoradiography. *Regulatory Toxicology and Pharmacology* **31** (2), 1-3.
- Comar, C. L. (1955) 'Radioisotopes in biology and agriculture.' (McGraw-Hill: London)
- Condon, L. M., Frossard, E., Tiessen, H., Newmans, R. H., Stewart, J. W. B. (1990) Chemical nature of organic phosphorus in cultivated and uncultivated soils under different environmental conditions. *Journal of Soil Science* **41** (1), 41-50.
- Condon, L. M., Newman, S. (2011) Revisiting the fundamentals of phosphorus fractionation of sediments and soils. *Soils Sediments* **11** 830-840.
- Cordell, D., Drangert, J.-O., White, S. (2009) The story of phosphorus: Global food security and food for thought. *Global Environmental Change-Human and Policy Dimensions* **19** (2), 292-305.
- Cordell, D., White, S. (2011) Peak phosphorus: Clarifying the key issues of a vigorous debate about long-term phosphorus security. *Sustainability* **3** (10), 2027-2049.
- Cremer, C. M., Cremer, M., Escobar, J. L., Speckmann, E.-J., Zilles, K. (2009) Fast, quantitative in situ hybridization of rare mRNAs using 14C-standards and phosphorus imaging. *Journal of Neuroscience Methods* **185** (1), 56-61.
- Crosland, A. R., Zhao, F. J., McGrath, S. P., Lane, P. W. (1995) Comparison of aqua regia digestion with sodium carbonate fusion for the determination of total phosphorus in soils by inductively coupled plasma atomic emission spectroscopy (ICP). *Communications in Soil Science and Plant Analysis* **26** (9-10), 1357-1368.
- Cross, A. F., Schlesinger, W. H. (1995) A literature review and evaluation of the Hedley fractionation - Applications to the biogeochemical cycle of soil - Phosphorus in natural ecosystems. *Geoderma* **64** (3-4), 197-214.
- Daroub, S., Pierce, F. J., Ellis, B. G. (2000) Phosphorus fractions and fate of phosphorus-33 in soils managed under plowing and no-tillage. *Soil Science Society of America Journal* **64** 170-176.
- Dawson, C. J., Hilton, J. (2011) Fertiliser availability in a resource-limited world: Production and recycling of nitrogen and phosphorus. *Food Policy* **36**, **Supplement 1** S14-S22.
- de Campos, M., Antonangelo, J. A., Alleoni, L. R. F. (2016) Phosphorus sorption index in humid tropical soils. *Soil and Tillage Research* **156** 110-118.
- Debreczeni, K., Körschens, M. (2003) Long-term field experiments of the world. *Archives of Agronomy and Soil Science* **49** (5), 465-483.
- Decagon Devices Inc., 2016. MPS-2 & MPS-6 dielectric water potential sensors operator's manual. Decagon Devices, Pullman, Washington.
- Degryse, F., Smolders, E., Zhang, H., Davison, W. (2009) Predicting availability of mineral elements to plants with the DGT technique: a review of experimental data and interpretation by modelling. *Environmental Chemistry* **6** (3), 198-218.
- Delgado, A., Torrent, J. (2000) Phosphorus forms and desorption patterns in heavily fertilized calcareous and limed acid soils. *Soil Science Society of America Journal* **64** (6), 2031-2037.
- Di, H. J., Condon, L. M., Frossard, E. (1997) Isotope techniques to study phosphorus cycling in agricultural and forest soils: A review. *Biology and Fertility of Soils* **24** (1), 1-12.
- Doolette, A. L., Smernik, R. J. (2011) Soil organic phosphorus speciation using spectroscopic techniques. In 'Phosphorus in Action: Biological Processes in Soil Phosphorus Cycling'. Eds EK Bunemann, A Oberson, E Frossard.) Vol. 26, pp. 3-36. (Springer-Verlag: Berlin)

- Dorahy, C. G., Blair, G. J., Rochester, I. J., Till, A. R. (2007) Availability of P from ^{32}P -labelled endogenous soil P and ^{33}P -labelled fertilizer in an alkaline soil producing cotton in Australia. *Soil Use and Management* **23** (2), 192-199.
- Dubus, I. G., Becquer, T. (2001) Phosphorus sorption and desorption in oxide-rich Ferralsols of New Caledonia. *Soil Research* **39** (2), 403-414.
- Eakin, T. J., Baskin, D. G., Breining, J. F., Stahl, W. L. (1994) Calibration of ^{14}C -plastic standards for quantitative autoradiography with ^{33}P . *Journal of Histochemistry & Cytochemistry* **42** (9), 1295-1298.
- Eckhardt, K. U., Leinweber, P. (1997) P-Fraktionen zur Vorhersage von P-Austrägen aus landwirtschaftlich genutzten Böden. *Mitteilung der Deutschen Bodenkundlichen Gesellschaft* **85** (II), 871-874.
- Edmeades, D. C. (2003) The long-term effects of manures and fertilisers on soil productivity and quality: a review. *Nutrient Cycling in Agroecosystems* **66** (2), 165-180.
- Epstein, E. (1972) Mineral Nutrition of Plants: Principles and Perspectives. John Wiley and Sons, Inc., New York, London, Sydney, Toronto. 1972. *Zeitschrift für Pflanzenernährung und Bodenkunde* **132** (2), 158-159.
- Eriksson, A. K., Gustafsson, J. P., Hesterberg, D. (2015) Phosphorus speciation of clay fractions from long-term fertility experiments in Sweden. *Geoderma* **241-242** 68-74.
- Eriksson, A. K., Hesterberg, D., Klysubun, W., Gustafsson, J. P. (2016a) Phosphorus dynamics in Swedish agricultural soils as influenced by fertilization and mineralogical properties: Insights gained from batch experiments and XANES spectroscopy. *Science of the Total Environment* **566-567** (Supplement C), 1410-1419.
- Eriksson, A. K., Hillier, S., Hesterberg, D., Klysubun, W., Ulén, B., Gustafsson, J. P. (2016b) Evolution of phosphorus speciation with depth in an agricultural soil profile. *Geoderma* **280** 29-37.
- Fardeau, J. C. (1995) Dynamics of phosphate in soils. An isotopic outlook. *Fertilizer research* **45** (2), 91-100.
- Fardeau, J. C., Guiraud, G., Marol, C. (1995) The role of isotopic techniques on the evaluation of the agronomic effectiveness of P fertilizers. *Fertilizer research* **45** (2), 101-109.
- Fink, J. R., Inda, A. V., Tiecher, T., Barrón, V. (2016) Iron oxides and organic matter on soil phosphorus availability. *Ciência e Agrotecnologia* **40** (4), 369-379.
- Forster, J. C. (1995) Soil sampling, handling, storage and analysis A2 - Alef, Kassem. In 'Methods in Applied Soil Microbiology and Biochemistry'. (Ed. P Nannipieri.) pp. 49-121. (Academic Press: London)
- Fox, R. L., Kang, B. (1978) Influence of phosphorus fertilizer placement and fertilization rate on maize nutrition. *Soil Science* **125** (1), 34-40.
- Friesen, D. K., Blair, G. J. (1988) A dual radiotracer study of transformations of organic, inorganic and plant residue phosphorus in soil in the presence and absence of plants. *Australian Journal of Soil Research* **26** (2), 355-366.
- Frossard, E., Achat, D. L., Bernasconi, S. M., Bünemann, E. K., Fardeau, J. C., Jansa, J., Morel, C., Rabeharisoa, L., Randriamanantsoa, L., Sinaj, S. t., Tamburini, F., Oberson, A. Eds E Bünemann, A Oberson, E Frossard (2011) 'Phosphorus in Action: Biological Processes in Soil Phosphorus Cycling.' (Springer Berlin Heidelberg: Berlin, Heidelberg)
- Frossard, E., Condon, L. M., Oberson, A., Sinaj, S., Fardeau, J. C. (2000) Processes governing phosphorus availability in temperate soils. *Journal of Environmental Quality* **29** (1), 15-23.
- Fuentes, B., de la Luz Mora, M., Bolan, N. S., Naidu, R. (2008) Assessment of phosphorus bioavailability from organic wastes in soil. *Developments in Soil Science* **32** 363-411.
- Garz, J., Schliephake, W., Merbach, W. (2000) Changes in the subsoil of long-term trials in Halle (Saale), Germany, caused by mineral fertilization. *Journal of Plant Nutrition and Soil Science* **163** (6), 663-668.
- Gatiboni, L. C., Dos Santos Rheinheimer, D., Claro Flores, A. F., Anghinoni, I., Kaminski, J., De Lima, M. A. S. (2005) Phosphorus forms and availability assessed by ^{31}P -NMR in successively cropped soil. *Communications in Soil Science and Plant Analysis* **36** (19-20), 2625-2640.
- Gérard, F. (2016) Clay minerals, iron/aluminum oxides, and their contribution to phosphate sorption in soils - A myth revisited. *Geoderma* **262** 213-226.

- Gilbert, N. (2009) The disappearing nutrient. *Nature Climate Change* **461** (7267), 716-718
- Gliński, J., Lipiec, J. (1990) 'Soil physical conditions & plant roots.' (CRC Press Inc.: Boca Raton, FL 33431)
- Godlinski, F., Leinweber, P., Meissner, R., Seeger, J. (2004) Phosphorus status of soil and leaching losses: results from operating and dismantled lysimeters after 15 experimental years. *Nutrient Cycling in Agroecosystems* **68** (1), 47-57.
- Goldberg, S., Kapoor, B., Rhoades, J. (1990) Effect of aluminum and iron oxides and organic matter on flocculation and dispersion of arid zone soils. *Soil Sci* **150** (3), 588-593.
- Goldberg, S., Sposito, G. (1985) On the mechanism of specific phosphate adsorption by hydroxylated mineral surfaces: A review. *Communications in Soil Science and Plant Analysis* **16** (8), 801-821.
- Golterman, H., Booman, A. (1988) Sequential extraction of iron-phosphate and calcium-phosphate from sediments by chelating agents. *Internationale Vereinigung für theoretische und angewandte Limnologie: Verhandlungen* **23** (2), 904-909.
- Golterman, H. L. (2002) Hydrobiologia: Editorial. *Hydrobiologia* **472** (1), 3-4.
- Gorenstein, D. G. (2012) 'Phosphorous-31 NMR: Principles and applications.' (Academic Press:
- Granssee, A., Merbach, W. (2000) Phosphorus dynamics in a long-term P fertilization trial on Luvic Phaeozem at Halle. *Journal of Plant Nutrition and Soil Science* **163** (4), 353-357.
- Grant, C., Bittman, S., Montreal, M., Plenchette, C., Morel, C. (2005) Soil and fertilizer phosphorus: Effects on plant P supply and mycorrhizal development. *Canadian Journal of Plant Science* **85** (1), 3-14.
- Günther, H. (1992) 'NMR-Spektroskopie: Grundlagen, Konzepte und Anwendungen der Protonen-und Kohlenstoff-13-Kernresonanz-Spektroskopie in der Chemie; 49 Tabellen.' (Thieme: Stuttgart)
- Guo, F., Yost, R., Hue, N. V., Evensen, C. I., Silva, J. A. (2000) Changes in Phosphorus Fractions in Soils under Intensive Plant Growth. *Soil Science Society of America Journal* **64** 1681-1689.
- Guppy, C. N., Menzies, N. W., Blamey, F. P. C., Moody, P. W. (2005) Do Decomposing Organic Matter Residues Reduce Phosphorus Sorption in Highly Weathered Soils? *Soil Science Society of America Journal* **69** (5), 1405-1411.
- Gustafsson, J. P., Mwamila, L. B., Kergoat, K. (2012) The pH dependence of phosphate sorption and desorption in Swedish agricultural soils. *Geoderma* **189-190** 304-311.
- Gypser, S., Hirsch, F., Schleicher, A. M., Freese, D. (2018) Impact of crystalline and amorphous iron- and aluminum hydroxides on mechanisms of phosphate adsorption and desorption. *Journal of Environmental Sciences* **70** 175-189.
- Hao, X. Y., Godlinski, F., Chang, C. (2008) Distribution of phosphorus forms in soil following long-term continuous and discontinuous cattle manure applications. *Soil Science Society of America Journal* **72** (1), 90-97.
- Hartner, A. (2013) Test und Evaluierung von neuartigen Matrixpotenzialsensoren. Diploma 'thesis', Universität für Bodenkultur, Wien.
- Hawkes, G. E., Powlson, D. S., Randall, E. W., Tate, K. R. (1984) A ³¹P nuclear magnetic resonance study of the phosphorus species in alkali extracts of soils from long-term field experiments *Journal of Soil Science* **35** (1), 35-45.
- Hayes, J., Richardson, A., Simpson, R. (2000) Components of organic phosphorus in soil extracts that are hydrolysed by phytase and acid phosphatase. *Biology and Fertility of Soils* **32** (4), 279-286.
- He, Y., Hou, L., Wang, H., Hu, K., McConkey, B. (2014) A modelling approach to evaluate the long-term effect of soil texture on spring wheat productivity under a rain-fed condition. *Scientific Reports* **4** 5736.
- He, Z., Fortuna, A.-M., Senwo, Z. N., Tazisong, I. A., Honeycutt, C. W., Griffin, T. S. (2006) Hydrochloric fractions in Hedley fractionation may contain inorganic and organic phosphates. *Soil Science Society of America Journal* **70** (3), 893-899.
- Hedley, M., McLaughlin, M. (2005) Reactions of phosphate fertilizers and by-products in soils. *Phosphorus: agriculture and the environment* (phosphorusagric), 181-252.
- Hedley, M. J., Stewart, J. W., Chohan, B. S. (1982) Changes in inorganic and organic soil phosphorus fractions induced by cultivation practices and by laboratory incubations. *Soil Science Society of America Journal* **46** 970-976.

- Heffer, P., Prud'homme, M. (2017) Fertilizer Outlook 2017–2021. In '85th IFA Annual Conference, Marrakech (Morocco)'. pp. 1-7. (International Fertilizer Association (IFA): Available at www.fertilizer.org/images/Library_Downloads/2018_IFA_Annual_Report_2017_Public.pdf
- Hinsinger, P. (2001) Bioavailability of soil inorganic P in the rhizosphere as affected by root-induced chemical changes: a review. *Plant and Soil* **237** 173-195.
- Hirose, A., Yamawaki, M., Kanno, S., Igarashi, S., Sugita, R., Ohmae, Y., Tanoi, K., Nakanishi, T. (2013) Development of a ¹⁴C detectable real-time radioisotope imaging system for plants under intermittent light environment. *Journal of Radioanalytical and Nuclear Chemistry* **296** (1), 417-422.
- Ho, M. D., Rosas, J. C., Brown, K. M., Lynch, J. P. (2005) Root architectural tradeoffs for water and phosphorus acquisition. *Functional Plant Biology* **32** (8), 737-748.
- Holmgren, G. G. S. (1967) A rapid citrate-dithionite extractable iron procedure. *Soil Science Society of America Journal* **31** (2), 210-211.
- Hooda, P., Truesdale, V., Edwards, A., Withers, P., Aitken, M., Miller, A., Rendell, A. (2001) Manuring and fertilization effects on phosphorus accumulation in soils and potential environmental implications. *Advances in Environmental Research* **5** (1), 13-21.
- Horta, M. D., Torrent, J. (2007) Phosphorus desorption kinetics in relation to phosphorus forms and sorption properties of Portuguese acid soils. *Soil Science* **172** (8), 631-638.
- Hue, N. V. (1991) Effects of Organic Acids/Anions on P Sorption and Phytoavailability in Soils With Different Mineralogies. *Soil Science* **6** (152), 463-471.
- Hue, N. V., Ikawa, H., Silva, J. A. (1994) Increasing plant-available phosphorus in an ultisol with a yard-waste compost. *Communications in Soil Science and Plant Analysis* **25** (19-20), 3291-3303.
- Hüve, K., Merbach, W., Remus, R., Lüttschwager, D., Wittenmayer, L., Hertel, K., Schurr, U. (2007) Transport of phosphorus in leaf veins of *Vicia faba* L. *Journal of Plant Nutrition and Soil Science* **170** (1), 14-23.
- Igwe, C. A., Zarei, M., Stahr, K. (2010) Fe and Al oxides distribution in some ultisols and inceptisols of southeastern Nigeria in relation to soil total phosphorus. *Environmental Earth Sciences* **60** (5), 1103-1111.
- IUSS Working Group WRB (2015) 'World Reference Base for Soil Resources 2014, update 2015. International soil classification system for naming soils and creating legends for soil maps. World Soil Resources Reports No. 106.' (Food and Agriculture Organization of the United Nations: Rome)
- Iyamuremye, F., Dick, R. P., Baham, J. (1996) Organic amendments and phosphorus dynamics: I. phosphorus chemistry and sorption. *Soil Science* **161** (7), 426-435.
- Jasinski, S. M. (2018) Mineral commodity summaries 2018: Phosphate Rock. US Geological Survey, Reston, Virginia. Available at www.minerals.usgs.gov/minerals/pubs/mcs/2018/mcs2018
- Johnston, A. E., Poulton, P. R. (2018) The importance of long-term experiments in agriculture: their management to ensure continued crop production and soil fertility; the Rothamsted experience. *European Journal of Soil Science* **69** (1), 113-125.
- Johnston, R. F., Pickett, S. C., Barker, D. L. (1990) Autoradiography using storage phosphor technology. *Electrophoresis* **11** (5), 355-360.
- Jørgensen, C., Turner, B. L., Reitzel, K. (2015) Identification of inositol hexakisphosphate binding sites in soils by selective extraction and solution ³¹P NMR spectroscopy. *Geoderma* **257–258** 22-28.
- Jungk, A. (1984) Phosphatdynamik in der Rhizosphäre und Phosphatverfügbarkeit für Pflanzen. *Bodenkultur*
- Kanno, S., Yamawaki, M., Ishibashi, H., Kobayashi, N. I., Hirose, A., Tanoi, K., Nussaume, L., Nakanishi, T. M. (2012) Development of real-time radioisotope imaging systems for plant nutrient uptake studies. *Philosophical Transactions of the Royal Society B: Biological Sciences* **367** (1595), 1501.
- Kautz, T., Amelung, W., Ewert, F., Gaiser, T., Horn, R., Jahn, R., Javaux, M., Kemna, A., Kuzyakov, Y., Munch, J., Pätzold, S., Peth, S., Scherer, H. W., Schlöter, M., Schneider, H., Vanderborght, J., Vetterlein, D., Walter, A., Wiesenberger, G., Köpke, U. (2012) Nutrient acquisition from arable subsoil in temperate climates: A review. *Soil Biology & Biochemistry* **57** 1003 - 1022.

- Khan, A., Lu, G., Ayaz, M., Zhang, H., Wang, R., Lv, F., Yang, X., Sun, B., Zhang, S. (2018) Phosphorus efficiency, soil phosphorus dynamics and critical phosphorus level under long-term fertilization for single and double cropping systems. *Agriculture, Ecosystems & Environment* **256** 1-11.
- Khasawneh, F. E., Sample, E., Kamprath, E. (1980) 'The role of phosphorus in agriculture.' (American Society of Agronomy, Crop Science Society of America, Soil Science Society of America.: Madison)
- Khatriwada, R., Hettiarachchi, G. M., Mengel, D. B., Fei, M. W. (2012) Speciation of phosphorus in a fertilized, reduced-till soil system: In-field treatment incubation study. *Soil Science Society of America Journal* **76** (6), 2006-2018.
- Kirkham, M. B. (2014) Field capacity, wilting point, available water, and the nonlimiting water range. In 'Principles of Soil and Plant Water Relations (Second Edition)'. pp. 153-170. (Academic Press: Boston)
- Kizewski, F., Liu, Y. T., Morris, A., Hesterberg, D. (2011) Spectroscopic approaches for phosphorus speciation in soils and other environmental systems. *Journal of Environmental Quality* **40** (3), 751-766.
- Kladivko, E. J., Keeney, D. R. (1987) Soil nitrogen mineralization as affected by water and temperature interactions. *Biology and Fertility of Soils* **5** (3), 248-252.
- Klopfenstein, T. J., Angel, R., Cromwell, G., Erickson, G. E., Fox, D. G., Parsons, C., Satter, L. D., Sutton, A. L., Baker, D. H., Lewis, A. (2002) Animal diet modification to decrease the potential for nitrogen and phosphorus pollution. *Faculty Papers and Publications in Animal Science* **518**
- Körschens, M. (1994) 'Der statische Düngungsversuch Bad Lauchstädt nach 90 Jahren: Einfluss der Düngung auf Boden, Pflanze und Umwelt: mit einem Verzeichnis von 240 Dauerfeldversuchen der Welt.' (BG Teubner Verlagsgesellschaft: Stuttgart)
- Körschens, M. (2006) The importance of long-term field experiments for soil science and environmental research - A review. *Plant Soil Environment* **52** 1-8.
- Kratz, S., Schnug, E. (2006) Rock phosphates and P fertilizers as sources of U contamination in agricultural soils. In 'Uranium in the environment'. pp. 57-67. (Springer: Berlin, Heidelberg)
- Kruse, J., Abraham, M., Amelung, W., Baum, C., Bol, R., Kühn, O., Lewandowski, H., Niederberger, J., Oelmann, Y., Rüger, C., Santner, J., Siebers, M., Siebers, N., Sphon, M., Verstergren, J., Vogts, A., Leinweber, P. (2015) Innovative methods in soil phosphorus research: A review. *Journal of Plant Nutrition and Soil Science* **178** 43-88.
- Kruse, J., Leinweber, P. (2008) Phosphorus in sequentially extracted fen peat soils: A K-edge X-ray absorption near-edge structure (XANES) spectroscopy study. *Journal of Plant Nutrition and Soil Science* **171.4** 613-620.
- Kruse, J., Negassa, W., Appathuria, N., Zuin, L., Leinweber, P. (2010) Phosphorus speciation in sequentially extracted agro-industrial by-products: evidence from X-ray absorption near edge structure spectroscopy. *Journal of Environmental Quality* **39** 2179-2184.
- Kuhlmann, H., Baumgartel, G. (1991) Potential importance of the subsoil for P and Mg nutrition of wheat. *Plant and Soil* **137** (2), 259-266.
- L'annunziata, M. F. (1979) 'Radiotracers in agricultural chemistry.' (Academic Press Inc.(London) Ltd.:
- L'Annunziata, M. F. (2012) Chapter 1 - Radiation Physics and Radionuclide Decay. In 'Handbook of Radioactivity Analysis (Third Edition)'. (Ed. MF L'Annunziata.) pp. 1-162. (Academic Press: Amsterdam)
- Lal, R., Stewart, B. A. (2016) 'Soil Phosphorus.' (CRC Press: Boca Raton)
- Lambers, H., Shane, M. W., Cramer, M. D., Pearse, S. J., Veneklaas, E. J. (2006) Root structure and functioning for efficient acquisition of phosphorus: matching morphological and physiological traits. *Annals of botany* **98** (4), 693-713.
- Large, E. C. (1954) Growth stages in cereals illustration of the Feekes scale. *Plant Pathology* **3** (4), 128-129.
- Leinweber, P., Hagemann, P., Kebelmann, L., Kebelmann, K., Morshedizad, M. (2019) Bone Char As a Novel Phosphorus Fertilizer. In 'Phosphorus Recovery and Recycling'. Eds H Ohtake, S Tsuneda.) pp. 419-432. (Springer: Singapore)

- Leinweber, P., Haumaier, L., Zech, W. (1997) Sequential extractions and ³¹P-NMR spectroscopy of phosphorus forms in animal manures, whole soils and particle-size separates from a densely populated livestock area in northwest Germany. *Biology and Fertility of Soils* **25** (1), 89-94.
- Levy, E. T., Schlesinger, W. H. (1999) A comparison of fractionation methods for forms of phosphorus in soils. *Biogeochemistry* **47** (1), 25-38.
- Lewis, D. G., Quirk, J. P. (1967) Phosphate diffusion in soil and uptake by plants. *Plant and Soil* **26** (1), 99-118.
- Lindsay, W. L. (1979) 'Chemical equilibria in soils.' (John Wiley and Sons Ltd.: New York, USA)
- Lindsay, W. L., Peech, M., Clark, J. S. (1959) Solubility criteria for the existence of cariscite in soils. *Soil Science Society of America Journal* **23** (5), 357-360.
- Lindsay, W. L., Vlek, P. L., Chien, S. H. (1989) Phosphate minerals. *Minerals in soil environments* (mineralsinsoile), 1089-1130.
- Liu, F., Zhang, Y.-Y., Yan, Y.-P., Liu, F., Tan, W.-F., Liu, M.-M., Feng, X.-H. (2013a) Sorption and desorption characteristics of different structures of organic phosphorus onto aluminum (oxyhydr) oxides. *Chinese Journal of Environmental Science* **34** (11), 4482-9.
- Liu, J., Hu, Y., Yang, J., Abdi, D., Cade-Menun, B. J. (2014a) Investigation of Soil Legacy Phosphorus Transformation in Long-term Agricultural Fields Using Sequential Fractionation, P K-edge Xanes and Solution P NMR Spectroscopy. *Environmental Science & Technology* **49** 168-176.
- Liu, J., Yang, J., Cade-Menun, B. J., Liang, X., Hu, Y., Liu, C. W., Zhao, Y., Li, L., Shi, J. (2013b) Complementary Phosphorus Speciation in Agricultural Soils by Sequential Fractionation, Solution ³¹P Nuclear Magnetic Resonance, and Phosphorus K-edge X-ray Absorption Near-Edge Structure Spectroscopy. *Journal of Environmental Quality* **42** 1763-1770.
- Liu, J., Yang, J. J., Liang, X. Q., Zhao, Y., Cade-Menun, B. J., Hu, Y. F. (2014b) Molecular Speciation of Phosphorus Present in Readily Dispersible Colloids from Agricultural Soils. *Soil Science Society of America Journal* **78** (1), 47-53.
- Lombi, E., Scheckel, K. G., Armstrong, R. D., Forrester, S., Cutler, J. N., Paterson, D. (2006) Speciation and distribution of phosphorus in a fertilized soil: A synchrotron-based investigation. *Soil Science Society of America Journal* **70** (6), 2038-2048.
- Lookman, R., Grobet, P., Merckx, R., Vlassak, K. (1994) Phosphate sorption by synthetic amorphous aluminium hydroxides: a ²⁷Al and ³¹P solid-state MAS NMR spectroscopy study. *European Journal of Soil Science* **45** (1), 37-44.
- Luckey, G. W., 1975. Apparatus and method for producing images corresponding to patterns of high energy radiation. Google Patents, USA.
- LWK Nordrhein-Westfalen (2015) Düngung mit Phosphat, Kali, Magnesium. *Ratgeber 2015* **8**, Available at www.landwirtschaftskammer.de/landwirtschaft/ackerbau/pdf/phosphat-kalium-magnesium-pdf
- LWK Nordrhein-Westfalen, 2017. Nährstoffbericht 2017 über Wirtschaftsdünger und andere organische Düngemittel für Nordrhein-Westfalen. Landwirtschaftskammer Nordrhein-Westfalen, Münster.
- Magid, J., Nielsen, N. E. (1992) Seasonal variation in organic and inorganic phosphorus fractions of temperate-climate sandy soils. *Plant and Soil* **144** (2), 155-165.
- Mallarino, A. P., Borges, R. (2006) Phosphorus and Potassium Distribution in Soil Following Long-term Deep-Band Fertilization in Different Tillage Systems Research supported in part by the Iowa Soybean Promotion Board and the Leopold Center for Sustainable Agriculture. *Soil Science Society of America Journal* **70** (2), 702-707.
- McBeath, T. M., McLaughlin, M. J., Kirby, J. K., Armstrong, R. D. (2012) The effect of soil water status on fertiliser, topsoil and subsoil phosphorus utilisation by wheat. *Plant and Soil* **358** (1-2), 337-348.
- McKeague, J. A., Day, J. H. (1966) Dithionite and oxalate extractable Fe and Al as aids in differentiating various classes of soils. *Canadian Journal of Soil Science* **46** (1), 13-22.
- McKercher, R. B., Anderson, G. (1968) Content of Inositol Penta- and Hexaphosphates in some Canadian Soils. *Journal of Soil Science* **19** (1), 47-55.
- McLaren, T., Bell, M., J. Rochester, I., Guppy, C., Tighe, M., Flavel, R. (2013) Growth and phosphorus uptake of faba bean and cotton are related to Colwell-P concentrations in the subsoil of Vertosols. *Crop and Pasture Science* **64** 825-833.

- McLaren, T. I., McLaughlin, M. J., McBeath, T. M., Simpson, R. J., Smernik, R. J., Guppy, C. N., Richardson, A. E. (2016) The fate of fertiliser P in soil under pasture and uptake by subterranean clover – a field study using ^{33}P -labelled single superphosphate. *Plant and Soil* **401** (1), 23-38.
- McLaughlin, M., Alston, A., Martin, J. (1988a) Phosphorus cycling in wheat pasture rotations .I. The source of phosphorus taken up by wheat. *Soil Research* **26** (2), 323-331.
- McLaughlin, M., Alston, A., Martin, J. (1988b) Phosphorus cycling in wheat pasture rotations .II. The role of the microbial biomass in phosphorus cycling. *Soil Research* **26** (2), 333-342.
- McLaughlin, M. J., McBeath, T. M., Smernik, R. J., Stacey, S. P., Ajiboye, B., Guppy, C. N. (2011) The chemical nature of P accumulation in agricultural soils - implications for fertiliser management and design: an Australian perspective. **349** (1-2), 87.
- Medinski, T., Freese, D., Reitz, T. (2018) Changes in soil phosphorus balance and phosphorus-use efficiency under long-term fertilization conducted on agriculturally used Chernozem in Germany. *Canadian Journal of Soil Science* **98** (0), 1-13.
- Mengel, K., Kirkby, E. A., Kosegarten, H., Appel, T. (2006) 'Principles of plant nutrition.' (Springer: Mertens, F., Pätzold, S., Welp, G. (2008) Spatial heterogeneity of soil properties and its mapping with apparent electrical conductivity. *Journal of Plant Nutrition and Soil Science* **171** (2), 146-154.
- Miller, J. A. (1991) The calibration of ^{35}S or ^{32}P with ^{14}C -labeled brain paste or ^{14}C -plastic standards for quantitative autoradiography using LKB Ultrofilm or Amersham Hyperfilm. *Neuroscience Letters* **121** (1), 211-214.
- Morel, J. L., Fardeau, J. C., Béruff, M. A., Guckert, A. (1989) Phosphate fixing capacity of soils: A survey, using the isotopic exchange technique, or soils from north-eastern France. *Fertilizer research* **19** (2), 103-111.
- Murphy, J., Riley, J. P. (1962) A modified single solution method for the determination of phosphate in natural waters. *Analytica Chimica Acta* **27** 31-36.
- Nadeem, M., Mollier, A., Morel, C., Vives, A., Prud'homme, L., Pellerin, S. (2011) Relative contribution of seed phosphorus reserves and exogenous phosphorus uptake to maize (*Zea mays* L.) nutrition during early growth stages. *Plant and Soil* **346** (1), 231-244.
- Nakajima, E. Eds K Mukherjee, N Weber (1993) 'CRC Handbook of Chromatography: Analysis of Lipids.' (CRC Press: London, Tokyo)
- Negassa, W., Dultz, S., Schlichting, A., Leinweber, P. (2008) Influence of specific organic compounds on phosphorus sorption and distribution in a tropical soil. *Soil Science* **173** (9), 587-601.
- Negassa, W., Leinweber, P. (2009) How does the Hedley sequential phosphorus fractionation reflect impacts of land use and management on soil phosphorus: A review. *Journal of Plant Nutrition and Soil Science* **172** (3), 305-325.
- Newman, R. H., Tate, K. R. (1980) Soil-phosphorus characterization by ^{31}P nuclear magnetic-resonance. *Communications in Soil Science and Plant Analysis* **11** 835-842.
- Nielsen, J. S., Joner, E. J., Declerck, S., Olsson, S., Jakobsen, I. (2002) Phospho-imaging as a tool for visualization and noninvasive measurement of P transport dynamics in arbuscular mycorrhizas. *New Phytologist* **154** (3), 809-819.
- Nziguheba, G., Palm, C. A., Buresh, R. J., Smithson, P. C. (1998) Soil phosphorus fractions and adsorption as affected by organic and inorganic sources. *Plant and Soil* **198** (2), 159-168.
- Nziguheba, G., Smolders, E. (2008) Inputs of trace elements in agricultural soils via phosphate fertilizers in European countries. *Science of the Total Environment* **390** (1), 53-57.
- Oberson, A., Fardeau, J. C., Besson, J. M., Sticher, H. (1993) Soil phosphorus dynamics in cropping systems managed according to conventional and biological agricultural methods. *Biology and Fertility of Soils* **16** (2), 111-117.
- Oehl, F., Oberson, A., Tagmann, H. U., Besson, J. M., Dubois, D., Mäder, P., Roth, H. R., Frossard, E. (2002) Phosphorus budget and phosphorus availability in soils under organic and conventional farming. *Nutrient Cycling in Agroecosystems* **62** (1), 25-35.
- Ohlinger, R. (1996) Methods in soil biology In 'Soil Sampling and Sample Preparation'. Eds F Schinner, R Ohlinger, E Kandeler, R Margesin.) Vol. 1, pp. 7-11. (Springer-Verlag Berlin Heidelberg: Berlin)
- Olsen, S. R. (1954) 'Estimation of available phosphorus in soils by extraction with sodium bicarbonate.' (United States Department Of Agriculture: Washington)

- Panda, S. K., Baluska, F., Matsumoto, H. (2009) Aluminum stress signaling in plants. *Plant Signaling & Behavior* **4** (7), 592-597.
- Pheav, S., Bell, R., White, P., Kirk, G. (2003) Fate of applied fertilizer phosphorus in a highly weathered sandy soil under lowland rice cropping, and its residual effect. *Field Crops Research* **81** (1), 1-16.
- Pierzynski, G. M., McDowell, R. W., Sims, J. T. (2005) 'Chemistry, cycling, and potential moment of inorganic phosphorus in soils.' (American Society of Agronomy: Madison)
- Pizzeghello, D., Berti, A., Nardi, S., Morari, F. (2011) Phosphorus forms and P-sorption properties in three alkaline soils after long-term mineral and manure applications in north-eastern Italy. *Agriculture, Ecosystems & Environment* **141** (1-2), 58-66.
- Randriamanantsoa, L., Morel, C., Rabeharisoa, L., Douzet, J.-M., Jansa, J., Frossard, E. (2013) Can the isotopic exchange kinetic method be used in soils with a very low water extractable phosphate content and a high sorbing capacity for phosphate ions? *Geoderma* **200-201** 120-129.
- Rasmussen, P. E., Goulding, K. W. T., Brown, J. R., Grace, P. R., Janzen, H. H., Körschens, M. (1998) Long-term Agroecosystem Experiments: Assessing Agricultural Sustainability and Global Change. *Science* **282** (5390), 893-896.
- Ravel, B., Newville, M. (2005) Athena, Artemis, Hephaestus: data analysis for X-ray absorption spectroscopy using IFEFFIT. *Journal of Synchrotron Radiation* **12** (4), 537-541.
- Reddy, D. D., Rao, S. A., Singh, M. (2005) Changes in P fractions and sorption in an Alfisol following crop residues application. *Journal of Plant Nutrition and Soil Science* **168** (2), 241-247.
- Reichert, W. L., Stein, J. E., French, B., Goodwin, P., Varanasi, U. (1992) Storage phosphor imaging technique for detection and quantitation of DNA adducts measured by the ³²P-postlabeling assay. *Carcinogenesis* **13** (8), 1475-1479.
- Requejo, M. I., Eichler-Löbermann, B. (2014) Organic and inorganic phosphorus forms in soil as affected by long-term application of organic amendments. *Nutrient Cycling in Agroecosystems* (2), 245-255.
- Richardson, A. E., George, T. S., Jakobsen, I., Simpson, R. J. (2007) Plant Utilization of Inositol Phosphates. In 'Inositol phosphates: Linking agriculture and the environment'. Eds BL Turner, AE Richardson, E Mullaney.) pp. 242-260. (CABI Publishing: Wallingford, UK)
- Richardson, A. E., Hocking, P. J., Simpson, R. J., George, T. S. (2009) Plant mechanisms to optimise access to soil phosphorus. *Crop and Pasture Science* **60** (2), 124-143.
- Richter, F., Döriung, C., Jansen, M. (2012) Tagesgänge in Tensiometermessungen – Signal oder Artefakt? In 'Messung, Monitoring und Modellierung von Prozessen im System Boden – Pflanze - Atmosphäre'. 16-17.11.2012, Helmholtzzentrum (Deutsche bodenkundliche Gesellschaft (DBG): Leipzig) Available at www.eprints.dbges.de/866/
- Riehm, H. (1948) Arbeitsvorschrift zur Bestimmung der Phosphorsäure und des Kaliums nach lactatverfahren. *Zeitschrift für Pflanzenernährung und Bodenkunde* **40** 152-156.
- Rittmann, B. E., Mayer, B., Westerhoff, P., Edwards, M. (2011) Capturing the lost phosphorus. *Chemosphere* **84** (6), 846-853.
- Roberts, T. L. (2014) Cadmium and Phosphorous Fertilizers: The Issues and the Science. *Procedia Engineering* **83** 52-59.
- Robu, E., Giovani, C. (2009) Gamma-ray self-attenuation corrections in environmental samples. *Romanian Reports in Physics* **61** (2), 295-300.
- Römer, W., Schilling, G. (1986) Phosphorus requirements of the wheat plant in various stages of its life cycle. *Plant and Soil* **91** (2), 221-229.
- Rosemarin, A., Schroder, J. J., Dagerskog, L., Cordell, D., Smit, A. L. (2011) Future supply of phosphorus in agriculture and the need to maximise efficiency of use and reuse. *International Fertiliser Society. Proceedings* **685** 1-28.
- Rothamsted Research (2017) Mean long-term winter wheat grain yields, t ha⁻¹ at 85% dry matter. Available at www.era.rothamsted.ac.uk/.../Broadbalk_YieldsJune2017.xlsx [Verified 12.07.2018]
- Rubæk, G. H., Kristensen, K., Olesen, S. E., Østergaard, H. S., Heckrath, G. (2013) Phosphorus accumulation and spatial distribution in agricultural soils in Denmark. *Geoderma* **209-210** 241-250.

- Rubio, G., Sargonà, A., Lynch, J. P. (2004) Spatial mapping of phosphorus influx in bean root systems using digital autoradiography. *Journal of Experimental Botany* **55** (406), 2269-2280.
- Rupp, H., Meissner, R., Leinweber, P. (2018) Plant available phosphorus in soil as predictor for the leaching potential: Insights from long-term lysimeter studies. *Ambio* **47** (1), 103-113.
- Sample, E., Soper, R., Racz, G. (1980) Reactions of phosphate fertilizers in soils. *The role of phosphorus in agriculture* 263-310.
- Santner, J., Smolders, E., Wenzel, W. W., Degryse, F. (2012) First observation of diffusion-limited plant root phosphorus uptake from nutrient solution. *Plant Cell Environ* **35** (9), 1558-1566.
- Sanyal, S. K., De Datta, S. K. (1991) Chemistry of Phosphorus Transformations in Soil. In 'Advances in Soil Science'. (Ed. BA Stewart.) pp. 1-120. (Springer: New York)
- Sato, S., Solomon, D., Hyland, C., Ketterings, Q. M., Lehmann, J. (2005) Phosphorus speciation in manure and manure-amended soils using XANES spectroscopy. *Environmental Science & Technology* **39** (19), 7485-7491.
- Sattari, S. Z., Bouwman, A. F., Giller, K. E., van Ittersum, M. K. (2012) Residual soil phosphorus as the missing piece in the global phosphorus crisis puzzle. *Proceedings of the National Academy of Sciences of the United States of America* **109** (16), 6348-6353.
- Saunders, W. M. H. (1959) Effect of phosphate topdressing on a soil from andesitic volcanic ash. *New Zealand. J. Agr. Res.* **2** 427-444.
- Saunders, W. M. H., Metson, A. J. (1971) Seasonal variation of phosphorus in soil and pasture. *New Zealand Journal of Agricultural Research* **14** (2), 307-328.
- Schachtman, D. P., Reid, R. J., Ayling, S. M. (1998) Phosphorus Uptake by Plants: From Soil to Cell. *Plant Physiology* **116** (2), 447-453.
- Schmidt, L., Hummel, G. M., Thiele, B., Schurr, U., Thorpe, M. R. (2015) Leaf wounding or simulated herbivory in young *N. attenuata* plants reduces carbon delivery to roots and root tips. *Planta* **241** (4), 917-928.
- Schmieder, F., Bergström, L., Riddle, M., Gustafsson, J.-P., Klysubun, W., Zehetner, F., Condron, L., Kirchmann, H. (2018) Phosphorus speciation in a long-term manure-amended soil profile – Evidence from wet chemical extraction, 31P-NMR and P K-edge XANES spectroscopy. *Geoderma* **322** 19-27.
- Schoenau, J. J., Stewart, J. W. B., Bettany, J. R. (1989) Forms and Cycling of Phosphorus in Prairie and Boreal Forest Soils. *Biogeochemistry* **8** (3), 223-237.
- Schweitzer, A., Fahr, A., Niederberger, W. (1987) A simple method for the quantitation of ¹⁴C-whole-body autoradiograms. *International Journal of Radiation Applications and Instrumentation. Part A. Applied Radiation and Isotopes* **38** (5), 329-333.
- Schwertmann, U. (1964) Differenzierung der Eisenoxide des Bodens durch Extraktion mit Ammoniumoxalat-Lösung. *Zeitschrift für Pflanzenernährung, Düngung, Bodenkunde* **105** (3), 194-202.
- Schwertmann, U., Taylor, R. M. (1989) Iron Oxides. In 'Minerals in soil environments'. Eds JB Dixon, SB Weed.) pp. 379-438. (Soil Science Society of America: Madison)
- Selles, F., Campbell, C. A., Zentner, R. P. (1995) Effect of cropping and fertilization on plant and soil phosphorus. *Soil Science Society of America Journal* **59** (1), 140-144.
- Selles, F., Campbell, C. A., Zentner, R. P., Curtin, D., James, D. C., Basnyat, P. (2011) Phosphorus use efficiency and long-term trends in soil available phosphorus in wheat production systems with and without nitrogen fertilizer. *Canadian Journal of Soil Science* **91** (1), 39-52.
- Sharpley, A. N. (1986) Disposition of Fertilizer Phosphorus Applied to Winter Wheat1. *Soil Science Society of America Journal* **50** (4), 953-958.
- Shinde, K. N., Dhoble, S. J., Swart, H. C., Park, K. (2012) Basic Mechanisms of Photoluminescence. In 'Phosphate Phosphors for Solid-State Lighting'. pp. 41-59. (Springer Berlin Heidelberg: Berlin, Heidelberg)
- Siebers, N., Kruse, J., Leinweber, P. (2013) Speciation of phosphorus and cadmium in a contaminated soil amended with bone char: sequential fractionations and XANES spectroscopy. *Water Air & Soil Pollution* **224** (1564),
- Sinaj, S., Stamm, C., Toor, G. S., Condron, L. M., Hendry, T., Di, H. J., Cameron, K. C., Frossard, E. (2002) Phosphorus exchangeability and leaching losses from two grassland soils. *Journal of Environmental Quality* **31** (1), 319-330.

- Smil, V. (2000) Phosphorus in the environment: Natural Flows and Human Interferences. *Annual Review of Energy and the Environment* **25** (1), 53-88.
- Smil, V. (2002) Phosphorus: Global Transfers. In 'Causes and Consequences of Global Environmental Change'. (Ed. I Douglas.) pp. 536 – 542. (John Wiley & Sons: Chichester)
- Smith, V. H., Schindler, D. W. (2009) Eutrophication science: where do we go from here? *Trends in Ecology & Evolution* **24** (4), 201-207.
- Soinne, H., Uusitalo, R., Sarvi, M., Turtola, E., Hartikainen, H. (2011) Characterization of Soil Phosphorus in Differently Managed Clay Soil by Chemical Extraction Methods and P-31 NMR Spectroscopy. *Communications in Soil Science and Plant Analysis* **42** (16), 1995-2011.
- Speirs, S. D., Scott, B. J., Moody, P. W., Mason, S. D. (2013) Soil phosphorus tests II: A comparison of soil test–crop response relationships for different soil tests and wheat. *Crop and Pasture Science* **64** (5), 469-479.
- Spratt, E. D., Warder, F. G., Bailey, L. D., Read, D. W. L. (1980) Measurement of fertilizer phosphorus residues and its utilization. *Soil Science Society of America Journal* **44** (6), 1200-1204.
- Statistisches Bundesamt, 2017. Statistisches Jahrbuch 2017. 1., Auflage ed. Statistisches Bundesamt Wiesbaden.
- Stevenson, F. J., Cole, M. A. (1999) 'Cycles of Soils: Carbon, Nitrogen, Phosphorus, Sulfur, Micronutrients 2nd Edition.' (Wiley-Interscience: New York)
- Subbarao, Y., R. Ellis, AND Jr. (1977) Determination of kinetics of phosphorus mineralization in soils under oxidizing conditions. *Environmental Protection Technology* **180** (600), 2-77.
- Syers, J., Johnston, A., Curtin, D. (2008) Efficiency of soil and fertilizer phosphorus use. *FAO Fertilizer and plant nutrition bulletin* **18** 108.
- Takahashi, K. (2006) Phosphor for X-ray and ionizing radiation. In 'Practical Applications of Phosphors'. Eds WM Yen, S Shionoya, H Yamamoto.) pp. 319-325. (CRC Press: Boca Raton)
- Takahashi, K., Kohda, K., Miyahara, J., Kanemitsu, Y., Amitani, K., Shionoya, S. (1984) Mechanism of photostimulated luminescence in BaFX:Eu²⁺ (X=Cl,Br) phosphors. *Journal of Luminescence* **31-32** (Part 1), 266-268.
- Takahashi, K., Miyahara, J., Shibahara, Y. (1985) Photostimulated Luminescence (PSL) and Color Centers in BaFX:Eu²⁺ (X = Cl, Br, I) Phosphors. *Journal of The Electrochemical Society* **132** (6), 1492-1494.
- Tiess, G. (2010) Minerals policy in Europe: Some recent developments. *Resources Policy* **35** (3), 190-198.
- Tiessen, H., Stewart, J. W. B., Moir, J. O. (1983) Changes in organic and inorganic phosphorus composition of two grassland soils and their particle size fractions during 60–90 years of cultivation. *Journal of Soil Science* **34** (4), 815-823.
- Tiessen, H. J., Moir, J. O. (1993) Characterization of available P by sequential extraction. In 'Soil Sampling and Methods of Analysis'. pp. 75-86. (Lewis Publishers: Boca Raton)
- Tiessen, H. J., Moir, J. O. (2008) Characterization of available P by sequential extraction. In 'Soil Sampling and Methods of Analysis'. pp. 293-306. (Carter, M.R.:
- Tiessen, H. J., Sweart, W. B., Cole, C. V. (1984) Pathways of Phosphorus Transformation in Soils of Differing Pedogenesis. *Soil Science Society of America Journal* **48** 853-858.
- Toor, G. S., Peak, J. D., Sims, J. T. (2005) Phosphorus speciation in broiler litter and turkey manure produced from modiried diets. *Journal of Environmental Quality* **34** (2), 687-697.
- Torrent, J. (1997) Interactions between phosphate and iron oxide. *Advances in Geoecology* **30** 321-344.
- Tóth, G., Guicharnaud, R.-A., Tóth, B., Hermann, T. (2014) Phosphorus levels in croplands of the European Union with implications for P fertilizer use. *European Journal of Agronomy* **55** 42-52.
- Tunney, H., Csatho, P., Ehlert, P. (2003) Approaches to calculating P balance at the field-scale in Europe. *Journal of Plant Nutrition and Soil Science-Zeitschrift Fur Pflanzenernahrung Und Bodenkunde* **166** (4), 438-446.
- Turner, B. L., Cade-Menun, B. J., Condon, L. M., Newman, S. (2005) Extraction of Soil organic phosphorus. *Talanta* **66** 294-306.

- Turner, B. L., Cheeseman, A. W., Godage, H. Y., Riley, A. M., Potter, B. V. L. (2012) Determination of neo- and d-chiro-Inositol Hexakisphosphate in Soils by Solution ^{31}P NMR Spectroscopy. *Environmental Science & Technology* **9** (46), 4994-5002.
- Turner, B. L., Leytem, A. B. (2004) Phosphorus compounds in sequential extracts of animal manures: chemical speciation and a novel fractionation procedure. *Environmental Science & Technology* **38** (22), 6101-6108.
- Turner, B. L., Mahieu, N., Condon, L. M. (2003a) The phosphorus composition of temperate pasture soils determined by NaOH-EDTA extraction and solution ^{31}P NMR spectroscopy. *Organic Geochemistry* **34** (8), 1199-1210.
- Turner, B. L., Mahieu, N., Condon, L. M. (2003b) Quantification of myo-inositol hexakisphosphate in alkaline soil extracts by solution ^{31}P NMR spectroscopy and spectral deconvolution. *Soil Science* **168** (7), 469-478.
- Turner, B. L., Richardson, A. E. (2004) Identification of scyllo-Inositol Phosphates in Soil by Solution Phosphorus- 31 Nuclear Magnetic Resonance Spectroscopy. *Soil Science Society of America Journal* **68** (3), 802-808.
- Ulen, B., Snall, S. (2007) Forms and retention of phosphorus in an illite-clay soil profile with a history of fertilisation with pig manure and mineral fertilisers. *Geoderma* **137** (3-4), 455-465.
- Upham, L. V., Englert, D. F. (2003) Chapter 13 - Radionuclide imaging - L'Annunziata, Michael F. In 'Handbook of Radioactivity Analysis (Second Edition)'. pp. 1063-1127. (Academic Press: San Diego)
- Vaccari, D. A. (2009) Phosphorus: a looming crisis. *Scientific American* **300** (6), 54-59.
- Veith, J. A., Sposito, G. (1977) Reactions of Aluminosilicates, Aluminum Hydrous Oxides, and Aluminum Oxide with o-Phosphate: The Formation of X-ray Amorphous Analogs of Variscite and Montebasite. *Soil Science Society of America Journal* **41** (5), 870-876.
- Velásquez, G., Ngo, P. T., Rumpel, C., Calabi-Floody, M., Redel, Y., Turner, B. L., Condon, L. M., Mora, M. D. L. L. (2016) Chemical nature of residual phosphorus in Andisols. *Geoderma* **271** 27-31.
- Veneklaas, E. J., Lambers, H., Bragg, J., Finnegan, P. M., Lovelock, C. E., Plaxton, W. C., Price, C. A., Scheible, W. R., Shane, M. W., White, P. J., Raven, J. A. (2012) Opportunities for improving phosphorus-use efficiency in crop plants. *New Phytologist* **195** (2), 306-320.
- Wahid, P. (2001) An introduction to isotopes and radiations. (Allied Publishers LTD.: New Dehli)
- Walker, T. W., Syers, J. K. (1976) The fate of phosphorus during pedogenesis. *Geoderma* **15** (1), 1-19.
- Wang, J., Liu, W.-Z., Mu, H.-F., Dang, T.-H. (2010) Inorganic Phosphorus Fractions and Phosphorus Availability in a Calcareous Soil Receiving 21-Year Superphosphate Application. *Pedosphere* **20** (3), 304-310.
- Wang, X., Lester, D. W., Guppy, C. N., Lockwood, P. V., Tang, C. (2007) Changes in phosphorus fractions at various soil depths following long-term P fertiliser application on a Black Vertosol from south-eastern Queensland. *Australian Journal of Soil Research* **45** (7), 524-532.
- Wechsung, G., Pagel, H. (1993) Akkumulation und Mobilisation von Phosphaten in einer Schwarzerde im Statischen Dauerversuch Lauchstädt-Betrachtung der P-Bilanz nach 84 Versuchsjahren. *Zeitschrift für Pflanzenernährung und Bodenkunde* **156** (4), 301-306.
- Weihrauch, C., Opp, C. (2018) Ecologically relevant phosphorus pools in soils and their dynamics: The story so far. *Geoderma* **325** 183-194.
- Williams, E. G., Saunders, W. M. H. (1956) Distribution of Phosphorus in Profiles and Particle-Size Fractions of Some Scottish Soils. *Journal of Soil Science* **7** (1), 91-108.
- Williams, J. D. H., Syers, J. K., Harris, R. F., Armstrong, D. E. (1971) Fractionation of Inorganic Phosphate in Calcareous Lake Sediments1. *Soil Science Society of America Journal* **35** (2), 250-255.
- Wilson, M. A. (2013) 'NMR Techniques & Applications in Geochemistry & Soil Chemistry.' (Pergamon Press: Sydney)
- Xavier, F. A. d. S., de Oliveira, T. S., Andrade, F. V., de Sá Mendonça, E. (2009) Phosphorus fractionation in a sandy soil under organic agriculture in Northeastern Brazil. *Geoderma* **151** (3-4), 417-423.
- Yan, X., Wang, D., Zhang, H., Zhang, G., Wei, Z. (2013) Organic amendments affect phosphorus sorption characteristics in a paddy soil. *Agriculture, Ecosystems & Environment* **175** 47-53.

- Yan, Y., Koopal, L. K., Liu, F., Huang, Q., Feng, X. (2015) Desorption of myo-inositol hexakisphosphate and phosphate from goethite by different reagents. *Journal of Plant Nutrition and Soil Science* **178** (6), 878-887.
- Yan, Y., Li, W., Yang, J., Zheng, A., Liu, F., Feng, X., Sparks, D. L. (2014) Mechanism of myo-inositol hexakisphosphate sorption on amorphous aluminum hydroxide: Spectroscopic evidence for rapid surface precipitation. *Environmental Science and Technology* **48** (12), 6735-6742.
- Yang, X., Post, W. M. (2011) Phosphorus transformations as a function of pedogenesis: A synthesis of soil phosphorus data using Hedley fractionation method *Biogeosciences* **8** (10), 2907-2916.
- YanHong, W., Prietzel, J., Jun, Z., Haijian, B., Ji, L., Dong, Y., ShouQin, S., JianHong, L., HongYang, S. (2014) Soil phosphorus bioavailability assessed by XAnes and Hedley sequential fractionation technique in a glacier foreland chronosequence in Gingga Mountain, Southwestern China. *Science China Earth Science* **57** (8), 1860-1868.
- Yuan, G., Lavkulich, L. M. (1994) Phosphate Sorption in Relation to Extractable Iron and Aluminum in Spodosols. *Soil Science Society of America Journal* **58** (2), 343-346.

VII

APPENDIX A

Supporting information for chapter II

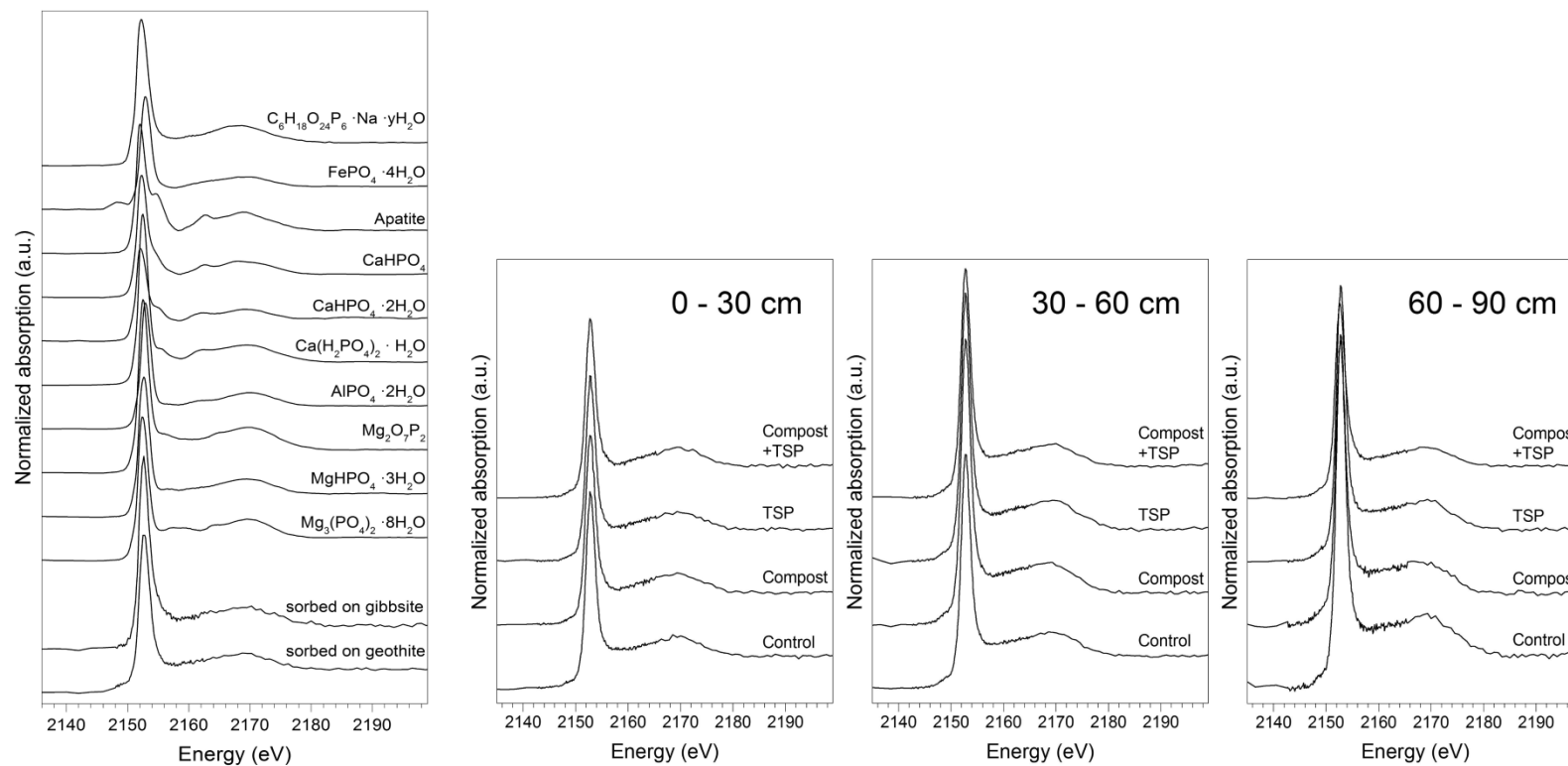


Figure A1: Stacked normalized P K-edge XANES spectra of used P reference compounds and the four treatments separated by sampling depths 0 to 30 cm, 30 to 60 cm, and 60 to 90 cm.

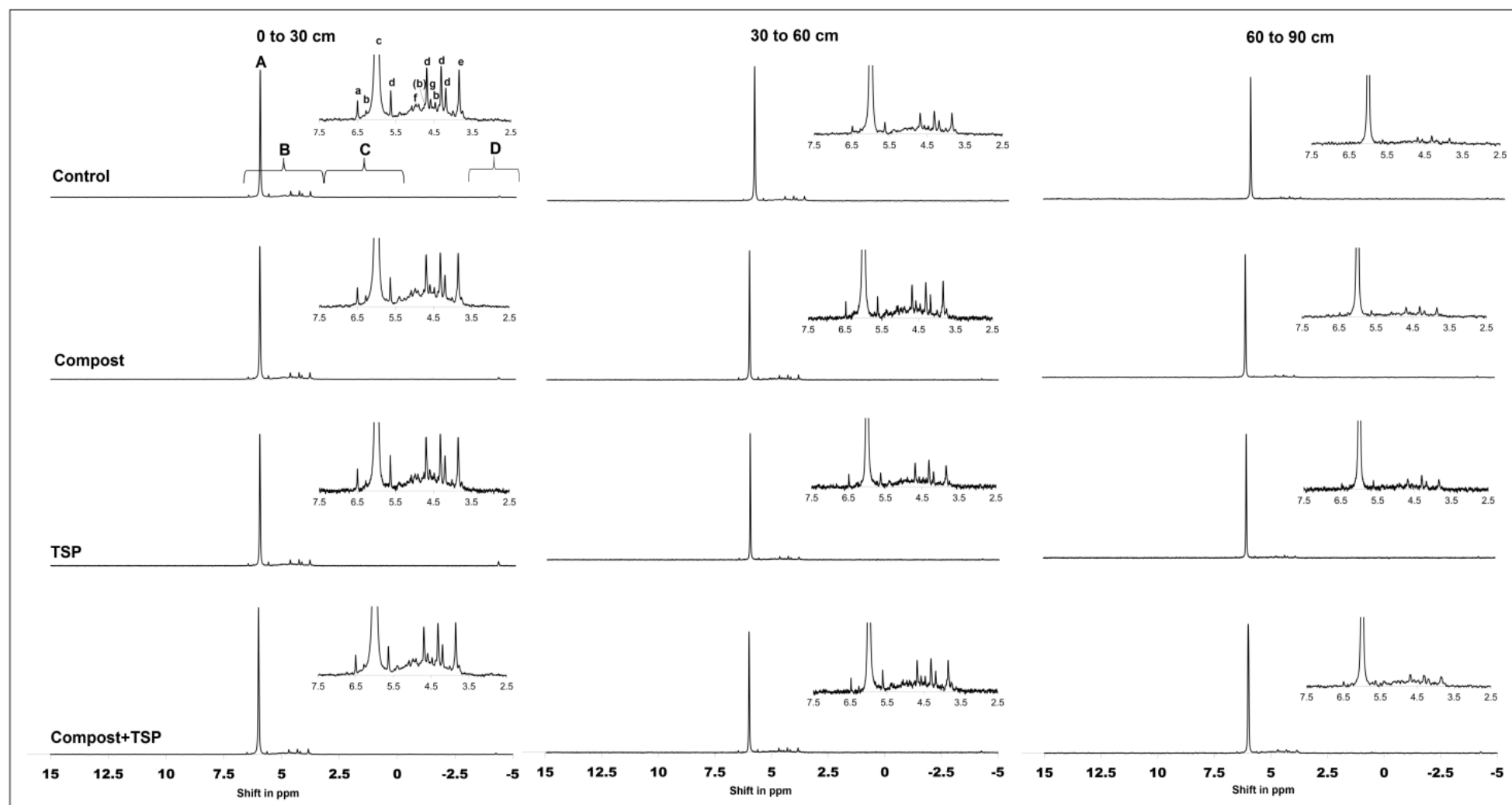


Figure A2: Solution ^{31}P -NMR spectra of the NaOH-EDTA extracts of the topsoil and subsoil samples from 0 to 90 cm soil depths of the control and the fertilizer treatments compost, TSP and compost+TSP with highlighted orthophosphate and orthophosphate monoester region. Shift regions of P compounds are marked with capital letters. Showing orthophosphate (A), the orthophosphate monoester region (B), the orthophosphate diester region (C), and the pyrophosphate region (D). The identified orthophosphate monoester species, are illustrated with small letters from a to e, displaying (a) *neo*-inositol hexakisphosphate, (b) *chiro*-inositol hexakisphosphate, (c) orthophosphate, (d) *myo*-inositol hexakisphosphate, and (e) *scyllo*-inositol hexakisphosphate. Spiking experiments revealed the diester degradation products (f) *alpha*-glycerophosphate, and (g) *beta*-glycerophosphate.

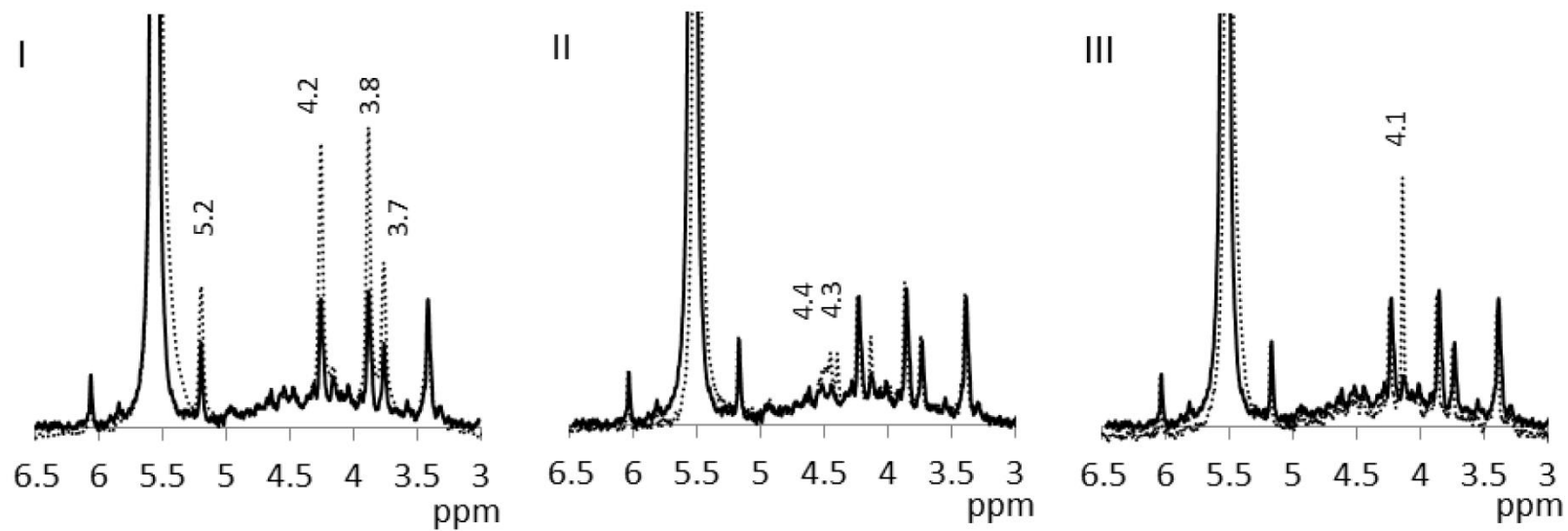


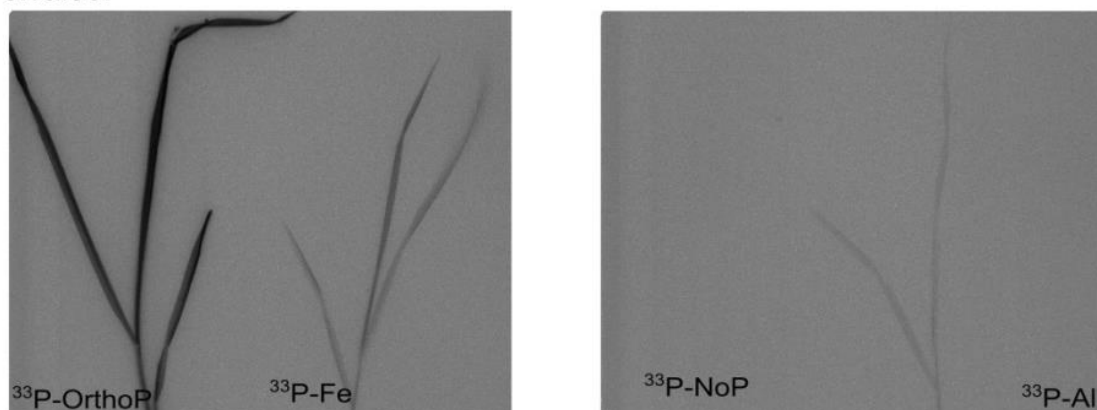
Figure A3: Spiking experiment of a topsoil sample of the TSP treatment, showing the orthophosphate and orthophosphate monoester region. The original solution ^{31}P -NMR spectrum is presented (black line) and the spiked spectra (dotted line) of (I) *myo*-inositol hexakisphosphate, (II) *alpha*-glycerophosphate, and (III) *beta*-glycerophosphate is superimposed to identify and separate these monoesters.

VIII

APPENDIX B

Supporting information for chapter III

Ferralsol



Luvisol

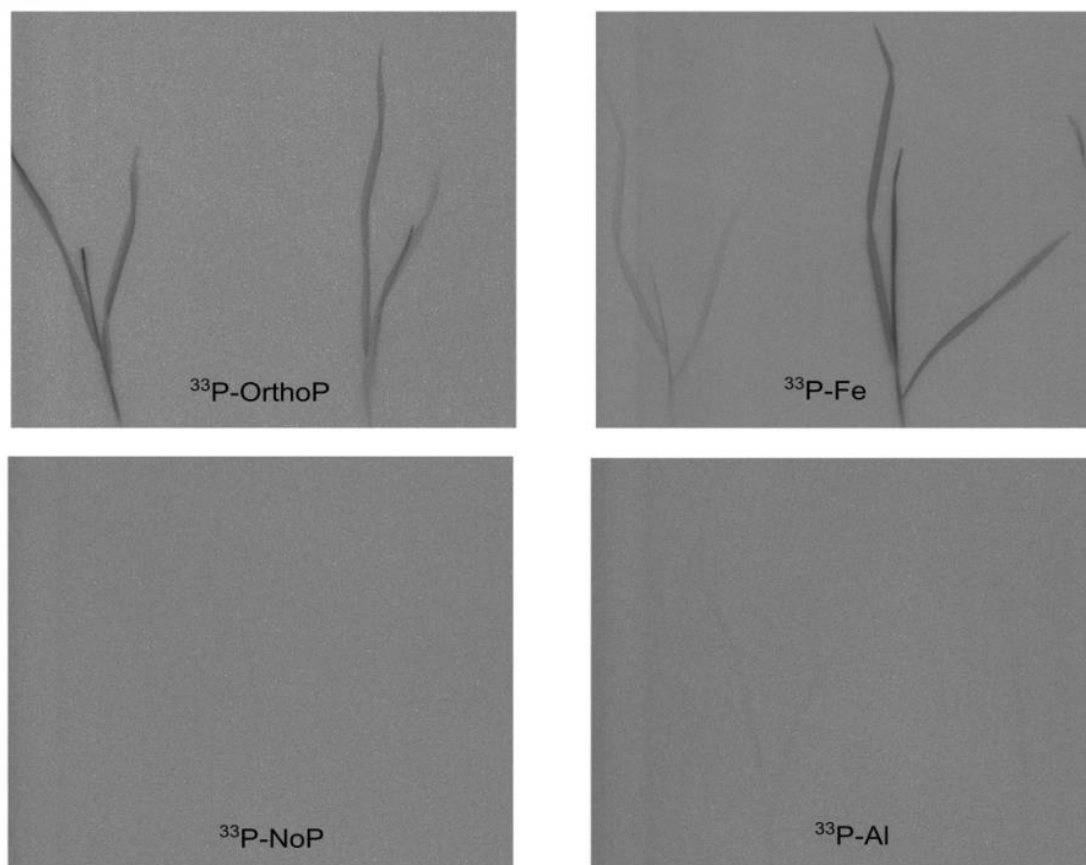


Figure B1: Digital autoradiographic images of 14 days old wheat plants grown in rhizoboxes with different ^{33}P labeled treatments ($^{33}\text{P}\text{-Fe}$: ^{33}P associated to amorphous Fe hydroxide; $^{33}\text{P}\text{-Al}$: ^{33}P associated to amorphous Al hydroxide; $^{33}\text{P}\text{-OrthoP}$: ^{33}P applied in KH_2PO_4 solution; $^{33}\text{P}\text{-NoP}$: ^{33}P radiotracer applied alone without P addition) in Ferralsol and Luvisol subsoil. Imaging plates were exposed for 4 h to the plant material followed by a 100 μm sensitive scan with the scanner unit Bioimager CR35 Bio. Images are processed with AIDA software and presented with a gamma resolution at 2.

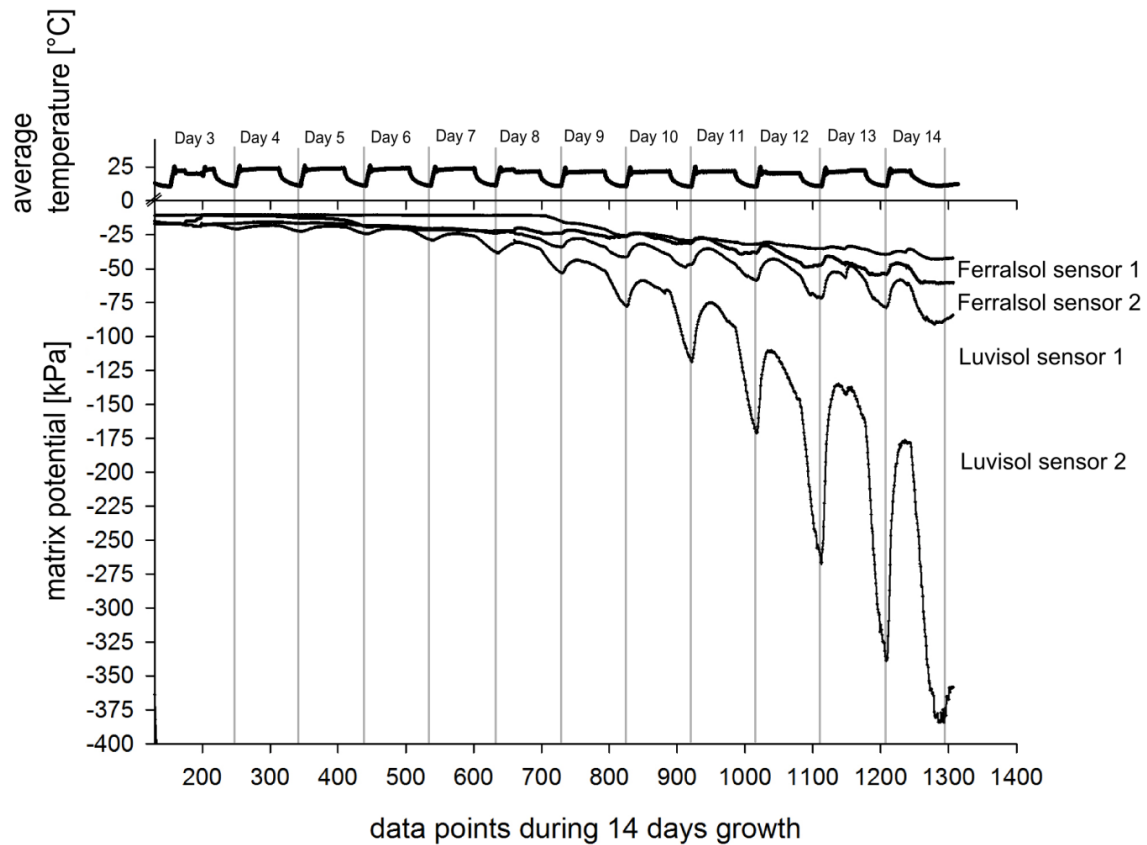


Figure B2: Average diurnal temperature [°C] and soil matrix potentials [kPa] data points from Luvisol (Luvisol sensor 1 + 2) Ferralsol (Ferralsol sensor 1 + 2) subsoil during a 14 days growth period of wheat plants in rhizoboxes. Valid measurement started after filling the ^{33}P radioactive-labeled soil treatments in soil bands of rhizoboxes, which were sealed with plastic foil at day 2 of growth. The data was conducted by dielectric water potential sensors (MPS2) and moisture sensors for the volumetric water content. In this figure all data points from night and day measurements are presented. It is obvious, that matrix potentials were artificially affected by increasing temperature at the start of each day time similar observations are stated by other users. Others authors also assumed effects by plant transpiration when plants reached the sensor area, but these effects were not that pronounced than the effects of temperature variations. However, plant transpiration can be expected to gain influence on the matrix potential after day 7. Furthermore, matrix potential producer estimated the sensor accuracy at -9 to -100 kPa to be approximately 25% (Decagon Devices Inc. 2016). However, these variations cannot explain the steep increase of the matrix potentials measured by Luvisol Sensor 2, and we therefore assume that sensor-soil connectivity was not appropriate for this sensor.

IX

APPENDIX C

Supporting information for chapter IV

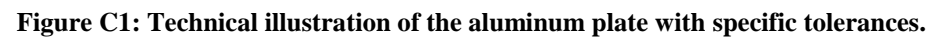


Table C1: Average leaf tissue thickness, leaf area, weight, and density of the excised leaves of maize and wheat plants.

Maize					Wheat				
	Average thickness	Leaf area	Leaf weight	Leaf density		Average thickness	Leaf area	Leaf weight	Leaf density
Leaf No.	μm	mm^2	g	g cm^{-3}	Leaf No.	μm	mm^2	g	g cm^{-3}
1	114	353	0.01323	0.33	1	104	137	0.00719	0.45
2	127	275	0.01343	0.38	2	105	166	0.00865	0.45
3	128	248	0.00974	0.31	3	103	168	0.00957	0.49
4	77	340	0.01091	0.42	4	117	196	0.01025	0.49
5	89	371	0.01581	0.48	5	112	154	0.00777	0.44
6	104	322	0.01442	0.43	6	119	153	0.00828	0.46
7	85	346	0.01354	0.46	7	121	143	0.00857	0.47
8	134	303	0.0119	0.29	8	112	178	0.00997	0.49
9	92	239	0.00859	0.39	9	102	195	0.00925	0.46
10	88	270	0.0092	0.39	10	101	173	0.00811	0.45
11	106	319	0.01197	0.36	11	99	169	0.00776	0.45
12	152	219	0.00955	0.29	12	109	170	0.00896	0.45
13	80	280	0.00895	0.40	13	116	173	0.0085	0.44
14	91	330	0.01141	0.38	14	117	160	0.00834	0.44
15	85	248	0.00819	0.39	15	116	158	0.00843	0.44
					16	108	152	0.00766	0.45
					17	116	179	0.00801	0.44
					18	117	183	0.00859	0.47
					19	128	178	0.00818	0.46
					20	113	175	0.00858	0.45

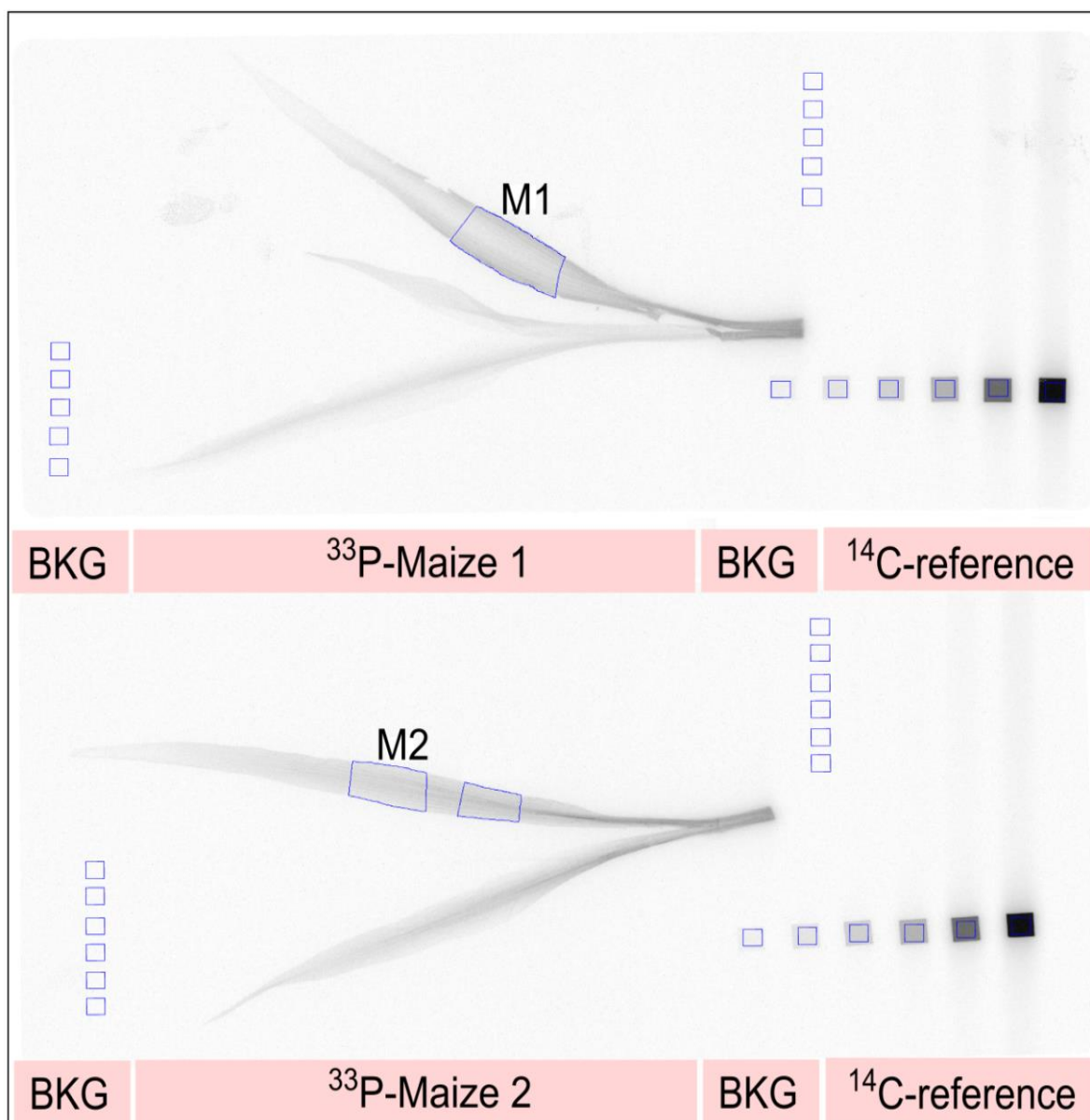


Figure C2: In this example, the ^{33}P activity in specific plant sections of whole plants was analyzed. Results showed that $101 \pm 4\%$ ($n=2$; 3 plate exposures) of the measured activity by liquid scintillation counting (LSC) (in both, M1 and M2) was quantified. Whole maize plants in the three leaf stage were cut at the rhizome and directly placed in 20 mL of dH_2O spiked with $3.6 \text{ Bq } \mu\text{L}^{-1} \text{ }^{33}\text{P}$. After 2 days of incubation in a climate chamber, the plants were carefully removed from the solution. Thereafter, the first 2 cm from the bottom of the stem that were in contact with the solution were cut and discarded. The plants were dried at 40°C for 24 h and thereafter leaf sections of 5 to 10 cm were marginally incised at the edge of a leaf. This was done to retrieve the specific leaf area for processing with AIDA Image Analyzer 2D software (ELYSIA-Raytest, Straubenhardt, Germany). For plate exposure, single plants were placed together with a ^{14}C polymer reference set in a cassette for radiography and exposed for 4 h to a freshly erased imaging plate, covered with a thin plastic foil. The ROI, representing the labeled leaf section were surrounded within the software, giving the PSL intensity and the size of the region in mm^2 . Overall, 3 different imaging plates were exposed to two maize plants (giving $n=6$), respectively. After exposure, the marked leaf sections were carefully cut at the incisions. Then, the tissue thickness was measured and the material was digested with subsequent ^{33}P activities liquid scintillation counting (LSC). The Figure demonstrates that even within a whole plant it is possible to identify and quantify ^{33}P uptake into individual plant sections.

X

APPENDIX D

Supporting information for chapter V

Additional data of long-term fertilizer experiments located in Rostock and Bad Lauchstädt. The data from Bad Lauchstädt are already summarized in a master thesis (Theresa Funk, FZ-Jülich 2018).

Additional data of the ^{33}P loaded hydroxides from analysis for Chapter III and from a plant-agar system testing Al phytotoxicity is included.

Table D1: Basic soil characteristics and elemental stocks of the samples of the four studied treatments (control (no P additions), manure, superphosphate (SP), and manure + SP), and three sampling depths (0 to 30, 30 to 60, and 60 to 90 cm). Long-term fertilizer experiment Bad Lauchstädt (data analysis by Theresa Funk – Master Thesis FZJ 2018)

Treatment		control			manure			SP			manure+SP		
Soil depth		0 - 30 cm	30 - 60 cm	60 - 90 cm	0 - 30 cm	30 - 60 cm	60 - 90 cm	0 - 30 cm	30 - 60 cm	60 - 90 cm	0 - 30 cm	30 - 60 cm	60 - 90 cm
Sand		28	19	16	26	25	19	28	27	19	25	26	20
Silt	%	68	71	77	67	69	71	67	68	72	64	67	70
Clay		5	9	7	7	6	11	6	5	9	11	7	10
pH _{CAC12}		5,97 ± 0,02	7,42 ± 0,01	7,55 ± 0,06	6,94 ± 0,04	7,37 ± 0,03	7,58 ± 0,03	5,19 ± 0,04	6,07 ± 0,08	7,13 ± 0,04	6,77 ± 0,04	6,92 ± 0	7,47 ± 0,02
bulk density	g cm ⁻³	1,6 ± 0,002	1,4 ± 0,002	1,4 ± 0	1,5 ± 0,001	1,4 ± 0,002	1,5 ± 0	1,6 ± 0,002	1,2 ± 0	1,4 ± 0,001	1,5 ± 0,004	1,3 ± 0,003	1,4 ± 0,003
C/N		13,4 ± 0,1	27,5 ± 0,8	72,5 ± 1,2	12,4 ± 0,2	16,5 ± 0,6	47,4 ± 4,2	13,6 ± 0,3	13,3 ± 0,1	11,2 ± 0,1	11,8 ± 0	11,6 ± 0,1	16,2 ± 0,2
P _{tot}		2162 ± 141	1473 ± 82	1385 ± 294	3504 ± 263	1957 ± 125	1756 ± 132	3577 ± 191	1772 ± 148	1564 ± 169	4938 ± 437	2794 ± 116	1920 ± 167
Al _{tot}		22539 ± 451	79725 ± 450	61041 ± 210	89398 ± 350	98986 ± 292	67381 ± 351	111803 ± 525	72564 ± 627	74310 ± 465	106550 ± 810	87353 ± 582	83415 ± 459
Fe _{tot}		92483 ± 376	70603 ± 573	62930 ± 336	82478 ± 394	83203 ± 333	68654 ± 263	97923 ± 572	70054 ± 591	75620 ± 507	90930 ± 900	77815 ± 376	75441 ± 376
Mn _{tot}	kg ha ⁻¹	2613 ± 14	1714 ± 25	1566 ± 8	2510 ± 13	2245 ± 17	1589 ± 26	2895 ± 24	1834 ± 15	1649 ± 17	2611 ± 32	2193 ± 16	1954 ± 17
K _{tot}		21053 ± 752	15953 ± 818	14106 ± 798	21550 ± 613	22446 ± 708	15276 ± 746	23944 ± 715	14764 ± 738	14921 ± 803	27504 ± 855	19946 ± 699	18370 ± 835
Ca _{tot}		20865 ± 141	115762 ± 1227	232199 ± 714	24266 ± 131	87451 ± 833	234844 ± 1317	20892 ± 143	17458 ± 148	19275 ± 211	27504 ± 270	21041 ± 62	65630 ± 668
Mg _{tot}		15522 ± 75	23234 ± 245	35642 ± 294	14542 ± 88	20697 ± 167	32966 ± 219	15645 ± 95	11553 ± 111	13230 ± 127	15260 ± 180	13427 ± 78	17869 ± 125
N _{tot}		5169 ± 47	2454 ± 82	1259 ± 42	7884 ± 175	4164 ± 42	1756 ± 88	6678 ± 191	4798 ± 74	2113 ± 42	9453 ± 360	5821 ± 116	3340 ± 83
C _{tot}	kg ha ⁻¹	71900 ± 752	64222 ± 82	84383 ± 1092	100305 ± 1139	70794 ± 2124	90426 ± 3073	93010 ± 1622	62008 ± 591	24516 ± 592	109386 ± 4186	66747 ± 737	51769 ± 2296
S _{tot}		1410 ± 94	409 ± 41	420 ± 42	2190 ± 44	1249 ± 83	878 ± 88	1908 ± 143	1107 ± 37	1691 ± 42	2701 ± 135	1552 ± 39	835 ± 83
Mn _{ox}		2050 ± 63	931 ± 64	556 ± 14	1873 ± 44	1527 ± 83	760 ± 50	2095 ± 49	1621 ± 19	1199 ± 10	1881 ± 20	1656 ± 4	1173 ± 34
P _{ox}	kg ha ⁻¹	959 ± 8	420 ± 10	380 ± 14	1912 ± 31	812 ± 35	530 ± 13	1965 ± 21	1521 ± 16	550 ± 17	2783 ± 27	1430 ± 37	711 ± 32
Fe _{ox}		6431 ± 41	3513 ± 134	2653 ± 137	5620 ± 121	4168 ± 180	2892 ± 69	6892 ± 60	5333 ± 40	4715 ± 60	6183 ± 114	4773 ± 91	3625 ± 25
Al _{ox}		5728 ± 5	3338 ± 128	1762 ± 72	4457 ± 90	4154 ± 107	2206 ± 42	6012 ± 14	4652 ± 21	3891 ± 65	4774 ± 57	4240 ± 49	3507 ± 46
PSC	mmol kg ⁻¹	39	25	15	34	31	17	40	36	30	36	35	26
DPS	%	17	13	20	41	20	23	33	21	14	56	34	21
P _{DL}		121 ± 6	0 ± 0	0 ± 0	1154 ± 86	195 ± 16	8 ± 16	511 ± 20	118 ± 142	55 ± 5	2011 ± 50	779 ± 53	177 ± 34
K _{DL}	kg ha ⁻¹	446 ± 18	202 ± 14	171 ± 15	1898 ± 39	559 ± 22	224 ± 19	811 ± 44	340 ± 28	306 ± 13	2215 ± 66	978 ± 50	393 ± 10
Mg _{DL}		1183 ± 68	2161 ± 20	2479 ± 63	1673 ± 29	3387 ± 149	2881 ± 46	906 ± 45	716 ± 21	591 ± 8	1606 ± 17	1150 ± 13	2766 ± 555
P _{CAL}		36 ± 5	8 ± 9	6 ± 8	581 ± 27	56 ± 6	8 ± 8	228 ± 31	51 ± 3	18 ± 2	908 ± 203	400 ± 60	45 ± 8
K _{CAL}	kg ha ⁻¹	185 ± 85	132 ± 26	107 ± 36	1225 ± 171	347 ± 71	132 ± 53	480 ± 41	185 ± 7	167 ± 16	1227 ± 486	538 ± 133	210 ± 74
Mg _{CAL}		610 ± 289	1665 ± 273	1912 ± 511	1180 ± 122	1961 ± 311	2241 ± 769	608 ± 54	502 ± 11	413 ± 35	905 ± 391	732 ± 177	1455 ± 440

SP = Super phosphate

tot = Total elemental stocks

Pox, Feox, Alox, Mnox = Ammonium-oxalate extractable stocks of P, Fe, Al, and Mn

DPS = Degree of phosphorus sorption

PSC = Phosphorus sorption capacity

Table D2: Stocks of extractable P of the individual fractions determined by sequential fractionation (n=2) in kg ha⁻¹, extractability with respect to total P stocks (P_t), proportions of inorganic P (P_i) and organic P (P_o) in %, and the ratio of P_i and P_o stocks. The P stocks of the four fertilizer treatments, control (no P additions), manure, superphosphate (SP), and the combination with manure and SP within three soil depths (0 to 30, 30 to 60 and 60 to 90 cm) and the standard deviation are listed. Significant differences between the control and the treatments with fertilizer inputs are marked by * (p < 0.5). Long-term fertilizer experiment Bad Lauchstädt (data analysis by Theresa Funk – Master Thesis FZJ 2018)

107

Treatment	Depth	Resin-P	NaHCO ₃ P _i	NaHCO ₃ P _o	NaOH P _i	NaOH P _o	H ₂ SO ₄ P	Residual-P	P _t	extractability	P _i	P _o	P _i /P _o ratio
	cm	kg ha ⁻¹ (%)								%			
control	0-30	92±3* (5%)	67±1* (4%)	58±27 (3%)	237±21* (13%)	313±12 (18%)	611±53* (34%)	402±17* (23%)	2162±141	64	57	21	3
	30-60	13±19* (1%)	31±19* (2%)	11±7 (1%)	16±22* (1%)	23±33* (2%)	847±6 (64%)	374±49* (28%)	1473±82	64	69	3	27
	60-90	0±0* (0%)	6±8* (0%)	22±31 (1%)	0±0 (0%)	0±0 (0%)	1213±6* (77%)	338±27 (21%)	1385±294	89	77	1	55
manure	0-30	493±3 (15%)	172±70 (5%)	92±72 (3%)	446±32 (13%)	292±11 (9%)	1266±105* (37%)	635±93 (19%)	3504±263	79	70	11	6
	30-60	162±77 (8%)	87±1 (4%)	46±0 (2%)	133±22 (6%)	123±22 (6%)	929±112 (45%)	604±29 (29%)	1957±125	76	63	8	8
	60-90	70±43 (4%)	41±5 (2%)	14±5 (1%)	n.a.	n.a.	1154±19 (67%)	437±34 (25%)	1756±132	73	74	1	90
SP	0-30	423±4 (14%)	256±6* (9%)	49±48 (2%)	613±34* (21%)	419±4 (14%)	777±47 (26%)	445±19 (15%)	3577±191	71	69	16	4
	30-60	132±11 (7%)	76±3 (4%)	39±1 (2%)	249±9* (14%)	295±15* (16%)	565±16 (32%)	437±8 (24%)	1772±148	77	57	19	3
	60-90	57±3 (4%)	27±28 (2%)	40±9 (3%)	87±6 (6%)	82±18 (5%)	782±42 (51%)	444±30 (29%)	1564±169	69	63	8	8
manure + SP	0-30	797±0* (16%)	353±2* (7%)	44±16 (1%)	588±8 (12%)	450±203 (9%)	1805±19 (36%)	990±191* (20%)	4938±437	82	70	10	7
	30-60	435±19* (17%)	161±6* (6%)	33±6 (1%)	319±15* (12%)	248±51* (10%)	896±38 (34%)	506±58* (19%)	2794±116	75	70	11	6
	60-90	95±7* (5%)	93±10* (5%)	33±2 (2%)	96±9 (5%)	59±8 (3%)	939±41* (53%)	451±30 (26%)	1920±167	68	69	5	13

X APPENDIX D

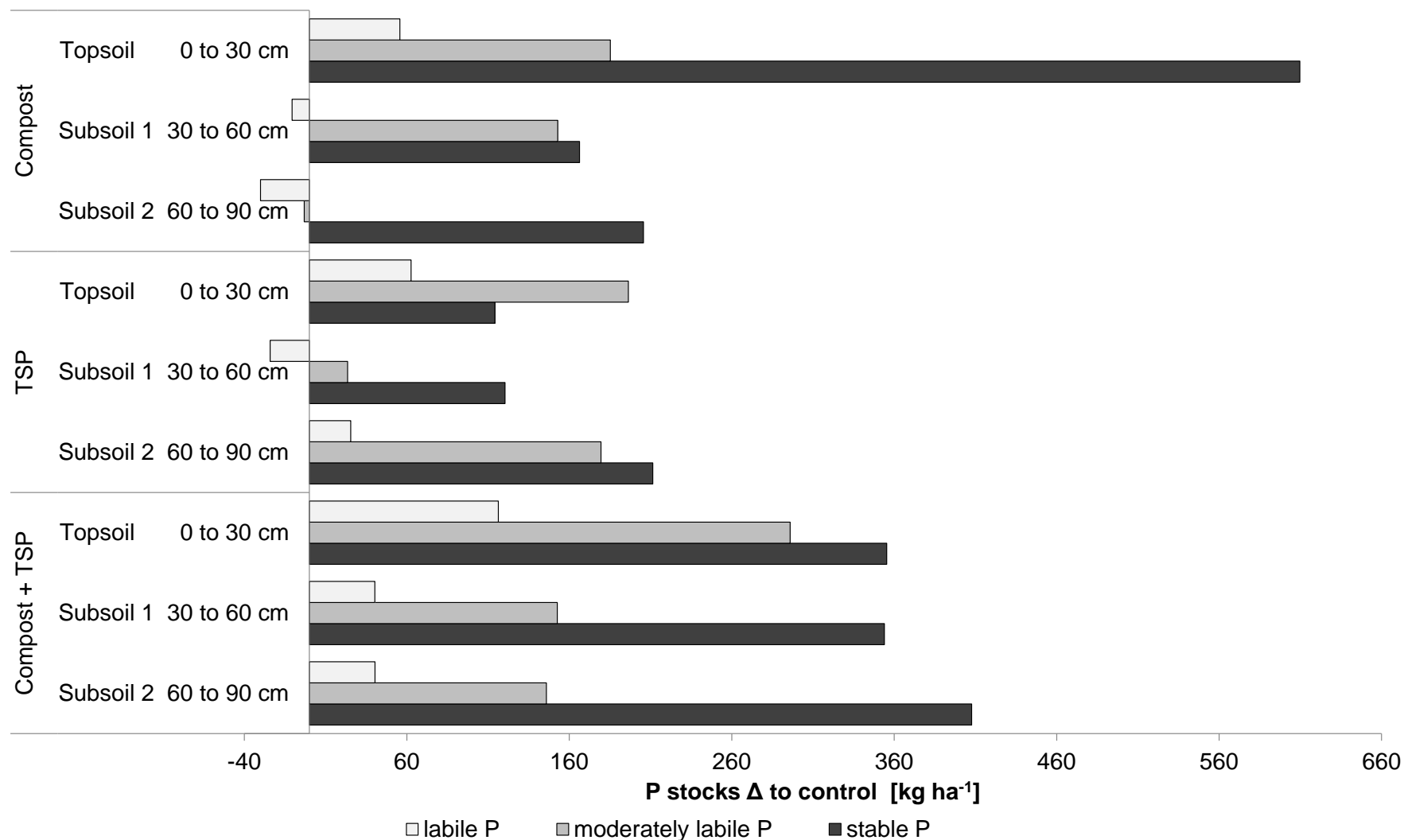


Figure D1: Averaged stocks of labile (sum of Resin-P, $\text{NaHCO}_3\text{-P}_i$, and $\text{NaHCO}_3\text{-P}_o$), moderately labile (sum of NaOH-P_i , NaOH-P_o), and stable P fractions (sum of $\text{H}_2\text{SO}_4\text{-P}$ and Residual-P) of the three sampling depths (0 to 30 cm, 30 to 60 cm, and 60 to 90 cm) of fertilizer treatments (compost, triple superphosphate (TSP), and the combination compost + TSP ($n=3$)) as delta to the P stocks of the unfertilized control treatment (kg ha^{-1}). Long-term fertilizer experiment Rostock

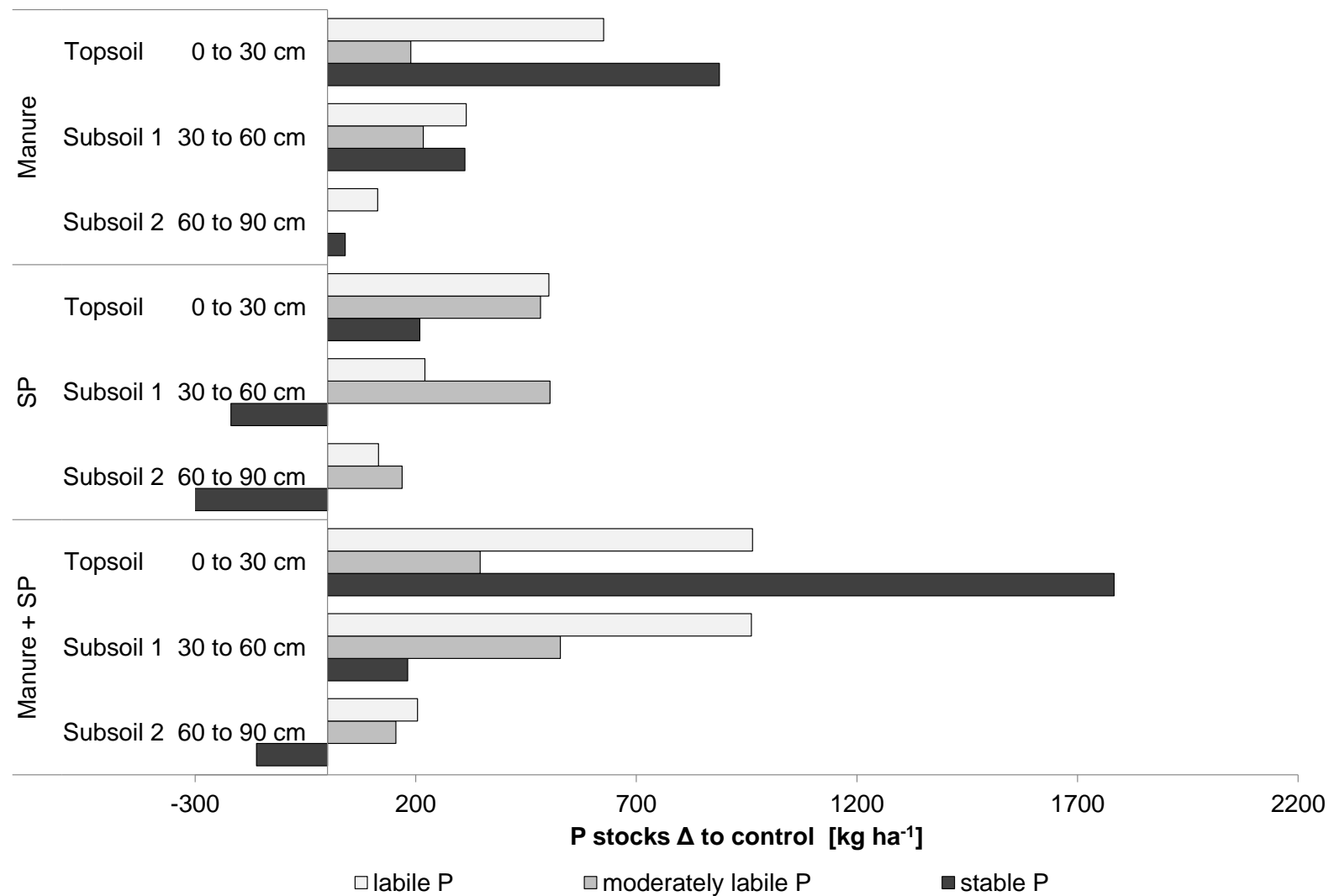


Figure D2: Averaged stocks of labile (sum of Resin-P, $\text{NaHCO}_3\text{-P}_i$, and $\text{NaHCO}_3\text{-P}_o$), moderately labile (sum of NaOH-P_i , NaOH-P_o), and stable P fractions (sum of $\text{H}_2\text{SO}_4\text{-P}$ and Residual-P) of the three sampling depths (0 to 30 cm, 30 to 60 cm, and 60 to 90 cm) of fertilizer treatments (manure, superphosphate (SP), and the combination manure + SP ($n=1$)) as delta to the P stocks of the unfertilized control treatment (kg ha^{-1}). Long-term fertilizer experiment Bad Lauchstädt (data analysis by Theresa Funk - Master Thesis FZJ 2018)

Table D3: Phosphorus (P) speciation (% proportion of total P (P_t)) as obtained by linear combination fitting (LCF) on averaged ($n=3$) P K -edge XANES spectra of two treatments (Control (no P additions) and Manure + Superphosphate (SP) from the long-term fertilizer treatments Bad Lauchstädt. All possible combinations with up to four standard components (total 12 standard components) were calculated comprising P associated with calcium species (Ca-P and Apatite), aluminum species (Al-P), iron species (Fe-P) and organic P species (here phytic acid). Best fit was chosen according to the lowest r-factor and fits were tested for significant differences using the Hamilton test ($p < 0.05$). Long-term fertilizer experiment Bad Lauchstädt (data analysis by Theresa Funk – Master Thesis FZJ 2018)

Treatment	Depth	Ca-P	Apatite	Al-P	Fe-P	Phytic acid
	cm	%				
Control	0 to 30	52.3		18.7	13.7	15.4
	30 to 60	39.0		31.9	0.0	29.2
	60 to 90	52.2		24.3	0.0	23.6
Manure + SP	0 to 30	21.4		0.0	50.2	28.4
	30 to 60	48.7		22.9	0.0	28.3
	60 to 90	0.0	59.9	25.8	0.0	14.3

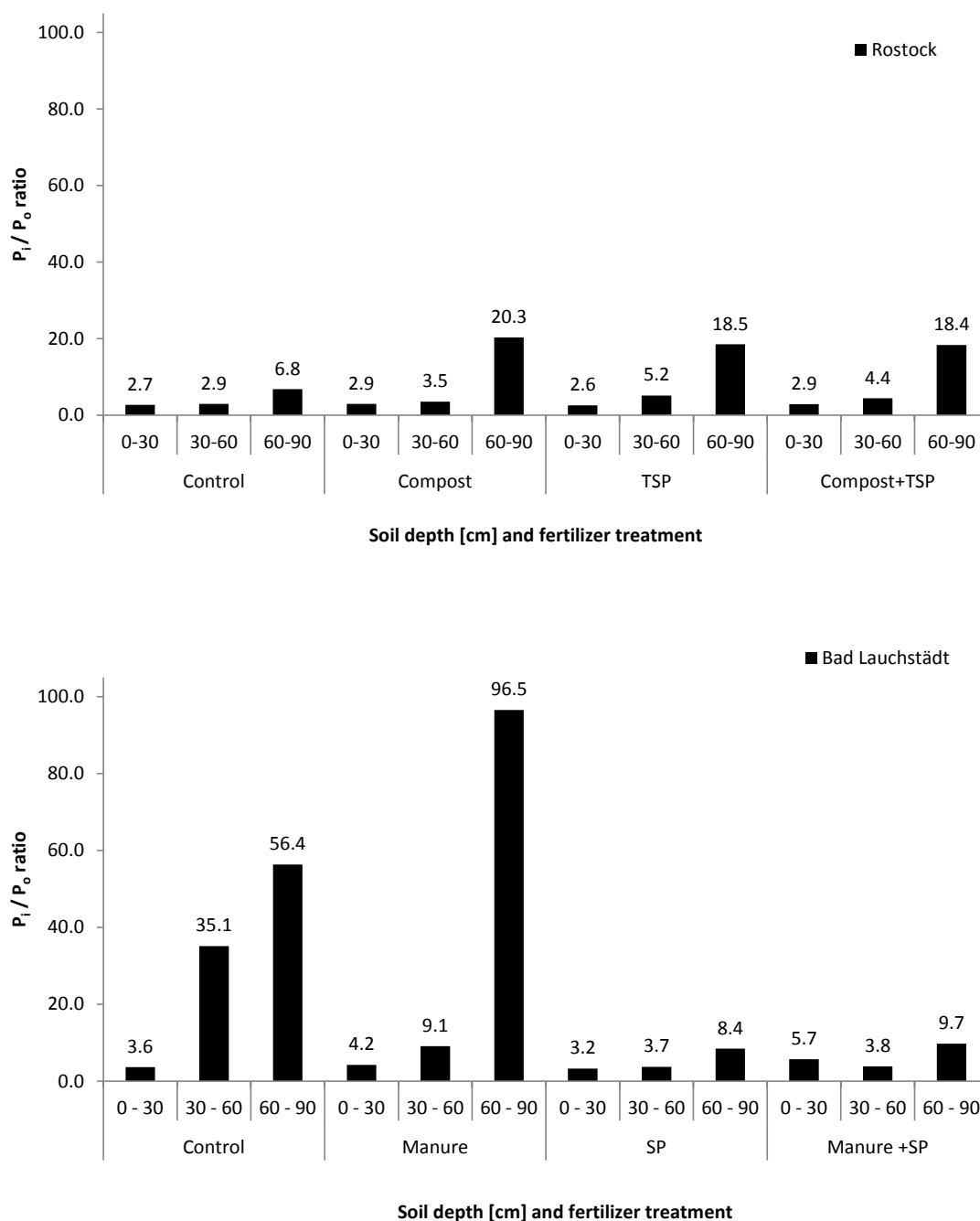


Figure D3: Inorganic P (P_i) to organic P (P_o) ratio, estimated from sequential P fractionation procedure in three sampling depths (0 to 30 cm, 30 to 60 cm, and 60 to 90 cm) of fertilizer treatments of a fertilizer experiment in Rostock (control (no P), compost, triple superphosphate (TSP), and the combination compost + TSP (n=3) and of a fertilizer experiment in Bad Lauchstädt (control (no P), manure, superphosphate (SP), and the combination manure + SP (n=1)).

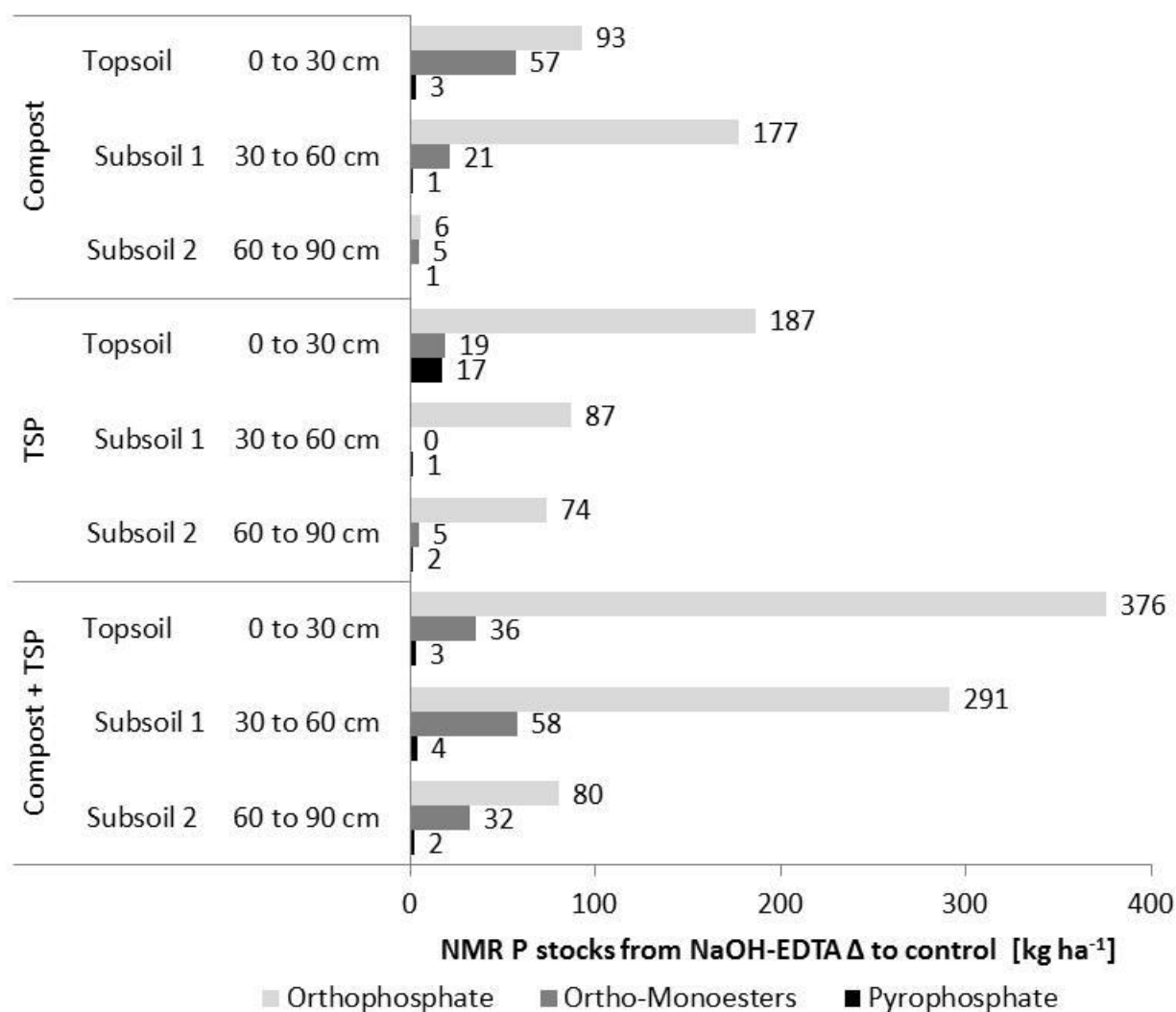


Figure D4: ³¹P-NMR P stocks of orthophosphate (ortho-P), ortho-P monoesters and ortho-P diesters after NaOH-EDTA extraction of fertilizer treatments (compost, triple superphosphate (TSP), and the combination compost + TSP (n=3)) as delta to the NaOH-EDTA P stocks of the unfertilized control treatment (kg ha⁻¹). Long-term fertilizer experiment Rostock

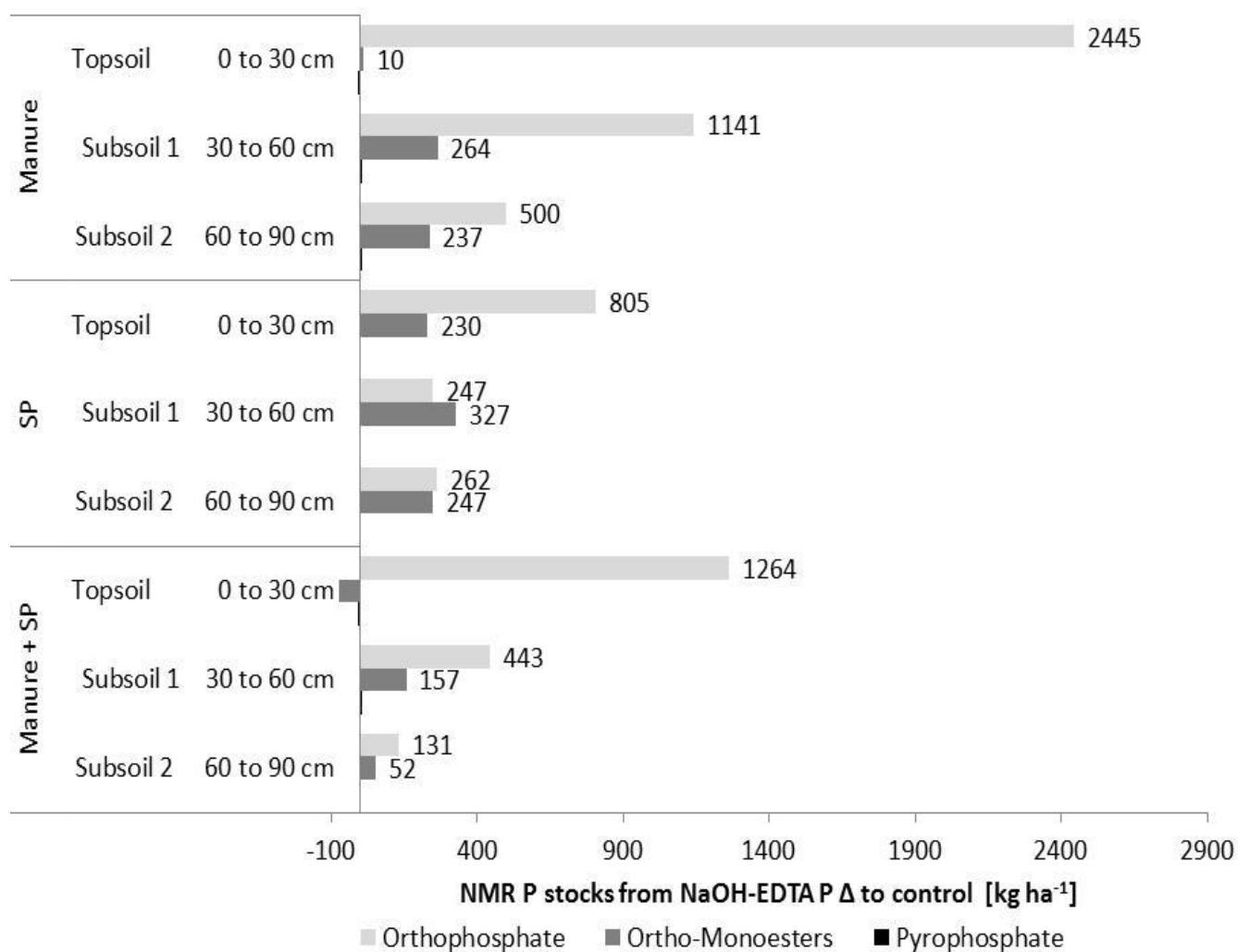


Figure D5: ³¹P-NMR P stocks of orthophosphate (ortho-P), ortho-P monoesters and ortho-P diesters after NaOH-EDTA extraction of fertilizer treatments of fertilizer treatments (manure, superphosphate (SP), and the combination manure + TSP (n=1)) as delta to the NaOH-EDTA P stocks of the unfertilized control treatment (kg ha⁻¹). Long-term fertilizer experiment Bad Lauchstädt (data analysis by Theresa Funk – Master Thesis FZJ 2018)

Table D4: Phosphorus loading levels on amorphous Fe and Al hydroxide surfaces. The weight proportions are shown after acid digestion of the P loaded hydroxides and subsequent inductively coupled plasma emission spectroscopy (ICP-OES) measurement. For acid digestion 50 mg replicate sample were dissolved in 3 mL HCl / 3 mL HNO₃ each and make up to 50 mL volume. For the ICP-OES element determination, two aliquots of each of the sample solutions obtained were diluted to 1 to 100. SD = Standard deviation.

	P loading	Replicates	Fe	SD	Al	SD	P	SD
	$\mu\text{mol g}^{-1}$				% w/w			
Fe hydroxide	370	1	53.5	0.3	<0.009		0.3	0
		2	54.3	0.2	<0.009		0.3	0
		3	55.2	0.2	<0.01		0.3	0
	750	1	53.5	0.2	<0.01		1.3	0.1
		2	53.12	0.19	<0.01		1.3	0.1
		3	53.3	0.18	<0.01		1.3	0
Al hydroxide	370	1	<0.02		28.9	0.17	0.4	0
		2	<0.03		27.76	0.09	0.4	0
		3	<0.02		27.75	0.14	0.4	0
	750	1	<0.02		27.11	0.09	1.8	0
		2	<0.02		26.27	0.14	1.7	0
		3	<0.02		27.43	0.13	1.7	0

Table D5: Dry weights (DW) and ^{32}P proportions of selected plant compartments and agar nutrition medium after 18 d of growth. ^{32}P recovery was between 96% and 100% at the end of experiment.

Significant at * $p < 0.05$. $n = 3$

P concentration	Fe hydroxide		Al hydroxide		Control
	5mM (1a)	0,2 mM (1b)	5mM (2a)	0,2 mM (2b)	0,6 mM
Shoot DW [mg]	178±33	183±28	120±6	146±15	176±39
Root DW [mg]	42±20	37±3	36±3	41±2	45±9
Shoot ^{32}P (%)	1.1±0.3	3.9±0.7*	0.1±0.0	0.3±0.0	-
Root ^{32}P (%)	1.2±1.0	1.9±0.0	1.1±0.2	1.8±0.3	-
Agar ^{32}P (%)	98±1.1	94±0.7	99±0.4	98±0.2	-

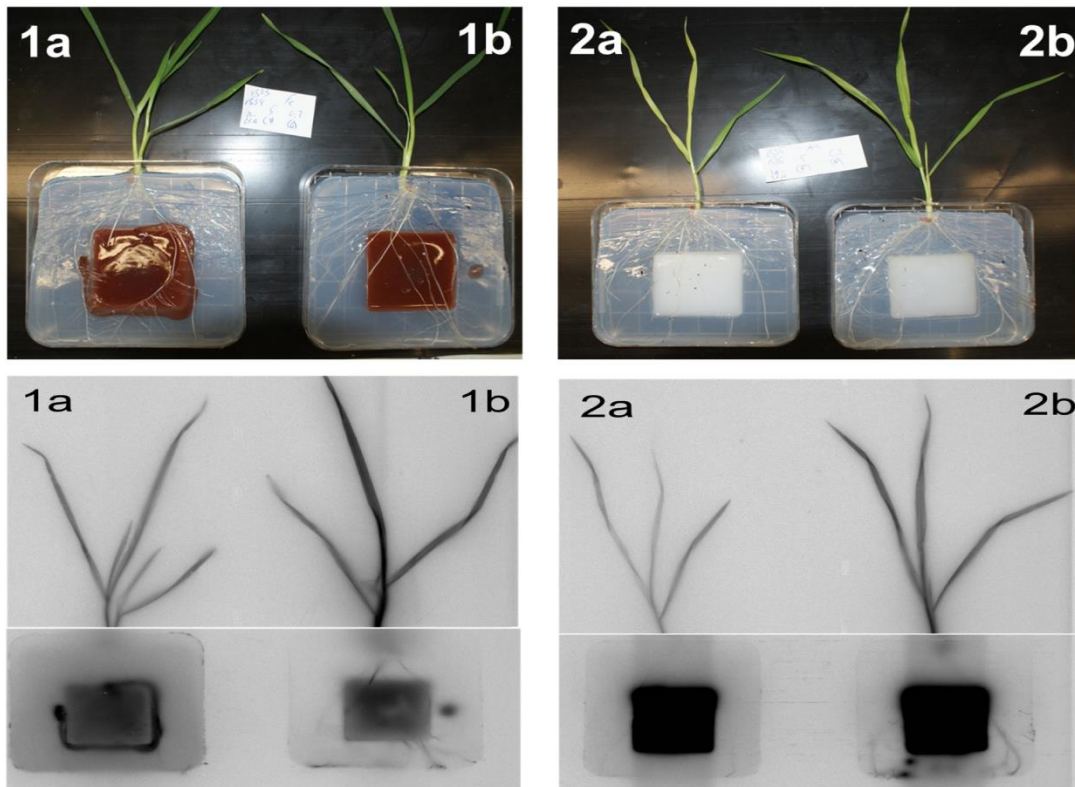


Figure D6: Photo and bioimager image of plant-agar system after 18 days of growth. P sources were provided as (1) P sorbed on to amorphous iron oxide and (2) on to amorphous aluminum oxide, both labelled with ^{32}P -orthophosphate mixed in agar gel and implemented in surrounding agar gel with basal nutrition solution containing (a) 5 mM and (b) 0.2 mM of KH_2PO_4 . The experiment was performed in a growth chamber with 16 h day-length at a light intensity of $320 \mu\text{mol m}^{-2} \text{s}^{-1}$ (PAR). Day-time conditions were 20°C and 60% relative air humidity, while at night temperature decreased to 12°C at 80% relative air humidity. Imaging plates were exposed for 6 h and scanned with $100\mu\text{m}$ sensitivity.

Further information (Table D5 and Figure D6):

The experiment was conducted with ^{32}P radioisotopes (beta emission energy of 1.7 MeV), since it enabled an adequate contrasted imaging via digital autoradiography in agar (containing $< 90\%$ of water). ^{32}P radiotracer activities in the 18 day-old wheat plants confirmed significant better ^{32}P accessibility from the Fe hydroxide treatment (Table D5). However, the digital images showed contrasted regions of the agar area surrounding the ^{32}P loaded hydroxide spots (Fig. D6, red: Fe, white: Al) indicating abiotic ^{32}P desorption (free, unbound ^{32}P on the hydroxide surfaces can be excluded because of two washing steps during hydroxide preparation).

XI

APPENDIX E

Modified Material and Methods section and results according to the manuscript

Combination of ^{33}P digital autoradiography and 2D in situ diffusive gradient in thin films to determine labile phosphorus in soils

Nina Siebers^a, Maximilian Koch^a, Jens Kruse^{ab}

^a Agrosphere Institute, Institute of Bio- and Geosciences (IBG-3), Forschungszentrum Jülich, D-52425 Jülich, Germany

^b Institute of Crop Science and Resource Conservation (INRES), Soil Science and Soil Ecology, University of Bonn, Nussallee 13, 53115 Bonn, Germany

1 MATERIAL AND METHODS

1.1 Soil characteristics and ^{33}P labeling

The soil used in this study was an subsoils from a Haplic Luvisol (50 to 60 cm soil depths) taken from an unfertilized control plot (no P since 1931) at the former experimental research station Dikopshof of the University of Bonn, Germany (50°48'17" N, 6°57'17" E). Soil sampling and basic analyses are described in Chapter III. The soil was characterized by 9% sand, 62% silt, and 29% clay, a pH (0.1 M CaCl_2) of 6.4, C/N ratio of 6.2, and the following total elemental composition: P = 500 mg kg^{-1} , iron (Fe) = 28 g kg^{-1} , and aluminum (Al) = 32 g kg^{-1} .

We prepared four different P sources of different availabilities, i.e., P adsorbed to i) Al-hydroxide, ii) to Fe hydroxide, and iii) KH_2PO_4 which were all labeled with 1.65 MBq ^{33}P -phosphoric acid, being negligibly small compared to the soil P concentration. This was done by applying ^{33}P solved in deionized water (dH_2O) to Al hydroxide (^{33}P -Al), Fe hydroxide (^{33}P -Fe), and KH_2PO_4 (^{33}P -K). Furthermore, in a fourth treatment, iv) we used carrier-free ^{33}P radioisotopes to mimic a 100% bioavailable P-source (^{33}P -solution).

For the ^{33}P -Fe and ^{33}P -Al treatment, respectively Fe and Al hydroxides were produced and loaded with P according to Chapter III. For the ^{33}P -K treatment we spiked a KH_2PO_4 solution with the ^{33}P -phosphoric acid radiotracer and let it dry again to precipitate the KH_2PO_4 with incorporated ^{33}P . The ^{33}P labeled and P associated Fe and Al hydroxides as well as the ^{33}P - KH_2PO_4 were then homogenous blended with a subsample of soil using a drum hop mixer for 24 h according to Chapter III. Thereby the amount of Fe and Al hydroxide addition to soil was chosen to increase the total Fe and Al concentrations in the treatments by 50%, equaling an addition of 14 g Fe kg^{-1} soil and 15.75 g Al kg^{-1} soil and yielding an addition of 40 kg P ha^{-1} , except for the ^{33}P -NoP treatment without additional P application.

1.2 DGT application

For *in situ* chemical imaging of labile ^{33}P the front-lid of the soil container (quadratic petri dish 12 x 12 cm) was removed. We used 12 x 12 cm sheets of the polyethersulfone membrane as diffusive layer overlaid by 10 x 10 x 0.06 cm (length x width x thickness) ferrihydrite gel sheets (DGT Research Ltd.). These DGT sheets were applied 6 h after labeling and filling the soil spaces and DGT gels were deployed at closed soil containers for 48 h to ensure potential ^{33}P gel-diffusion also from less labile P sources. Afterwards, DGT sheets were carefully remove from the soil surface, the polyethersulfone membrane was discarded, and the ferrihydrite gels pressed and dried for 24 h using a gel drier (Gibco GD40/50, LIFE Technologies, Carlsbad, CA) to ensure spatial no distortion due to wrapping.

1.3 ^{33}P imaging

Imaging of the ^{33}P radiotracer 2D distribution in the soil and DGT gels were done using digital autoradiography technology (cf. Chapter VI).

Spatial distribution of the total ^{33}P activity in soils was analyzed by placing imaging plates (20 x 40 cm). For this plates were wrapped in a thin plastic foil to avoid contamination directly on the soils. After an exposure time of 2 h in shielded autoradiographic boxes the image plates were scanned using a scanner unit (Bioimager CR 35 Bio, Raytest, Straubenhardt, Germany) in sensitive mode at a resolution of 100 μm .

Dried DGT sheets were exposed for 15.5 h to the imaging plates to account for low activities in the gels also from less labile P sources. Different to the exposure of the soil no plastic foil was necessary during exposure of the dried DGT sheets. All obtained digital images were processed using the AIDA software (AIDA Bio-package, Raytest, Straubenhardt, Germany).

1.4 ^{33}P quantification

To estimate the bioavailable ^{33}P concentration of the four tested different P sources the DGT sheets were subsequently analyzed for their total ^{33}P activity using liquid scintillation counting (LSC; Tri-Carb 3110TR, PerkinElmer Inc., USA). For LSC analyses all DGT sheet pieces were previously digested and subsamples were supplied with 10 mL scintillation cocktail (Ultima Gold XR, PerkinElmer Inc., USA). The ^{33}P activity quantification from digital images was conducted using the approach as described in Chapter IV; thereby, as a first step AIDA 2D (Raytest, Straubenrath, Germany) was used to correct the background of the obtained photostimulable intensities (PSL) images by using areas in the image, which are known to originate from regions of the imaging plates not exposed ^{33}P . For single plate exposures the ^{33}P activities were calculated using the linear interrelation between PSL intensities and activities in combination with ^{14}C reference standards described in Chapter IV.

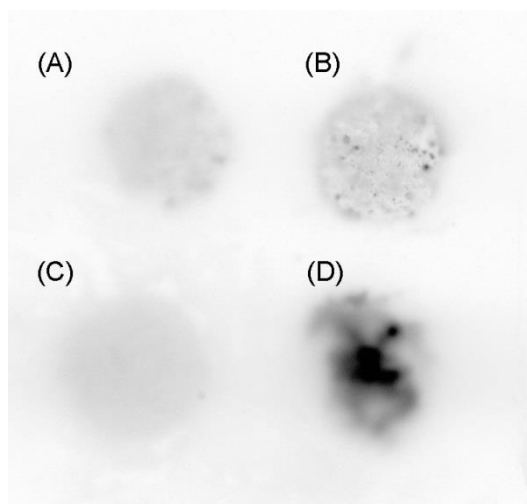


Figure E1: Exemplified ^{33}P autoradiographic image of soil blended with (A) $^{33}\text{P}\text{-Fe}$, (B) $^{33}\text{P}\text{-Al}$, (C) $^{33}\text{P}\text{-K}$, and (D) $^{33}\text{P}\text{-solution}$.

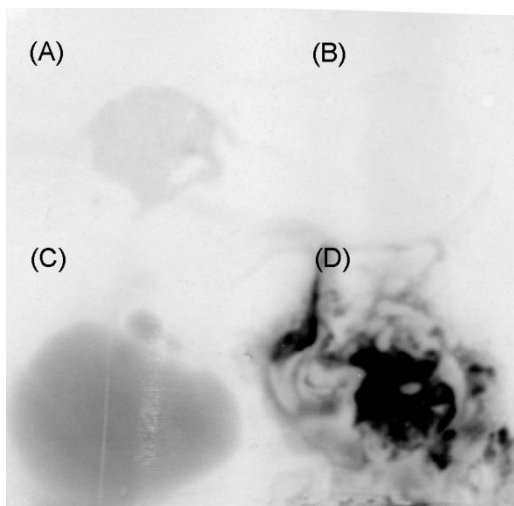


Figure E2: Exemplified ^{33}P autoradiographic image of a diffusive gradient in thin films (DGT) sheet applied for 48 h to soil blended with (A) ^{33}P -Fe, (B) ^{33}P -Al, (C) ^{33}P -K, and (D) ^{33}P -solution. Following the order, ^{33}P -solution ($3841 \pm 721^c \text{ Bq cm}^{-2}$) > ^{33}P -K ($1389 \pm 543^b \text{ Bq cm}^{-2}$) > ^{33}P -Fe ($84 \pm 22^a \text{ Bq cm}^{-2}$) = ^{33}P -Al ($53 \pm 54^a \text{ Bq cm}^{-2}$).

REFERENCES

Decagon Devices Inc., 2016. MPS-2 & MPS-6 dielectric water potential sensors operator's manual. Decagon Devices, Pullman, Washington.

XII

APPENDIX F

Full manuscript of *M. Koch et al. 2016*:

Instructions for homogenous ^{33}P labeling of soil using digital autoradiography for visualization (*not submitted*)

Maximilian Koch¹, Richard Flavel², Christopher Guppy², Nina Siebers¹

¹ Forschungszentrum Jülich GmbH, Agrosphere (IBG-3) Institute of Bio- and Geosciences, Wilhelm Johnen Straße, 52425 Jülich, Germany

² School of Environmental and Rural Science, UNE, Armidale, NSW 2351, Australia

1 ABSTRACT

Homogenous soil-radiotracer blending is essential for reliable data on fertilization and plant nutrition. We tested homogenous blending of ^{33}P associated Fe and Al hydroxides and a carrier-free ^{33}P spiked potassium phosphate solution with a Ferralsol and a Luvisol using a drum hoop mixer and ^{33}P digital autoradiography. The carrier-free ^{33}P radiotracer treatments were more evenly blended than ^{33}P associated to hydroxides. We recommend liquid applications for good soil-radiotracer homogeneities.

2 INTRODUCTION

The use of ^{33}P and ^{32}P isotopes as P radiotracers enables the characterization of agronomic effects, e.g., the labeling of P forms added to soils to determine their spatial distribution within soil (e.g., Daroub *et al.* 2000; Bühler *et al.* 2002; McLaren *et al.* 2016) and the uptake and redistribution by plants (e.g., McLaughlin *et al.* 1988; Bühler *et al.* 2003; Hüve *et al.* 2007). In these studies the radiotracers were applied associated to a surface, located in plant residues, as a powder, or sprayed as a liquid and afterwards mixed thoroughly by hand or in a mixer, but however, with little quantified knowledge of how well the radiotracer was mixed within the soil matrix. Several radioisotope techniques are summarized by Frossard *et al.* (2011) and Di *et al.* (1997), but to the best of our knowledge no practical guidance to achieve homogenous soil-tracer blending is detailed in the literature. Homogeneous blending of the P radiotracers into soil is of particular interest to establish equilibrium with and simulate the natural occurrence of P forms in soils, and does not affect soil P dynamic by changing soil chemical equilibria and structure, as opposed to the buildup of chemical gradients that occur in concentrated hotspots. Likewise, homogenous incorporated radiotracers also ensure the maximum interaction of the proliferating plant roots with the labeled material in the bulk soil. This ensures the reliability to answer scientific questions, which always are extrapolating to field levels. The study was supported by a digital autoradiography which bases on radio-sensitive phosphors image plates being a suitable tool to visualize radiotracer distribution of a variety of isotopes emitting ionizing β -radiation (see Upham and Englert (2003)).

The aims of this work were to test (i) if the mixing process and the application form of ^{33}P radiotracers are crucial determinants for homogenous blending into soils and (ii) if digital autoradiography is suitable to document and statistically analyze homogenous spatial distribution of ^{33}P labeled P forms in soils, being crucial before comparing P uptake from various forms in plant-soil systems.

3 MATERIAL AND METHODS

3.1 Hydroxide preparation and soil blending

In a rhizobox experiment, we introduced a radioactive labeled soil band, the radioisotope labeling and soil blending were implemented as follows: Singly 1.9 MBq ^{33}P phosphoric acid spiked to potassium phosphate either in powdered form (^{33}P associated to iron (^{33}PFe) and aluminum (^{33}PAl) hydroxide) or in liquid form (^{33}P applied with additions of a potassium phosphate solution ($^{33}\text{P-SurplusP}$) or without KH_2PO_4 additions ($^{33}\text{P-NoP}$)) were blended with a Ferralsol (n=3) and a Luvisol (n=5) subsoil. The treatments $^{33}\text{P-SurplusP}$ and $^{33}\text{P-NoP}$ were applied as liquid and added in 5mL drop by drop to 174 g soil (which equals approx. 23% of total soil mass of the rhizobox), whereas the hydroxide treatments (^{33}PFe and ^{33}PAl) were applied in powdered form to the 174 g soil.

Every soil band, except $^{33}\text{P-NoP}$ was supplied with 2.1 mmol PO_4 (Ferralsol) and 2.8 mmol PO_4 (Luvisol). Because of the high specific activity of the ^{33}P radiotracer the P concentration introduced into the system by labeling was negligibly small (1.8×10^{-8} mmol P). For hydroxide P loading, the same amounts of PO_4 spiked with ^{33}P were associated according to the method outlined by Gypser *et al.* (2018). After hydroxide P loading, ^{33}P losses due to P-hydroxide preparation accounted in the Ferralsol for 3.1% (^{33}PFe) and 25.24% (^{33}PAl), and in the Luvisol for 2.7% (^{33}PFe), 6.4% (^{33}PAl). In sum we added 3.4 g with of ^{33}P loaded Fe-hydroxide and 2.9 g of ^{33}P loaded Al for the treatments in the Ferralsol and 4.5 g of ^{33}P loaded Fe and 3.7 g of ^{33}P loaded Al in the Luvisol treatments, having 1.5 to 1.9 MBq ^{33}P in 174 g soil of the soil band.

After applying the four ^{33}P treatments to the appropriate soil amount of the soil band (174 g soil) the labeled soils were blended in a drum hoop mixer (Rhönradmischer JEL RRM Mini-II, J. Engelsmann AG, Ludwigshafen am Rhein, Germany) with 25% to 30% of the total mixer volume filled with the soil and a speed of 30 turns per minute for 24 h. The drum hoop mixer was previously used by Mehmood *et al.* (2017) for soil blending of ^{137}Cs and ^{90}Sr , but no success of the blending was stated.

The bulk soil and the blended ^{33}P soil treatments were separately stored in darkness for 24 h at 5 °C at 75% of their water holding capacity (Luvisol, 207 g kg⁻¹ soil dry weight; Ferralsol, 264 g kg⁻¹ soil dry weight) in order to equilibrate soil moisture. Afterwards, the ^{33}P soil treatments were placed in a previously prepared, recessed band, within the depths of 20 to 25 cm of a two chambered petri dish (243 x 243 x 20mm; Laboglob), with the area being 5 cm in length, 11.2 cm wide, and having a depth of 2 cm. Every chamber was sealed with plastic foil to limit desiccation. After 14 days of plant growth, we applied the digital autoradiography to the surface soil areas to document the distribution of ^{33}P radiotracer in the soil bands.

3.2 Validation of blending

To trace the spatial distribution of ^{33}P within blended soil, we analyzed the surface of the chambers using imaging plates (20 x 40 cm; Raytest, Straubenhardt, Germany) as described in Bauke *et al.* (2017). Rhizoboxes were placed in lead shielded boxes and imaging plates were exposed for 16 h. Imaging plates were analyzed using a Bioimager scanner unit (CR35Bio, Raytest, Straubenhardt, Germany) producing a digital contrasted image (DI) with the mapped signal intensity distributions of the radioactive emitters in accordance to the soil band plate area. The DI was processed using the software “AIDA Image Analyzer 2 D densitometry program” (Raytest, Straubenhardt, Germany). The image of each sample (acquired at 8-bit depth) was subsampled three times to create spatial replicates 60 mm by 50 mm (3000 mm²) using ImageJ (FIJI ImageJ 2.0.0.0-rc-56/1.5 h) (Schindelin *et al.* 2012). These subsamples were allocated to regions where image clarity was the greatest. Images were imported into R (R Development Core Team 2010) using the package ‘tiff’ (Urbanek 2013). A mixture model with two Gaussian peaks was applied to the grey value histogram with the package ‘mixtools’ (Benaglia *et al.* 2009). The intersection of the two normal distributions was used to determine which threshold values would later be used for image processing. The standard deviation of the most common peak (indicating the ‘bulk’ soil) was used as a measure of the homogeneity of ^{33}P distribution through the soil matrix since this measure avoided bias from localized regions either higher than average or lower than average radioactivity. These phases (with the former more common than the later) were quantified as regions above and below the intersection points of the two Gaussian curves. Using the intersection points, the subsampled regions were thresholded using ImageJ to identify either regions of high or low activity. These regions were then quantified using the “Analyze Particles” tool to determine the number, average size and area (as a proportion of the image).

3.3 Statistical analysis

Statistical analysis was performed using the R statistical package (R Development Core Team 2010). Linear models were fitted to the data. Subsample (spatial pseudo-replicate) observations were treated as true replicates due to the small sample quantity available. Models were initially fitted with true replicate (n=2) and treatment predictor variables where there was 3 pseudo-replicates (n=3) of each combination. In no case was there any significant replicate effects or interactions with replicates and so measures were analyzed at the treatment level (with n=6). Low activity regions were also measured where present in samples. Since only one sample had measurable low attenuation regions statistical analysis was not performed on this measure; instead means and standard errors are presented for this sample. Model diagnostic measures were checked and models were transformed (boxcox power transformation (package MASS)), where necessary, to uphold model assumptions. Having determined the most parsimonious model, least squares means and multiple comparisons (Tukey’s method) were performed using the ‘lsmeans’ package (Lenth 2016) with significance determined at the 95% confidence level ($\alpha=0.05$). Back-transformed model means and standard errors are presented.

4 RESULTS AND DISCUSSION

Digital autoradiography bases on the photostimulable luminescence of radio-sensitive phosphor image plates (IP), and was recently applied to trace the transport and distribution of radioactive labeled P in the plant (Hüve *et al.* 2007; Anil Kumar *et al.* 2009) but also for the spatial mapping of P influxes in root systems (Rubio *et al.* 2004). In this study, which was part of a rhizobox experiment analysing the P supply efficiency of P from oxidic surfaces to wheat plants, to the best of our knowledge for the first time the technology was used to compare homogenous distribution of radioactive labeled P forms blended in soil bands. Due to the high fixation potential of the two subsoils, being low in soluble P concentrations and the small P uptake rates (< 1% of total radioactivity applied) of the wheat plants grown in the soils for 14 days (data not shown) no modification of ^{33}P distribution and any soil P diffusion during the period of growth were expected, however, plant roots indicated by low contrasted lines in the digital autoradiographic image were visible mainly due to shielding of radioactivity mediated by their higher water content (Fig.F 1).

For comparison of spatial homogeneity, regions of high resolution without plant roots were selected and the standard deviation (SD) of the mean bulk soil area was calculated; generally, heterogeneity was higher in samples of the Ferralsol compared to the Luvisol (Fig. F1). The SD of 'bulk' soil indicated that the ^{33}P PAI treatment in the Ferralsol had the highest inhomogeneity. This is most likely due to the friable structure of the ^{33}P -hydroxides but also due to lower total radioactivity (approx. 22.6 % less activity) located in the same amount of soil in the soil band, which is thought to be a direct result of the oxide preparation method. The SD of ^{33}P -SurplusP and ^{33}P -NoP treatments, in both soils, was lower indicating that the spatial ^{33}P distribution was more homogeneous. It is thought this is a result of applying ^{33}P as a solution.

The number of high activity regions and the average size of high activity regions (Fig. F2) in the Ferralsol were on average 1.1 and 1.6 times higher than in those measured in the Luvisol. However, number of high activity regions of ^{33}P Fe in Luvisol was 2.5 times higher compared to the treatment in the Ferralsol, while the average size of high activity regions of ^{33}P Fe in the Luvisol was significantly 4.6 times lower than in the Ferralsol. The opposite was visible for the ^{33}P PAI treatment with a significantly 4 times lower average size of high activity regions in Ferralsol than in Luvisol but a 1.9 times higher number of high activity regions. Direct reasons for this can be addressed to the differences in the total amount of activity in the ^{33}P PAI treatment compared to other treatments. However, the importance of close contact of the IP and the radioactive material has to be highlighted, being a limitation of resolution in this experiment.

For the ^{33}P treatments with and without carrier free KH_2PO_4 addition, both soils showed high homogeneity as indicated by low numbers of high activity regions and the average size of high activity regions. This result was also visible by comparing the percentage area covered by high activity regions (Fig. F2). Both of the P treatments that were applied as liquid (^{33}P -SurplusP and ^{33}P -NoP) produced the lowest area proportions that were covered by high activity regions. This intuitively indicated that the liquid application produced a more homogeneous spatial distribution of ^{33}P in the soil band as compared to the oxide application. In summary, the mixing procedure used lead to less-uniform distributions of radioactivity for treatments with ^{33}P radiotracer associated with a carrier and applied as friable powder, and thus the mixing procedure should be adjusted according to sample characteristics (we recommend a longer mixing and/or a previous fine grinding procedure for particulate radiotracer applications). However, these results also imply that labeling solid fertilizer samples results in more discrete and heterogeneous distributions of labeled fertilizer in soil volumes than when applying labeled liquids. Hence estimates of root interception and isotope recovery will vary with application techniques where P is being measured due to the high reliance on spatial root interception in P acquisition in soils. In addition, we showed that the digital autoradiography technology is a suitable tool to visualize ^{33}P distributions in soils to statistically quantify the homogeneity of incorporation methods.

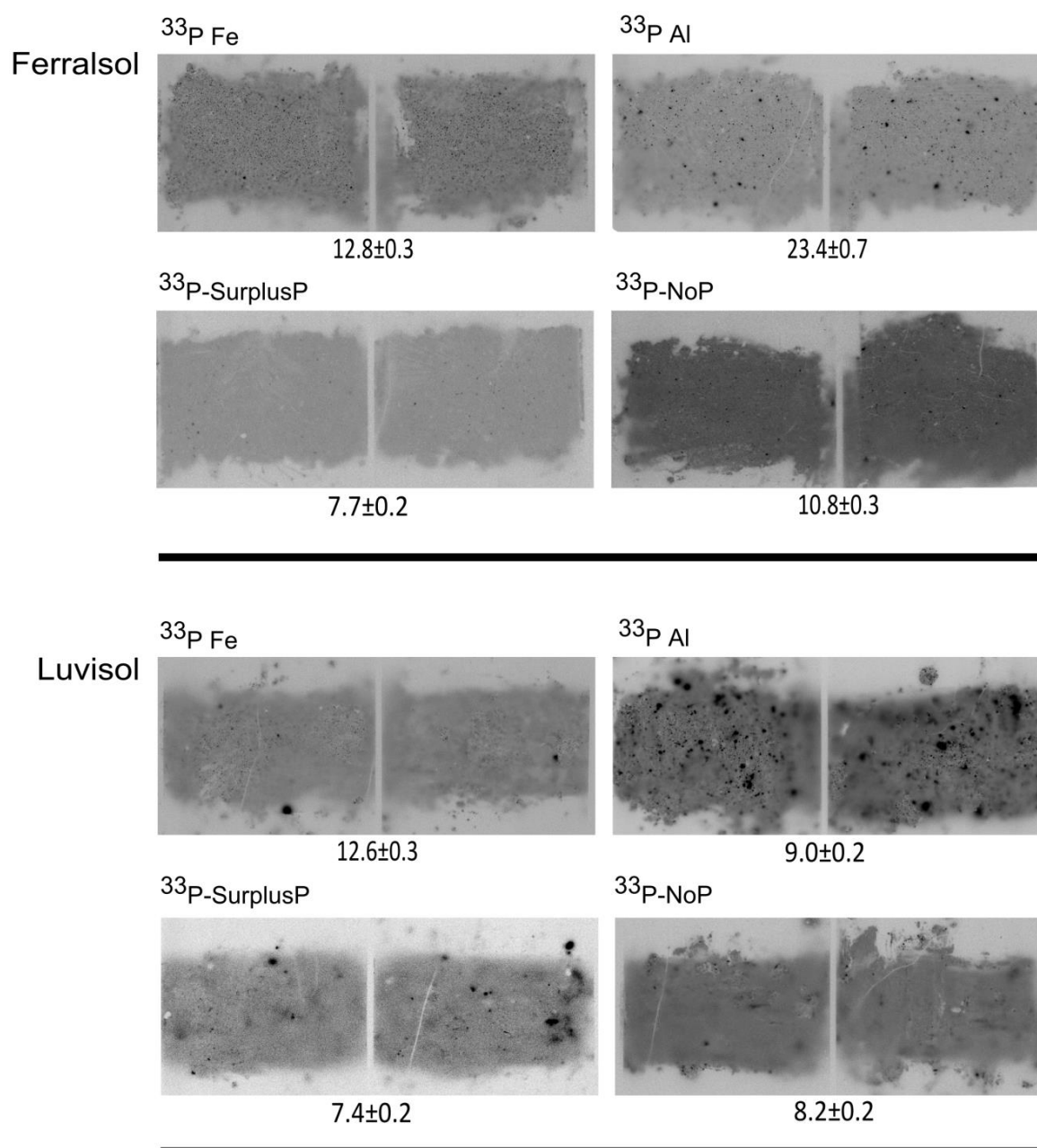


Figure F1: Digital autoradiographic images of ³³P labeled soil bands of a Ferralsol and a Luvisol with associated and ³³P radioisotopes (³³PFe hydroxide, ³³PAl hydroxide, ³³P-SurplusP, and ³³P-NoP) in duplicates (two replicated chambers). The standard deviation (SD) ± standard error of the mean bulk soil signature is displayed below the digital image.

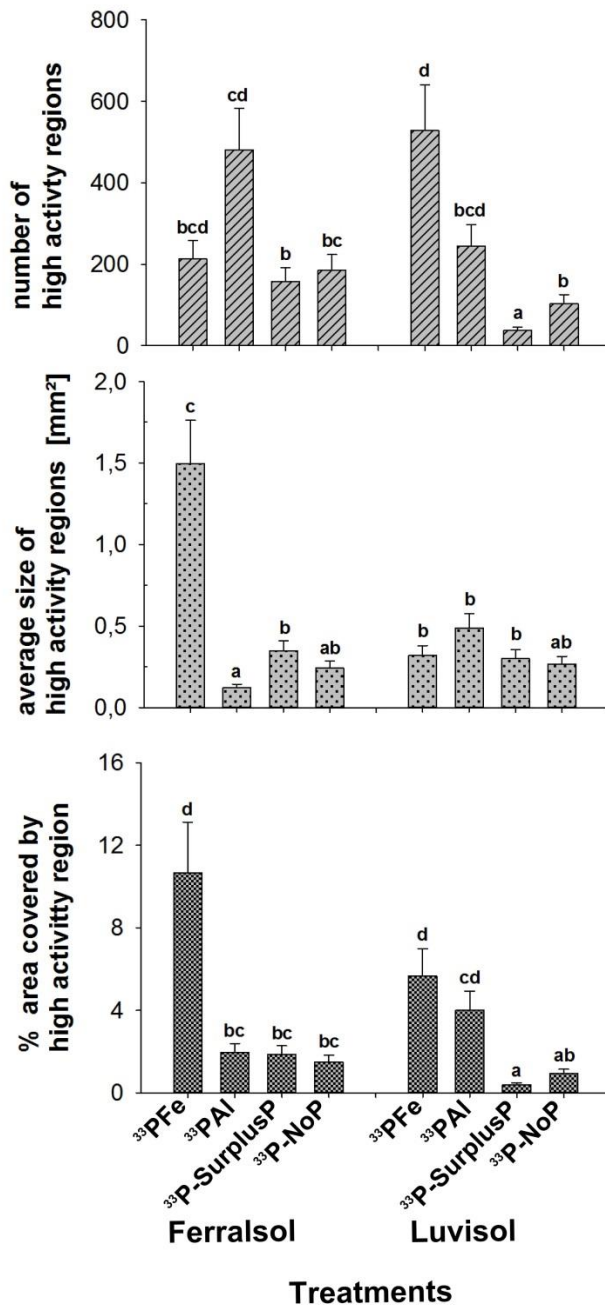


Figure F2: Statistical analysis of blending homogeneities evaluated by the digital image data of the soil bands (with the treatments ^{33}PFe hydroxide, ^{33}PAI hydroxide, $^{33}\text{P-SurplusP}$, and $^{33}\text{P-NoP}$). The analysis is separated into the number of high activity regions, the average size of high activity regions, and the percentage area covered by high activity regions as parameters for soil radiotracer blending homogeneity. Significant differences at 5% probability level between samples are designated by different letters.

REFERENCES

- Anil Kumar, R., Vasu, K., Velayudhan, K. T., Ramachandran, V., Suseela Bhai, R., Unnikrishnan, G. (2009) Translocation and distribution of ^{32}P labelled potassium phosphonate in black pepper (*Piper nigrum* L). *Crop Protection* 28 (10), 878-881. <https://doi.org/10.1016/j.cropro.2009.06.016>
- Bauke, S. L., Landl, M., Koch, M., Hofmann, D., Nagel, K. A., Siebers, N., Schnepf, A., Amelung, W. (2017) Macropore effects on phosphorus acquisition by wheat roots – a rhizotron study. *Plant and Soil* 416 (1-2), 67-82. <https://10.1007/s11104-017-3194-0>
- Benaglia, T., Chauveau, D., Hunter, D. R., Young, D. (2009) mixtools: An R Package for Analyzing Finite Mixture Models. *Journal of Statistical Software* 32 1-29.
- Bühler, S., Oberson, A., Rao, I. M., Friesen, D. K., Frossard, E. (2002) Sequential Phosphorus Extraction of ^{33}P -Labeled Oxisol under Contrasting Agricultural Systems. *Soil Science Society of America Journal* 66 868-877. 10.2136/sssaj2002.8680
- Bühler, S., Oberson, A., Sinaj, S., Friesen, D. K., Frossard, E. (2003) Isotope methods for assessing plant available phosphorus in acid tropical soils. *European Journal of Soil Science* 54 (3), 605-616. <https://10.1046/j.1365-2389.2003.00542.x>
- Daroub, S., Pierce, F. J., Ellis, B. G. (2000) Phosphorus fractions and fate of phosphorus-33 in soils managed under plowing and no-tillage. *Soil Science Society of America Journal* 64 170-176. 10.2136/sssaj2000.641170x
- Di, H. J., Condon, L. M., Frossard, E. (1997) Isotope techniques to study phosphorus cycling in agricultural and forest soils: A review. *Biology and Fertility of Soils* 24 (1), 1-12. <https://10.1007/bf01420213>
- Frossard, E., Achat, D. L., Bernasconi, S. M., Bünemann, E. K., Fardeau, J. C., Jansa, J., Morel, C., Rabeharisoa, L., Randriamanantsoa, L., Sinaj, S. t., Tamburini, F., Oberson, A. Eds E Bünemann, A Oberson, E Frossard (2011) 'Phosphorus in Action: Biological Processes in Soil Phosphorus Cycling.' (Springer Berlin Heidelberg: Berlin, Heidelberg)
- Gypser, S., Hirsch, F., Schleicher, A. M., Freese, D. (2018) Impact of crystalline and amorphous iron- and aluminum hydroxides on mechanisms of phosphate adsorption and desorption. *Journal of Environmental Sciences* <https://doi.org/10.1016/j.jes.2017.12.001>
- Hüve, K., Merbach, W., Remus, R., Lüttschwager, D., Wittenmayer, L., Hertel, K., Schurr, U. (2007) Transport of phosphorus in leaf veins of *Vicia faba* L. *Journal of Plant Nutrition and Soil Science* 170 (1), 14-23. 10.1002/jpln.200625057
- Lenth, R. (2016) Least-Squares Means: The R Package lsmean. *Journal of Statistical Software* 69 1-33.
- McLaren, T. I., McLaughlin, M. J., McBeath, T. M., Simpson, R. J., Smernik, R. J., Guppy, C. N., Richardson, A. E. (2016) The fate of fertiliser P in soil under pasture and uptake by subterranean clover – a field study using ^{33}P -labelled single superphosphate. *Plant and Soil* 401 (1), 23-38. <https://10.1007/s11104-015-2610-6>
- McLaughlin, M., Alston, A., Martin, J. (1988) Phosphorus cycling in wheat pasture rotations .I. The source of phosphorus taken up by wheat. *Soil Research* 26 (2), 323-331. <https://doi.org/10.1071/SR9880323>
- Mehmood, K., Berns, A. E., Pütz, T., Burauel, P., Vereecken, H., Opitz, T., Zoriy, M., Hofmann, D. (2017) No effect of digestate amendment on Cs-137 and Sr-90 translocation in lysimeter experiments. *Chemosphere* 172 310-315. <https://doi.org/10.1016/j.chemosphere.2016.12.134>
- R Development Core Team (2010) 'R: A language and environment for statistical computing.' (R Foundation for Statistical Computing: Vienna, Austria)
- Rubio, G., Sorgonà, A., Lynch, J. P. (2004) Spatial mapping of phosphorus influx in bean root systems using digital autoradiography. *Journal of Experimental Botany* 55 (406), 2269-2280. 10.1093/jxb/erh246
- Schindelin, J., Arganda-Carreras, I., Frise, E., Kaynig, V., Longair, M., Pietzsch, T., Preibisch, S., Rueden, C., Saalfeld, S., Schmid, B., Tinevez, J., White, D., Hartenstein, V., Eliceiri, K., Tomancak, P., Cardona, A. (2012) FiJI: and open-source platform for biological-image analysis. *Nature Methods* 9 676-682.
- Upham, L. V., Englert, D. F. (2003) 13 - RADIONUCLIDE IMAGING A2 - L'Annunziata, Michael F. In 'Handbook of Radioactivity Analysis (Second Edition)'. pp. 1063-1127. (Academic Press: San Diego)
- Urbanek (2013) 'tiff: Read and write TIFF images. R package.'

LEBENSLAUF

LEBENSLAUF / CURRICULUM VITAE

[Content not available in the electronic version]

DANKSAGUNG

DANKSAGUNG

[Content not available in the electronic version]